

# Ecological and molecular insights into the function of colourful signals in aquatic environments

## **Inauguraldissertation**

zur

Erlangung der Würde eines Doktors der Philosophie  
vorgelegt der  
Philosophisch-Naturwissenschaftlichen Fakultät  
der Universität Basel

von

**Fabio Cortesi**

aus

**Poschiavo, Graubünden  
Schweiz**

Basel, 2016

Originaldokument gespeichert auf dem Dokumentenserver der Universität Basel  
[edoc.unibas.ch](http://edoc.unibas.ch)

Genehmigt von der Philosophisch-Naturwissenschaftlichen Fakultät

Auf Antrag von

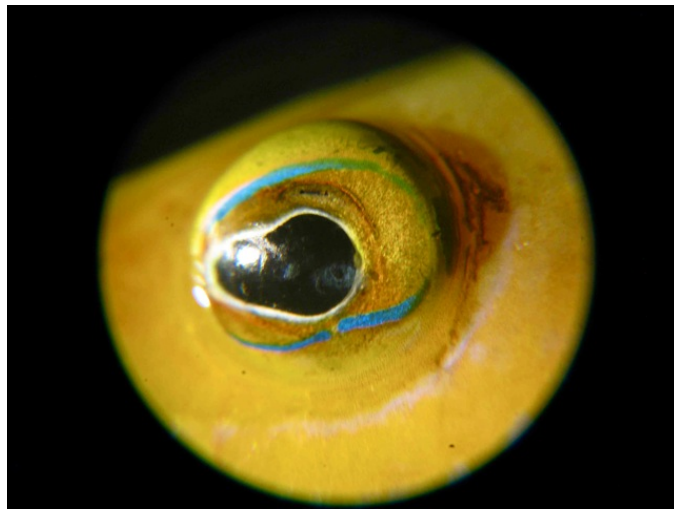
Prof. Dr. Walter Salzburger, Prof. Dr. Redouan Bshary

Basel, den 11.11.2014

Prof. Dr. Jörg Schibler  
Dekan



# Ecological and molecular insights into the function of colourful signals in aquatic environments



Dissertation zur  
Erlangung der Würde eines Doktors der Philosophie  
vorgelegt der  
Philosophisch-Naturwissenschaftlichen Fakultät  
der Universität Basel

**Fabio Cortesi**

under supervision of

Prof. Dr. Walter Salzburger, Dr. Karen Cheney, Prof. Dr. Justin Marshall

examined by

Prof. Dr. Walter Salzburger and Prof. Dr. Redouan Bshary

Basel, 2014



# Table of Contents

<b>Introduction.....</b>	<b>7</b>
<b>Main Body of Work.....</b>	<b>15</b>
<b>Chapter 1</b> Phenotypic plasticity confers multiple fitness benefits to a mimic.....	17
1.1. Manuscript.....	19
1.2. Supporting Information .....	26
<b>Chapter 2</b> From crypsis to mimicry: changes in colour and the configuration of the visual system during ontogenetic habitat transitions in a coral reef fish.....	45
2.1. Manuscript.....	47
2.2. Supporting Information .....	61
<b>Chapter 3</b> Ancestral duplications and highly dynamic opsin gene evolution in percomorph fishes.....	65
3.1. Manuscript.....	67
3.2. Supporting Information .....	73
3.3. Commentary by Harris R.M. & Hofmann H.A. ....	89
<b>Side Projects.....</b>	<b>91</b>
<b>Chapter 4</b> Conspicuousness is correlated with toxicity in marine opisthobranchs.....	93
4.1. Manuscript.....	95
4.2. Supporting Information .....	105
<b>Chapter 5</b> Conspicuous visual signals not coevolve with increased body size in marine sea slugs.....	107
5.1. Cover work .....	109
5.2. Manuscript.....	110
5.3. Supporting Information .....	122
<b>Chapter 6</b> Honesty of a plastic visual signal is maintained by receiver retaliation ...	127
6.1. Manuscript.....	129
6.2. Supporting Information .....	139
<b>Discussion and Future Perspectives .....</b>	<b>161</b>
<b>Acknowledgement .....</b>	<b>167</b>
<b>Curriculum Vitae .....</b>	<b>169</b>



# Introduction

"If you want beauty and wildlife, you want a coral reef. Put on a mask and stick your head under the water. The sight is mind-blowing. And that, actually, is still a mystery: why are coral reefs so beautiful and colourful? It is not immediately obvious, though the wildlife is wonderful: shell-less molluscs, crustaceans and shoals of fish that do not give a damn whether you are there or not. Your first trip to a coral reef will be one of the most transforming moments of your life."

Sir David Attenborough. 28th October 2012, The Guardian, UK

Discovering the processes that drive the emergence of new species and connecting it to biodiversity in its past, present, and future form has been one of the central questions of natural scientists for over a century [1-3]. Two ways in which we can start to unravel the mechanisms that have created such diversity is to investigate: 1) the selective pressures that can initiate/drive and 2) the molecular capacities allowing evolutionary changes to happen. Recently, advances in the field of genetics and genomics have started to dramatically improve our knowledge on how genetic diversity might promote speciation [4, 5]. Also, the growing field of 'evo-devo' is trying to shed light on how development and plasticity contribute to diversification (e.g. [3, 6-8]). Yet, despite these advances and with the exception of a few cases (e.g. [9-11]), we still have little knowledge on how molecular changes, development and the environment interrelate to create phenotypic variation, promote speciation and ultimately translate to organismal diversity.

## Main Body of Work

One way to study how environmental cues and molecular processes are linked to appearance is by investigating the emergence of similar phenotypes, whether they evolve in response to likewise selective pressures and/or in response to molecular or developmental constraints [3]. Here, mimics because they imitate unrelated species (the model), are a classical example in which to study phenotypic convergence (e.g. [12-14]).

Probably the most studied mimics are found in butterflies, in which ecological and genetic approaches have been used to investigate the processes driving signal convergence from geno- to phenotype (e.g. [15-18]). However, lately the field has started to expand and researchers are now beginning to uncover how differences in gene regulatory and developmental in addition to genetic and ecological variation, can lead to the evolution of mimicry. As before, it seems that most studies are focusing on invertebrate species (e.g. [19-22]), which raises the question on how environmental processes and molecular capacity interrelate to the emergence of mimicry in vertebrate species.

Coral reef fish are an excellent group to study vertebrate mimicry; more than sixty species of the most colourful and beautifully patterned reef fish are known to act as mimics [23]. Luckily, colouration is a favourable trait to study, as molecular modifications are easily traceable in phenotype. Also, colourful signals have been mentioned as an example of a 'magic trait' evolving under both, natural and sexual selection [24]. Hence, differences in observer visual systems (predators, competitors and potential mates) can drive the evolution of colourful signals [25-27]. Furthermore, habitat characteristics such as the background against which the signal is perceived, the prevalent light environment, as well as signalling behaviour can influence strength and directionality of signal evolution [25-27].

In teleost fishes, colourful signals are created by up to six different chromatophore cells, containing various types of pigmented molecules, located within the dermal layer of the skin [28]. Differences in interactions and position of these chromatophores are responsible for patterns and overall colouration. In addition, some fish can rapidly change colour (milliseconds – hours) via the aggregation or segregation of pigments inside chromatophores [29, 30]. Alternatively, colour change can also occur over days, weeks, or even months by altering the density, morphology and/or quality of different chromatophores [29, 31]. An example of the latter is found in the dusky dottyback, *Pseudochromis fuscus* (herein dottyback).

#### ***The dusky dottyback as a model system for research on vertebrate mimicry species***

Dottybacks are small (max. ~ 8cm total length), predatory fish with a wide distribution throughout the Indo-Pacific [32]. At least five differently coloured morphs, showing little or no other morphological variation, have been reported: brown, yellow, pink, grey, and orange [32]. Although there has been some effort to clarify the taxonomic status of these morphs, whether they are part of one polymorphic species or of a species complex, is still unclear [33]. On the Great Barrier Reef in Australia, only the yellow and brown colour morphs occur and colour differences are found independent of sex, ontogeny or season [34, 35]. However, it has been shown that yellow morphs can change to brown within two weeks [34]; whether colour change is bidirectional is unclear.

## Chapter 1

(Published in *Current Biology*, 2015)

Using a combination of behavioural, cell histological, neurophysiological and molecular approaches, the first chapter of my PhD thesis aimed to uncover the triggers for colour change in dottybacks. Yellow morphs are mainly found on live coral in association with yellow damselfish species such as the ambon- (*Pomacentrus amboinensis*) and the lemon damselfish (*P. moluccensis*), while brown morphs occur mainly on coral rubble in association with brown damselfishes such as the whitetail damselfish (*P. chrysurus*) [35] (Fig. 1).

Potential environmental cues that could be associated with colour change therefore include: i) aggressive mimicry, dottyback

morphs associate with similarly coloured damselfishes to increase foraging success by preventing detection by juvenile fish prey [23, 35]; ii) social mimicry, differently coloured morphs hide among similarly coloured damselfish to reduce detection and predation risk from their own predators (as per [36]); and iii) crypsis, different coloured morphs match the colour of their background habitat to prevent detection from predators or potential prey ([35]; as per [37]) (Fig. 1).

## Chapter 2

(Published in *The Journal of Experimental Biology*, 2016)

The second chapter aimed at investigating the triggers for ontogenetic colour changes and how these interrelate to the development of the visual system in dottybacks. Although adult dottybacks were found to be aggressive mimics that change colour to impersonate the colouration of the prevalent damselfish community, little was known about the early life stages of this fish. Using a developmental time series in combination with wild caught dottyback

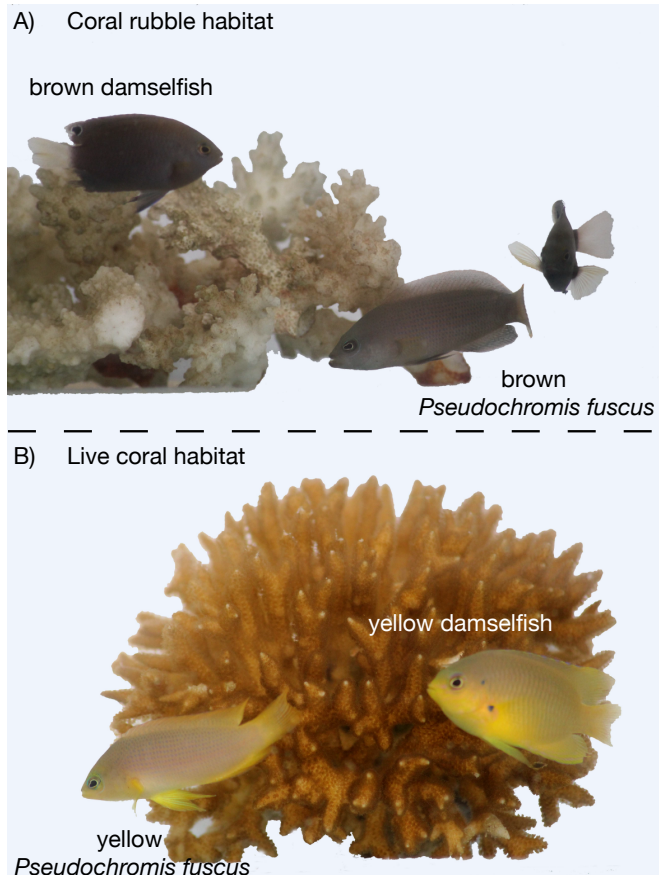


Figure 1. Morph specific habitat conditions. A) Brown dottyback morphs associate with brown damselfish on coral rubble habitat; B) yellow dottyback morphs associate with yellow damselfish on live coral.

specimens I show multiple colour changes during dottyback ontogeny and link them to crucial life history transitions of dottybacks. Moreover, changes in the visual system were found to precede OCC, and theoretical fish visual models were subsequently used to investigate the potential benefits of this pattern.

### **Chapter 3**

(Published in *PNAS*, 2015)

Work for chapter 3 was done in collaboration with Dr. Zuzana Musilová at the University of Basel and was based on the discovery of multiple novel visual genes (opsins) in the dottyback (Chapter 2), which arose through gene duplications (for classical work on the evolutionary significance of gene duplication see e.g. [38, 39]). One of these novel gene duplicates was found in the violet-blue opsin sub-family (SWS2); however, initial reconstruction of the SWS2 phylogeny suggested a much older, non- dottyback specific origin of the duplication event. Therefore, in chapter three we performed a thorough investigation of SWS2 by exploring the evolutionary history of this family in close to one 100 fish species representing most fish lineages across the modern fish phylogeny [40, 41].

### **Research Background of the PhD Candidate**

For more than six years now, my own research has evolved around the study of adaptation and the evolution of colourful signals in aquatic environments. Initially, as an assistant in the laboratory of Prof. Dr. Walter Salzburger, I helped to investigate the genetics underlying adaptive radiations in marine ice fish [42]. I then transferred to the groups of Dr. Lexa Grutter, Dr. Karen Cheney and Prof. Dr. Justin Marshall at the University of Queensland (UQ) in Australia, to accomplish my honours research (equivalent to a Swiss Masters degree) on the evolution of conspicuous signals and toxicity in marine opisthobranchs (sea slugs; see below).

My dissertation is based on the unique opportunity to combine these previous experiences, and represents collaborative work between the University of Basel and UQ. The ideas and design for the ‘Main Body of Work’ are my own and accordingly I raised most of the funding for it. My dissertation was possible due to the support from various sources including; start-up fellowships from the “Basler Foundation for Biological Research” and the “Janggen-Pöhn Foundation”; in 2012 through an “Australian Endeavour Research Fellowship”; and in 2013 - 2014 through a Swiss National Science Foundation “Doc.Mobility Fellowship”. Furthermore, I was awarded a “2013 Lizard Island Doctoral Fellowship” to specifically tackle some of the behavioural work described in Chapters 1 & 2.



## Side Projects

### Chapters 4 & 5

(Published in *The Journal of Evolutionary Biology*, 2010 & 2014)

*Evolution of aposematism in marine opisthobranchs.* In Australia, Dr. Cheney and collaborators are investigating the origins and evolution of conspicuous coloration and how this relates to levels of toxicity in marine opisthobranchs. These sea slugs have evolved an astonishing array of colourful signals, which coupled with distasteful/toxic chemicals are thought to deter predators from eating them (aposematism). However, some species within the group have chosen the opposite strategy and have either remained or returned to a cryptic state. A novel approach is currently used to study the evolution of conspicuous signals in opisthobranchs by combining behavioural experimentation, fish visual models, image analyses software and phylogenetic character state reconstructions. During the course of my PhD, I have been involved in two papers that have arisen from this work [43, 44].

### Chapter 6

(In review)

*Facial stripes signal dominance in the cichlid fish *Neolamprologus brichardi** This work is an expansion of Judith Bachman's Master thesis at the University of Basel during which she investigated the function of colour plasticity in the facial stripes of the cichlid fish, *Neolamprologus brichardi* (The Princess of Burundi). I have contributed to her work by taking spectral measurements of facial stripes and adjacent colours and combined them with theoretical fish visual models to predict the functionality of the stripes when perceived by *N. brichardi*. A manuscript describing this work is currently under review.

## References

1. Coyne J.A., Orr H.A. 2004 *Speciation*. Sunderland, Massachusetts, USA, Sinauer Associates.
2. Carroll S.B., Grenier J.K., Weatherbee S.D. 2009 *From DNA to diversity: molecular genetics and the evolution of animal design*. John Wiley & Sons.
3. Brakefield P.M. 2006 Evo-devo and constraints on selection. *Trends in Ecology & Evolution* **21**, 362-368.
4. Noor M.A.F., Feder J.L. 2006 Speciation genetics: evolving approaches. *Nature reviews Genetics* **7**, 851-861.
5. Nosil P., Schluter D. 2011 The genes underlying the process of speciation. *Trends in Ecology & Evolution* **26**, 160-167.
6. Beldade P., Brakefield P.M. 2002 The genetics and evo-devo of butterfly wing patterns. *Nature reviews Genetics* **3**, 442-452.
7. Müller G.B. 2007 Evo-devo: extending the evolutionary synthesis. *Nature Review Genetics* **8**, 943-949.
8. Moczek A.P., Sultan S., Foster S., Ledón-Rettig C., Dworkin I. et al. 2011 The role of developmental plasticity in evolutionary innovation. *Proceedings of the Royal Society B: Biological Sciences* **278**, 2705-2713.
9. Nachman M.W., Hoekstra H.E., D'Agostino S.L. 2003 The genetic basis of adaptive melanism in pocket mice. *Proceedings of the National Academy of Sciences of the United States of America (USA)* **100**, 5268-5273.
10. Manceau M., Domingues V.S., Mallarino R., Hoekstra H.E. 2011 The developmental role of Agouti in color pattern evolution. *Science* **331**, 1062-1065.
11. Santos M.E., Braasch I., Boileau N., Meyer B.S., Sauteur L. et al. 2014 The evolution of cichlid fish egg-spots is linked with a cis-regulatory change. *Nature communications* **5**.
12. Mallet J., Joron M. 1999 Evolution of diversity in warning color and mimicry: polymorphisms, shifting balance, and speciation. *Annual Review of Ecology and Systematics* **30**, 201-233.
13. Kapan D.D. 2001 Three-butterfly system provides a field test of Müllerian mimicry. *Nature* **409**, 338-340.
14. Baxter S.W., Papa R., Chamberlain N., Humphray S.J., Joron M. et al. 2008 Convergent evolution in the genetic basis of Müllerian mimicry in *Heliconius* butterflies. *Genetics* **180**, 1567-1577.
15. Brower J.v.Z. 1958 Experimental studies of mimicry in some North American butterflies: part I. the Monarch, *Danaus plexippus*, and Viceroy, *Limenitis archippus*. *Evolution* **12**, 32-47.

16. Scriber J.M., Hagen R.H., Lederhouse R.C. 1996 Genetics of mimicry in the Tiger Swallowtail butterflies, *Papilio glaucus* and *P. canadensis* (Lepidoptera: Papilionidae). *Evolution* **50**, 222-236.
17. Kapan D.D., Flanagan N.S., Tobler A., Papa R., Reed R.D. et al. 2006 Localization of Müllerian mimicry genes on a dense linkage map of *Heliconius erato*. *Genetics* **173**, 735-757.
18. Timmermans M.J.T.N., Baxter S.W., Clark R., Heckel D.G., Vogel H. et al. 2014 Comparative genomics of the mimicry switch in *Papilio dardanus*. *Proceedings of the Royal Society B: Biological Sciences* **281**, 20140465.
19. Brakefield P.M., Gates J., Keys D., Kesbeke F., Wijngaarden P.J. et al. 1996 Development, plasticity and evolution of butterfly eyespot patterns. *Nature* **384**, 236-242.
20. Counterman B.A., Araujo-Perez F., Hines H.M., Baxter S.W., Morrison C.M. et al. 2010 Genomic hotspots for adaptation: the population genetics of Müllerian mimicry in *Heliconius erato*. *PLoS Genetics* **6**, e1000796.
21. Ferguson L., Lee S.F., Chamberlain N., Nadeau N.J., Joron M. et al. 2010 Characterization of a hotspot for mimicry: assembly of a butterfly wing transcriptome to genomic sequence at the *HmYb/Sb* locus. *Molecular Ecology* **19**, 240-254.
22. Reed R.D., Papa R., Martin A., Hines H.M., Counterman B.A. et al. 2011 Optix drives the repeated convergent evolution of butterfly wing pattern mimicry. *Science* **333**, 1137-1141.
23. Moland E., Eagle J.V., Jones G.P. 2005 Ecology and evolution of mimicry in coral reef fishes. *Oceanography and Marine Biology: An Annual Review* **45**, 455-482.
24. Servedio M.R., Doorn G.S.V., Kopp M., Frame A.M., Nosil P. 2011 Magic traits in speciation: 'magic' but not rare? *Trends in Ecology & Evolution* **26**, 389-397.
25. Endler J.A. 1992 Signals, signal conditions, and the direction of evolution. *The American Naturalist* **139**, 125-153.
26. Marshall N.J., Cheney K.L. 2011 Color vision and color communication in reef fish. In *Encyclopedia of fish physiology: from genome to environment* (eds Farrell A.P.), pp. 150-158. San Diego, Academic Press.
27. Collin S.P., Marshall N.J., Atema J. 2003 *Sensory processing in aquatic environments*. Springer.
28. Fujii R. 1993 Cytophysiology of fish chromatophores. In *International Review of Cytology* (eds Kwang W. Jeon M.F., Jonathan J.), pp. 191-255. Academic Press.
29. Sugimoto M. 2002 Morphological color changes in fish: regulation of pigment cell density and morphology. *Microscopy Research and Technique* **58**, 496-503.
30. Sköld H.N., Aspögren S., Wallin M. 2013 Rapid color change in fish and amphibians - function, regulation, and emerging applications. *Pigment Cell & Melanoma Research* **26**, 29-38.

31. Leclercq E., Taylor J.F., Migaud H. 2009 Morphological skin colour changes in teleosts. *Fish and Fisheries* **11**, 159-193.
32. Gill A.C. 2004 *Revision of the Indo-Pacific dottyback fish subfamily Pseudochrominae*. Grahamstown, South Africa, Smithiana Monographs 1.
33. Messmer V., van Herwerden L., Munday P.L., Jones G.P. 2005 Phylogeography of colour polymorphism in the coral reef fish *Pseudochromis fuscus*, from Papua New Guinea and the Great Barrier Reef. *Coral Reefs* **24**, 392-402.
34. Messmer V., Jones G.P., Herwerden L., Munday P.L. 2005 Genetic and ecological characterisation of colour dimorphism in a coral reef fish. *Environmental Biology of Fishes* **74**, 175-183.
35. Munday P.L., Eyre P.J., Jones G.P. 2003 Ecological mechanisms for coexistence of colour polymorphism in a coral-reef fish: an experimental evaluation. *Oecologia* **137**, 519-526.
36. Moynihan M. 1968 Social mimicry; character convergence versus character displacement. *Evolution* **22**, 315-331.
37. Marshall N.J. 2000 Communication and camouflage with the same 'bright' colours in reef fishes. *Philosophical Transactions of the Royal Society of London. Series B: Biological Sciences* **355**, 1243-1248.
38. Ohno S. 1970 *Evolution by gene duplication*. London: George Allen & Unwin Ltd., Berlin, Heidelberg and New York: Springer-Verlag.
39. Taylor J.S., Raes J. 2004 Duplication and divergence: the evolution of new genes and old ideas. *Annual Review of Genetics* **38**, 615-643.
40. Near T.J., Eytan R.I., Dornburg A., Kuhn K.L., Moore J.A. et al. 2012 Resolution of ray-finned fish phylogeny and timing of diversification. *Proceedings of the National Academy of Sciences of the United States of America (USA)* **109**, 13698-13703.
41. Near T.J., Dornburg A., Eytan R.I., Keck B.P., Smith W.L. et al. 2013 Phylogeny and tempo of diversification in the superradiation of spiny-rayed fishes. *Proceedings of the National Academy of Sciences of the United States of America (USA)* **110**, 12738-12743.
42. Matschiner M., Hanel R., Salzburger W. 2011 On the origin and trigger of the notothenioid adaptive radiation. *PLoS ONE* **6**, e18911.
43. Cortesi F., Cheney K.L. 2010 Conspicuousness is correlated with toxicity in marine opisthobranchs. *Journal of Evolutionary Biology* **23**, 1509-1518.
44. Cheney K.L., Cortesi F., How M.J., Wilson N.G., Blomberg S.P. et al. 2014 Conspicuous visual signals do not coevolve with increased body size in marine sea slugs. *Journal of Evolutionary Biology* **27**, 676-687.

# Main Body of Work

*Pseudochromis fuscus* as a model system for research on vertebrate mimics



## Chapter 1

# Phenotypic plasticity confers multiple fitness benefits to a mimic

F. Cortesi, W. E. Feeney, M. C. O. Ferrari, P. A. Waldie,  
G. A. C. Phillips, E. C. McClure, H. N. Sköld,  
W. Salzburger, J. Marshall, K. L. Cheney

Current Biology (2015)

1.1. Manuscript p. 19 – 25

1.2. Supporting Information p. 26 – 44

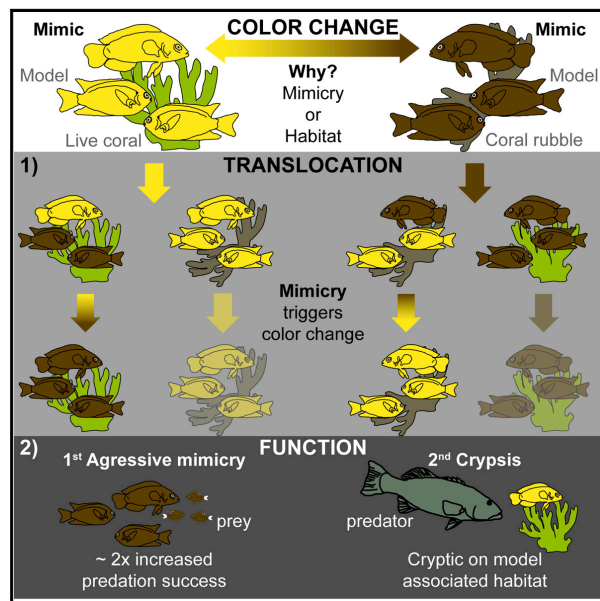




# Current Biology

## Phenotypic Plasticity Confers Multiple Fitness Benefits to a Mimic

### Graphical Abstract



### Authors

Fabio Cortesi, William E. Feeney, ..., N. Justin Marshall, Karen L. Cheney

### Correspondence

fabio.cortesi@uqconnect.edu.au

### In Brief

Cortesi et al. show that a predatory fish changes color to mimic various surrounding fishes. This prevents detection by prey, increasing predation success, and reduces detection by larger predators. Phenotypic plasticity is a novel strategy to maintain the effectiveness of deceptive signals.

### Highlights

- Fish mimics can flexibly change color to imitate multiple model species
- Flexible mimicry increases predation success by preventing detection by prey
- Changing color also increases protection by deceiving larger predatory fish
- Phenotypic plasticity thus enables the continuous use of deceptive signals



Cortesi et al., 2015, Current Biology 25, 949–954  
March 30, 2015 ©2015 Elsevier Ltd All rights reserved  
<http://dx.doi.org/10.1016/j.cub.2015.02.013>

CellPress

# Phenotypic Plasticity Confers Multiple Fitness Benefits to a Mimic

Fabio Cortesi,<sup>1,2,3,\*</sup> William E. Feeney,<sup>2,4,5</sup> Maud C.O. Ferrari,<sup>6</sup> Peter A. Waldie,<sup>2,7</sup> Genevieve A.C. Phillips,<sup>3</sup> Eva C. McClure,<sup>2</sup> Helen N. Sköld,<sup>8</sup> Walter Salzburger,<sup>1</sup> N. Justin Marshall,<sup>3</sup> and Karen L. Cheney<sup>2</sup>

<sup>1</sup>Zoological Institute, University of Basel, 4051 Basel, Switzerland

<sup>2</sup>School of Biological Sciences, University of Queensland, Brisbane, QLD 4072, Australia

<sup>3</sup>Queensland Brain Institute, University of Queensland, Brisbane, QLD 4072, Australia

<sup>4</sup>Research School of Biology, Australian National University, Canberra, ACT 0200, Australia

<sup>5</sup>Department of Zoology, University of Cambridge, Cambridge CB23EJ, UK

<sup>6</sup>Department of Biomedical Sciences, WCVN, University of Saskatchewan, Saskatoon, SK S7N 5B4, Canada

<sup>7</sup>ARC Centre of Excellence for Coral Reef Studies, James Cook University, Townsville, QLD 4811, Australia

<sup>8</sup>The Sven Lovén Centre for Marine Sciences, University of Gothenburg, 45178 Fiskebäckskil, Sweden

\*Correspondence: [fabio.cortesi@uqconnect.edu.au](mailto:fabio.cortesi@uqconnect.edu.au)

<http://dx.doi.org/10.1016/j.cub.2015.02.013>

## SUMMARY

Animal communication is often deceptive; however, such dishonesty can become ineffective if it is used too often, is used out of context, or is too easy to detect [1–3]. Mimicry is a common form of deception, and most mimics gain the greatest fitness benefits when they are rare compared to their models [3, 4]. If mimics are encountered too frequently or if their model is absent, avoidance learning of noxious models is disrupted (Batesian mimicry [3]), or receivers become more vigilant and learn to avoid perilous mimics (aggressive mimicry [4]). Mimics can moderate this selective constraint by imperfectly resembling multiple models [5], through polymorphisms [6], or by opportunistically deploying mimetic signals [1, 7]. Here we uncover a novel mechanism to escape the constraints of deceptive signaling: phenotypic plasticity allows mimics to deceive targets using multiple guises. Using a combination of behavioral, cell histological, and molecular methods, we show that a coral reef fish, the dusky dottyback (*Pseudochromis fuscus*), flexibly adapts its body coloration to mimic differently colored reef fishes and in doing so gains multiple fitness benefits. We find that by matching the color of other reef fish, dottybacks increase their success of predation upon juvenile fish prey and are therefore able to deceive their victims by resembling multiple models. Furthermore, we demonstrate that changing color also increases habitat-associated crypsis that decreases the risk of being detected by predators. Hence, when mimics and models share common selective pressures, flexible imitation of models might inherently confer secondary benefits to mimics. Our results show that phenotypic plasticity can act as a mechanism to ease constraints that are typically associated with deception.

## RESULTS AND DISCUSSION

Animals commonly use deceptive signals to increase access to food [1], reproductive opportunities [8], or protection from predation [9]. These uses of deception, however, bear a common risk: if deceptive signals are used too frequently or out of context, receivers can learn to recognize them and eventually ignore or even punish the signaler [1–3, 10]. Animals are known to “negotiate” such deceptive constraints with genetic adaptations (i.e., polymorphisms) [6] or by opportunistically switching between deceptive and nondeceptive signals [1, 7, 8]. Nonetheless, how obligate deceivers, such as many mimics, limit the costs imposed by deceptive constraints remains unclear.

In this context, we explored the function of color changes in the dusky dottyback, *Pseudochromis fuscus*, a small predatory fish (total length [TL] ~ 8 cm) common to Indo-Pacific coral reefs [11]. Dottybacks vary in coloration, with brown, yellow, pink, orange, and gray morphs being reported throughout their range [11]. On the reefs surrounding Lizard Island, Great Barrier Reef, Australia, two of these color morphs (yellow and brown) co-occur, and while yellow morphs are mostly seen on live coral together with similar-looking yellow damselfishes (*Pomacentrus* spp., such as the Ambon damselfish, *P. amboinensis*, and lemon damselfish, *P. moluccensis*) (Figure 1A), brown morphs are mostly seen on coral rubble together with similar-looking brown damselfishes (such as the whitetail damselfish, *P. chrysurus*) [12] (Figure 1B). In general, dottybacks are solitary and territorial, and although both yellow and brown damselfishes, live coral, and coral rubble habitat can be found within their territories [12], yellow morphs occupy significantly smaller home ranges compared to brown morphs (home range size,  $n = 10$  morphs each, mean  $\pm$  SEM: yellow dottyback  $5.5 \pm 1.6$  m<sup>2</sup>, brown dottyback  $11.2 \pm 1.7$  m<sup>2</sup>; independent t test,  $t_{18} = 2.86$ ,  $p = 0.01$ ). Color dimorphism is not sex linked [12], though, and yellow and brown morphs are genetically indistinguishable using either mitochondrial [13] or microsatellite markers (this study;  $n = 31$  yellow/39 brown morphs,  $F_{ST} = 0$ ,  $p = 0.68$ ; Figure S1), precluding color assortative mating as a driver for color dimorphism. Yellow dottybacks have previously



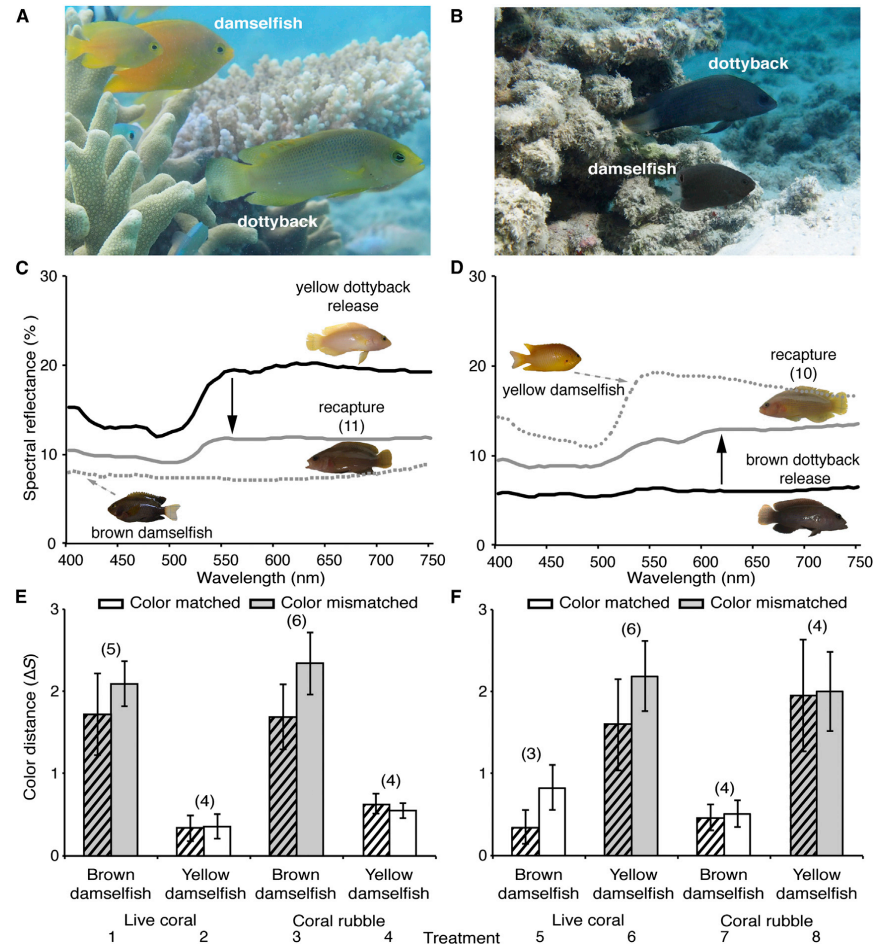


**Figure 1. Environmental Cues for Color Change in Dottybacks**

(A and B) In the field, yellow dottybacks associate with yellow damselfish on live coral (A), and brown dottybacks associate with brown damselfish on coral rubble (B). (See Figure S1 for population genetic assessment.)

(C and D) Mean spectral reflectance measurements from yellow dottybacks (C) and brown dottybacks (D) that changed color during the translocation experiment. (See Figure S3 for histological assessments of color change.)

(E and F) Color distances ( $\Delta S$ , mean  $\pm$  SEM) between body coloration before release and after recapture for yellow dottybacks (E) and brown dottybacks (F) as perceived by the potentially tetrachromatic visual systems of a dottyback predator, the coral trout (hatched bars), and a dottyback prey, the juvenile Ambon damselfish (plain bars). (See Figure S2 for  $\Delta S$  of potentially trichromatic visual systems.) Numbers in parentheses denote sample size.

Images by K.L.C. and F.C.

been shown to change their body coloration to brown within two weeks when translocated to artificial patch reefs comprising primarily dark coral rubble [13], indicating that coloration is a plastic trait. Furthermore, it has been suggested that dottybacks aggressively mimic similarly colored adult damselfishes to gain increased access to juvenile damselfishes, upon which

they prey [12]. However, the cues that drive color change and the associated fitness benefits remain unclear.

In this study, we first conducted a translocation experiment to investigate whether habitat composition or, alternatively, the color of resident adult damselfish would induce color change in dottybacks. To this end, we built experimental patch reefs

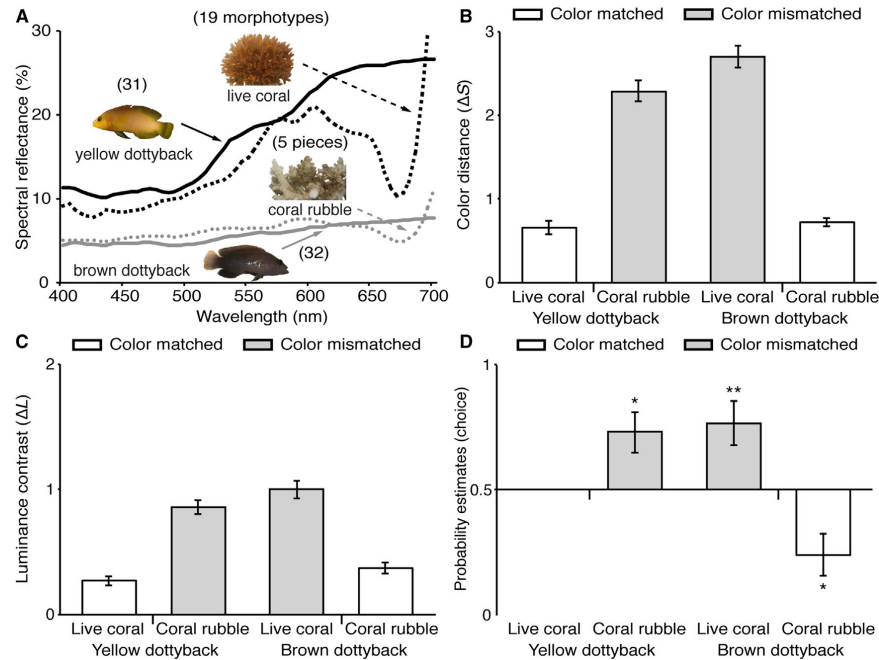


**Figure 2. Cryptic Benefits of Color Change**

(A) Mean spectral reflectance measurements used to assess the conspicuousness of dottedbacks (yellow and brown) when perceived on model-associated habitat types (live coral and coral rubble) by the predatory coral trout. Numbers in parentheses denote sample size. Images by F.C. (B and C) Color distance (B) ( $\Delta S$ , mean  $\pm$  SEM), and luminance contrast (C) ( $\Delta L$ , mean  $\pm$  SEM) between dottedback morphs and different habitat types. (D) Probability estimates (mean  $\pm$  SEM) of coral trout striking at yellow and brown dottedback morphs when placed against different habitat backgrounds (see also Movie S1). Yellow dottedback on live coral was used as the baseline treatment against which the other treatments were compared. The 0.5 line indicates equal choice between treatments and the baseline (significant difference from baseline, \* $z \leq -2.51$  or  $\geq 2.35$ ,  $p < 0.05$ ; \*\* $z \leq -2.43$ ,  $p < 0.01$ ).

comprising primarily live coral (60%–70% cover, light green to yellow background coloration; Figure 2A) or coral rubble (80%–90% cover, darker brown background coloration; Figure 2A) and stocked them with yellow (Ambon and lemon) or brown (whitetail) adult damselfish ( $n = 15$  per patch reef). We then added a single yellow or brown dottedback (individually marked with elastomer tags) and assessed whether they changed color after two weeks. Our setup was equivalent to a  $2 \times 2 \times 2$  experimental design (dottedback color  $\times$  damselfish color  $\times$  habitat type, each with two levels: yellow/brown dottedback, yellow/brown damselfish, live coral/coral rubble) (Table 1). To quantify color change, we measured the spectral reflectance of each dottedback in the laboratory prior to their release and again after recapture ( $n = 36$ ; Figures 1C and 1D; Table 1). Yellow dottedback morphs were defined as those that exhibited spectral reflectance curves with a cut-on step around 500 nm, reaching a plateau around 625 nm, whereas brown dottedback morphs were defined as those that showed a low overall reflectance with a gradual rise after 500 nm (for a framework of color categorizations, see [14]) (Figures 1C, 1D, and 2A). Next, we used the Vorobyev-Osorio theoretical vision model [15, 16] to quantify

changes in body coloration using color distance ( $\Delta S$ ).  $\Delta S$  was modeled using visual templates of a common predator of dottedbacks and damselfishes, the coral trout, *Plectropomus leopardus* [17], and a prey item of dottedbacks, juvenile Ambon damselfish [18]. Theoretical fish visual models were used to assure that color change was assessed from the point of view of the relevant signal receivers and independently of human perception. Because it is currently unknown whether these fishes use three or four distinct visual receptors to perceive color, we modeled color change from the perspective of both potentially trichromatic and tetrachromatic visual systems. We found using both models (Figures 1E, 1F, and S2) that independent of habitat type (all interactions involving habitat as a factor were nonsignificant; Table S1), dottedback morphs changed color (from yellow to brown and vice versa) in treatments where dottedbacks were released onto patch reefs with damselfishes of a coloration mismatched to their own (potentially tetrachromatic visual system, coral trout: linear model [LM], dottedback color  $\times$  damselfish color:  $F_{1,31} = 34.59$ ,  $p < 0.001$ ; Ambon damselfish: LM, dottedback color  $\times$  damselfish color:  $F_{1,31} = 60.39$ ,  $p < 0.001$ ; Figures 1E and 1F; for potentially trichromatic visual systems, see Figure S2

**Table 1. Variables Used to Examine the Cues for Color Change in Dottybacks**

Treatment	Dottyback Color at Release	Habitat	Damselfish Color (Model) n = 15/Reef	Dottyback n = Release, Recapture	Dottyback Color at Recapture
1	yellow	live coral	brown	6, 5	brown*
2	yellow	live coral	yellow	12, 4	yellow
3	yellow	coral rubble	brown	7, 6	brown*
4	yellow	coral rubble	yellow	9, 4	yellow
5	brown	live coral	brown	8, 3	brown
6	brown	live coral	yellow	9, 6	yellow*
7	brown	coral rubble	brown	5, 4	brown
8	brown	coral rubble	yellow	11, 4	yellow*

A 2 × 2 × 2 translocation experiment (dottyback color × damselfish color × habitat type, each with two levels: yellow/brown dottyback, yellow/brown damselfish, live coral/coral rubble) was used to examine whether habitat or mimicry would induce color change in dottybacks. Note that dottybacks changed color only when mismatched to the color of the damselfish, independent of habitat type (indicated by asterisk). Therefore, dottybacks change color to mimic the local damselfish community. (See also [Figures 1](#) and [S2](#).)

and [Table 1](#)). This demonstrates that dottybacks can change their body coloration to match the color of the resident damselfish community.

Subsequent histological examination of skin sections from yellow and brown dottybacks (n = 8 each) revealed that, although morphs did not change the overall number of chromatophores within their skin (number of chromatophores per 0.1 mm<sup>2</sup>: yellow dottyback 73.4 ± 4.1, brown dottyback 83.9 ± 4.0; independent t test,  $t_{14} = 1.83$ ,  $p = 0.09$ ), color change was achieved by an alteration in the relative proportion of xanthophores (yellow pigment cells) compared to melanophores (black pigment cells) (percentage of xanthophores: yellow dottyback 71.6% ± 0.7%, brown dottyback 52.1% ± 1.4%; independent t test,  $t_{14} = -11.09$ ,  $p < 0.001$ ; [Figure S3](#)). This change in the relative proportion of chromatophore types appears to be different from other reported cases of color change in fishes, which usually occur as a result of changes in the number of a single chromatophore type (mostly melanophores; “slow” morphological changes) [19] or dispersion and aggregation of pigments inside chromatophores (“fast” physiological changes) [20].

As a second step, we investigated whether dottybacks gain a fitness benefit in terms of increased capture success of juvenile damselfish prey when matching the color of adult damselfish. To examine this, we conducted laboratory predation experiments, in which dottybacks (n = 10 of each color morph per treatment) were placed in a tank with five adult damselfish (TL 45–57 mm, either color matched or mismatched) and ten juvenile brown damselfish (TL < 14.5 mm) for 24 hr. We found that dottybacks were significantly more successful at capturing juvenile damselfish when their color matched that of adult damselfish (generalized linear mixed model [GLMM; binomial], color of dottyback × color of damselfish:  $\chi^2_1 = 57.92$ ,  $p < 0.001$ ; [Figure 3](#)), suggesting that by flexibly matching the coloration of adult damselfishes, dottybacks facilitate predation by increased deception of juvenile damselfish prey. This is probably due to the prey exhibiting reduced anti-predator vigilance when unable to detect differences between harmless models (adult damselfishes) and predatory mimics (dottybacks).

In the field, dottyback predation rates are very high (up to ~30 prey fish per day [21]), forcing juvenile fish to learn quickly about

the risk that dottybacks impose (either through direct experience or socially) in order to survive [22]. Therefore, similar to the benefits gained from polymorphic adaptations [6] or the deployment of facultative mimetic signals [1, 7], the flexible imitation of multiple models might enable dottybacks to continuously dupe signal receivers by limiting learning in juvenile fish prey. Alternatively, phenotypic plasticity may also enable dottybacks to expand their niche by moving to novel locations devoid of experienced receivers, which may occur both within home ranges and by relocating across reef habitats.

Interestingly, although there was no difference in predatory success when dottyback morphs were matching the color of adult damselfish (prey survival, matched colors: yellow dottyback 5.0 ± 0.7, brown dottyback 3.4 ± 0.9; pairwise post hoc Tukey contrast,  $p > 0.05$ ), brown dottybacks were significantly more successful at capturing prey compared to yellow dottybacks when mismatched in color to the damselfish (prey survival, mismatched colors: yellow dottyback 9.2 ± 0.3, brown dottyback 6.2 ± 1.1; pairwise post hoc Tukey contrast,  $p < 0.05$ ; [Figure 3](#)). However, we found no difference in the number of strikes against prey between yellow or brown dottybacks (number of strikes within the first 60 min: yellow dottyback 9.2 ± 3.3, brown dottyback 8.9 ± 3.0;  $W = 178$ ,  $p = 0.56$ ). Hence, when mismatched to the color of the adult damselfish, the probability of capturing a prey item per strike was lower in yellow dottybacks, which may be due to an innate higher level of vigilance in juvenile fish prey toward dottybacks of a different color to their own (and the use of only juvenile brown prey during our experiment).

To investigate this, we conducted an additional experiment without adult damselfish, and we found that when given the choice between a juvenile brown or yellow prey, dottybacks more frequently directed their first strike at prey fish that matched their own body coloration (GLMM; binomial:  $\chi^2_1 = 17.97$ ,  $p < 0.001$ ). Dottybacks could exhibit a preference for prey that match their own coloration, but in this scenario, we would expect that yellow dottybacks would strike less frequently at brown prey, which was not observed in the experiment above. Instead, our results suggest that predator avoidance behavior in juvenile prey fish is enhanced when dottybacks are of a different coloration from their own and that, by changing color to imitate

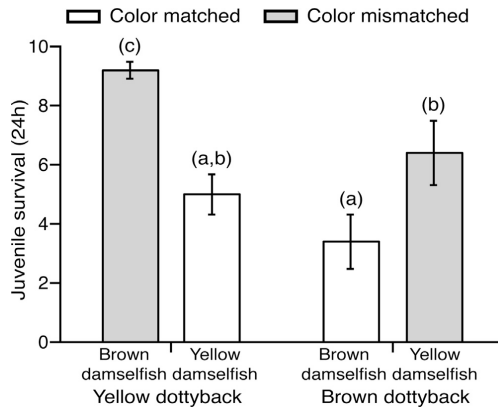


**Figure 3. Aggressive Mimicry Benefits of Color Change**

Juvenile damselfish prey survival (mean  $\pm$  SEM, out of 10) after 24 hr when exposed to dottybacks that were matched or mismatched in color to adult damselfish coloration ( $n = 10$  per treatment). Letters above bars denote significant differences between treatments (pairwise post hoc Tukey contrast,  $p < 0.05$ ).

the local damselfish community, dottybacks are able to overcome this innate vigilance. This is comparable to a “wolf in a sheep’s clothing” scenario where distinguishing the predator from harmless heterospecifics becomes increasingly difficult when the predator and the heterospecific look alike, regardless of whether or not the model species matches the appearance of the prey.

Finally, although changes in dottyback coloration were not driven by habitat variables (see the translocation experiment in Figures 1E and 1F), damselfish models match the color of the different habitat types they are naturally found upon (i.e., yellow damselfish on live coral; brown damselfish on coral rubble [23]), which is likely to reduce predation pressure due to cryptic benefits [23]. To investigate whether dottybacks experience similar benefits when matching the color of their habitat, we used the coral trout theoretical vision model to assess dottyback conspicuousness against the different habitat types (Figure 2A). We found that, similar to the damselfish they imitate, dottyback morphs also match the habitat they are commonly found upon, in terms of both color distance ( $\Delta S$ , linear mixed model [LMM], dottyback color  $\times$  habitat type:  $\chi^2_1 = 171.41$ ,  $p < 0.001$ ; Figure 2B) and luminance contrast ( $\Delta L$ , LMM, dottyback color  $\times$  habitat type:  $\chi^2_1 = 90.05$ ,  $p < 0.001$ ; Figure 2C). Next, to test the predictions of the visual model, we conducted a predator choice experiment in the laboratory. Coral trout ( $n = 5$ ) were trained to strike at laminated images of yellow or brown dottybacks placed against an image of live coral or coral rubble background to receive a food reward. Images were adjusted in Adobe Photoshop CS4 v11.0.2 to ensure that their spectral reflectance matched the predicted coral trout visual receptor response (in  $\Delta S$  and  $\Delta L$ ) from the visual model. In each trial, coral trout were given the choice between two randomly allocated backgrounds with either a yellow or brown dottyback image placed

in front of them. A third background without a dottyback image in front of it was used as a distractor to ensure that trout would not strike haphazardly at backgrounds to elicit the food reward (Movie S1). Coral trout struck significantly more often at dottybacks that were color mismatched with the background (110 trials;  $22 \pm 4.1$  trials per trout; Bradley-Terry model for paired choices, GLMM, yellow dottyback on coral rubble:  $z = 2.35$ ,  $p < 0.05$ ; brown dottyback on live coral:  $z = 2.43$ ,  $p < 0.01$ ) compared to dottybacks that were color matched with the background (Figure 2D). Therefore, while dottybacks change color to aggressively mimic damselfish models, they may also gain a secondary benefit of reduced predation risk when matching the color of model-associated habitat types. Moreover, although not specifically tested in our study, predation risk to dottybacks may be further reduced through dilution when they are associated with a school of similarly colored damselfish models (social mimicry [24]).

Our findings demonstrate that phenotypic plasticity facilitates aggressive mimicry of multiple models in our study system. Dottybacks can change their body coloration depending on the availability of suitable models to gain fitness benefits in terms of increasing access to food. Furthermore, our results highlight that phenotypic plasticity may inherently confer secondary benefits to mimics when mimics and models share ecological pressures: dottybacks benefit from reduced predation risk when living on model-associated habitat. Therefore, phenotypic plasticity may offer a solution to reduce the constraints of deceptive signaling, and dottybacks provide a good example of this adaptive ingenuity.

#### SUPPLEMENTAL INFORMATION

Supplemental Information includes three figures, one table, Supplemental Experimental Procedures, and one movie and can be found with this article online at <http://dx.doi.org/10.1016/j.cub.2015.02.013>.

#### AUTHOR CONTRIBUTIONS

F.C. conceived the study and designed the experiments together with K.L.C., N.J.M., W.S., and M.C.O.F. F.C., W.E.F., P.A.W., G.A.C.P., E.C.M., and M.C.O.F. performed the experiments. F.C., W.E.F., G.A.C.P., H.N.S., and K.L.C. analyzed the data. F.C., W.E.F., and K.L.C. wrote the initial manuscript. All authors reviewed and approved the final version of the manuscript.

#### ACKNOWLEDGMENTS

All experiments were approved by the Animal Ethics Committee of the University of Queensland (AEC approval numbers SBS/196/13/LIDF, SBS/427/10/ARC, and QBI/192/13/ARC). Fish collection and behavioral experiments were further approved by the Great Barrier Reef Marine Park Authority (permit numbers G11/34104.01, G09/30113.1, and G12/35005.1) and the Queensland Government Department of Employment, Economic Development and Innovation (General Fisheries permit numbers 146505, 161624, and 140763). We thank Hans-Jochen Wagner and Yuri Kläeffer for technical support, Marshall and Cheney group members for help in the field, the staff at the Lizard Island Research Station for logistical help, and four anonymous referees for insightful comments. F.C. was supported by the Janggen-Pöhn-Stiftung, the Basler Stiftung für Biologische Forschung, an Australian Endeavour Research Fellowship (2012), a Swiss National Science Foundation (SNSF) Doc.Mobility Fellowship (P1BSP3\_148460), and a Doctoral Fellowship (2013) from the Lizard Island Research Station, a facility of the Australian Museum. J.M. was supported by the Australian Research Council (ARC). W.E.F. was supported by the Australian National University. W.S. was supported by the SNSF and the



European Research Council (ERC; CoG "CICHLID-X"). K.L.C. was supported by the ARC and the University of Queensland.

Received: October 21, 2014

Revised: January 7, 2015

Accepted: February 2, 2015

Published: March 19, 2015

## REFERENCES

1. Flower, T.P., Gribble, M., and Ridley, A.R. (2014). Deception by flexible alarm mimicry in an African bird. *Science* 344, 513–516.
2. Laidre, M.E., and Johnstone, R.A. (2013). Animal signals. *Curr. Biol.* 23, R829–R833.
3. Pfennig, D.W., Harcombe, W.R., and Pfennig, K.S. (2001). Frequency-dependent Batesian mimicry. *Nature* 410, 323.
4. Cheney, K.L., and Côté, I.M. (2005). Frequency-dependent success of aggressive mimics in a cleaning symbiosis. *Proc. Biol. Sci.* 272, 2635–2639.
5. Penney, H.D., Hassall, C., Skevington, J.H., Abbott, K.R., and Sherratt, T.N.A. (2012). A comparative analysis of the evolution of imperfect mimicry. *Nature* 483, 461–464.
6. Thorogood, R., and Davies, N.B. (2012). Cuckoos combat socially transmitted defenses of reed warbler hosts with a plumage polymorphism. *Science* 337, 578–580.
7. Côté, I.M., and Cheney, K.L. (2005). Animal mimicry: choosing when to be a cleaner-fish mimic. *Nature* 433, 211–212.
8. le Roux, A., Snyder-Mackler, N., Roberts, E.K., Beehner, J.C., and Bergman, T.J. (2013). Evidence for tactical concealment in a wild primate. *Nat. Commun.* 4, 1462.
9. Wickler, W. (1965). Mimicry and the evolution of animal communication. *Nature* 208, 519–521.
10. Hauser, M.D. (1992). Costs of deception: cheaters are punished in rhesus monkeys (*Macaca mulatta*). *Proc. Natl. Acad. Sci. USA* 89, 12137–12139.
11. Gill, A.C. (2003). Revision of the Indo-Pacific Dottyback Fish Subfamily Pseudochrominae (Perciformes: Pseudochromidae) (Smithiana Monographs 1) (The South African Institute for Aquatic Biodiversity), pp. 1–214.
12. Munday, P.L., Eyre, P.J., and Jones, G.P. (2003). Ecological mechanisms for coexistence of colour polymorphism in a coral-reef fish: an experimental evaluation. *Oecologia* 137, 519–526.
13. Messmer, V., Jones, G.P., Herwerden, L., and Munday, P.L. (2005). Genetic and ecological characterisation of colour dimorphism in a coral reef fish. *Environ. Biol. Fish.* 74, 175–183.
14. Marshall, N.J. (2000). The visual ecology of reef fish colors. In *Animal Signals: Signalling and Signal Design in Animal Communication*, Y. Espmark, T. Amundsen, and G. Rosenqvist, eds. (Akademika Publishing), pp. 83–120.
15. Vorobyev, M., and Osorio, D. (1998). Receptor noise as a determinant of colour thresholds. *Proc. Biol. Sci.* 265, 351–358.
16. Vorobyev, M., Brandt, R., Peitsch, D., Laughlin, S.B., and Menzel, R. (2001). Colour thresholds and receptor noise: behaviour and physiology compared. *Vision Res.* 41, 639–653.
17. St. John, J. (1999). Ontogenetic changes in the diet of the coral reef grouper *Plectropomus leopardus* (Serranidae): patterns in taxa, size and habitat of prey. *Mar. Ecol. Prog. Ser.* 180, 233–246.
18. McCormick, M.I., and Meekan, M.G. (2007). Social facilitation of selective mortality. *Ecology* 88, 1562–1570.
19. Leclercq, E., Taylor, J.F., and Migaud, H. (2009). Morphological skin colour changes in teleosts. *Fish Fish.* 11, 159–193.
20. Nilsson Sköld, H., Aspögren, S., and Wallin, M. (2013). Rapid color change in fish and amphibians - function, regulation, and emerging applications. *Pigment Cell Melanoma Res.* 26, 29–38.
21. Feeney, W.E., Lönnstedt, O., Bosiger, Y., Martin, J., Jones, G., Rowe, R., and McCormick, M.I. (2012). High rate of prey consumption in a small predatory fish on coral reefs. *Coral Reefs* 31, 909–918.
22. Crane, A.L., and Ferrari, M.C.O. (2013). Social learning of predation risk: a review and prospectus. In *Social Learning Theory: Phylogenetic Considerations across Animal, Plant, and Microbial Taxa*, K.B. Clark, ed. (Nova Science Publishers), pp. 53–82.
23. Marshall, N.J. (2000). Communication and camouflage with the same 'bright' colours in reef fishes. *Philos. Trans. R. Soc. Lond. B Biol. Sci.* 355, 1243–1248.
24. Moynihan, M. (1968). Social mimicry: character convergence versus character displacement. *Evolution* 22, 315–331.

Current Biology

Supplemental Information

## **Phenotypic Plasticity Confers**

## **Multiple Fitness Benefits to a Mimic**

Fabio Cortesi, William E. Feeney, Maud C.O. Ferrari, Peter A. Waldie,  
Genevieve A.C. Phillips, Eva C. McClure, Helen N. Sköld, Walter Salzburger,  
N. Justin Marshall, and Karen L. Cheney



## Supplemental Figures and Tables:

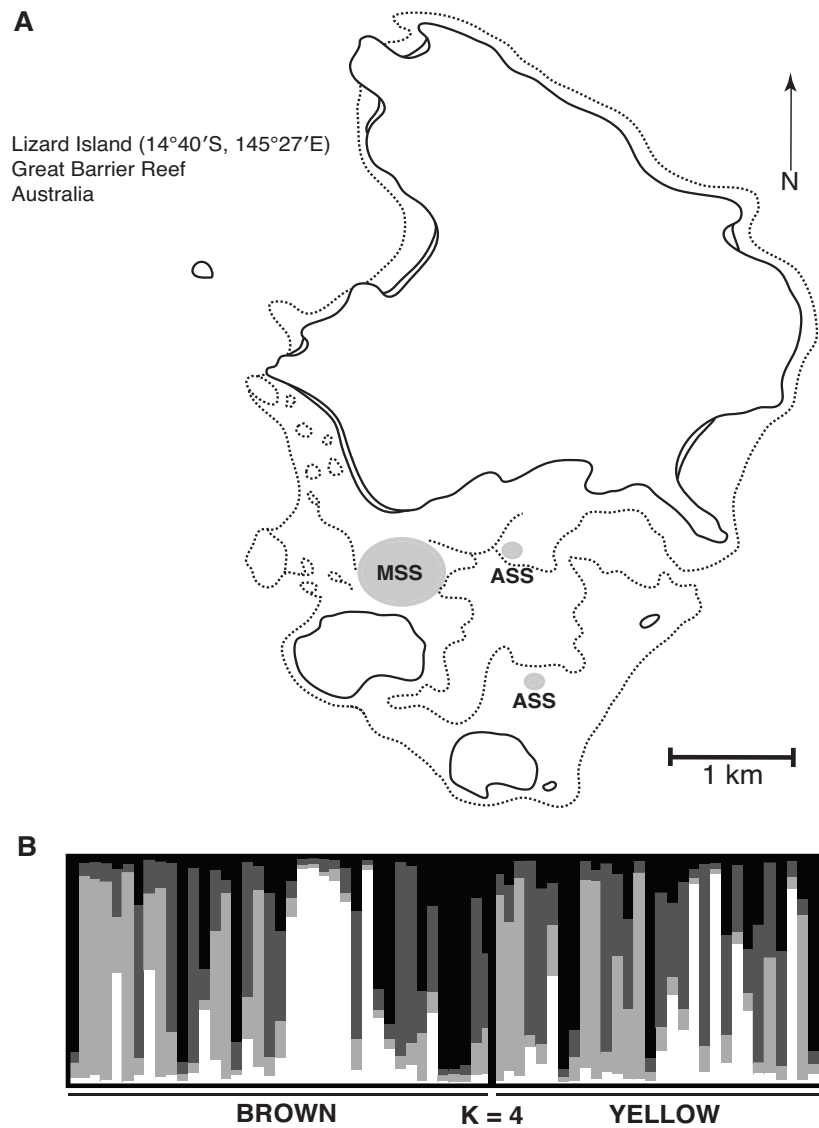


### Figure S1. Population Genetic Analysis

(A) Collection sites for dottyback individuals: main sampling site (MSS; 62 individuals), additional sampling sites (ASS; 8 individuals). (B) Structure plot for  $K = 4$ , brown ( $n = 39$ ) and yellow ( $n = 31$ ) dottyback morphs genotyped at eight microsatellite loci. Between color morphs pairwise  $F_{ST} = 0$ ,  $P = 0.7$ . Refer to Figure 1A, B for field photographs of dottyback morphs.

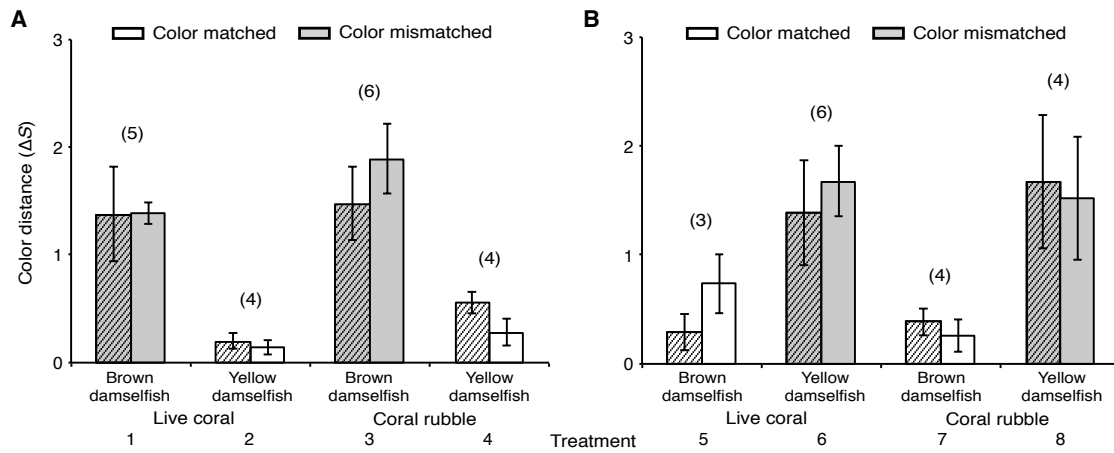


### Figure S2. Dottyback Color Change

Color distances ( $\Delta S$ , mean  $\pm$  SEM) between body coloration before release and after recapture for: (A) yellow dottybacks, and (B) brown dottybacks as perceived by the potentially trichromatic visual systems of a dottyback predator, the coral trout (patterned bars), and a dottyback prey, the juvenile ambon damselfish (clear bars). Numbers in parentheses denote sample size. Note that, independent of the habitat type dottybacks were released onto (all interactions comprising habitat as a factor were non-significant; Table S1), dottybacks changed color when released onto patch reefs with damselfishes of a mismatched coloration to their own [coral trout: linear model (LM), dottyback color  $\times$  damselfish color:  $F_{1,31} = 36.75$ ,  $P < 0.001$ ; ambon damselfish: LM, dottyback color  $\times$  damselfish color:  $F_{1,31} = 49.19$ ,  $P < 0.001$ ; Table 1].  $\Delta S$  of potentially tetrachromatic visual systems are shown in Figure 1E, F.

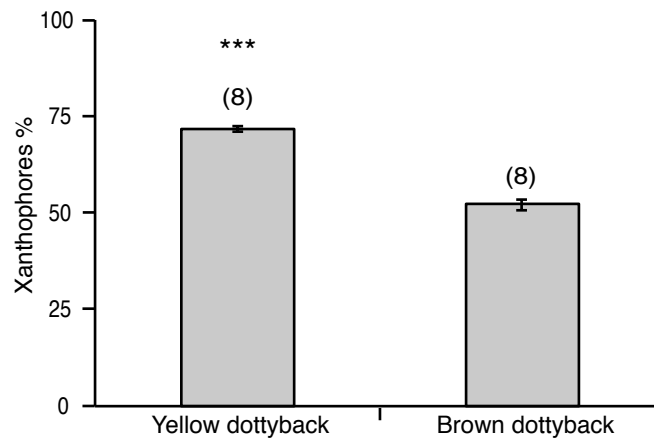


**Figure S3. Histological Assessment of Color Change**

The mean ( $\pm$  SEM) proportion of xanthophores (yellow pigment cells) found in the skin of yellow and brown dottyback morphs (\*\*\*) indicates  $P < 0.001$ ). Numbers in parentheses denote sample size. Refer to Figure 1E,D and Figure S2 for visual assessments of color change.

**Table S1.** Analyses of color change from the translocation experiment, showing interactions comprising habitat type as a factor (all non significant). The setup was equivalent to a 2 x 2 x 2 experimental design (dottyback color x damselfish color x habitat type, each with 2 levels: yellow/brown dottyback, yellow/brown damselfish, live coral/coral rubble). All analyses were conducted using linear models (LM's). Also see Figure 1, Figure S2, and Table 1.

Interaction	Visual system	Visual receiver	F	P
dottyback color <i>X</i> damselfish color <i>X</i> habitat type	Tetra	CT	$F_{1,28} = 1.00$	<b>0.33</b>
		AD	$F_{1,28} = 0.00$	<b>0.95</b>
	Tri	CT	$F_{1,28} = 1.64$	<b>0.21</b>
		AD	$F_{1,28} = 0.52$	<b>0.48</b>
dottyback color <i>X</i> habitat type	Tetra	CT	$F_{1,29} = 0.03$	<b>0.86</b>
		AD	$F_{1,29} = 1.83$	<b>0.19</b>
	Tri	CT	$F_{1,29} = 0.39$	<b>0.54</b>
		AD	$F_{1,29} = 3.97$	<b>0.06</b>
damselfish color <i>X</i> habitat type	Tetra	CT	$F_{1,29} = 0.80$	<b>0.38</b>
		AD	$F_{1,29} = 0.44$	<b>0.51</b>
	Tri	CT	$F_{1,29} = 1.02$	<b>0.32</b>
		AD	$F_{1,29} = 0.36$	<b>0.56</b>

**Tetra** Tetrachromatic (four distinct visual receptors)

**Tri** Trichromatic (three distinct visual receptors)

**CT** Coral trout

**AD** Ambon damselfish

## **Supplemental Experimental Procedures**

### **Study Site and Species**

The study was conducted at Lizard Island (14°40'S, 145°27'E), Great Barrier Reef, Australia, between December 2009 and November 2013. Dottybacks and adult damselfishes were collected on snorkel from shallow reefs (depth 2 – 5 m) surrounding the island using an anesthetic clove oil solution (10% clove oil; 40% ethanol; 50% seawater), hand nets and small barrier nets. All dottybacks used in the study were adults, ranging in size from 35 – 86 mm (total length, TL: mean  $\pm$  SEM = 68.05  $\pm$  0.78 mm).

Statistical analyses were conducted in R v.3.0.2 [S1] using the package lme4 v.1.1-7 [S2]. Assumptions of normality and homogeneity of variance were graphically assessed using histograms, residuals plots and quantile-quantile plots. For linear mixed-effect models (LMM's) and generalized linear mixed-effect models (GLMM's) we compared the adequacy of models with random intercepts-only to models with random slopes and intercepts using likelihood ratio tests (LRT), and the final models were fit by maximum likelihood (using a Laplace approximation for GLMM's). However, we found no significant difference between approaches and all random effect models were consequently fit with random intercepts-only.

### **Assessment of Home Range Size**

To assess differences between the home ranges of yellow and brown dottyback morphs, we haphazardly located twenty dottyback individuals (10 yellow and 10 brown) on SCUBA and observed them for approximately 60 min (mean  $\pm$  SEM = 61.65  $\pm$  1.06 min, total 1233 min) between 0800-1700 in December 2009, from a minimum distance of 2 metres. Dottybacks have previously been found to show no diurnal patterns in activity [S3] and this observational time period has been shown to be adequate for dottybacks to patrol the full extent of their home ranges (W.E. Feeney, unpublished data). To assess the home range of each individual, a single observer took notes of visual references of the extents of the used habitat by each fish. Following the observation a transect tape was used to measure the boundaries of the habitat range of each individual, and each habitat range was sub-sectioned for calculation of the area use (home range) of each individual (similar to [S4]). For statistical analysis, we transformed home range size to the natural logarithm to conform to normality.

## Population Genetic Assessment using Microsatellites

A total of 70 (31 yellow and 39 brown) dottybacks were collected in April and May 2011 from three locations in the lagoon (Figure S1). A piece of muscle tissue from behind the pectoral fin and a fin clip from each individual were preserved in 95% ethanol until total DNA was extracted using a standard salt precipitation protocol [S5]. In a previous study, genetic differentiation between morphs (9 yellow and 9 brown) was absent when using mtDNA as a marker [S6]; therefore, to investigate color differences in this study, we used microsatellite markers that allow for a finer-scale approach.

Initially, we tested 56 microsatellite markers, which were previously isolated and characterized from various cichlid species, whereby eight could successfully be amplified using multiplex PCRs: HchiST06, HchiST38, HchiST46, HchiST68, HchiST94 [S7], Pzeb3 [S8], Abur 45 [S9] and UME003 [S10]. Amplification was performed using Qiagen-Multiplex PCR kit and thermal cycler profiles for microsatellites as recommended by the manufacturer (Qiagen Inc., Valencia, CA). Samples were successfully amplified at all loci for 52 individuals, at seven out of eight loci for 16 individuals, and at six loci for the remaining two individuals. The average missing data over all loci was 3.6%.

Genotyping was performed on an AB3130xl sequencer and microsatellites were scored using GENEMAPPER v.4.0 (ABI) and edited by eye. TANDEM v.1.09 [S11] was used to automatically bin allele sizes. We then used STRUCTURE v.2.3.4 [S12] to assess population structuring between yellow and brown morphs. In STRUCTURE, individuals are not *a priori* assigned to a population but instead the program infers the number of clusters based on an *ad hoc* approximation of unknown performance [S12]. An admixture model with correlated gene allele frequencies [S13] was chosen with each run producing  $5 * 10^5$  burn in steps followed by  $10^6$  MCMC steps. The number of presumed clusters ( $K$ ) was set to be 1 – 10 with 10 independent runs for each value of  $K$ . Estimates of the posterior probability of the data  $\Pr(X|K)$  [S12] was analyzed using STRUCTURE-HARVESTER v.0.6.93 [S15] and estimated  $\Delta K$  [S15] was used as criteria to infer the number of genetic clusters present in the data set.

Pairwise  $F_{ST}$  was used to quantify the genetic differentiation between: 1) all yellow and brown morphs, and 2) yellow and brown morphs within clusters, as identified with STRUCTURE analysis.  $F_{ST}$  was calculated using ARLEQUIN v.3.11

[S16] with 1000 permutations and 5% missing data. Bonferroni corrections [S17] were used to adjust P-values in all tests.

Using clustering analysis and pairwise  $F_{ST}$  as a measurement of population differentiation, we could not separate between yellow and brown morphs based on microsatellite data (main text, Figure S1). However, STRUCTURE estimated the most probable number of clusters in the data set to be  $K = 4$  ( $\Delta K = 20.5$ , all other  $\Delta K$ 's between 0.04 – 9.2), with a mixture of brown and yellow fish present in each of these four clusters (individuals/cluster,  $n = 15 - 21$ ). When comparing between color morphs within clusters we did not find any evidence for color specific population differentiation ( $F_{ST}$  between - 0.018 – 0.045,  $P = 0.75 - 0.06$ ).

### Translocation Experiment

Patch reefs were initially created in April – May 2011 ( $n = 30$ ) by SCUBA divers on sandy flats in the lagoon of Lizard Island (2 – 5 m depth). A subset of reefs were then re-built in January – February 2012 ( $n = 15$ ), June – July 2013 ( $n = 15$ ) and October – November 2013 ( $n = 7$ ) to ensure enough replicates for each treatment were obtained. Reefs were constructed using loose live coral or coral rubble from nearby natural continuous reefs, and were built approximately 1 m in diameter and 50 cm in height. Once a site for a new patch reef was located, it was pseudo-randomly constructed of either a high percentage of live coral (60 – 70%;  $n = 35$ ) or a high percentage of coral rubble (80 – 90%;  $n = 32$ ). Reefs were located at a minimum distance of 20 m from the continuous reef and at least 15 m apart to reduce the movement of fishes between patches (similar to [S6]). Fishes present on the patch reefs prior to the experiment were carefully removed using hand nets and an anesthetic clove oil solution. Fifteen yellow damselfish (ambon damselfish, *Pomacentrus amboinensis* and yellow damselfish, *P. moluccensis*) and 15 brown damselfish (whitetail damselfish, *P. chrysurus*) of all size classes were then placed on patch reefs according to treatment, and their numbers were re-adjusted after 24 hours if there had been any movement between patches. Damselfish were left on the reefs for two days before one dottyback morph was added. This experimental setup was equivalent to a 2 x 2 x 2 design (dottyback color x damselfish color x habitat type, each with 2 levels: yellow/brown dottyback, yellow/brown damselfish, live coral/coral rubble) (Table 1).

To recognize individual dottybacks upon recapture, individuals were uniquely marked on their caudal peduncle using an injection of fluorescent elastomer (green,

orange and/or pink; Northwest Marine Technology, Inc., Shaw Island, USA). This marking procedure has been shown not to impact the behavior of coral reef fishes [S18]. After tagging, dottybacks were kept in holding tanks overnight before they were released onto experimental patch reefs, after which they were located and observed every other day. Additional fishes (dottybacks and any other fish species) that appeared on the patch reefs during the experiment were removed. New fish settlement occurred infrequently (1 – 3 fish per week) and was made up of mostly small recruiting individuals, which appeared more often through the summer months (October – February) during larval recruitment pulses. Dottybacks were left on the experimental patch reefs for two weeks before being recaptured and color change was assessed (see below). In total, we successfully recaptured and identified 36 dottybacks (initially yellow,  $n = 19$ ; initially brown = 17) out of the 67 dottybacks that were released. The remaining individuals were presumably lost through relocation to other reefs or due to predation.

### **Measurement of Body Coloration and Habitat Reflectance**

Spectral reflectance measurements of dottybacks (yellow,  $n = 38$ ; brown,  $n = 41$ ) and of an additional eight yellow colored damselfish (five ambon damselfish, three lemon damselfish) and eight brown colored damselfish (whitetail damselfish) were obtained using an Ocean Optics (Dunedin, FL, USA) USB2000 spectrophotometer connected to a laptop computer running Ocean Optics OOIBASE32 software (Figure 1C, D and Figure 2A). Fishes were measured in the laboratory by removing them from the water and placing them on a wet towel to facilitate handling. Spectral reflectance curves measured in this way do not significantly differ from those measured in water [S19]. Colors were measured with a 200 $\mu$ m bifurcated optic UV/visible fiber connected to a PX-2 pulse xenon light source (Ocean Optics). The bare end of the fiber was held at a 45° angle to prevent specular reflectance. A Spectralon 99% white reflectance standard was used to calibrate the percentage of light reflected at each wavelength from 400 – 750 nm (dottybacks did not reflect any light below 400 nm). The spectral reflectance of dottybacks from the translocation experiment (yellow,  $n = 19$ ; brown,  $n = 17$ ) was measured twice, once before releasing them onto the experimental patch reefs and then again when recaptured two weeks later.



Overall body coloration of fishes was quantified by taking measurements from different locations on the body (behind pectoral fin, ventral, center of the body, towards caudal peduncle, and dorsal). At least ten measurements per individual were taken from each location. Because no substantial difference in the shape of spectral curves was found between different areas of the body, measurements were subsequently averaged.

We also measured the spectral reflectance of the different habitats each color morph was found upon. To do so, pieces of different coral morphotypes and of coral rubble collected from the experimental patch reefs were measured in the laboratory. Coral morphotypes ( $n = 19$ ) and coral rubble pieces ( $n = 5$ ) were measured inside a shallow tray containing enough water to cover pieces completely and measurements were taken as previously described. Because rubble and some coral species were heterogeneously colored, color reflectance of each distinct color patch  $> 4 \text{ mm}^2$  was measured and an average of the color reflectance curves was used (Figure 2A).

### Visual Modeling of Color Change

To quantify color changes that occurred in dottybacks during the translocation experiment, we used a theoretical fish vision model [S20, 21] that calculates color distance ( $\Delta S$ ) within the visual ‘space’ of the fish, where  $\Delta S = 1$  is an approximate threshold of discrimination,  $\Delta S < 1$  indicates colors are chromatically indistinguishable, and  $\Delta S > 1$  indicates colors are discriminable from one another. Signal luminosity is disregarded, while color differences are calculated as chromatic distances encoded by an opponency mechanism based on the spectral sensitivities of the receiver (see e.g. [S22, 23]).

We used the visual sensitivities from a predator of dottybacks and damselfish: the coral trout *Plectropomus leopardus* [S24], which has peak spectral sensitivities ( $\lambda_{\text{max}}$ ) for single cones at 455 nm and 507 nm, and for twin cones (paired cones with a similar morphology) at 507 nm and 531 nm (N.J. Marshall, unpublished data). We also modeled the color changes from the perspective of a dottyback prey species: the juvenile ambon damselfish [S25], with  $\lambda_{\text{max}}$  for single cones at 370 nm and 501 nm, and for double cones (paired cones with a different morphology) at 480 nm and 523 nm [S26]. To generate visual templates of these fish, we furthermore incorporated the 50% light transmission cut-off from their whole eyes: coral trout,  $T_{50} = 414 \text{ nm}$  [S27] and juvenile ambon damselfish,  $T_{50} = 327 \text{ nm}$  [S28]. Cone receptor ratios were based

on previously conducted morphological assessments of retinas and set to be 1:1:2:2 for coral trout (N.J. Marshall, unpublished data), and 1:2:4:4 for ambon damselfish [S26]. In accordance with previous studies [S22, 23], and in the absence of any behavioral data, we set the Weber's fraction ( $\omega$ ) for the LWS noise threshold to be at 0.05; a conservative estimate at approximately half the sensitivity of the human LWS cone [S29]. A measurement of illumination taken at the experimental site at 5 m depth was used [S23], which represents the maximum depth of patch reefs during the translocation experiment. Color change in dottybacks was then calculated as the difference ( $\Delta S$ ) between the dottyback body coloration at the beginning of the experiment and after being recaptured two weeks later (Figure 1E, F and Figure S2).

Although members of twin/double cones have previously been shown to contribute individually to color vision in some coral reef fishes [S30], whether this is also the case for either the coral trout or the ambon damselfish is currently unknown. Therefore, to assess color change in dottybacks we modeled two scenarios for each visual receiver; one in which twin/double cones would work independently from one another, resulting in four distinct cone receptors (tetrachromacy), and one in which they would be optically coupled by combining the output of the twin/double cones, resulting in three distinct cone receptors (trichromacy). However, we found no difference in our conclusion when modeling either scenario (Figure 1 E, F and Figure S2).

To examine whether damselfish coloration or background habitat triggered color change in dottybacks, we used linear models (LM's) with  $\Delta S$  transformed to the natural logarithm for the coral trout, and  $\Delta S$  square root transformed for the ambon damselfish as the response variable. Dottyback morph (yellow, brown), damselfish coloration (yellow, brown), and habitat type (live coral, coral rubble) were set as fixed factors. To determine the best model in all analyses, we compared the full model with models in which one of the explanatory terms was dropped using the "drop1" function [S31]. If the analysis of variance found that a dropped term had no significant effect on the model then the term was permanently dropped (based on AIC value comparisons).

### **Histological Assessment of Color Change**

To investigate the cellular mechanisms underlying color change, we took skin biopsies (approximately 1 cm<sup>2</sup>) from a random set of adult dottybacks located and caught between February – May 2012 and October – November 2013. Morphs were classified according to the shape of their spectral reflectance curve as brown or yellow (see main text). Biopsies were taken from behind the pectoral fin of yellow and brown morphs (n = 8 per morph) and kept in a phosphate buffered saline (PBS) solution (Astral Scientific, GyMEA NWS, Australia) for no more than 10 min. All scales were carefully removed and ten randomly chosen micrographs were taken per biopsy by using a SPOT digital camera (DIAGNOSTIC Instruments, Inc., Sterling Heights, Michigan, USA) connected to a Zeiss Axioskop microscope and a bench top computer running SPOT v.3.0.5 software. Micrographs were recorded at 40x/0.9 (0.145 mm<sup>2</sup>/micrograph) and the number of melanophores (black pigment cells) and xanthophores (yellow pigment cells) were counted in ImageJ v.1.36r (National Institute of Health, USA). The counts of cells in 5 – 10 micrographs per individual were subsequently averaged and standardized to 0.1 mm<sup>2</sup> (main text, Figure S3).

### **Assessment of Aggressive Mimicry Benefits**

Brown juvenile damselfish (whitetail damselfish) were caught overnight using light traps at Lizard Island during the recruitment pulses in October and November 2013. After capture, juvenile fish were kept in holding tanks (22 L) for 3 – 4 days and fed *ad libitum* with freshly hatched *Artemia nauplii*, before being used in experiments. Adult damselfish (n = 5 per treatment, either yellow ambon damselfish or brown whitetail damselfish) were left to acclimatize in experimental tanks (reef mesocosms) for 24 hours while being fed fish-flakes *ad libitum* before experiments started. Dottybacks were caught approximately 48 hours before experimental trials began, kept in separate holding tanks and fed one small piece of prawn (approx. 0.5 cm<sup>2</sup>) 24 hours prior to the experiment. All holding and experimental tanks were flow-through and continuously supplied with fresh seawater pumped directly from the ocean.

Aquarium tanks (80 cm x 37 cm x 35 cm; n = 5) were used for trials, and to make each tank into a reef mesocosm we added: 2 cm of sand substrate on the bottom of each tank, a live coral colony (cauliflower coral, *Pocillopora damicornis*, c. 90 cm in circumference and c. 20 cm in height) in the middle of the tank, and pieces of coral rubble (c. 30 cm in circumference and c. 10 cm in height) were placed in each corner.

Ten juvenile damselfish were added and left to acclimatize for 60 min before a dottyback morph was introduced. Fishes were left to acclimatize for 30 min before strike rates of dottybacks directed at juvenile damselfish were recorded over a 60 min period. Dottybacks of the same color were size matched between treatments (mean  $\pm$  SEM: yellow dottyback/yellow damselfish =  $69.1 \pm 1.7$  mm, yellow dottyback/brown damselfish =  $69.3 \pm 2.2$  mm,  $t_{18} = 0.07$ ,  $P = 0.94$ ; brown dottyback/yellow damselfish =  $74.0 \pm 2.2$  mm, brown dottyback/brown damselfish =  $75.2 \pm 1.8$  mm,  $t_{18} = 0.42$ ,  $P = 0.68$ ). Additional control trials were conducted with adult and juvenile damselfish only to ensure that the survival of juvenile fish was dependent on the presence of dottybacks alone (yellow or brown adult damselfish,  $n = 10$  trials each). After 24 hours, all fish were removed from the mesocosm and the number of surviving juvenile damselfish was recorded ( $n = 10$  trials per treatment, Figure 3). Live coral colonies and coral rubble were removed and mesocosms were drained and flushed before being reset for subsequent trials. Each day we conducted between 2 – 4 trials and the treatments were switched randomly between tanks. Adult damselfish were replaced every 3 – 4 trials.

In control treatments, the majority of juveniles survived the 24-hour trial period (mean  $\pm$  SEM: yellow damselfish =  $9.7 \pm 0.3$ , brown damselfish =  $9.5 \pm 0.4$ ;  $W = 55$ ,  $P = 0.58$ ). We used a GLMM with logit-link function and a binomial distribution to analyze differences in juvenile survival between treatments: dottyback color (yellow/brown) and adult damselfish color (yellow/brown) were fixed factors, and dottyback size was included as a random effect. Pairwise post-hoc Tukey contrast tests were conducted using the function `glht` implemented in the package `multcomp` v.1.3-7 [S32].

### **Prey Color Choice Experiment**

To examine whether dottybacks had a preference for a particular colored prey fish, additional similarly sized dottyback morphs (9 yellow, 7 brown, size mean  $\pm$  SE =  $75 \pm 1.8$  mm;  $t_{15} = 0.93$ ,  $P = 0.37$ ) were placed in a tank with one juvenile yellow ambon damselfish and one brown whitetail damselfish (3 – 4 days old). Juvenile fish were size matched to the nearest mm ( $\sim 14.5$  mm TL) and released into an experimental tank (15 L), which had 1 cm of sand on the bottom and a standard, white plastic coral object (c. 30 cm in circumference and c. 10 cm in height) in the middle for shelter. Fish were left to acclimatize for 30 min before a dottyback of a random color was

added to the tank. We recorded which prey color the dottyback first struck at and consumed.

The same dottyback individuals were tested twice to assure repeatability of results. We used a GLMM with logit-link function and a binomial distribution to analyze differences in prey color preferences: dottyback color (yellow/brown) was used as fixed factor, and dottyback identity was included as a random effect.

We found that dottyback color morphs directed their first strike at (main text), and first captured (GLMM (binomial):  $\chi^2_1 = 16.50$ ,  $P < 0.001$ ), prey fish that matched their own body coloration.

### **Assessment of the Cryptic Benefits of Color Change**

We used the coral trout theoretical vision model (see above, visual modeling of color change) to investigate whether dottybacks also benefit from matching the color of the habitat when associating with the damselfish they mimic (Figure 2A). A measurement of illumination taken from the coral trout experimental arena (see below) at 0.5 m depth was used. Conspicuousness of dottybacks was then calculated as the color distance ( $\Delta S$ ) between dottybacks (yellow,  $n = 31$ ; brown,  $n = 32$ ) and the average color of the habitat (live coral or coral rubble) they are seen against, using the coral trout tetrachromatic visual system (Figure 2B). In addition to  $\Delta S$ , coral trout may also use differences in luminance contrast ( $\Delta L$ ) to distinguish dottybacks from their habitat background. Long wavelength sensitive receptors (LWS) are thought to be responsible to perceive luminance contrast [S22, 33] and we therefore, used the differences in the natural logarithm quantum catch ( $Q$ ) of the coral trout LWS receptor ( $\lambda_{\max} = 532$  nm) to calculate luminance differences between dottybacks and habitat types (Figure 2C):

$$\Delta L = \ln(Q_{LWSdottyback}) - \ln(Q_{LWS\text{habitat}})$$

To assess whether dottybacks would be more cryptic against the habitat they are usually found upon we used LMM's with  $\Delta S$  or  $\Delta L$  square root transformed as the response variable. Dottyback morph (yellow, brown) and habitat type (live coral, coral rubble) were set as fixed factors, and dottyback identity was included as a random effect.

To test the predictions of the visual model, we caught coral trout ( $n = 5$ ) off Lizard Island using de-barbed hooks and line in June and September 2013. Fish were placed in individual oval tanks (220 cm x 120 cm x 50 cm) and left to acclimatize for

2 – 3 days before training commenced. Coral trout were trained twice a day (c. 9:00 and 16:00) and initially learned to feed on a piece of prawn (c. 1.5 cm<sup>3</sup>) attached to a transparent monofilament line (c. 50 cm) held randomly against either of the far-end walls of the oval. A black divider was introduced in the middle of the tank, and the fish were then trained to enter through a door in the divider and feed on a piece of prawn attached to a laminated A4 black or white background. Next, they were trained to approach and attack a laminated image of a neutral grey dottyback to receive a food reward given from above. The training was considered successful after each fish would swim through the black divider and pick at the grey dottyback replica for two days in a row.

Following training, coral trout were given the choice between two randomly chosen laminated live coral or coral rubble backgrounds with either a yellow or brown dottyback image on them (the dottyback location on the background was randomized between trials). Additionally, each trial also contained a background without dottyback on it, which was used as a distractor to assure the coral trout would search for and strike at dottyback images, rather than strike haphazardly at backgrounds to elicit a food reward (Movie S1). In total there were four dottyback/background combinations (2 x 2 design; dottyback color x habitat type, each with 2 levels: yellow/brown and live coral/coral rubble; Figure 2D). The experimental backgrounds were based on a picture of a *Pocillopora damicornis* coral colony, a common habitat for dottybacks and damselfishes. The same picture was used for both backgrounds to ensure that variables other than color and luminance e.g. branch length, branch angle, and degree of branching were kept constant. Similarly, dottyback images were based on laminated photographs of fish from the field. The color and luminance of the background and the dottyback images was adjusted in Adobe Photoshop CS4 v.11.0.2 to ensure their spectral reflectance matched the predicted coral trout visual receptor response (in  $\Delta S$  and  $\Delta L$ ) from the visual model (see above).

To assess whether coral trout would differ in their choice, we conducted a GLMM with a binomial distribution (logit-link), based on a Bradley-Terry model approach for paired choices [S34, 35]. The yellow dottyback on live coral treatment was used as the baseline against which the other treatments were compared, and dottyback identity was included as a random effect (Figure 2D). To account for the relatively small sample size, we calculated the P-values for the likelihood of being chosen using a permutation test approach [S36]. In detail, the permutation test was

used to compare the distribution of the actual model to the distribution of a simulated null model with equal probabilities of choice for all treatments compared to the baseline (based on 5000 permutations and a 0.5 probability of choice for each treatment).

## Supplemental References

- S1. R Core Team. (2013). R: a language and environment for statistical computing. (Vienna, Austria: R foundation for statistical computing), <http://www.R-project.org/>.
- S2. Bates, D., Maechler, M., Bolker, B., and Walker, S. (2012). Lme4: linear mixed-effects models using Eigen and S4. (R package version 1.0-4), <http://CRAN.R-project.org/package=lme4>.
- S3. Feeney, W.E., Lönnstedt, O., Bosiger, Y., Martin, J., Jones, G., Rowe, R., and McCormick, M.I. (2012). High rate of prey consumption in a small predatory fish on coral reefs. *Coral Reefs* 31, 909-918.
- S4. Jones, K. M. M. (2005). Home range areas and activity centres in six species of Caribbean wrasses (Labridae). *J. Fish Biol.* 66, 150-166.
- S5. Miller, S.A., Dykes, D.D., and Polesky, H.F. (1988). A simple salting out procedure for extracting DNA from human nucleated cells. *Nucleic acids res.* 16, 1215.
- S6. Messmer, V., Jones, G.P., Herwerden, L., and Munday, P.L. (2005). Genetic and ecological characterisation of colour dimorphism in a coral reef fish. *Environ. Biol. Fishes* 74, 175-183.
- S7. Maeda, K., Takeshima, H., Mizoiri, S., Okada, N., Nishida, M., and Tachida, H. (2008). Isolation and characterization of microsatellite loci in the cichlid fish in Lake Victoria, *Haplochromis chilotes*. *Mol. Ecol. Res.* 8, 428-430.
- S8. Van Oppen, M.J.H., Rico, C., Deutsch, J.C., Turner, G.F., and Hewitt, G.M. (1997). Isolation and characterization of microsatellite loci in the cichlid fish *Pseudotropheus zebra*. *Mol. Ecol.* 6, 387-388.
- S9. Sanetra, M., Henning, F., Fukamachi, S., and Meyer, A.A. (2009). Microsatellite-based genetic linkage map of the cichlid fish, *Astatotilapia burtoni* (Teleostei): a comparison of genomic architectures among rapidly speciating cichlids. *Genetics* 182, 387-397.
- S10. Parker, A., and Kornfield, I. (1996). Polygynandry in *Pseudotropheus zebra*, a cichlid fish from Lake Malawi. *Environ. Biol. Fishes* 47, 345-352.
- S11. Matschiner, M., and Salzburger, W. (2009). TANDEM: integrating automated allele binning into genetics and genomics workflows. *Bioinformatics* 25, 1982-1983.



- S12. Pritchard, J.K., Stephens, M., and Donnelly, P. (2000). Inference of population structure using multilocus genotype data. *Genetics* 155, 945-959.
- S13. Falush, D., Stephens, M., and Pritchard, J.K. (2003). Inference of population structure using multilocus genotype data: linked loci and correlated allele frequencies. *Genetics* 164, 1567-1587.
- S14. Earl, D.A., and vonHoldt, B.M. (2012). STRUCTURE HARVESTER: a website and program for visualizing STRUCTURE output and implementing the Evanno method. *Conserv. Genet. Res.* 4, 359-361.
- S15. Evanno, G., Regnaut, S., and Goudet, J. (2005). Detecting the number of clusters of individuals using the software structure: a simulation study. *Mol. Ecol.* 14, 2611-2620.
- S16. Excoffier, L., Laval, G., and Schneider, S. (2005). Arlequin (version 3.0): an integrated software package for population genetics data analysis. *Evol. bioinformatics online* 1, 47-50.
- S17. Rice, W.R. (1989). Analyzing tables of statistical tests. *Evolution* 43, 223-225.
- S18. Whiteman, E.A., and Côté, I.M. (2002). Cleaning activity of two Caribbean cleaning gobies: intra-and interspecific comparisons. *J. Fish Biol.* 60, 1443-1458.
- S19. Marshall, N.J., Jennings, K., McFarland, W.N., Loew, E.R., Losey, G.S., and Motgomery, W.L. (2003). Visual biology of Hawaiian coral reef fishes. II. Colours of Hawaiian coral reef fish. *Copeia* 3, 455-466.
- S20. Vorobyev, M., and Osorio, D. (1998). Receptor noise as a determinant of colour thresholds. *Proc. R. Soc. B Biol. Sci.* 265, 351-358.
- S21. Vorobyev, M., Brandt, R., Peitsch, D., Laughlin, S.B., and Menzel, R. (2001). Colour thresholds and receptor noise: behaviour and physiology compared. *Vision Res.* 41, 639-653.
- S22. Cheney, K.L., and Marshall, N.J. (2009). Mimicry in coral reef fish: how accurate is this deception in terms of colour and luminance? *Behav. Ecol.* 20, 459-468.
- S23. Cortesi, F., and Cheney, K.L. (2010). Conspicuousness is correlated with toxicity in marine opisthobranchs. *J. Evol. Biol.* 23, 1509-1518.
- S24. John, J.St. (1999). Ontogenetic changes in the diet of the coral reef grouper *Plectropomus leopardus* (Serranidae): patterns in taxa, size and habitat of prey. *Mar. Ecol. Prog. Ser.* 180, 233-246.

- S25. McCormick, M.I., and Meekan, M.G. (2007). Social facilitation of selective mortality. *Ecology* 88, 1562-1570.
- S26. Siebeck, U.E., Parker, A.N., Sprenger, D., Mathger, L.M., and Wallis, G. (2010). A species of reef fish that uses ultraviolet patterns for covert face recognition. *Curr. Biol.* 20, 407-210.
- S27. Siebeck, U.E., and Marshall, N.J. (2001). Ocular media transmission of coral reef fish - Can coral reef fish see ultraviolet light? *Vision Res.* 41, 133-149.
- S28. Siebeck, U.E., and Marshall, N.J. (2007). Potential ultraviolet vision in pre-settlement larvae and settled reef fish - A comparison across 23 families. *Vision Res.* 47, 273-282.
- S29. Wyszecki, G., and Stiles, W.S. (1982). *Colour science: concepts and methods, quantitative data and formulae* (Wiley).
- S30. Pignatelli, V., Champ, C., Marshall, J., Vorobyev M. (2010). Double cones are used for colour discrimination in the reef fish, *Rhinecanthus aculeatus*. *Biol. Lett.* 6, 537-539.
- S31. Chambers, J.M. (1992). Linear models. In *Statistical models*, J.M. Chambers, and T.J. Hastie, eds. (London: Wadsworth S. & Brooks/Cole).
- S32. Hothorn, T., Bretz, F., and Westfall, P. (2008). Simultaneous inference in general parametric models. *Biom. J.* 50, 346-363.
- S33. Marshall, N.J., Jennings, K., McFarland, W.N., Loew, E.R., and Losey, G.S. (2003). Visual biology of Hawaiian coral reef fishes. III. Environmental light and an integrated approach to the ecology of reef fish vision. *Copeia* 3, 467–480.
- S34. Bradley, R.A., and Terry, M.E. (1952). Rank analysis of incomplete block designs: I. The method of paired comparisons. *Biometrika*, 324-345.
- S35. David, H.A. (1963). *The method of paired comparisons* (DTIC Document).
- S36. Good, P. (2000). *Permutation tests: a practical guide to resampling methods for testing hypothesis* (New York: Springer).

## Chapter 2

### From crypsis to mimicry: changes in colour and the configuration of the visual system during ontogenetic habitat transitions in a coral reef fish

F. Cortesi, Z. Musilová, S. M. Stieb, N. S. Hart,  
U. E. Siebeck, K. L. Cheney, W. Salzburger,  
J. Marshall,

Journal of Experimental Biology (2016)

2.1. Manuscript p. 47 – 60

2.2. Supporting Information p. 61 – 63



## RESEARCH ARTICLE

# From crypsis to mimicry: changes in colour and the configuration of the visual system during ontogenetic habitat transitions in a coral reef fish

Fabio Cortesi<sup>1,2,3,\*</sup>, Zuzana Musilová<sup>3,4</sup>, Sara M. Stieb<sup>1</sup>, Nathan S. Hart<sup>5</sup>, Ulrike E. Siebeck<sup>6</sup>, Karen L. Cheney<sup>2</sup>, Walter Salzburger<sup>3,7</sup> and N. Justin Marshall<sup>1</sup>

## ABSTRACT

Animals often change their habitat throughout ontogeny; yet, the triggers for habitat transitions and how these correlate with developmental changes – e.g. physiological, morphological and behavioural – remain largely unknown. Here, we investigated how ontogenetic changes in body coloration and of the visual system relate to habitat transitions in a coral reef fish. Adult dusky dotybacks, *Pseudochromis fuscus*, are aggressive mimics that change colour to imitate various fishes in their surroundings; however, little is known about the early life stages of this fish. Using a developmental time series in combination with the examination of wild-caught specimens, we revealed that dotybacks change colour twice during development: (i) nearly translucent cryptic pelagic larvae change to a grey camouflage coloration when settling on coral reefs; and (ii) juveniles change to mimic yellow- or brown-coloured fishes when reaching a size capable of consuming juvenile fish prey. Moreover, microspectrophotometric (MSP) and quantitative real-time PCR (qRT-PCR) experiments show developmental changes of the dotyback visual system, including the use of a novel adult-specific visual gene (*RH2* opsin). This gene is likely to be co-expressed with other visual pigments to form broad spectral sensitivities that cover the medium-wavelength part of the visible spectrum. Surprisingly, the visual modifications precede changes in habitat and colour, possibly because dotybacks need to first acquire the appropriate visual performance before transitioning into novel life stages.

**KEY WORDS:** Vision, Development, Gene duplication, Opsin, Colour change, Co-expression

## INTRODUCTION

Throughout different life stages, animals may change their morphology, physiology and behaviour. Such ontogenetic variability often correlates with changes in diet, predation pressure or social status, which in turn are often associated with major habitat transitions (e.g. Booth, 1990; Childress and

Herrnkind, 2001; Dahlgren and Eggleston, 2000; Evans and Fernald, 1990; Grant, 2007). However, despite a large body of literature on ontogenetic variability, studies looking at the development of multiple traits within individuals and how they relate to habitat transitions remain scarce. For example, it is well established that many animals alter some aspects of their visual system when shifting to novel habitats during ontogeny (Hunt et al., 2014), but how these changes interrelate with developmental changes in other traits such as body coloration remains poorly understood.

The complex and varied life histories of coral reef fishes make them particularly well suited for studies of the causes and consequences of ontogenetic habitat transitions. Most coral reef fishes experience a change in environment when moving from a pelagic larval phase in the open ocean to reef-associated juvenile and adult phases. In association with these migrations, the visual system as well as the pigmentation of the skin may be modified (Collin and Marshall, 2003; Evans and Browman, 2004; Evans and Fernald, 1990; Youson, 1988). Ontogenetic changes to the visual system are generally extensive and involve multiple morphological and/or physiological adaptations that cause a shift in peak spectral sensitivity ( $\lambda_{\text{max}}$ ), which is used to adapt vision to varying light conditions or to solve novel visual tasks (Collin and Marshall, 2003; Evans and Browman, 2004; Evans and Fernald, 1990). This can be achieved through a gain or loss of different photoreceptor types in the retina (rod cells used for scotopic vision and/or various cone cell types used for photopic vision), qualitative and/or quantitative changes in the expression of visual pigments (opsins) within the photoreceptors themselves, or the use of different light-absorbing chromophores that bind to the opsin pigment: shorter wavelength sensitive vitamin A<sub>1</sub>-based (retinal) or longer wavelength sensitive vitamin A<sub>2</sub>-based (3,4-didehydroretinal) chromophores, respectively (Collin and Marshall, 2003).

Ontogenetic colour changes, in contrast, are less well documented in coral reef fishes, but generally include a change from transparent or silvery larval stages in the open ocean to often differently coloured juvenile and adult stages on the reef (Booth, 1990; Youson, 1988). While a transparent/silvery appearance may be used to camouflage fish larvae in open water light environments (McFall-Ngai, 1990), juvenile fish use their coloration for a number of strategies that facilitate access to food and reduce predation risks, including: aggressive mimicry, protective mimicry and several mechanisms of crypsis (Booth, 1990; Moland et al., 2005). When morphing into adults, however, many coral reef fishes become large enough or acquire appropriate defensive strategies to avoid predation. Coloration may from this point on also be used for sexual displays or during territorial behaviour (e.g. Booth, 1990; Kodric-Brown, 1998; Sale, 1993).

<sup>1</sup>Queensland Brain Institute, The University of Queensland, Brisbane, QLD 4072, Australia. <sup>2</sup>School of Biological Sciences, The University of Queensland, Brisbane, QLD 4072, Australia. <sup>3</sup>Zoological Institute, University of Basel, Basel 4051, Switzerland. <sup>4</sup>Department of Zoology, Charles University in Prague, Prague 128 44, Czech Republic. <sup>5</sup>Department of Biological Sciences, Macquarie University, North Ryde, NSW 2109, Australia. <sup>6</sup>School of Biomedical Sciences, The University of Queensland, Brisbane, QLD 4072, Australia. <sup>7</sup>Centre for Ecological and Evolutionary Synthesis, Department of Biosciences, University of Oslo, Oslo 0316, Norway.

\*Author for correspondence (fabio.cortesi@uqconnect.edu.au)

© F.C., 0000-0002-7518-6159

Received 22 February 2016; Accepted 9 June 2016

**List of abbreviations**

dps	days post-settlement
JND	just noticeable difference
LWS	long-wavelength sensitive
LWS	long-wavelength sensitive opsin gene
MSP	microspectrophotometry
MWS	mid-wavelength sensitive
qRT-PCR	quantitative real-time PCR
RH1	rhodopsin 1 opsin gene
RH2A $\alpha$ , RH2A $\beta$ , RH2B	rhodopsin like 2 opsin genes
SL	standard length
SWS	short-wavelength sensitive
SWS1	short-wavelength sensitive 1 opsin gene
SWS2A $\alpha$ , SWS2A $\beta$ , SWS2B	short-wavelength sensitive 2 opsin genes
$\Delta L$	luminance contrast
$\Delta S$	chromatic colour contrast
$\lambda_{\max}$	peak spectral sensitivity

The dusky dottyback, *Pseudochromis fuscus* Müller and Troschel 1849, is a small (maximum standard length ~7 cm) predatory reef fish common to reefs throughout the Indo-Pacific ocean, including at our study site at Lizard Island, Australia, where both yellow and brown colour morphs can be found in sympatry (Munday et al., 2003). It has recently been shown that adult dottybacks flexibly adapt their colour from yellow to brown and vice versa to mimic the coloration of damselfishes (*Pomacentrus* spp.) in their surroundings (Cortesi et al., 2015a). By doing so, dottybacks gain multiple fitness benefits including an increase in predatory success on juvenile fish prey (aggressive mimicry) and habitat-associated crypsis (yellow morphs on live coral, brown morphs on coral rubble) that decreases predation risk (Cortesi et al., 2015a). It has also been shown that dottybacks, amongst other fish species, possess an additional gene that is part of a triplet of opsins responsible for visual discrimination in the short-wavelength 'violet–blue' region of the visible spectrum (*SWS2B*, *SWS2A $\alpha$*  and *SWS2A $\beta$* ; Cortesi et al., 2015b). Interestingly, in dottybacks, these opsins are spectrally distinct from one another and are differentially expressed between ontogenetic stages: larval dottybacks express *SWS2A $\beta$*  ( $\lambda_{\max}$ =457 nm), whereas adult dottybacks express *SWS2A $\alpha$*  ( $\lambda_{\max}$ =448 nm) and *SWS2A $\beta$*  (Cortesi et al., 2015b). Finally, dottybacks are demersal spawners that guard their eggs until they hatch, after which larvae undergo a pelagic phase before returning to settle on coral reefs (Michael, 2004; Kuitert, 2004). Taken together, a pelagic larval phase, ontogenetic modifications of the visual system, adult-specific feeding and habitat associations provide a rich substrate for the study of multi-trait ontogeny and its relationship to habitat transitions.

In this context, we explored the relationship between habitat transitions and ontogeny in dottybacks using histological, neurophysiological and molecular approaches. We conducted a developmental time series in the laboratory and explored wild-caught dottyback specimens to examine when, and under what conditions, ontogenetic colour changes would take place. We then assessed how these changes related to modifications of the dottyback visual system by using a combination of microspectrophotometry (MSP) and quantitative real-time PCR (qRT-PCR) approaches. Finally, we used theoretical fish visual models from the perspectives of the dottyback and of a dottyback predator, the coral trout, *Plectropomus leopardus* (St John, 1999), to assess whether changes of the visual system and skin colour would benefit the various life history strategies dottybacks adopt throughout ontogeny.

**MATERIALS AND METHODS****Study site and species**

The field part of the study was conducted at Lizard Island (14°40'S, 145°27'E) and Heron Island (23°44'S, 151°91'E), Great Barrier Reef, Australia, between March 2007 and November 2013. Adult and juvenile dottybacks were collected on snorkel from shallow reefs (depth 2–5 m; yellow morphs from live coral, brown morphs from coral rubble, juveniles independent of habitat type) surrounding Lizard Island using an anaesthetic clove oil solution (10% clove oil, 40% ethanol, 50% seawater) and hand nets. Larval dottybacks and damselfishes (*Pomacentrus* spp.) were caught overnight at Lizard Island using light traps during the summer recruitment pulses in November 2007 and October–November 2013. Adult coral trout ( $N=1$  Heron Island, no morphometrics;  $N=2$  Lizard Island, total length 35.5 and 46 cm) were caught using debarbed hooks and line in March 2007 (Heron Island) and November 2007 (Lizard Island). After capture, fish were placed in sealed bags of seawater, or in large plastic containers, and taken back to the laboratory for further examination. Coral trout and adult and larval dottybacks were used immediately for MSP, or eyes (adult and juvenile dottybacks) and in some cases the whole body (larval dottybacks) were stored on RNAlater (Life Technologies) for subsequent gene expression analysis. The skin of juvenile dottybacks was also used for cell histological assessments. Additional larval dottybacks and damselfishes were used for a developmental time series (see below). Fish sizes are reported in standard length (SL) throughout the study.

For the purpose of this study, we define larval dottybacks as those that are translucent (settlement stage larvae; 11–13 mm SL). After settlement has taken place (2–3 days), fish start to develop skin pigments and turn grey to light brown and are henceforth described as juveniles (SL $\leq$ 48 mm). Adult stages are reached as soon as fishes adopt a mimic colour (either yellow or dark brown; SL $\geq$ 43 mm; Figs 1 and 2). Juvenile and adult morphs were initially differentiated by eye based on their coloration, and the categorization was later reviewed based on the shape of their spectral reflectance curves (according to Marshall, 2000). Although our classification might not conform entirely to the traditional way ontogenetic stages in fishes are allocated (Balon, 1975), i.e. adult dottybacks in our study might not all have started to produce gametes, this classification coincides with two major life history transitions of dottybacks (also see Results and Discussion below).

Statistical analyses were conducted in R v.3.3.0 (R Core Team, 2013) using the package lme4 v.1.1-12 (Bates et al., 2015). Assumptions of normality and homogeneity of variance were assessed using histograms, residual plots and quantile–quantile plots.

**Developmental time series**

To investigate the course of ontogenetic colour change in dottybacks and eventual changes of the visual system associated with it, we placed single larval dottybacks ( $N=8$ ) in holding tanks (40 cm $\times$ 30 cm $\times$ 25 cm) together with either yellow (*Pomacentrus amboinensis*) or brown juvenile damselfish (*Pomacentrus chrysurus*; four replicates per colour with five individuals each). Adult dottybacks are known to change their body coloration to imitate yellow and brown damselfishes (Cortesi et al., 2015a); therefore, we investigated whether juvenile dottybacks would adopt their mimic coloration immediately post-settlement.

Larval holding tanks (40 cm $\times$ 30 cm $\times$ 25 cm) were placed in daylight under shade cloth at the Lizard Island Research Station, with a constant supply of fresh seawater sourced directly from the

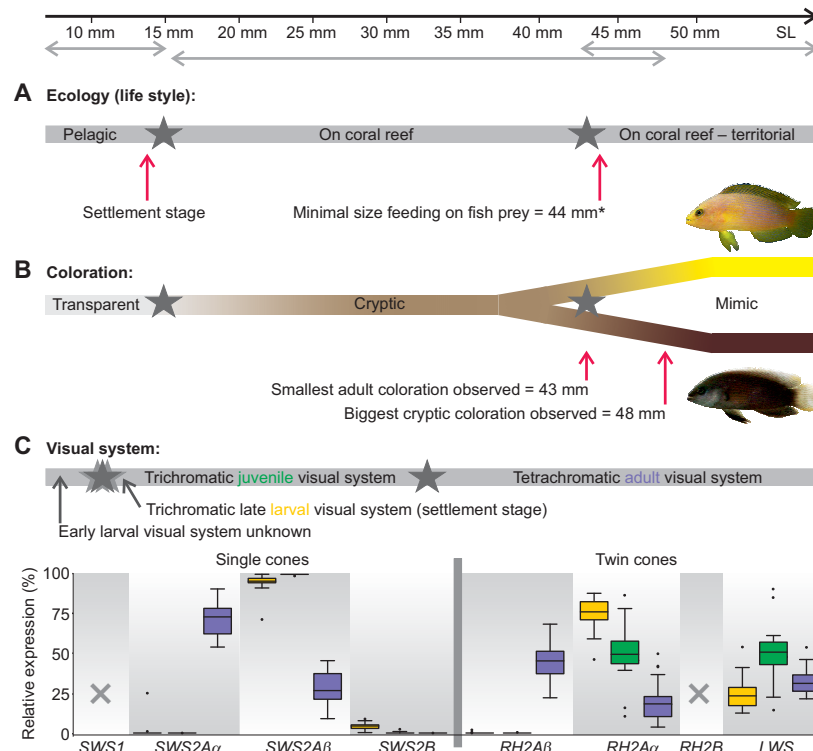


**Fig. 1. Integrative approach to study multi-trait developmental adaptations during ontogenetic habitat shifts in the dusky dottyback, *Pseudochromis fuscus*.** Developmental adaptations are marked with a star. (A) Dottybacks experience two major ontogenetic habitat transitions: settlement on coral reefs when returning from the pelagic environment as larvae, and reaching a size that enables them to feed on juvenile fish prey when turning into mimics as adults. (B) When returning to the reef, larval dottybacks are almost translucent (~13 mm in standard length, SL), after which they quickly become pigmented and cryptic against their habitat background, before changing to their mimic colorations when turning into adults (~43 mm). (C) Changes of the dottyback visual system precede ontogenetic colour change, probably because dottybacks need to alter their visual system to complete complex visual tasks before ontogenetic colour change can occur (see Discussion). The graph at the bottom shows the relative single (*SWS1* and *SWS2s*) and twin (*RH2s* and *LWS*) cone opsin gene expression measured by quantitative real-time PCR (qRT-PCR) for larval expression profiles ( $N=18$ ), juvenile expression profiles ( $N=17$ ) and adult expression profiles ( $N=18$ ). The smallest dottyback to express an adult profile was 26 mm. Note that larvae/juveniles mainly express three cone opsin genes within their retina, while adults mostly express five (also see Fig. S2). Crosses indicate no expression of *SWS1* and *RH2B* genes. The box indicates Q2 and Q3, with the line indicating the median. The whiskers indicate Q1 and Q4 of the data, with dots marking outliers. \*Holmes and McCormick, 2010.

ocean in front of the station. To make each tank into a reef mesocosm, we added 1 cm of sand substrate to the bottom of each tank, a live coral colony (cauliflower coral, *Pocillopora damicornis*, ~30 cm in circumference and ~10 cm in height) in the middle of the tank, and pieces of coral rubble (~20 cm in circumference and ~10 cm in height), placed in each corner. All larval fish were fed *ad libitum* with freshly hatched *Artemia nauplii*, twice daily.

To measure their size and take photographs of individual fish, dottybacks were temporarily removed from their tanks at different time points. Measurements were taken to the closest millimetre and photographs of various body parts were taken under a Zeiss Discovery v8 Stereoscope with an integrated AxioCam Erc5s microscope camera attached to a standard desktop computer running Zen2011 software (www.zeiss.com; Fig. 2). On day 34 post-settlement (dps), individuals from the developmental time series started to overlap in length (18–24 mm, mean±s.e.m. SL=22.3±0.8 mm) with the juveniles caught from the reef ( $N=16$ ,

19–48 mm, 35.4±1.9 mm), and fish were then killed using an overdose of clove oil (40 mg l<sup>-1</sup>). Sections of their skin were taken for histological assessments and the eyes were transferred to RNAlater for subsequent gene expression analysis. As a control, additional larval dottybacks were kept in four separate holding tanks without damselfishes. Control fish were killed with an overdose of clove oil (40 mg l<sup>-1</sup>) either 1 dps ( $N=8$ ) or 7–9 dps ( $N=8$ ), before their bodies were transferred to RNAlater for subsequent gene expression analysis (see below).

#### Skin histological assessment

To assess the type of chromatophores (skin pigment cells) that were present at different ontogenetic time points, we took skin biopsies (0.5–1 cm<sup>2</sup>) from fish at the end of the developmental time series (34 dps,  $N=8$ ; see above) and of larger juveniles ( $N=3$ , 38.0±2.3 mm) located and caught from the reef in January–February 2012. Biopsies were taken from behind the



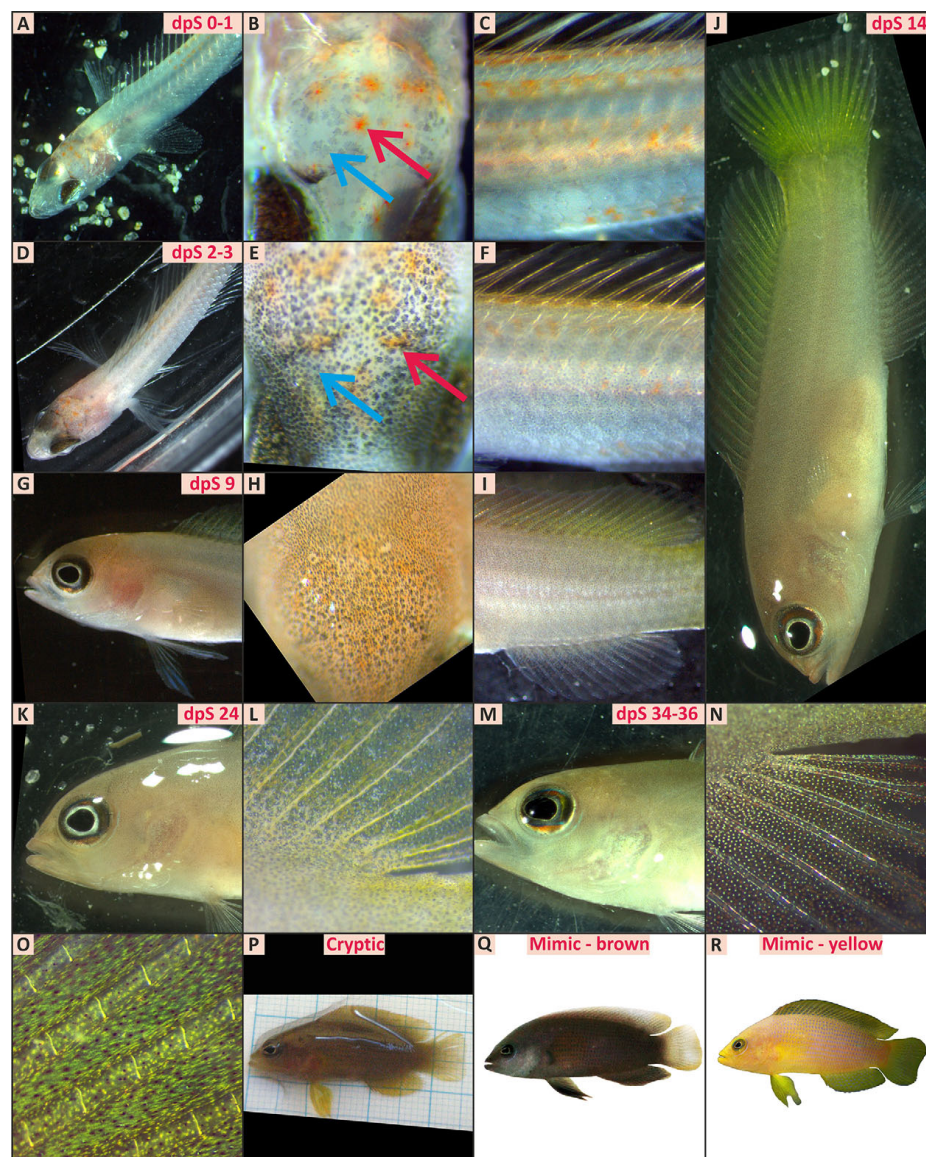


**Fig. 2. Developmental time series tracing ontogenetic colour change in dottybacks.** (A) When returning from the pelagic environment, larval dottybacks are almost translucent, showing only a little pigmentation on their cranial plate (B), and along the dorsal axis (C). (D–F) Within the first 2–3 days post-settlement (dps), black pigment rapidly starts to form inside melanophores and disperses over the whole body. (G–I) At 7–9 dps, dottybacks attain an overall grey to light-brown coloration, which is maintained (J,K,M,P) until juvenile dottybacks change into their mimic colorations as adults (Q,R). Note, yellow- and red-pigmented cells (xanthophores and erythrophores) first accumulate along the dorsal axis (C,F), spreading to the dorsal, caudal and anal fin (I,J,L,N,O), before migrating across the lateral axis to spread to the entire body (K,M,P). Red arrows point to developing xanthophores, blue arrows point to developing melanophores.

pectoral fin and were treated following the methods of Cortesi et al. (2015a). Results from juvenile fish were subsequently compared with skin histological assessments previously attained

from adult dottyback morphs (data taken from Cortesi et al., 2015a;  $N=8$  morphs each, yellow  $55.4 \pm 3.1$  mm, brown  $61.6 \pm 2.8$  mm; Fig. 3).



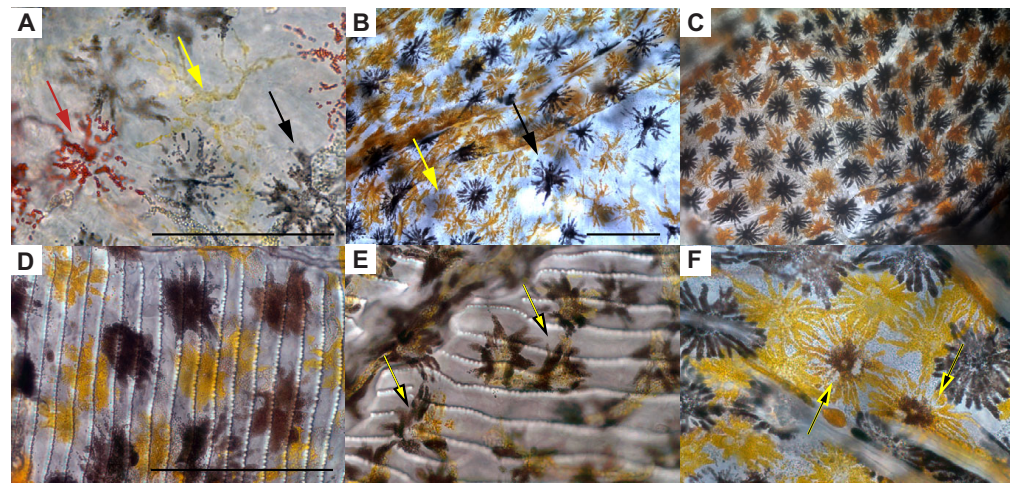


**Fig. 3. Skin micrographs of dottybacks across ontogeny.** (A) Typical skin biopsies of juvenile dottybacks at the end of the developmental time series (~24 mm SL). Arrows depict red-pigmented cells (presumable erythrophores), yellow-pigmented cells (presumable xanthophores) and black-pigmented cells (melanophores). The red cells are absent in the skin (B,C) and scales (D) of larger juvenile dottybacks (~38 mm) and adult dottybacks (yellow and brown morphs, ~58 mm). Instead, larger dottybacks show low numbers (<1%) of 'hybrid' cells containing yellow and black pigment within their scales (E) and skin (F) (*sensu* Bagnara and Hadley, 1973). Scale bars: 100  $\mu$ m.

### MSP

We used MSP to measure the spectral absorbance of different photoreceptor types in the retina of larval ( $N=1$ ) and adult dottybacks ( $N=3$ ), and of adult coral trout ( $N=3$ ). MSP and raw absorbance spectra were analysed following the methods of Hart et al. (2011) and fitted with visual pigment absorbance spectrum templates of Stavenga et al. (1993) to be used for subsequent fish visual models (see below; Table 1, Fig. 4; Table S1, Fig. S1). Both the dottyback and coral trout contained single as well as twin cones within their retina. The individual members of the twin cones had a very similar overall morphology; however, one member generally contained a shorter shifted mid-wavelength sensitive visual pigment (MWS), while the other member contained a longer shifted long-wavelength sensitive visual pigment (LWS) (this was not always the case for the coral trout twin cones; see Results). Single cones contained a short-wavelength sensitive pigment (SWS).

### Opsin genes, synteny and their phylogeny

Dottyback opsin genes were searched for in the genomic raw reads of the specimen that was sequenced as part of the whole-genome sequencing project at the Centre for Ecological and Evolutionary Synthesis (CEES) in Oslo, and the opsin gene sequences of the Nile tilapia, *Oreochromis niloticus* (Spady et al., 2006), were used as a reference against which to map the reads. Mapping and extraction of dottyback opsins followed the methods described in Cortesi et al. (2015b). Opsin sequences from 16 species were subsequently combined with the dottyback sequences to generate a dataset for the phylogenetic reconstruction of genes (Fig. 5). Genomes from three species were accessed from the Assembly or the SRA databases in GenBank (<http://www.ncbi.nlm.nih.gov/genbank>) and opsin genes were extracted following the methods of Cortesi et al. (2015b). Additional single gene coding sequences from 14 species were directly accessed from GenBank.

**Table 1. Spectral characteristics of visual pigment found in the scotopic rod and the photopic single and twin cone photoreceptors of the dusky dottyback, *Pseudochromis fuscus***

	Twin cones								
	Single cones		Broad spectra						
			MWS member		LWS member	MWS		LWS	Rod
	SWS2A $\alpha$	SWS2A $\beta$	RH2A $\beta$	RH2A $\alpha$	LWS	RH2A $\alpha$ & RH2A $\beta$		LWS & RH2A $\beta$	RH1
$\lambda_{\max}$	Adult	Adult & larval	Adult	Adult & larval	Adult & larval	Adult	Adult	Adult	Adult & larval
Pre-bleach absorbance spectra (nm)	447.5 $\pm$ 0.9	456.8 $\pm$ 1.5	512.5 $\pm$ 0.7	524.1 $\pm$ 0.7	560.6 $\pm$ 1.7	522.8	551.8 $\pm$ 2.1	497.8 $\pm$ 0.5	
Difference spectra (nm)	446.7 $\pm$ 1.0	456.1 $\pm$ 1.4	513.4 $\pm$ 0.1	524.3 $\pm$ 1.0	561.5 $\pm$ 1.8	524.2 $\pm$ 0.9	554.3 $\pm$ 2.2	502.4 $\pm$ 0.5	
No. cells pre-bleach/difference spectra	11/16	4/5	2/2	19/19	9/9	1/2	12/12	24/28	

The pigment spectral range and corresponding opsin gene are given below the morphological distinction.  $\lambda_{\max}$  data means $\pm$ s.e.m. were obtained from adults/larvae as shown.

Note that most twin cones contained a mid-wavelength sensitive (MWS) and a long-wavelength sensitive (LWS) member with absorbance spectra that fitted an A<sub>1</sub> visual template (Stavenga et al., 1993). However, some twin cone members showed unusually broad absorbance spectra that are likely to be caused by pigment co-expression within outer segments (see Discussion).

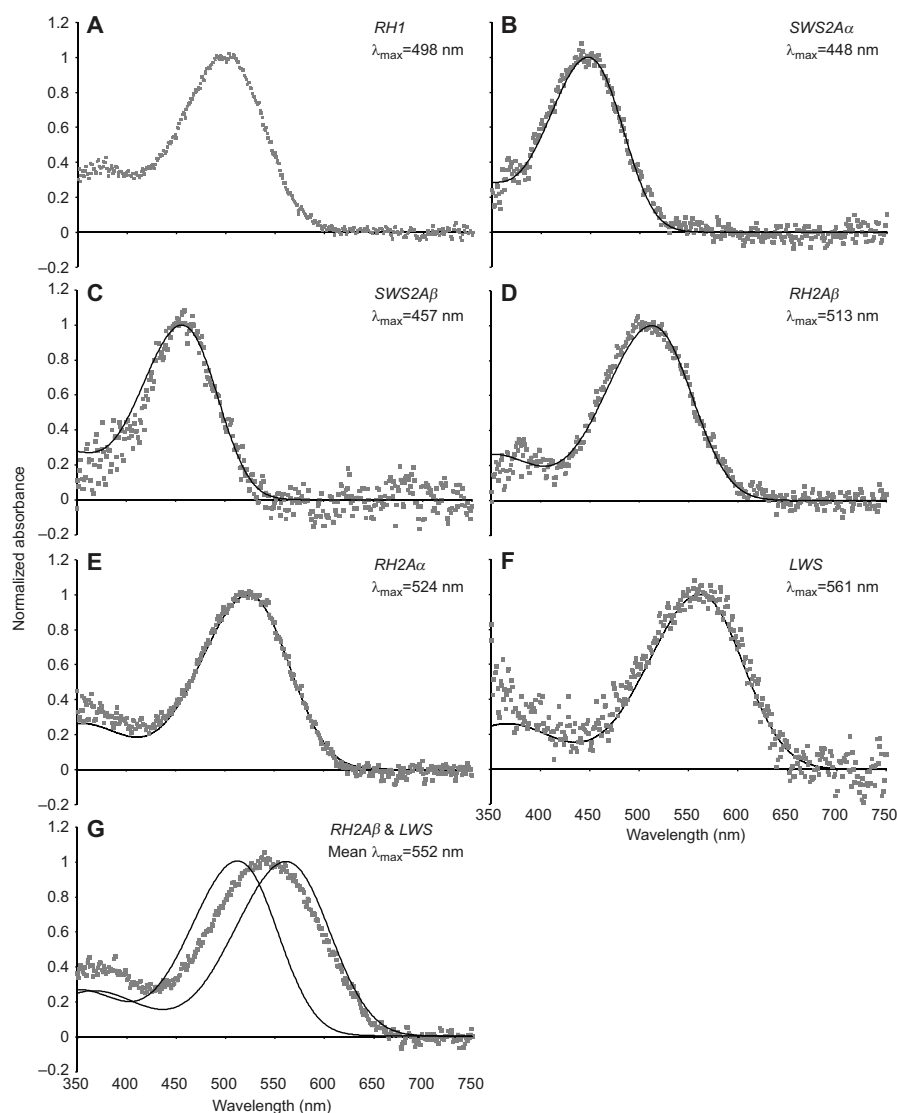


**Fig. 4. Normalized pre-bleach absorbance spectra of the dottyback visual pigments measured with microspectrophotometry (MSP).** (A) The visual pigment found in the rod photoreceptor used for scotopic vision ( $N=24$ ). (B,C) The 'violet-blue' short-wavelength sensitive (SWS) single cones (B, short SWS,  $N=11$ ; C, long SWS,  $N=4$ ). (D) The 'short-green' mid-wavelength sensitive (MWS) member of the twin cones ( $N=2$ ). (E) The 'long-green' MWS member of the twin cones ( $N=19$ ). (F) The 'red' LWS member of the twin cones ( $N=9$ ). (G) The mean of the broad absorbance spectra found mostly in the LWS member of twin cones and thought to be the result of co-expression of RH2A $\beta$  and LWS visual pigments ( $N=13$ ). The corresponding opsin genes are shown in the top right of each panel. Spectra were fitted with vitamin A<sub>1</sub>-based rhodopsin templates of the appropriate  $\lambda_{\text{max}}$  calculated using the equations of Stavenga et al. (1993). Note that in G, no visual template was fitted, but instead the visual templates for the short MWS-twin and LWS-twin are shown.

The combined opsin dataset was aligned using the I-ins-i algorithm in MAFFT 6.8 (Katoh and Toh, 2008) and the most appropriate model of sequence evolution was estimated in jModeltest v.2 (Darriba et al., 2012), using the Akaike

information criterion (AIC) for model selection. A Bayesian inference phylogenetic hypothesis was calculated on the CIPRES platform (Miller et al., 2010), using the GTR+I+ $\Gamma$  model and an MCMC search with two independent runs and four chains each in



2551

MrBayes v.3.2.1 (Ronquist et al., 2012). Each run was set to 10 million generations, with trees sampled every 1000 generations (i.e. 10,000 trees/run) and a burn-in of 25%. Vertebrate-ancestral opsin gene sequences (VA-opsins) from four fish species were used as outgroups to reconstruct the phylogenetic relationship between opsins. The Dottyback genome data have been submitted to GenBank; other accession numbers are depicted after the species names in Fig. 5.

### Opsin gene expression

To investigate whether the expression of cone opsins changed throughout ontogeny, we extracted RNA from the whole head of larvae prior to settlement ( $N=10$ , 11–13 mm,  $12.2\pm0.4$  mm) and at 1 dps ( $N=8$ , 12–13 mm,  $12.8\pm0.3$  mm), and small juveniles from the developmental time series 7–9 dps ( $N=8$ , 13–15 mm,  $13.9\pm0.3$  mm) and 34 dps ( $N=8$ , 18–24 mm,  $22.3\pm0.8$  mm). Additionally, RNA was extracted from retina tissue of larger juveniles ( $N=7$ , 19–41 mm,  $31.8\pm3.1$  mm) and adult morphs ( $N=6$  each; yellow, 51–68 mm,  $57.5\pm3.1$  mm; brown, 49–65 mm,  $58.5\pm2.7$  mm) located and caught from the reef between April 2011 and February 2012. Importantly, juveniles from the reef overlapped in size with individuals from the developmental time series and reached all the way to the adult size class.

RNA extraction and qRT-PCR experiments were conducted following the methods of Stieb et al. (2016). In brief, unique primers were designed for each cone opsin gene, whereby either the forward or the reverse primer spanned an exon–exon boundary to warrant cDNA amplification (Table S2). Primer efficiency was validated using a fivefold dilution series of an opsin pool with a starting concentration of  $0.1\text{--}0.5\text{ nmol }\mu\text{l}^{-1}$ , making sure that the critical threshold cycle (Ct) values of the dilution series encompassed the Ct values of the samples (Table S2). The opsin pool contained equal ratios of fragments of each opsin gene that were amplified from cDNA (measured on an Agilent 2100 BioAnalyzer, Agilent Technologies). Opsin expression was calculated for short-wavelength sensitive genes (*SWS1* and *SWS2* expressed in single cones) and long-wavelength sensitive genes (*RH2* and *LWS*, expressed in twin cones) separately as the fraction of total opsin gene expression within either single or twin cones, using the opsin pool as a reference to normalize between PCR plates. Individuals from different ontogenetic stages were randomly assigned to each RT reaction plate, and experiments were carried out with three technical replicates each (for further details on the approach, refer to Carleton and Kocher, 2001 and Stieb et al., 2016).

Expression data were transformed to the natural logarithm to compare opsin gene expression between different ontogenetic stages. Initially, a principal component analysis (PCA) followed by MANOVA revealed three distinct groups among ontogenetic stages: larvae prior to settlement and 1 dps (MANOVA, single cones: Pillai's  $\lambda=0.3$ ,  $P=0.2$ ; twin cones: Pillai's  $\lambda=0.2$ ,  $P=0.4$ ), small juveniles 7–9 and 34 dps (MANOVA, single cones: Pillai's  $\lambda=0.3$ ,  $P=0.2$ ; twin cones: Pillai's  $\lambda=0.3$ ,  $P=0.1$ ), and larger juveniles and adult morphs (yellow and brown dottybacks; MANOVA, single cones: Pillai's  $\lambda=0.5$ ,  $P=0.2$ ; twin cones: Pillai's  $\lambda=0.3$ ,  $P=0.5$ ). Importantly, PCA revealed that one large juvenile from the reef at 19 mm overlapped in expression with the small juvenile expression profile (Fig. S2A). Ontogenetic stages were subsequently joined into three different subgroups for expression analysis: larval expression ( $N=18$ ), juvenile expression ( $N=17$ ) and adult expression ( $N=18$ ; Fig. 1; Fig. S2).

### Measurement of body coloration and visual models of colour discrimination

Spectral reflectance measurements of juvenile dottybacks ( $N=6$ ,  $38.0\pm3.2$  mm) located and caught between April and May 2011 were obtained following the methods of Cortesi et al. (2015a). Juvenile spectra were combined with measurements previously attained from adult dottybacks (yellow,  $N=31$ ; brown,  $N=32$ ), and from the yellow (*Pomacentrus amboinensis* and *P. moluccensis*) and brown (*P. chrysurus*) damselfishes they imitate as adults ( $N=8$  each; data taken from Cortesi et al., 2015a; Fig. 6A). These spectra were then used in theoretical fish visual models (Vorobyev and Osorio, 1998; Vorobyev et al., 2001) to determine: (i) whether an adult expression profile would change the ability of dottybacks to discriminate between damselfishes compared with a juvenile expression profile (Fig. 6E), and (ii) how the predatory coral trout may perceive juvenile and adult dottybacks against a coral rubble or live coral background (Fig. 6F; for measurements of background spectra, see Cortesi et al., 2015a; Fig. 6B).

The visual models calculate the chromatic distance between two colours ( $\Delta S$ ) within the visual 'space' of the fish based on an opponent mechanism, which is limited by the noise of the different photoreceptors (Vorobyev and Osorio, 1998; Vorobyev et al., 2001), whereby,  $\Delta S=1$  is an approximate threshold of discrimination,  $\Delta S<1$  indicates colours are chromatically indistinguishable, and  $\Delta S>1$  indicates colours are discriminable from one another (just noticeable difference, JND; e.g. Cheney et al., 2014; Boileau et al., 2015). In addition, the coral trout might also use differences in luminance contrast ( $\Delta L$ ) to detect dottybacks against their habitat background. In general, coral reef fishes are assumed to use the LWS receptor to perceive differences in  $\Delta L$ , with some direct evidence in damselfishes (Siebeck et al., 2014). Hence, we used the differences in the natural logarithm quantum catch ( $Q$ ) of the coral trout LWS receptor (522 or 532 nm  $\lambda_{\text{max}}$ ; see Results) to calculate  $\Delta L$  between dottybacks and habitat types:

$$\Delta L = \ln(Q_{\text{LWSdottyback}}) - \ln(Q_{\text{LWSHabitat}}). \quad (1)$$

Members of twin cones have previously been shown to contribute individually to colour vision in some coral reef fishes (Pignatelli et al., 2010). Consequently, dottybacks with juvenile expression (*SWS2A $\beta$* , *RH2A $\alpha$* , *LWS*) were modelled as trichromatic and those with adult expression (*SWS2A $\alpha$* , *SWS2A $\beta$* , *RH2A $\alpha$* , *LWS* or *LWS/RH2A $\beta$* ; see Results) as tetrachromatic using different visual sensitivities for the LWS member of the adult twin cones: first, a vitamin A<sub>1</sub>-based visual template (561 nm  $\lambda_{\text{max}}$ ) and second, a broader absorbance spectrum presumably derived from opsin co-expression (552 nm  $\lambda_{\text{max}}$ ; Figs 4 and 6). Because broad absorbance spectra were also found in the coral trout twin cones, we modelled its visual system to be either trichromatic or dichromatic. These models were computed using two A<sub>1</sub>-based templates for the MWS (507 nm  $\lambda_{\text{max}}$ ) and LWS (532 nm  $\lambda_{\text{max}}$ ) members of the twin cones or using a broad absorbance spectrum for both twin cone members (522 nm  $\lambda_{\text{max}}$ ), respectively (Fig. 6, Fig. S1).

Spectral sensitivity curves were multiplied by the lens transmission cut-off (dottyback  $T_{50}=435$  nm; coral trout  $T_{50}=411$  nm; Siebeck and Marshall, 2001) to generate species-specific visual templates (Fig. 6C,D). Cone receptor ratios were based on previously conducted morphological assessments of coral reef fish retinas (N.J.M., unpublished) and set to 1:4 (SWS:LWS) for dichromatic, 1:2:2 for trichromatic (SWS:MWS:LWS) and

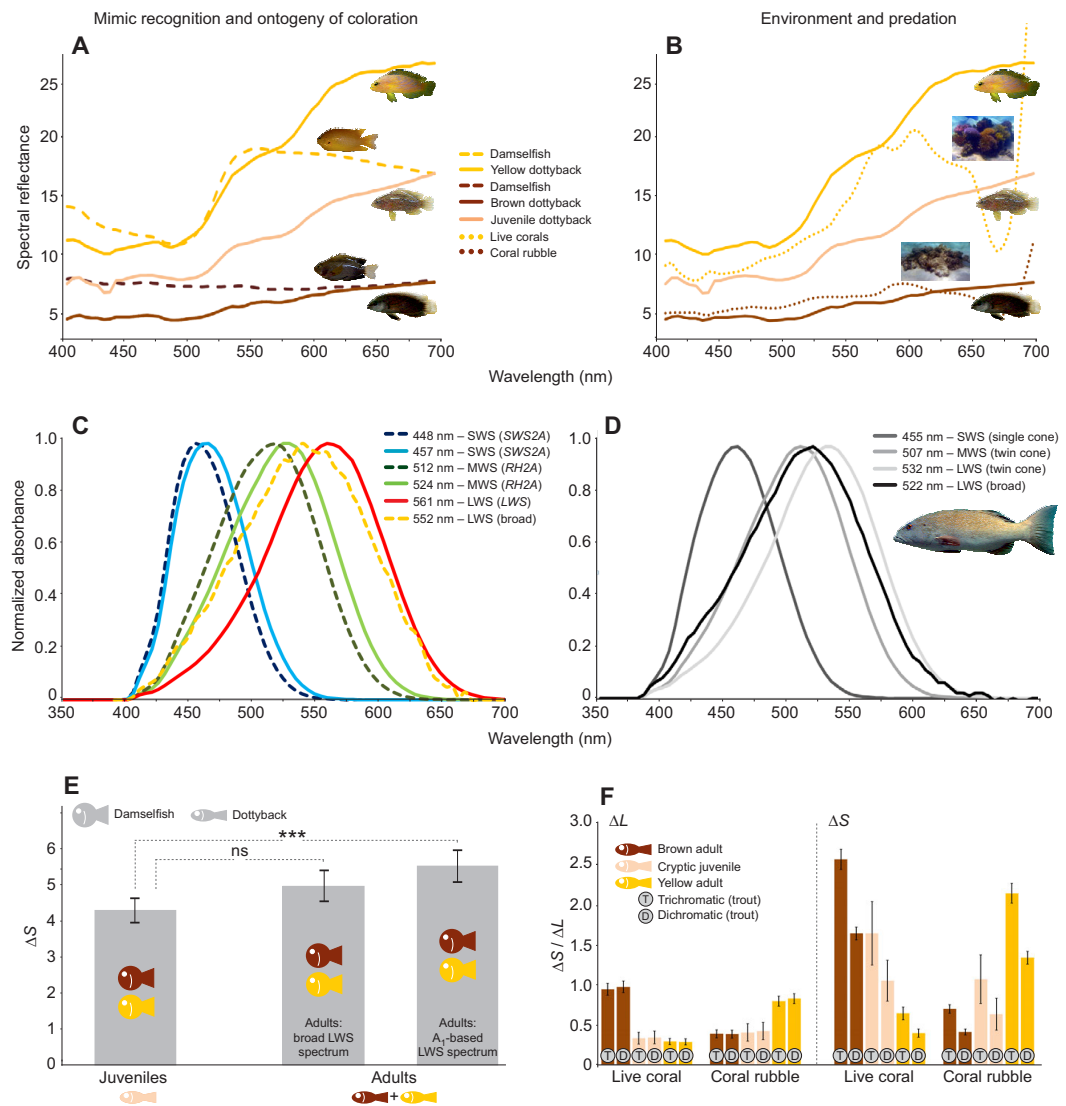


**Fig. 6. Theoretical fish vision models used to investigate the possible benefits of ontogenetic changes in dottybacks.** (A,B) Mean spectral reflectance measurements of juvenile ( $N=6$ ) and adult (yellow,  $N=31$ ; brown,  $N=32$ ) dottybacks and (A) the damselfish they mimic as adults (yellow and brown,  $N=8$  each) and (B) the habitat types that dottybacks are found on [yellow morphs on live coral, brown morphs on coral rubble (Munday et al., 2003) and juveniles across habitat types]. (C,D) Visual templates of juvenile and adult dottybacks (C) and the predatory coral trout, *Plectropomus leopardus* (D; see also Fig. 4, Fig. S2). In C, the dashed spectral curves are adult specific while the continuous curves belong to both larval/juvenile and adult dottyback visual systems. The genes corresponding to the visual pigments found in different photoreceptor types are shown (see also Fig. 4). These visual templates were used to calculate the chromatic (hue,  $\Delta S$ ) and luminance contrast ( $\Delta L$ ) (Vorobyev and Osorio, 1998; Vorobyev et al., 2001) between yellow and brown damselfish models (*Pomacentrus amboinensis* and *P. moluccensis*, yellow: *P. chrysurus*, brown) when perceived by different dottyback stages (*P. fuscus*; E), and between dottybacks and different habitat types when perceived by the coral trout (*P. leopardus*; F). In E, juvenile dottybacks were modelled to have three spectral sensitivities (trichromacy), while adult dottybacks were modelled to have four spectral sensitivities (tetrachromacy) using the long MWS (*RH2A $\alpha$* ) and either an  $A_1$ -based LWS (*LWS*) or a broad absorbance spectra-based LWS (putative *RH2A $\beta$*  and *LWS* co-expression) for the twin cone members. In F, the coral trout was modelled as a trichromat using separate values for the MWS and LWS twin cone members, or as a dichromat using the broad absorbance spectra for both twin cone members. Details on statistical values in F are provided in Table 2. Note that, independent of the visual receiver,  $\Delta S$  was lower when visual models were computed using the broad absorbance spectra. Coral trout image credit: G. A. C. Phillips.



1:1:2:2 (SWS:SWS:MWS:LWS) for tetrachromatic visual systems. To account for the light environment under which fish and the background habitat are viewed, we modelled colour discrimination using illumination measurements taken from their natural environments at a water depth of 5 m (as per Cortesi et al., 2015a).

To examine whether dottybacks with a juvenile or an adult expression would differ in their ability to discriminate between damselfish colours ( $N=8$  yellow,  $N=8$  brown damselfishes; 64 pairwise comparisons), we used a linear mixed model (LMM) in lmerTest v.2.0-11 (R package lme4) with  $\Delta S$  square-root transformed as the response variable. Signal receiver (juvenile, adult, adult co-expression) was set as fixed factor, and damselfish identities were set as random factors. We used likelihood ratio tests to compare a model with random intercepts-only to a model with random slopes and intercepts (models fitted by maximum likelihood). However, we found no significant difference between approaches and the final model was computed using random intercepts-only. Linear models (LMs) were used to investigate whether the coral trout would perceive juvenile and adult dottybacks differently when seen against various habitat backgrounds (trichromatic and dichromatic results were analysed separately). The nature of significant differences was further examined using Tukey–Kramer HSD means comparison tests.

## RESULTS

### Do dottybacks change colour during ontogenetic habitat shifts?

When larval dottybacks settle onto reefs after their pelagic larval stage, they are translucent and show only a few pigmented chromatophore cells, mostly along the dorsal axis and on the cranial plate (Fig. 2A–C). Within the first 2–3 dps, pigments rapidly start to form and to disperse over the whole body (Fig. 2D–F). At 7–9 dps, fish attain an overall grey to light-brown coloration (Fig. 2G–I). This coloration is maintained (Fig. 2K,M,P) until juvenile dottybacks change to either dark brown or yellow colour morphs as adults, when feeding and habitat specializations take place (Figs 1 and 2Q,R).

While melanophores (black pigment cells) immediately spread across the whole body, erythrophores and xanthophores (red and yellow pigment cells) first accumulate along the dorsal axis (Fig. 2C,F), spreading to the dorsal and caudal fin (Fig. 2I,J,L), before migrating across the lateral and ventral axis to spread across the entire body (Fig. 2K,M). At the end of the developmental time series, at 34 dps, juvenile dottybacks possessed a mixture of melanophores, erythrophores and xanthophores within their skin (Fig. 3A). However, erythrophores were absent in the skin of larger juvenile and adult dottybacks (Fig. 3B–D). Instead, in addition to melanophores and xanthophores, we sporadically found ‘mosaic’ cells (*sensu* Bagnara and Hadley, 1973) within the skin of these specimens (<1% of overall chromatophores), i.e. chromatophores that contained black and yellow pigments and thus appeared to be at a transitional stage between melanophores and xanthophores (Fig. 3E,F).

When returning from the pelagic environment, larval dottybacks measured 11–13 mm, after which fish continuously grew until reaching 18–24 mm at the end of the developmental time series at 34 dps. Juvenile dottybacks caught from the reef (independent of habitat type) ranged from 19 to 48 mm and did not differ in coloration from dottybacks that were raised with either yellow or brown damselfish in our developmental time series. The smallest dottyback to adopt a mimic coloration was 43 mm for yellow morphs and 44 mm for brown morphs.

### Does the dottyback visual system change during ontogenetic habitat shifts?

Using MSP, we found seven different types of visual pigments within dottyback retinas, of which two were adult specific (summarized in Table 1). Rods contained a MWS pigment with a mean  $\lambda_{\max}$  at 498 nm ( $N=24$  cells; Fig. 4A). There were two spectrally distinct types of single cones containing SWS (‘blue’) pigments: adult-specific cones containing a visual pigment with a mean  $\lambda_{\max}$  at 448 nm ( $N=11$  cells; Fig. 4B) and cones that occurred throughout ontogeny with a visual pigment having a mean  $\lambda_{\max}$  at 457 nm ( $N=4$  cells; Fig. 4C; see also Cortesi et al., 2015b). Most dottyback twin cones were made up of a member containing a MWS (‘green’)-sensitive visual pigment with a mean  $\lambda_{\max}$  at 524 nm (long MWS,  $N=19$  cells; Fig. 4E) and a second member containing a LWS (‘red’) visual pigment with a mean  $\lambda_{\max}$  at 561 nm ( $N=9$  cells; Fig. 4F). However, we also found one twin cone in adult dottybacks that contained two shorter shifted MWS pigments with a mean  $\lambda_{\max}$  at 512 nm (short MWS,  $N=2$  cells; Fig. 4D). In addition, the LWS members of twin cones in adult fish were found to sporadically depict unusually broad absorbance spectra ( $N=12$  cells), with a mean  $\lambda_{\max}$  of 552 nm (Fig. 4G). Moreover, we also found one MWS member with a broad absorbance spectrum at 523 nm  $\lambda_{\max}$  (see Discussion on the possible origin of these broad spectra; Fig. 4G, Table 1).

Using whole-genome sequencing, we recovered 10 different opsin genes from the dottyback genome, nine of which are orthologous to visual opsin genes from other vertebrates and similar in synteny to the visual opsin genes of the Nile tilapia (O’Quin et al., 2011), and one of which is orthologous to exorhodopsin, the opsin gene expressed in the pineal gland of fishes (Mano et al., 1999; Fig. 5). Phylogenetic analyses revealed that dottyback visual opsins belong to the known visual opsin gene families in percomorph fishes (Rennison et al., 2012), including one rod opsin gene used for scotopic vision (*RH1*) and six cone opsin genes used for photopic vision: four ‘UV–blue’-sensitive genes (*SWS1*, *SWS2A $\alpha$* , *SWS2A $\beta$*  and *SWS2B*; see also Cortesi et al., 2015b), one ‘blue–green’-sensitive gene (*RH2B*) and one ‘red’-sensitive gene (*LWS*). In addition, we discovered a novel, possibly dottyback-specific duplication of the ‘green’-sensitive *RH2A* gene: *RH2A $\alpha$*  and *RH2A $\beta$* , which cluster together in the phylogeny (Fig. 5).

Independent of ontogeny, dottybacks did not express the UV-sensitive *SWS1* or the green-sensitive *RH2B* genes (Fig. 1C; Fig. S2). Larval dottybacks were found to express three single (*SWS2*) and two twin cone (*RH2* and *LWS*) opsins within their retina (percentage of overall single or twin cone opsin expression): *SWS2B*, 4.2 $\pm$ 0.5%; *SWS2A $\alpha$* , 1.6 $\pm$ 1.4%; *SWS2A $\beta$* , 94.1 $\pm$ 1.4%; *RH2A $\alpha$* , 74.9 $\pm$ 2.5%; and *LWS*, 23.9 $\pm$ 2.5%. However, both *SWS2B* and *SWS2A $\alpha$*  were expressed at very low levels and are therefore unlikely to be used for vision. Juvenile dottybacks, in contrast, were found to express one single and two twin cone opsins: *SWS2A $\beta$* , 99.4 $\pm$ 0.1%; *RH2A $\alpha$* , 50.2 $\pm$ 4.7%; and *LWS*, 49.6 $\pm$ 4.7%. Finally, dottybacks with an adult expression profile were found to express two single and three twin cone opsins: *SWS2A $\alpha$* , 71.71 $\pm$ 2.5%; *SWS2A $\beta$* , 28.23 $\pm$ 2.5%; *RH2A $\alpha$* , 20.5 $\pm$ 3.0%; *RH2A $\beta$* , 45.8 $\pm$ 2.7%; and *LWS*, 33.2 $\pm$ 2.0% (Fig. 1C; Fig. S2).

The largest juveniles with juvenile expression profiles were found to be between 19 mm (wild caught) and 24 mm (developmental time series), and the smallest juvenile with an adult expression profile was found to be 26 mm (wild caught). Hence, the transition between the juvenile and the adult expression profile occurs when dottybacks reach ~25 mm, well before the juvenile to adult colour

change and habitat specialization take place. Moreover, these data together with the MSP measurements enabled us to assign visual pigments (and sensitivities) to opsin genes: *SWS2Aa* at 448 nm  $\lambda_{\text{max}}$  (adult specific), *SWS2Ab* at 457 nm  $\lambda_{\text{max}}$ , *RH2Aa* at 524 nm  $\lambda_{\text{max}}$ , *RH2Ab* at 512 nm  $\lambda_{\text{max}}$  (adult specific) and *LWS* at 561 nm  $\lambda_{\text{max}}$  (Table 1 and Fig. 4).

### Coral trout visual system

The coral trout rod cells contained a MWS pigment with a mean  $\lambda_{\text{max}}$  at 497 nm ( $N=22$  cells; Fig. S1A), while single cones contained a SWS pigment with a mean  $\lambda_{\text{max}}$  at 455 nm ( $N=10$  cells; Fig. S1B). Similar to the dottybacks, the coral trout twin cone members were found to have absorbance spectra that were broader than would be expected based on the presence of only a single pigment binding either an  $A_1$  or an  $A_2$  chromophore. However, in this case, broad absorbance spectra were found for almost every cell and often both twin cone members had a similar spectral absorbance ranging from 507 to 532 nm  $\lambda_{\text{max}}$  (mean  $\lambda_{\text{max}}=522$  nm,  $N=48$  cells; Fig. S1C).

### Colour discrimination by juvenile and adult dottybacks and by the predatory coral trout

Using theoretical vision models, we found that the chromatic contrast ( $\Delta S$ ) between differently coloured damselfish models increased for adult dottybacks compared with juvenile dottybacks ( $\Delta S$  brown versus yellow damselfish: adult dottybacks with  $A_1$ -based LWS=5.5 $\pm$ 0.5; adult dottybacks with broad LWS spectrum=5.0 $\pm$ 0.4; juvenile dottybacks=4.3 $\pm$ 0.3; LMM:  $\chi^2=16.9$ ,  $P<0.001$ ). However, while adult dottybacks with an  $A_1$ -fitted LWS had a significantly higher  $\Delta S$  compared with juvenile dottybacks (pairwise *post hoc* Tukey contrast:  $z=-4.2$ ,  $P<0.001$ ), this difference was not apparent when using the broad LWS spectrum (pairwise *post hoc* Tukey contrast:  $z=-0.1$ ,  $P=0.1$ ; Fig. 6E).

From the perspective of the predatory coral trout, we found that when perceived against different habitat backgrounds, there was a

significant difference between juvenile and adult dottybacks for colour ( $\Delta S$ : LM, dottyback colour $\times$ habitat type, trichromat:  $F_{2,134}=134.9$ ,  $P<0.001$ ; dichromat:  $F_{2,134}=124.2$ ,  $P<0.001$ ) and luminance contrast ( $\Delta L$ : LM, dottyback colour $\times$ habitat type, trichromat:  $F_{2,134}=55.0$ ,  $P<0.001$ ; dichromat:  $F_{2,134}=48.4$ ,  $P<0.001$ ; Fig. 6F). While adult yellow and brown morphs have previously been shown to match their habitat (yellow on live coral and brown on coral rubble; Cortesi et al., 2015a), we found no difference in colour and luminance contrast for juveniles against either habitat type ( $\Delta S$  and  $\Delta L$  values as well as pairwise *post hoc* Tukey contrast tests are summarized in Table 2; Fig. 6F). However, although using different chromaticity models did not change our conclusions and  $\Delta L$  remained similar between models,  $\Delta S$  was consistently lower for the dichromatic models than for the trichromatic models (Table 2, Fig. 6F).

### DISCUSSION

Using a multidisciplinary approach, we show that dottybacks experience two major ontogenetic habitat shifts, which are associated with multi-trait developmental modifications. Starting their life as translucent larvae, dottybacks are likely to be well camouflaged within the open water of the pelagic environment. Upon returning to the reef to settle, larvae quickly become pigmented and adopt a coloration that, independent of the habitat background, appears cryptic from the perspective of their predators. The smallest adult dottybacks from our study were  $\sim 43$  mm, which coincides with the predicted minimum size at which dottybacks are capable of feeding on juvenile fish prey (Holmes and McCormick, 2010; Fig. 1A). Hence, adopting their characteristic mimic coloration at this ontogenetic stage is likely to deliver substantial fitness benefits in terms of deceiving and capturing prey, and – at the same time – maintaining cryptic benefits due to model-associated habitat specialization (see also Cortesi et al., 2015a, for further details on multiple fitness benefits of this mimicry system).

**Table 2. Summary of the chromatic and luminance (achromatic) contrast between dottyback ontogenetic stages when perceived against different habitat backgrounds by the coral trout, *Plectropomus leopardus***

Background	Visual system	Developmental stage	$\Delta S$	$t$	$P$	$\Delta L$	$t$	$P$
Live coral	Trichromatic	Adult (yellow)	0.6 $\pm$ 0.1	–13.1	<0.001	0.3 $\pm$ 0.04	–8.9	<0.001
		Adult (brown)	2.5 $\pm$ 0.1			1.0 $\pm$ 0.1		
	Dichromatic	Adult (yellow)	0.4 $\pm$ 0.1	–12.6	<0.001	0.3 $\pm$ 0.04	–8.2	<0.001
		Adult (brown)	1.6 $\pm$ 0.1			1.0 $\pm$ 0.1		
Coral rubble	Trichromatic	Adult (yellow)	2.1 $\pm$ 0.1	10.0	<0.001	0.8 $\pm$ 0.1	5.9	<0.001
		Adult (brown)	0.7 $\pm$ 0.1			0.4 $\pm$ 0.05		
	Dichromatic	Adult (yellow)	1.3 $\pm$ 0.1	9.7	<0.001	0.8 $\pm$ 0.1	5.4	<0.001
		Adult (brown)	0.4 $\pm$ 0.04			0.4 $\pm$ 0.05		
Live coral	Trichromatic	Adult (yellow)	0.6 $\pm$ 0.1	–4.1	0.001	0.3 $\pm$ 0.04	–0.8	1.0
		Juvenile (grey)	1.6 $\pm$ 0.4			0.3 $\pm$ 0.1		
	Dichromatic	Adult (yellow)	0.4 $\pm$ 0.1	–4.0	0.001	0.3 $\pm$ 0.04	–0.7	1.0
		Juvenile (grey)	1.0 $\pm$ 0.2			0.3 $\pm$ 0.1		
Coral rubble	Trichromatic	Adult (brown)	0.7 $\pm$ 0.1	1.6	0.6	0.4 $\pm$ 0.05	0.7	1.0
		Juvenile (grey)	1.1 $\pm$ 0.3			0.4 $\pm$ 0.1		
	Dichromatic	Adult (brown)	0.4 $\pm$ 0.04	1.4	0.7	0.4 $\pm$ 0.05	0.5	1.0
		Juvenile (grey)	0.6 $\pm$ 0.2			0.4 $\pm$ 0.1		
Live coral	Trichromatic	Juvenile (grey)	1.6 $\pm$ 0.4	–1.6	0.6	0.3 $\pm$ 0.1	0.6	1.0
Coral rubble	Dichromatic		1.1 $\pm$ 0.3	–1.8	0.5	0.4 $\pm$ 0.1	0.5	1.0
Live coral			1.0 $\pm$ 0.2			0.3 $\pm$ 0.1		
Coral rubble			0.6 $\pm$ 0.2			0.4 $\pm$ 0.1		

*Plectropomus leopardus* visual system was modelled as trichromatic or dichromatic.

Note that modelling the coral trout as either a dichromat or a trichromat did not change the overall results. However, while luminance contrast values ( $\Delta L$ , means $\pm$ s.e.m.) stayed consistent, chromatic contrast values ( $\Delta S$ , means $\pm$ s.e.m.) were always lower for the dichromatic compared with the trichromatic models. Tukey *post hoc* tests.

Interestingly, we found that the type of chromatophore within the skin of dottybacks changes throughout ontogeny. Smaller juveniles have a combination of erythrophores, xanthophores and melanophores, while larger juveniles and adults lose erythrophores, and instead possess low numbers of mosaic cells containing both yellow and black pigments. Note, however, that the occurrence of adult orange dottyback morphs in Papua New Guinea indicates that, in some populations, erythrophores may be maintained throughout ontogeny (Messmer et al., 2005). Furthermore, as erythrophores and xanthophores are characterized by their carotenoid (red/orange)- and/or pteridine (yellow)-derived coloration (Fujii, 1993; Skögl et al., 2016), dottybacks may only possess one ‘red–yellow’ chromatophore type. Changes in hue of this chromatophore could then be achieved by varying the amount and/or type of pigment within the cell. Such trans-differentiation of chromatophore cells is a rarely described phenomenon in fish (Leclercq et al., 2009), but could also explain the mosaic cells we found in larger dottybacks. If cells were able to change their pigment content, then the non-developmental colour changes in adult mimics (Cortesi et al., 2015a) could occur without having to invest in the production of novel cellular structures. However, chromatographic approaches are needed to unambiguously distinguish between chromatophore types and pigment contents thereof in dottybacks.

The visual systems of coral reef fish larvae often undergo major morphological changes when the fish return to the reef and metamorphose into their juvenile phenotypes (Evans and Browman, 2004; Evans and Fernald, 1990). Generally, early-stage larvae possess a pure cone retina and are sensitive to shorter wavelengths of light, which is ideal for a life in a well-lit epipelagic environment (Britt et al., 2001; Evans and Browman, 2004; Evans and Fernald, 1990; Hunt et al., 2014). Our study did not include larval dottybacks from their early planktonic stages, which could explain why we only found very low levels or no expression of the shorter SWS (*SWS1* ‘UV’ and *SWS2B* ‘violet’) and MWS (*RH2B* ‘blue–green’) pigments. What we found instead is that at the time when dottyback larvae return from the pelagic environment, they possess a fully developed retina containing all photoreceptor types (single cones, twin cones and rods) that are also present in adults. These photoreceptors mainly express three longer-wavelength shifted cone opsins (*SWS2A $\beta$* , *RH2A $\alpha$* , *LWS*), theoretically providing settlement-stage fish with the ability to see colours likely to be necessary for survival on the reef (Evans and Fernald, 1990).

Using qRT-PCR, we showed that juvenile dottybacks change to an adult visual system when reaching ~25 mm, thereby predating the ontogenetic colour change and juvenile to adult habitat transition, which only occurs when dottybacks are substantially larger (~43 mm). While it has previously been shown that dottybacks express an additional blue opsin gene as adults (*SWS2A $\alpha$* ; Cortesi et al., 2015b), we found that, just like in cichlids (Spady et al., 2006) and black bream, *Acanthopagrus butcheri* (Shand et al., 2008), larger dottybacks in addition start to express a second green opsin within their retina (*RH2A $\beta$* ; Fig. 1; Fig. S2). Strikingly, the synteny of green genes, while unknown for black bream, is alike in dottybacks and cichlids, with the *RH2A $\alpha$*  gene occurring in a prominent reversed orientation between the upstream *RH2B* and the downstream *RH2A $\beta$*  genes (O’Quin et al., 2011; Fig. 5). However, it remains to be investigated whether these findings are instances of convergence or whether it is a more commonly occurring pattern in fishes that possess multiple *RH2A* genes, such as the Japanese rice fish, *Oryzias latipes* (Matsumoto et al., 2006), or the tiger rockfish, *Sebastes nigrocinctus* (Fig. 5).

Interestingly, in adult dottybacks, *RH2A $\beta$*  was found to be the highest expressed twin cone gene, but pure *RH2A $\beta$*  pigment was only found in two out of 43 cells. This suggests that the large absorbance spectra in the adult LWS twin cones may derive from the co-expression of *RH2A $\beta$*  with *LWS* (*RH2A $\beta$*  with *RH2A $\alpha$*  in the case of the MWS twin cone). The proposed dottyback scenario of co-expression involving two orthologous green genes (*RH2A*) with a difference in  $\lambda_{\text{max}}$  of ~10 nm and a longer shifted red gene (*LWS*), has recently been reported for the freshwater cichlid *Metriactila zebra* (Dalton et al., 2014). In *M. zebra*, co-expressing multiple visual pigments within a single photoreceptor significantly enhances luminance discrimination, but the drawback seems to be a decrease in chromatic colour discrimination (Dalton et al., 2014). In support of these findings, we found a very similar pattern when modelling dottyback and coral trout visual tasks using the broad absorbance spectra instead of  $A_1$ -based visual templates. This suggests that pigment co-expression may serve a common function even across very distantly related species, which raises the question whether opsin co-expression has a long-lasting evolutionary history in fishes?

An alternative to opsin co-expression would be that both the dottyback and coral trout twin cone outer segments contained a mixture of  $A_1$  and  $A_2$  chromophores, something that has previously been found to cause broad absorbance spectra in frogs (Reuter et al., 1971). However, so far there are very few (if any) coral reef fishes that have been reported to contain  $A_2$  chromophores within their photoreceptors (e.g. Toyama et al., 2008). Moreover, given that for both species the rod and SWS cones and in the dottyback also the ‘normal’ MWS and LWS cones are fitted by  $A_1$  templates, it is unlikely that the broad spectra are due to chromophore mixtures. Nevertheless, methods such as *in situ* hybridization, gene knock-out approaches or chromophore extractions are necessary to unambiguously assess whether the broad spectra are caused by pigment co-expression or by chromophore mixtures.

Finally, the visual models showed that adult dottybacks might have an increased ability to distinguish between the colorations of the damselfishes they mimic compared with juvenile dottybacks, at least when relying on pure  $A_1$ -based LWS photoreceptors. Having excellent colour discrimination could be essential for dottybacks to determine the differences between the fishes they are going to mimic, which might partly explain why juvenile dottybacks switch their visual system well before ontogenetic colour changes take place. Interestingly, it has recently been observed that opsins are also expressed in a variety of non-eye tissues of fishes including the skin, where they are thought to mediate colour change via chromatophore light sensing (e.g. Chen et al., 2013; Davies et al., 2015). Whether the dottybacks also express opsins in their skin and how light sensing may contribute to colour change in this species warrants further investigation.

Using theoretical visual models as well as modelling only a few visual tasks, however, has its limitations. The assumption that juvenile dottybacks are trichromatic while adults are tetrachromatic, or, for that matter, that the coral trout is either dichromatic or trichromatic, needs to be verified by behavioural experimentation. Moreover, the models show that both juvenile and adult dottybacks should have colour vision and behavioural experiments are therefore needed to establish the significance (if any) of the changes in colour discrimination between different developmental stages. This is important because it is currently not understood what a change in JND beyond the discrimination threshold of 1 signifies for the animal, and whether the discrimination threshold varies depending on direction and position in colour space. Finally, behavioural



experiments are also needed to test the role putative opsin co-expression may play for vision in these species.

In conclusion, despite the evolutionary importance of ontogenetic habitat shifts, detailed studies investigating the triggers for the transitions and how these interrelate with multi-trait developmental adaptations remain scarce. Here, we examined ontogenetic habitat transitions in the dusky dotyback, an enigmatic mimic with the ability to imitate differently coloured model species in its surroundings. We show that dotybacks start their lives well camouflaged within their respective habitats and while their visual systems quickly adapt to a lifestyle on coral reefs, changes to their mimic adult coloration and associated habitat specialization only occur once dotybacks are big enough to feed on juvenile fish prey. Therefore, our study highlights the importance of comparative approaches to understand how species adapt and evolve to an ever-changing environment.

#### Acknowledgements

We would like to thank Eva C. McClure, Peter A. Waldie and William E. Feeney for assistance in the field, Mark McCormick and Mark Meekan for the use of light traps, and the staff at the Lizard Island Research Station for logistical help. We would furthermore like to thank the members of the Teleost Genome Project at CEES, University of Oslo, for providing unpublished raw sequence reads, and two anonymous referees for valuable suggestions.

#### Competing interests

The authors declare no competing or financial interests.

#### Author contributions

F.C. conceived the study and designed the experiments together with N.J.M., K.L.C. and W.S. F.C., Z.M., S.M.S., N.S.H. and U.E.S. performed the experiments and analysed the data. F.C., Z.M., K.L.C., W.S. and N.J.M. wrote the initial manuscript. All authors reviewed and approved the final version of the manuscript.

#### Funding

F.C. was supported by an Australian Endeavour Research Fellowship (2012), Schweizerischer Nationalfonds zur Förderung der Wissenschaftlichen Forschung Doctoral Mobility and Early Postdoctoral Mobility Fellowships (148460; 165364), and a Doctoral Fellowship (2013) from the Lizard Island Research Station, a facility of the Australian Museum; Z.M. was supported by Novartis – Universität Basel Excellence Scholarship for Life Sciences; S.M.S. was supported by the German Academic Exchange Service (Deutscher Akademischer Austauschdienst) (2012–2014); N.S.H. was supported by an Australian Research Council QEII Research Fellowship (DP0558681); U.E.S. was supported by an Australian Research Council APD Fellowship (DP557285); K.L.C. was supported by the University of Queensland and the Australian Research Council; W.S. was supported by the Schweizerischer Nationalfonds zur Förderung der Wissenschaftlichen Forschung and the European Research Council; and N.J.M. was supported by the Australian Research Council.

#### Data availability

#### Supplementary information

Supplementary information available online at <http://jeb.biologists.org/lookup/doi/10.1242/jeb.139501.supplemental>

#### References

- Bagnara, J. T. and Hadley, M. E. (1973). *Chromatophores and Color Change: The Comparative Physiology of Animal Pigmentation*. Englewood Cliffs, USA: Prentice-Hall.
- Balon, E. K. (1975). Terminology of intervals in fish development. *J. Fish. Res. Board. Can.* **32**, 1663–1670.
- Bates, D., Mächler, M., Bolker, B. and Walter, S. (2015). Fitting linear mixed-effects models using lme4. *J. Stat. Softw.* **67**, 1–48.
- Boileau, N., Cortesi, F., Egger, B., Muschick, M., Indermaur, A., Theis, A., Büscher, H. H. and Salzburger, W. (2015). A complex mode of aggressive mimicry in a scale-eating cichlid fish. *Biol. Lett.* **11**, 20150521.
- Booth, C. L. (1990). Evolutionary significance of ontogenetic colour change in animals. *Biol. J. Linn. Soc.* **40**, 125–163.
- Britt, L. L., Loew, E. R. and McFarland, W. N. (2001). Visual pigments in the early life stages of Pacific northwest marine fishes. *J. Exp. Biol.* **204**, 2581–2587.
- Carleton, K. L. and Kocher, T. D. (2001). Cone opsin genes of african cichlid fishes: tuning spectral sensitivity by differential gene expression. *Mol. Biol. Evol.* **18**, 1540–1550.
- Chen, S.-C., Robertson, R. M. and Hawryshyn, C. W. (2013). Possible involvement of cone opsins in distinct photoresponses of intrinsically photosensitive dermal chromatophores in tilapia *Oreochromis niloticus*. *PLoS ONE* **8**, e70342.
- Cheney, K. L., Cortesi, F., How, M. J., Wilson, N. G., Blomberg, S. P., Winters, A. E., Umantzör, S. and Marshall, N. J. (2014). Conspicuous visual signals do not coevolve with increased body size in marine sea slugs. *J. Evol. Biol.* **27**, 676–687.
- Childress, M. J. and Herrnkind, W. F. (2001). Influence of conspecifics on the ontogenetic habitat shift of juvenile Caribbean spiny lobsters. *Mar. Freshwater Res.* **52**, 1077–1084.
- Collin, S. P. and Marshall, N. J. (2003). *Sensory Processing in Aquatic Environments*. New York, USA: Springer-Verlag.
- Cortesi, F., Feeney, W. E., Ferrari, M. C. O., Waldie, P. A., Phillips, G. A. C., McClure, E. C., Sköld, H. N., Salzburger, W., Marshall, N. J. and Cheney, K. L. (2015a). Phenotypic plasticity confers multiple fitness benefits to a mimic. *Curr. Biol.* **25**, 949–954.
- Cortesi, F., Musilová, Z., Stieb, S. M., Hart, N. S., Siebeck, U. E., Malmström, M., Tørresen, O. K., Jentoft, S., Cheney, K. L., Marshall, N. J. et al. (2015b). Ancestral duplications and highly dynamic opsin gene evolution in percomorph fishes. *Proc. Natl. Acad. Sci. USA* **112**, 1493–1498.
- Dahlgren, C. P. and Eggleston, D. B. (2000). Ecological processes underlying ontogenetic habitat shifts in a coral reef fish. *Ecology* **81**, 2227–2240.
- Dalton, B. E., Loew, E. R., Cronin, T. W. and Carleton, K. L. (2014). Spectral tuning by opsin coexpression in retinal regions that view different parts of the visual field. *Proc. R. Soc. B Biol. Sci.* **281**, 20141980.
- Darriba, D., Taboada, G. L., Doallo, R. and Posada, D. (2012). jModelTest2: more models, new heuristics and parallel computing. *Nat. Methods* **9**, 772–772.
- Davies, W. I. L., Tamai, T. K., Zheng, L., Fu, J. K., Rihel, J., Foster, R. G., Whitmore, D. and Hankins, M. W. (2015). An extended family of novel vertebrate photopigments is widely expressed and displays a diversity of function. *Genome Res.* **25**, 1666–1679.
- Evans, B. I. and Browman, H. I. (2004). Variation in the development of the fish retina. In *Development of Form and Function in Fishes, and the Question of Larval Adaptation* (ed. J. J. Govoni), pp. 145–166. Bethesda, MD: American Fisheries Society Symposium 40.
- Evans, B. I. and Fernald, R. D. (1990). Metamorphosis and fish vision. *J. Neurobiol.* **21**, 1037–1052.
- Fujii, R. (1993). Cytophysiology of fish chromatophores. In *International Review of Cytology* (ed. W. Kwang, M. F. Jeon and J. Jonathan), pp. 191–255. San Diego, USA: Academic Press.
- Grant, J. B. (2007). Ontogenetic colour change and the evolution of aposmatism: a case study in panic moth caterpillars. *J. Anim. Ecol.* **76**, 439–447.
- Hart, N. S., Theiss, S. M., Harahush, B. K. and Collin, S. P. (2011). Microspectrophotometric evidence for cone monochromacy in sharks. *Naturwissenschaften* **98**, 193–201.
- Holmes, T. H. and McCormick, M. I. (2010). Size-selectivity of predatory reef fish on juvenile prey. *Mar. Ecol. Prog. Ser.* **399**, 273–283.
- Hunt, D. M., Hankins, M. W., Collin, S. P. and Marshall, N. J. (2014). *Evolution of Visual and Non-visual Pigments*. New York: Springer.
- Katoh, K. and Toh, H. (2008). Recent developments in the MAFFT multiple sequence alignment program. *Brief. Bioinform.* **9**, 286–298.
- Kodric-Brown, A. (1998). Sexual dichromatism and temporary color changes in the reproduction of fishes. *Am. Zool.* **38**, 70–81.
- Kuiter, R. H. (2004). *Basslets, Hamlets and Their Relatives: A Comprehensive Guide to Selected Serranidae and Plesiopidae*. London: TMC Publishing.
- Leclercq, E., Taylor, J. F. and Migaud, H. (2009). Morphological skin colour changes in teleosts. *Fish Fish.* **11**, 159–193.
- Mano, H., Kojima, D. and Fukada, Y. (1999). Exo-rhodopsin: a novel rhodopsin expressed in the zebrafish pineal gland. *Mol. Brain Res.* **73**, 110–118.
- Marshall, N. J. (2000). The visual ecology of reef fish colors. In *Animal Signals Signalling and Signal Design in Animal Communication* (ed. Y. Espmark, T. Amundsen and G. Rosenqvist), pp. 83–120. Trondheim, Norway: Akademika Publishing.
- Matsumoto, Y., Fukamachi, S., Mitani, H. and Kawamura, S. (2006). Functional characterization of visual opsin repertoire in Medaka (*Oryzias latipes*). *Gene* **371**, 268–278.
- McFall-Ngai, M. J. (1990). Cypsis in the pelagic environment. *Am. Zool.* **30**, 175–188.
- Messmer, V., van Herwerden, L., Munday, P. L. and Jones, G. P. (2005). Phylogeography of colour polymorphism in the coral reef fish *Pseudochromis fuscus*, from Papua New Guinea and the Great Barrier Reef. *Coral Reefs* **24**, 392–402.
- Michael, S. W. (2004). *Basslets, Dotybacks & Hawkfishes: Plus Seven More Aquarium Fish Families with Expert Captive Care Advice for the Marine Aquarist*. Neptune City, NJ: T. F. H. Publications.

- Miller, M. A., Pfeiffer, W. and Schwartz, T. (2010). Creating the CIPRES Science Gateway for inference of large phylogenetic trees. Gateway Computing Environments Workshop (GCE), IEEE, 1–8.
- Moland, E., Eagle, J. V. and Jones, G. P. (2005). Ecology and evolution of mimicry in coral reef fishes. In *Oceanography and Marine Biology: An Annual Review* (ed. R. N. Gibson, J. D. M. Gordon and R. J. A. Atkinson), pp. 455–482. Boca Raton, FL: CRC Press.
- Munday, P. L., Eyre, P. J. and Jones, G. P. (2003). Ecological mechanisms for coexistence of colour polymorphism in a coral-reef fish: an experimental evaluation. *Oecologia* **137**, 519–526.
- O'Quin, K. E., Smith, D., Naseer, Z., Schulte, J., Engel, S. D., Loh, Y.-H. E., Streelman, J. T., Boore, J. L. and Carleton, K. L. (2011). Divergence in cis-regulatory sequences surrounding the opsin gene arrays of African cichlid fishes. *BMC Evol. Biol.* **11**, 120.
- Pignatelli, V., Champ, C., Marshall, J. and Vorobyev, M. (2010). Double cones are used for colour discrimination in the reef fish, *Rhinecanthus aculeatus*. *Biol. Lett.* **6**, 537–539.
- R Core Team (2013). *R: A Language and Environment for Statistical Computing*. Vienna, Austria: R foundation for statistical computing, <http://www.R-project.org/>.
- Rennison, D. J., Owens, G. L. and Taylor, J. S. (2012). Opsin gene duplication and divergence in ray-finned fish. *Mol. Phylogenet. Evol.* **62**, 986–1008.
- Reuter, T. E., White, R. H. and Wald, G. (1971). Rhodopsin and porphyropsin fields in the adult bullfrog retina. *J. Gen. Physiol.* **58**, 351–371.
- Ronquist, F., Teslenko, M., van der Mark, P., Ayres, D. L., Darling, A., Höhna, S., Larget, B., Liu, L., Suchard, M. A. and Huelsenbeck, J. P. (2012). MrBayes 3.2: efficient Bayesian phylogenetic inference and model choice across a large model space. *Syst. Biol.* **61**, 539–542.
- Sale, P. F. (1993). *The Ecology of Fishes on Coral Reefs*. San Diego, USA: Academic Press, Inc.
- Shand, J., Davies, W. L., Thomas, N., Balmer, L., Cowing, J. A., Pointer, M., Carvalho, L. S., Trezise, A. E. O., Collin, S. P. and Beazley, L. D. (2008). The influence of ontogeny and light environment on the expression of visual pigment opsins in the retina of the black bream, *Acanthopagrus butcheri*. *J. Exp. Biol.* **211**, 1495–1503.
- Siebeck, U. E. and Marshall, N. J. (2001). Ocular media transmission of coral reef fish - can coral reef fish see ultraviolet light? *Vision Res.* **41**, 133–149.
- Siebeck, U. E., Wallis, G. M., Litherland, L., Ganeshina, O. and Vorobyev, M. (2014). Spectral and spatial selectivity of luminance vision in reef fish. *Front. Neural Circuits* **8**, 118.
- Sköld, H. N., Aspöngren, S., Cheney, K. L. and Wallin, M. (2016). Fish chromatophores—from molecular motors to animal behavior. In *International Review of Cell and Molecular Biology* (ed. W. J. Kwang), pp. 171–219. San Diego, USA: Academic Press, Inc.
- Spady, T. C., Parry, J. W. L., Robinson, P. R., Hunt, D. M., Bowmaker, J. K. and Carleton, K. L. (2006). Evolution of the cichlid visual palette through ontogenetic subfunctionalization of the opsin gene arrays. *Mol. Biol. Evol.* **23**, 1538–1547.
- St John, J. (1999). Ontogenetic changes in the diet of the coral reef grouper *Plectropomus leopardus* (Serranidae): patterns in taxa, size and habitat of prey. *Mar. Ecol. Prog. Ser.* **180**, 233–246.
- Stavenga, D. G., Smits, R. P. and Hoenders, B. J. (1993). Simple exponential functions describing the absorbance bands of visual pigment spectra. *Vision Res.* **33**, 1011–1017.
- Stieb, S. M., Carleton, K. L., Cortesi, F., Marshall, N. J. and Salzburger, W. (2016). Depth dependent plasticity in opsin gene expression varies between damselfish (Pomacentridae) species. *Mol. Ecol.* doi:10.1111/mec.13712.
- Toyama, M., Hironaka, M., Yamahama, Y., Horiguchi, H., Tsukada, O., Uto, N., Ueno, Y., Tokunaga, F., Seno, K. and Hariyama, T. (2008). Presence of rhodopsin and porphyropsin in the eyes of 164 fishes, representing marine, diadromous, coastal and freshwater species—a qualitative and comparative study. *J. Photochem. Photobiol.* **84**, 996–1002.
- Vorobyev, M. and Osorio, D. (1998). Receptor noise as a determinant of colour thresholds. *Proc. R. Soc. B Biol. Sci.* **265**, 351–358.
- Vorobyev, M., Brandt, R., Peitsch, D., Laughlin, S. B. and Menzel, R. (2001). Colour thresholds and receptor noise: behaviour and physiology compared. *Vision Res.* **41**, 639–653.
- Youson, J. H. (1988). First metamorphosis. In *The Physiology of Developing Fish: Volume 11B: Viviparity and Posthatching Juveniles* (ed. W. S. Hoar and D. J. Randall), pp. 135–194. San Diego, USA: Academic Press, Inc.

## SUPPLEMENTARY FIGURES

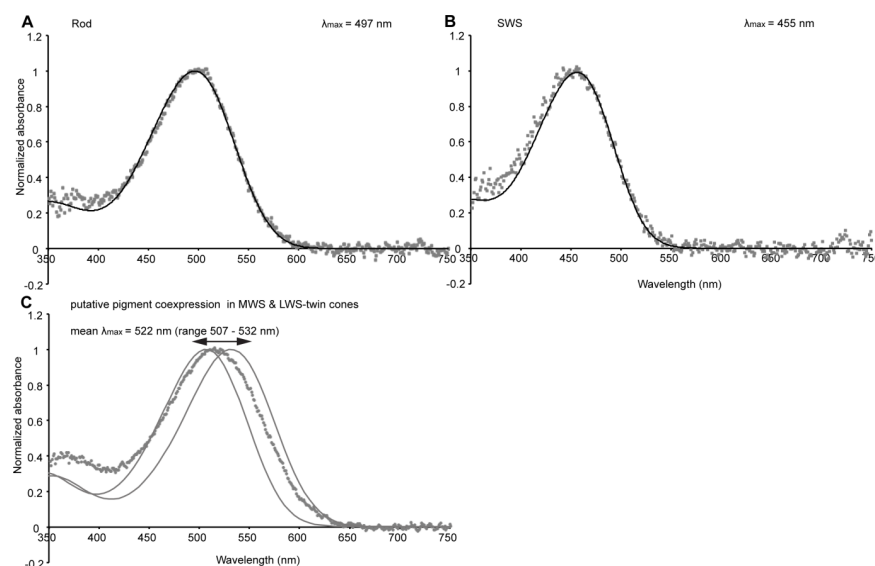


**Fig. S1. Normalized pre-bleach absorbance spectra of the coral trout visual pigments (measured with MSP).** (A) The visual pigment found in the rod photoreceptor used for scotopic vision ( $n = 22$ ), (B) the 'blue' SWS single cone ( $n = 10$ ), (C) the mean of the broad absorbance spectra found in the twin cones (MWS and LWS) and thought to be the result of a coexpression of two visual pigments with a range of 507 – 532 nm  $\lambda_{\text{max}}$  ( $n = 48$ ). Spectra are fitted with Vitamin A1 rhodopsin templates of the appropriate  $\lambda_{\text{max}}$  calculated using the equations of Stavenga et al., 1993. Note that in (C) no visual templates were fitted, instead the A1 based visual templates for 507 nm and 532 nm  $\lambda_{\text{max}}$  are shown in grey.

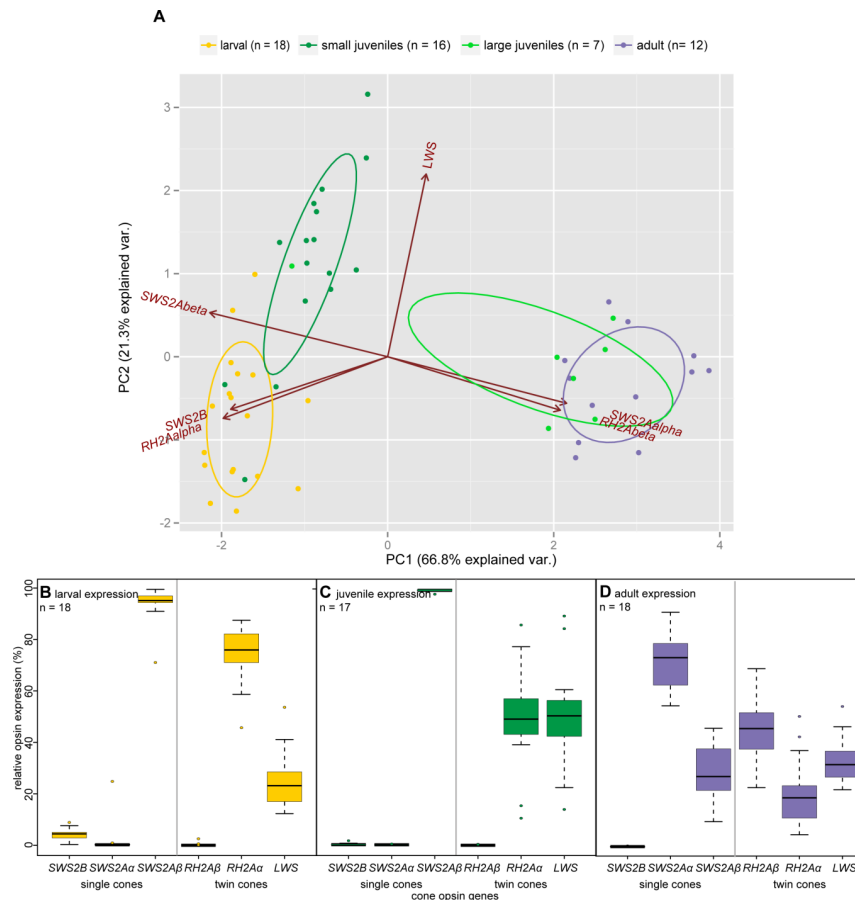


**Fig. S2. Difference in opsin gene expression throughout dottyback ontogeny.**

(A) A principle component analysis (PCA) shows dottyback cone opsin expression of larvae prior to settlement and one day post settlement (dps) in yellow (n = 18), small juveniles (7 – 9 dps and 34 dps) in dark green (n = 16), large juveniles in bright green (n = 7), and adults in violet (n = 12). The lines indicate differences in gene expression between individuals, separating ontogenetic stages into three distinct expression profiles: (B) larval-expression (n = 18), (C) juvenile-expression (n = 17), and (D) adult expression (n = 18). Note that the smallest of the large juveniles at 19 mm standard length (SL) clusters together with individuals of the juvenile-expression profile, while the remaining large juveniles (> 26 mm SL) already show an adult-expression profile. Gene expression was calculated for single and twin cone genes separately.

**Table S1. Spectral characteristics of visual pigment found in the scotopic rod, and the photopic single cone and twin cone photoreceptors of the coral trout, *Plectropomus leopardus*.** Both twin cone members showed broad absorbance spectra that are likely to be caused by pigment coexpression within outer segments with a range of 507 – 532 nm  $\lambda_{\text{max}}$  (also see discussion in the main article; Fig. S1).

	single cone	twin cone	rod
Morphological distinction	SWS	broad spectra (coexpression?) MWS & LWS	
$\lambda_{\text{max}}$ mean $\pm$ s.e.			
pre-bleach absorbance spectra (nm)	455.4 $\pm$ 0.7	522.1 $\pm$ 0.9	496.5 $\pm$ 0.6
difference spectra (nm)	457.3 $\pm$ 1.6	522.8 $\pm$ 1.1	501.9 $\pm$ 1.2
no. cells pre-bleach/difference spectra	10 / 11	48 / 39	22 / 23

**Table S2. qRT-PCR and pool primers used in this study**

method	gene (efficiency)	primer name	orientation	primer sequence
qRT_PCR	<i>SWS1</i> (90%) qPCR primers	<i>Pfus SWS1 2F</i> <i>Pfus SWS1 23R</i>	forward reverse	TTTGGAGCCTTCAAGTTCACCAG GATGTACCTGCTCCAGCCAAAG
qRT_PCR	<i>SWS2B</i> (94%) qPCR primers	<i>Pfus SWS2B 1F1</i> <i>Pfus SWS2B 12R1</i>	forward reverse	CCGTGGGCTCCTTCACCTG GGCTCACCATGCCTCCAATC
qRT_PCR	<i>SWS2Aa</i> (96%) qPCR primers	<i>Pfus SWS2Aalfa 12F1</i> <i>Pfus SWS2Aalfa 2R1</i>	forward reverse	CATGGCAACACTCGGGGGTATG CGCAAACACCCAGGTGAACC
qRT_PCR	<i>SWS2Ab</i> (96%) qPCR primers	<i>Pfus SWS2Abeta 1F2</i> <i>Pfus SWS2Abeta 12R1</i>	forward reverse	GGTGAACCTGGCTGCCGCG CCATACCTCCAAGTGTGCTAC
qRT_PCR	<i>RH2B</i> (91%) qPCR primers	<i>Pfus RH2B 23R new</i> <i>Pfus RH2B 2F new</i>	forward reverse	TGTACCTCGACCAGCCACC TGTGGTCTGTAAACCTATGGGC
qRT_PCR	<i>RH2Aa</i> (tba) qPCR primers	<i>qPCR RH2Aa ex4 F1</i> <i>qPCR RH2Aa ex45 R1</i>	forward reverse	GCTGCCTTACCGCCCTC GTCAGCATGCAGTTACGGAAC
qRT_PCR	<i>RH2Ab</i> (tba) qPCR primers	<i>qRH2Abeta ex2 F1</i> <i>qRH2Abeta ex23 R1</i>	forward reverse	GGAGCTTCAAGTTCGGTGGAT ATGTACCTGGACCAGCCAGC
qRT_PCR	<i>LWS</i> (91%) qPCR pool	<i>PFus LWS 34 F1</i> <i>PFus LWS 4 R1</i>	forward reverse	TGTCTCAACCTGTGGTATTACTGC GGATCCACCTGTGGCCCAT
Sanger sequencing	<i>SWS1</i> qPCR pool	<i>POOL Pfus SWS1 F</i> <i>SWS1 R2d dam</i>	forward reverse	CTGTGTGCCATGGAGTCTGCC TCGTTGTGGGTGTACCAGTC
Sanger sequencing	<i>SWS2B</i> qPCR pool	<i>POOL Pfus SWS2B F</i> <i>POOL Pfus SWS2B R</i>	forward reverse	GTGACTGGTACTGCCATCAATATC AACGATGGTGAAGAAGGGGATGGAA
Sanger sequencing	<i>SWS2Aa</i> qPCR pool	<i>POOL Pfus SWS2Aalfa F</i> <i>POOL Pfus SWS2Aalfa R</i>	forward reverse	CTCACTATTGCATGCACCGCC GCCCATGCCAGCATCGCT
Sanger sequencing	<i>SWS2Ab</i> qPCR pool	<i>POOL Pfus SWS2Abeta F</i> <i>POOL Pfus SWS2Abeta R</i>	forward reverse	CTTACC GTTGCATGCACCGTG TCCACTCATCCCCAGCATCTTC
Sanger sequencing	<i>RH2B</i> qPCR pool	<i>RH2B F2 Fuscus</i> <i>Rh2B R2c dam</i>	forward reverse	TTA TCCTGGTTAACTTGGC ATCACATAGGATTCTGTGTG
Sanger sequencing	<i>RH2Aa</i> qPCR pool	<i>poolRH2Aalpha ex1 F1</i> <i>poolRH2Aalpha ex5 R1</i>	forward reverse	TCCAACAGGACTGGGATAAC CCATCCCAATAGTCGTCAG
Sanger sequencing	<i>RH2Ab</i> qPCR pool	<i>poolRH2Abeta ex1 F1</i> <i>poolRH2Abeta ex5 R1</i>	forward reverse	CCAACAGGACGGGGATTGT GCCACCATTCCTCAATAGTG
Sanger sequencing	<i>LWS</i> qPCR pool	<i>LWS R4dFin dam</i> <i>LWS F6d dam</i>	forward reverse	CCCCAAACGAAGAACATGGA AAGTTCAAGAACTCCGTCA



## Chapter 3

# Ancestral duplications and highly dynamic opsin gene evolution in percomorph fishes

F. Cortesi<sup>†</sup>, Z. Musilová<sup>†</sup>, S. M. Stieb, N. S. Hart, U.E. Siebeck,  
M. Malmstrøm, O. K. Tørresen, S. Jentoft, K. L. Cheney,  
N. J. Marshall, K. L. Carleton, W. Salzburger

Proceedings of the National Academy of Sciences of the  
United States of America (2015)

3.1. Manuscript p. 67 – 72

3.2. Supporting Information & commentary p. 73 – 88

3.3. Commentary by Harris R.M. & Hofmann H.A p. 89 - 90





# Ancestral duplications and highly dynamic opsin gene evolution in percomorph fishes

Fabio Cortesi<sup>a,b,c,1,2</sup>, Zuzana Musilová<sup>a,1,2</sup>, Sara M. Stieb<sup>a,c</sup>, Nathan S. Hart<sup>d,e</sup>, Ulrike E. Siebeck<sup>f</sup>, Martin Malmström<sup>g</sup>, Ole K. Tørresen<sup>g</sup>, Sissel Jentoft<sup>g</sup>, Karen L. Cheney<sup>b</sup>, N. Justin Marshall<sup>c</sup>, Karen L. Carleton<sup>h</sup>, and Walter Salzburger<sup>a,g</sup>

<sup>a</sup>Zoological Institute, University of Basel, Basel 4051, Switzerland; Schools of <sup>b</sup>Biological Sciences and <sup>c</sup>Biomedical Sciences and <sup>d</sup>Queensland Brain Institute, The University of Queensland, Brisbane 4072, Australia; <sup>e</sup>School of Animal Biology and <sup>f</sup>The Oceans Institute, The University of Western Australia, Crawley 6009, Australia; <sup>g</sup>Centre for Ecological and Evolutionary Synthesis, Department of Biosciences, University of Oslo, Oslo 0316, Norway; and <sup>h</sup>Department of Biology, University of Maryland, College Park, MD 20742

Edited by Trudy F. C. Mackay, North Carolina State University, Raleigh, NC, and approved November 20, 2014 (received for review September 15, 2014)

Single-gene and whole-genome duplications are important evolutionary mechanisms that contribute to biological diversification by launching new genetic raw material. For example, the evolution of animal vision is tightly linked to the expansion of the opsin gene family encoding light-absorbing visual pigments. In teleost fishes, the most species-rich vertebrate group, opsins are particularly diverse and key to the successful colonization of habitats ranging from the bioluminescence-biased but basically dark deep sea to clear mountain streams. In this study, we report a previously unnoticed duplication of the violet-blue short wavelength-sensitive 2 (SWS2) opsin, which coincides with the radiation of highly diverse percomorph fishes, permitting us to reinterpret the evolution of this gene family. The inspection of close to 100 fish genomes revealed that, triggered by frequent gene conversion between duplicates, the evolutionary history of SWS2 is rather complex and difficult to predict. Coincidentally, we also report potential cases of gene resurrection in vertebrate opsins, whereby pseudogenized genes were found to convert with their functional paralogs. We then identify multiple novel amino acid substitutions that are likely to have contributed to the adaptive differentiation between SWS2 copies. Finally, using the dusky dottyback *Pseudochromis fuscus*, we show that the newly discovered SWS2A duplicates can contribute to visual adaptation in two ways: by gaining sensitivities to different wavelengths of light and by being differentially expressed between ontogenetic stages. Thus, our study highlights the importance of comparative approaches in gaining a comprehensive view of the dynamics underlying gene family evolution and ultimately, animal diversification.

gene duplication | gene conversion | gene resurrection | Percomorphs | SWS2

Gene and whole-genome duplications facilitate the acquisition of novel biological functions (1, 2) and are, hence, considered important forces to achieve major evolutionary transitions (3). For example, whole-genome duplications in the respective ancestors of yeast (4), vertebrates (5), and teleost fishes (6) are thought to have laid the genomic foundation for many key characteristics crucial to the evolutionary success of these lineages. More common, however, are single-gene duplications, which often act as a springboard for adaptive diversification of entire gene families as exemplified by the immune-regulatory MHC genes in hominids (7), hemoglobins in tetrapods (8) and bony fishes (9), or opsins in mantis shrimps (10), fishes (11), and primates (12).

Opsins are at the core of animal vision, an important sensory system involved in, for example, food gathering, communication, predator avoidance, mate selection, and navigation. In vertebrates, opsins are expressed primarily in ciliary photoreceptor cells (c-opsins) and encode for G protein-coupled receptors that bind to a light-absorbing, vitamin A-derived nonprotein retinal chromophore (13). The evolution of opsin genes is a prime textbook example of how changes at a molecular level—in the form of duplications (11, 12), mutations (14), and changes in gene

expression (11)—drive adaptation to divergent photic environments (15), which may ultimately lead to speciation (16). In addition, because of the possibility to directly link opsin genotypes to functional visual phenotypes (i.e., spectral sensitivities), opsins are among the best studied and functionally best characterized gene families in vertebrates (15, 17).

Other than rhodopsin (RH1), the rod-based visual pigment often used for scotopic vision, vertebrates possess four basic types of cone opsin genes, which mediate color vision: two short wavelength (UV-blue)-sensitive (SWS) genes (SWS1 and SWS2), a mid-wavelength (green)-sensitive gene (RH2), and a long wavelength (yellow-red)-sensitive gene (LWS) (17). Unlike in tetrapods, where this basic opsin setup remained relatively constant, teleost opsins have duplicated extensively, leading to an astonishing richness of opsin genes (18). Opsins are particularly diverse in spiny-rayed fishes [Acanthomorpha (18)]—with >18,000 species, it is the most species-rich taxon of vertebrates that also includes the highly diverse percomorphs (19).

## Significance

Gene and whole-genome duplications are important evolutionary forces promoting organismal diversification. Teleost fishes, for example, possess many gene duplicates responsible for photoreception (opsins), which emerged through gene duplication and allow fishes to adapt to the various light conditions of the aquatic environment. Here, we reevaluate the evolutionary history of the violet-blue-sensitive opsins [short wavelength-sensitive 2 (SWS2)] in modern teleosts using next generation genome sequencing. We uncover a gene duplication event specific to the most diverse lineage of vertebrates (the percomorphs) and show that SWS2 evolution was highly dynamic and involved gene loss, pseudogenization, and gene conversion. We, thus, clarify previous discrepancies regarding opsin annotations. Our study highlights the importance of integrative approaches to help us understand how species adapt and diversify.

Author contributions: F.C., Z.M., K. L. Carleton, and W.S. designed research; F.C., Z.M., S.M.S., N.S.H., U.E.S., and K. L. Carleton performed research; M.M., O.K.T., and S.J. contributed new reagents/analytic tools; F.C., Z.M., S.M.S., N.S.H., U.E.S., M.M., O.K.T., S.J., K. L. Cheney, N.J.M., and K. L. Carleton analyzed data; and F.C., Z.M., and W.S. wrote the paper.

The authors declare no conflict of interest.

This article is a PNAS Direct Submission.

Freely available online through the PNAS open access option.

Data deposition: New SWS2 sequences, SWS2 genomic regions, and the transcriptomic raw reads of the *P. fuscus* reference transcriptome have been deposited in the GenBank database (accession nos. [KM978043](#)–[KM978047](#), [KP004247](#)–[KP004345](#), and [SRX736911](#)).

See Commentary on page 1252.

<sup>1</sup>F.C. and Z.M. contributed equally to this work.

<sup>2</sup>To whom correspondence may be addressed. Email: [fabio.cortesi@uqconnect.edu.au](mailto:fabio.cortesi@uqconnect.edu.au) or [zuzmus@gmail.com](mailto:zuzmus@gmail.com).

This article contains supporting information online at [www.pnas.org/lookup/suppl/doi:10.1073/pnas.1417803112/-DCSupplemental](http://www.pnas.org/lookup/suppl/doi:10.1073/pnas.1417803112/-DCSupplemental).

Opsin duplications in teleosts occur at all taxonomic levels (18), affecting the visual systems of entire families (20), genera (21), or individual species (22). In addition, opsin diversity increases because of differences in the evolutionary fate of duplicates (18). In many fishes, novel opsins become pseudogenes (i.e., still detectable functionally disrupted genes) or are lost shortly after emerging through duplication (i.e., nonfunctionalization). However, novel opsins can persist if they acquire new functions (i.e., neofunctionalization). Neofunctionalization is primarily achieved through changes in amino acids at key tuning sites (typically of the retinal binding pocket), leading to shifts in the peak absorbance ( $\lambda_{\text{max}}$ ) of opsin proteins and consequently, sensitivities to different wavelengths of light (17, 18). However, neofunctionalization can also include differential expression of genes throughout ontogeny (20). Finally, opsin duplicates might be subject to gene conversion (18, 21), a common form of reticulate evolution that serves as an important homogenizing force or a repair mechanism between paralogous genes (23). Gene conversion typically occurs between functional paralogs, but it may also involve pseudogenized genes, thus leading to their resurrection (24).

The majority of known opsin gene duplications affecting a large number of fish species involve the midwavelength and long wavelength-sensitive genes (RH1, RH2, and LWS), whereas only one major duplication event of an SWS gene, that of the blue opsin SWS2 (SWS2A and SWS2B) at the base of the spiny-rayed fishes, has been described (18). However, phylogenetic and functional comparisons between different opsin gene families suggest that the evolutionary history of SWS2 might be more complex than previously thought. To begin with, based on a predicted duplication rate of approximately one duplication event every 100 My (25) and the estimated age of the clade [teleosts started to diversify in the Carboniferous to Permian 330–260 Mya (26, 27)], a larger number of SWS2 duplicates is to be expected. Furthermore, teleost SWS2 genes show surprisingly high rates of amino acid substitutions (28) but comparatively low rates of diversification postduplication (18), indicating major discrepancies in current SWS2 gene annotations.

Against this background, we reevaluate the evolutionary history of SWS2 in teleosts using next generation sequencing and open access data mining. We explored transcriptomic and genomic information on SWS2 from a phylogenetically representative set of close to 100 fish species and examined in detail the different evolutionary scenarios (gene duplication, loss, and conversion) that have shaped the SWS2 diversity in teleosts, with a particular focus on acanthomorphs. In doing so, we uncover a major SWS2A duplication, which coincides with the radiation of percomorph fishes. Using a combination of microspectrophotometric (MSP) and quantitative real-time RT-PCR (qRT-PCR) experiments in a species that retained both paralogs, the dusky dotyback *Pseudochromis fuscus*, we provide evidence for neofunctionalization in SWS2A. We finally show that the SWS2A duplication was followed by a complex pattern of gene loss and gene conversion in the different lineages of this highly diverse group of fish, offering an explanation for why this duplication event remained undetected so far.

## Results and Discussion

**SWS2 Duplication, Gene Synteny, and Phylogenetic Reconstruction.** Using a phylogenetic representative sample of 97 fish species (Table S1) covering most of the currently recognized neoteleostei lineages [Neoteleostei (19)], we first show that a duplication of SWS2 into SWS2A and SWS2B occurred around the appearance of the first neoteleosts 190–170 Mya (26, 27), thereby shifting the previously described acanthomorph-specific origin of this duplication deeper into the teleost phylogeny (18, 21) (Fig. 1). A closer inspection of the genomic region (~30 kb) between the highly conserved HCFC1 gene upstream and LWS or GNL3L downstream of SWS2 revealed two additional duplication events

and the retention of up to three SWS2 genes in some fish lineages (Fig. 1).

More ancestral fish only possess one SWS2 gene [Anguilliformes, Ostariophysi, and Salmoniformes (18)], whereas most of the basal neoteleosts have lost SWS2 entirely (Osmeriformes, Stomiiformes, Ateleopodiformes, and Myctophiformes) (Fig. 1). However, we discovered two SWS2 genes in lizardfishes (Aulopiformes), which cluster together with SWS2B from more derived taxa and therefore, mark the earliest appearance of SWS2B in the phylogeny (Fig. S1). Because the two SWS2B paralogs were only recovered in lizardfish and not in other neoteleosts, this duplication is likely lineage-specific (Fig. 2 and Fig. S1). Most interestingly, we discovered a duplication of SWS2A that is associated with the emergence of the first percomorph fishes 110–130 Mya (19, 27), the most species-rich clade of teleosts (Figs. 1 and 2 and Fig. S1). Several percomorph groups, including jacks (Carangiformes), dotybacks (Pseudochromidae), rockfishes (Sebastidae), and seabreams (Sparidae), retained three complete copies of SWS2 (SWS2A $\alpha$ , SWS2A $\beta$ , and SWS2B), whereas others, including tunas (Scombriformes; SWS2A $\alpha$  and SWS2B), pufferfishes (Tetraodontiformes; SWS2B), stickleback (Gasterosteiformes; SWS2A $\beta$  and SWS2B pseudogene), and cichlids (Cichlidae; SWS2A $\alpha$ , SWS2B, and SWS2A $\beta$  pseudogene), have secondarily lost one or two SWS2 copies and/or feature pseudogenized SWS2 paralogs (Figs. 1 and 2). The earliest indication for an SWS2A-specific duplication was found in toadfishes (Batrachoidiformes), which have a complete SWS2A $\alpha$  copy and an SWS2A $\beta$  pseudogene (Fig. 1).

**Evolutionary History of SWS2.** In general, teleosts vary substantially in the retention of SWS2 opsins between but also within lineages (e.g., Beryciformes, Gobiomorpharia, and Pleuronectiformes) (Figs. 1 and 2). Furthermore, high rates of gene conversion seem to promote the evolutionary dynamics in this gene family (Fig. 1). Using single-exon phylogenies (Fig. S4 and Fig. S2) and a sliding window analysis to measure the neutral divergence along SWS2 [rate of synonymous substitutions per synonymous sites (dS)] (Fig. 3B and Fig. S3), we found that gene conversion affects SWS2 copies in almost all fish lineages. However, the extent of gene conversion differed between SWS2 paralogs. When two SWS2A paralogs were involved, conversion affected larger sections of genes (mostly of exons 2 and 3) compared with SWS2B (mostly of exon 4) (Fig. 1 and Figs. S2 and S3). These differences could be explained by a higher similarity of SWS2A copies because of the additional duplication event in percomorphs, which is likely to increase the chances and extent of gene conversion (23).

Surprisingly, in the common mora (*Mora mora*) and the roughhead grenadier (*Macrourus berglax*; both Gadiformes), SWS2A is pseudogenized, but some exons do not contain stop codons or frame shifts; compared with the functional SWS2B, these parts produce highly congruent nucleotide alignments (>90% identical in both cases). A similar pattern was found for the SWS2A pseudogene in the opah (*Lampris guttatus*; Lampriformes; 86% identical to SWS2B) and the SWS2A $\beta$  pseudogene in the Asian swamp eel (*Monopterus albus*; Synbranchiformes), and the shortspine African angler (*Lophius vaillanti*; Lophiiformes; >94% identical to SWS2A $\alpha$  in both cases). Sliding window analyses revealed that, in these species, gene conversion occurred between pseudogenized and complete paralogs (Fig. S3). Moreover, using phylogenetic approaches, we could show that, at least for the grenadier and the swamp eel, the conversion occurred in the direction from the pseudogene to the potentially functional gene, providing what may be the first evidence, to our knowledge, for gene resurrection in vertebrate opsins (Fig. S4). However, a broader taxonomic sampling and functional approaches using expression analyses are needed to fully sustain our findings. Notably, in beryciformes, the dS values between SWS2A and SWS2B are very low, indicating that an almost



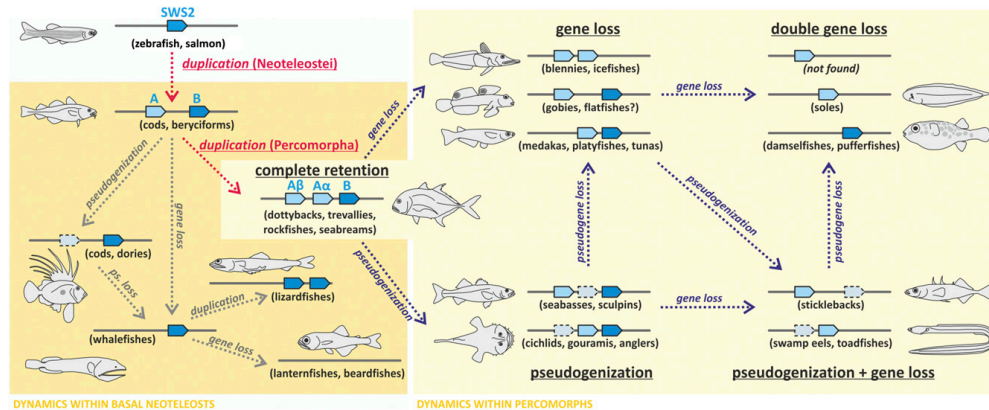


**Fig. 2.** Schematic of the evolutionary dynamics affecting SWS2 in teleosts. The orange box indicates lineages affected by the initial Neoteleostei-specific duplication of SWS2 (SWS2A and SWS2B); the yellow box shows the lineages additionally affected by the Percomorpha-specific duplication of SWS2A (SWS2A $\alpha$  and SWS2A $\beta$ ). Note that gene loss and pseudogenization happened repeatedly and independently between fish lineages (examples shown in parentheses), causing various stages of SWS2 retention in extant taxa. The missing genomic target region for flatfishes is marked with a question mark. Interestingly, no complete gene loss of SWS2 has been found within percomorphs.

complete conversion between those genes has recently occurred (Fig. S3). This observation is supported by the SWS2 phylogeny, where the beryciform SWS2A clusters close to the SWS2B clade and outside of the remaining SWS2As, thus suggesting that, in this case, a conversion occurred from SWS2B to SWS2A (Fig. S1).

Overall, the postduplication dynamics of SWS2 do not follow a phylogenetic pattern (Fig. 1) and are much more complex than previously reported for other opsin genes in fishes (18). The high rates of gene conversion were unexpected, because gene conversion usually affects larger gene families [more than five members (23)]. Our findings have strong implications for the interpretation of SWS2 gene evolution. Initially, we reconstructed gene phylogenies based on full coding regions; however, the SWS2A $\alpha$  clade in particular was poorly resolved, showing low or a lack of support for many of the nodes (Fig. S5). In contrast, when the converted regions were removed (based on the sliding window analysis) (Fig. S3), clades became well-resolved and supported (Fig. S1). Most importantly, high and variable rates of conversion even within lineages (e.g., Anabantiformes) (Fig. S3) constantly homogenize gene copies, making it impossible to reconstruct their evolutionary history on the basis of traditional phylogenetic methods.

If high rates of gene conversion are, in fact, a much more common phenomenon affecting not only opsin evolution but the evolution of many other gene families alike, then our results could have even farther reaching implications in that previous analyses based on common methods of gene evolution should potentially be reassessed.

**Neofunctionalization of SWS2 Genes.** The ancestral SWS2 was predicted to have had a  $\lambda_{\max}$  between 400 and 440 nm (17). However, SWS2As and SWS2Bs diversified and became maximally sensitive within the blue light (440–480 nm) and the violet light (400–440 nm) spectra, respectively (11). Comparing known (17) and potential key tuning sites (i.e., retinal binding pocket sites) between SWS2 copies (Fig. 3C and Fig. S6) combined with ancestral state reconstruction, we identified 11 amino acid sites with clade specificity (Fig. S1). Five of these sites also differed in physical properties between one another, making them prime candidates for sites under adaptive divergence by spectral tuning (29) (Fig. S1). In agreement with the older age of the initial neoteleost-specific SWS2 duplication, we found that most of

these amino acid substitutions occurred between SWS2B and both SWS2A paralogs ( $n = 9$  of 11 sites) (Fig. S1). The remaining two substitutions were found to be SWS2A $\beta$ -specific, whereas no SWS2A $\alpha$ -specific amino acid could be identified, thus suggesting that functional divergence between SWS2A paralogs occurred through a shift in spectral sensitivity in SWS2A $\beta$  (Fig. S1).

Interestingly, only three of the newly identified sites coincide with the eleven previously known key tuning sites of SWS2 (17): 94, 109, and 116 (amino acid positions standardized to bovine rhodopsin). Therefore, our approach highlights the importance of comparative approaches across a large number of species to identify amino acid substitutions that might have a more general impact on opsins.

**Neofunctionalization in the Percomorph-Specific SWS2A Duplicates.** MSP measurements of the dusky dotyback retina (*P. fuscus*; Pseudochromidae) revealed that dotybacks possess single cone cells with two distinct visual sensitivities, which fall within the expected range of SWS2A. Although both adult and larval dotybacks were found to have single cone cells sensitive to 457 nm  $\lambda_{\max}$  (prebleach  $\lambda_{\max}$  mean  $\pm$  SE: 456.78  $\pm$  1.53 nm;  $n = 4$  cells), adult dotybacks were additionally found to have single cone cells sensitive to 448 nm  $\lambda_{\max}$  (447.51  $\pm$  0.91 nm;  $n = 11$  cells) (Fig. 3D). Therefore, SWS2A paralogs may be differentially expressed between ontogenetic stages in dotybacks, a pattern that has previously been described from the cichlid-specific green opsin duplicates (RH2A $\alpha$  and RH2A $\beta$ ), which feature a similar difference in  $\lambda_{\max}$  (~11 nm) to the one found here (20).

To elaborate on the possibility of ontogenetic neofunctionalization in dotybacks and because single cones mostly express SWS1 and SWS2 (30), we compared the relative levels of gene expression across all SWS genes between adult and larval dotybacks. We found that the UV-sensitive SWS1 gene was not expressed (Fig. 3E), which is supported with transmission measurements that show UV-impermeable lenses in adult dotyback eyes (31). Likewise, although SWS2B expression was found to differ between ontogenetic stages (percentage of total SWS expression mean  $\pm$  SE: adults, 0.04%  $\pm$  0.01%; larvae, 4.45%  $\pm$  0.73%; two-tailed  $t$  test,  $t_9 = -9.43$ ,  $P < 0.001$ ), it is probably not relevant for dotyback vision, because it is expressed in very low levels overall (Fig. 3E). Consequently, dotyback single cones mostly express SWS2As. Importantly, the SWS2A paralogs differed



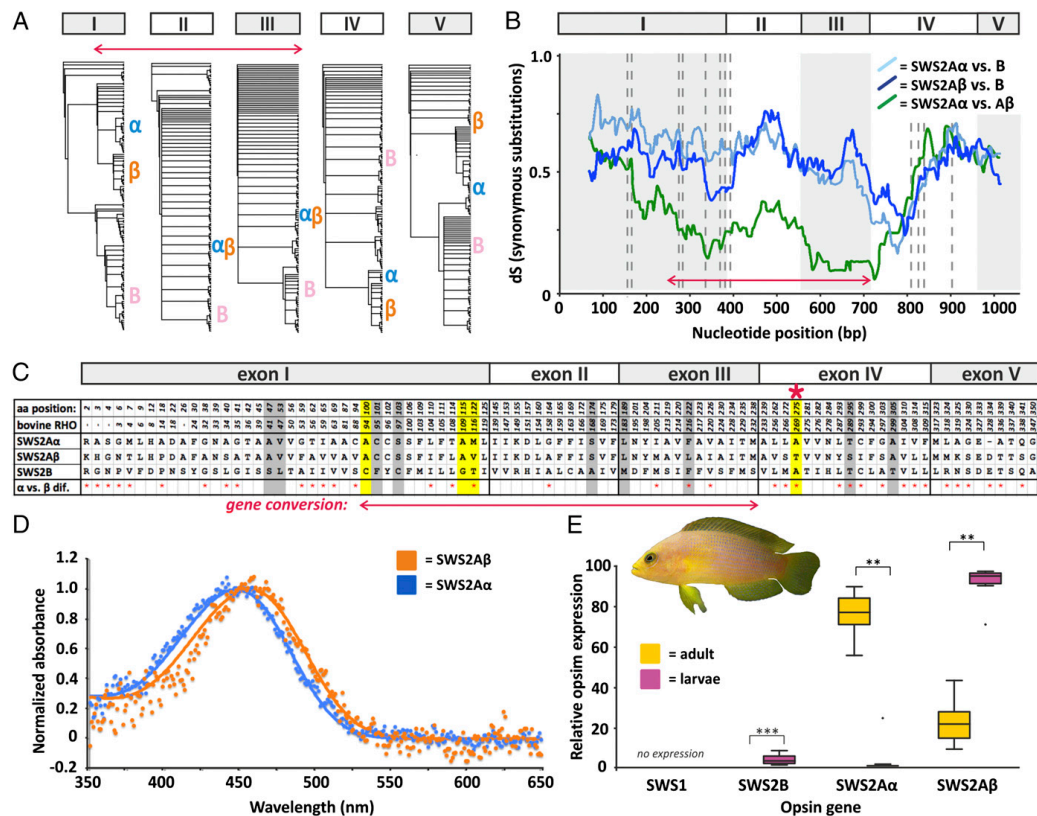


**Fig. 3.** Integrative approach to study opsin gene evolution exemplified in the dusky dotyback *P. fuscus*. (A–C) Gene conversion approach. (A) Single-exon phylogenies show distinct phylogenetic placements of SWS2 copies when exon 1, 4, or 5 is used, whereas SWS2A copies are resolved as sister groups when exons 2 and 3 are analyzed. Letters  $\alpha$ ,  $\beta$ , and B mark the position of the corresponding dotyback gene in the trees. (B) Sliding window analysis. Pairwise dS rate between SWS2 copies calculated with a window of 30 and a step size of 1. The red arrow depicts low dS rates between SWS2A copies in exons 2 and 3 and part of exon 1, corresponding to gene conversion. (C) Amino acid alignment of known key tuning (yellow) (17) and retinal binding pocket sites, showing all variable positions across dotyback SWS2s. Additional putative key substitutions that were identified across fish families are highlighted in gray. The red asterisk marks the substitution A269T in SWS2A $\beta$ , which is known to cause a positive shift in visual sensitivity of 6 nm (17). (D) MSP of adult and larval dotybacks. Orange shows spectral absorbance curves for adult and larval single cones at 457 nm  $\lambda_{max}$  ( $n = 4$ ), and blue shows spectral absorbance curves for adult-specific single cones at 448 nm  $\lambda_{max}$  ( $n = 11$ ). (E) Relative SWS gene expression measured by qRT-PCR in adult ( $n = 12$ ) and larval ( $n = 10$ ) dotybacks. Note that larvae almost exclusively express SWS2A $\beta$ , whereas adults predominantly express SWS2A $\alpha$ . \*\* $P < 0.01$ ; \*\*\* $P < 0.001$ .

substantially in their relative levels of gene expression between ontogenetic stages: adults primarily expressed SWS2A $\alpha$  (adults,  $75.91\% \pm 2.96\%$ ; larvae,  $2.66\% \pm 2.46\%$ ; Wilcoxon test,  $Z = -2.803$ ,  $P = 0.005$ ), whereas larvae mostly expressed SWS2A $\beta$  (adults,  $24.05\% \pm 2.95\%$ ; larvae,  $92.87\% \pm 2.53\%$ ;  $Z = -2.803$ ,  $P = 0.005$ ) (Fig. 3E). These results together with the MSP measurements (see above) suggest that SWS2A $\beta$  is the longer wavelength-tuned paralog, which is consistent with the occurrence of an amino acid substitution at site A269T that is known to induce a positive shift in spectral sensitivity of 6 nm (17). Coincidentally, A269T is the only amino acid substitution within our dataset for which the resulting shift in spectral sensitivity has been experimentally confirmed by in vitro mutagenesis (17). Moreover, the A269T amino acid substitution was never found in the putatively more conserved SWS2A $\alpha$  copy, but it arose multiple times independently in other SWS2 copies of fishes, including in SWS2A $\beta$  of jacks and seabreams (two other families that retained

a full set of SWS2 copies) and one of the SWS2B duplicates of lizardfishes (Fig. S1).

Although at this point, we can only speculate about the biological significance of the ~10-nm shift in spectral sensitivity between the dotyback SWS2A copies, small spectral shifts in sensitivity of other opsin genes in fishes (4–15 nm) have previously been implicated to drive ecological adaptations to various light environments (32) or in some cases, even lead to speciation (16, 33). Similarly, the biological significance of the ontogenetic neofunctionalization of SWS2A copies remains to be investigated but could be tied to major life history changes when larval dotybacks transition in light environment and/or food source from a pelagic life in the open water to a benthic adult life on shallow coral reefs.

**Summary and Significance of Findings.** Despite the importance of opsin genes as key components of the animal visual system, little is known about the evolutionary history of this gene family within

a larger phylogenetic context. Here, we examine the molecular evolution of SWS2 opsins across teleost fishes. We report multiple gene duplication events in SWS2, including a newly discovered duplication of SWS2A that is specific to the most species-rich lineage of vertebrates (percomorph fish), and provide a novel classification of teleost SWS2 genes, calling for the reinterpretation of previous results. Furthermore, we uncover a complex pattern of gene loss, pseudogenization, and gene conversion (in some cases, possibly leading to the resurrection of pseudogenized gene copies) after SWS2 duplications in fishes. Finally, we provide evidence for functional (adaptive) divergence through neofunctionalization between the percomorph-specific SWS2A paralogs. Our study highlights, once more, the importance of comparative approaches in gaining a comprehensive understanding of the dynamics underlying gene family evolution and ultimately, speciation.

## Materials and Methods

Detailed methods are described in *SI Materials and Methods*.

**Data Collection, Gene Synteny, and Phylogenetic Analysis.** Our analyses focused on the genomic region containing SWS2 genes between the upstream HCFC1 and downstream LWS or GNL3L genes (~30 kbp) in 97 fish species. Genomes, transcriptomes, or single SWS2 genes of 44 species were accessed from public databases at GenBank ([www.ncbi.nlm.nih.gov/genbank/](http://www.ncbi.nlm.nih.gov/genbank/)) and Ensembl ([www.ensembl.org/index.html](http://www.ensembl.org/index.html)) (Table S1); the sequences for 53 taxa are new to this study. Raw reads of 38 teleost genomes were used to BLAST search and assemble the target genomic region; for nine species, we sequenced the region using PGM IonTorrent ([www.lifetechnologies.com](http://www.lifetechnologies.com)) (Table S2). PGM IonTorrent was also used to generate a reference transcriptome for the dusky dotyback, and an Illumina HiSeq 2000 DNA sequencer ([www.illumina.com](http://www.illumina.com)) was used to generate retina-specific transcriptomes for five additional species (Table S1). Coding regions of the SWS2 genes were individually retrieved from the genomic region containing

SWS2. To test for gene conversion, we used single-exon gene phylogenies and combined them with a sliding window approach on one member of each fish family to compare the dS ratio of gene copies (Figs. S2 and S3). Bayesian phylogenetic analyses were performed on coding regions of SWS2 genes (exons one to five; excluding converted parts) (Fig. S1). Results from synteny, gene phylogeny, and conversion approaches were subsequently mapped onto a consensus of the latest fish phylogenies (19, 27) (Fig. 1).

**Functional Analysis.** Potentially functional amino acid substitutions were searched for by comparing known key tuning (17) and retinal binding pocket sites of genes from one fish species per family (based on alignments in ref. 34) and extracting those sites that differed in the clade consensus (applying a majority rule consensus after removal of the converted parts) between paralogs (Fig. S6). Mesquite v.3.0 (35) was used to reconstruct the ancestral state of 15 identified sites, which confirmed that 11 of them were clade-specific. Key amino acids were then mapped onto the SWS2 gene phylogeny (standardized to bovine rhodopsin) (Fig. S1). Additionally, we also marked those species with a substitution of A269T, which is known to cause a positive shift in visual sensitivity of 6 nm (17) (Fig. S1). A functional analysis of the percomorph-specific SWS2A duplicates was conducted in the dusky dotyback using a combination of MSP (36) and qRT-PCR approaches (29) (Fig. 3 D and E and Table S2).

**ACKNOWLEDGMENTS.** We thank Nicolas Boileau for support with IonTorrent sequencing, Michael Matschiner for help during data mining, the staff at the Lizard Island Research Station for logistical help, and two anonymous referees for valuable suggestions. F.C. was supported by an Australian Endeavour Research Fellowship, Swiss National Science Foundation (SNSF) Doc. Mobility Fellowship P1BSP3\_148460, and a Doctoral Fellowship from the Lizard Island Research Station, a facility of the Australian Museum. Z.M. was supported by a Novartis–University of Basel Excellence Scholarship for Life Sciences. N.S.H. was supported by Australian Research Council (ARC) Queen Elizabeth II Research Fellowship DP0558681. M.M. was supported by a Doctoral Fellowship from the Molecular Life Science Foundation. The Teleost Genome Project lead by S.J. is supported by Research Council of Norway Grant 222378. K. L. Cheney and N.J.M. were supported by the ARC. W.S. was supported by the SNSF and European Research Council Grants StG “INTERGENADAPT” and CoG “CICHLID-X.”

- Taylor JS, Raes J (2004) Duplication and divergence: The evolution of new genes and old ideas. *Annu Rev Genet* 38:615–643.
- Ohno S (1970) *Evolution by Gene Duplication* (Springer, Heidelberg).
- Wagner GP, Pavlicev M, Cheverud JM (2007) The road to modularity. *Nat Rev Genet* 8(12):921–931.
- Wolfe KH, Shields DC (1997) Molecular evidence for an ancient duplication of the entire yeast genome. *Nature* 387(6634):708–713.
- Dehal P, Boore JL (2005) Two rounds of whole genome duplication in the ancestral vertebrate. *PLoS Biol* 3(10):e314.
- Meyer A, Van de Peer Y (2005) From 2R to 3R: Evidence for a fish-specific genome duplication (FSGD). *BioEssays* 27(9):937–945.
- Parham P, Moffett A (2013) Variable NK cell receptors and their MHC class I ligands in immunity, reproduction and human evolution. *Nat Rev Immunol* 13(2):133–144.
- Grispo MT, et al. (2012) Gene duplication and the evolution of hemoglobin isoform differentiation in birds. *J Biol Chem* 287(45):37647–37658.
- de Souza PC, Bonilla-Rodríguez GO (2007) Fish hemoglobins. *Braz J Med Biol Res* 40(6):769–778.
- Porter ML, Zhang Y, Desai S, Caldwell RL, Cronin TW (2010) Evolution of anatomical and physiological specialization in the compound eyes of stomatopod crustaceans. *J Exp Biol* 213(Pt 20):3473–3486.
- Hofmann CM, Carleton KL (2009) Gene duplication and differential gene expression play an important role in the diversification of visual pigments in fish. *Integr Comp Biol* 49(6):630–643.
- Dulai KS, von Dornum M, Mollon JD, Hunt DM (1999) The evolution of trichromatic color vision by opsin gene duplication in New World and Old World primates. *Genome Res* 9(7):629–638.
- Palczewski K, et al. (2000) Crystal structure of rhodopsin: A G protein-coupled receptor. *Science* 289(5480):739–745.
- Sugawara T, et al. (2005) Parallelism of amino acid changes at the RH1 affecting spectral sensitivity among deep-water cichlids from Lakes Tanganyika and Malawi. *Proc Natl Acad Sci USA* 102(15):5448–5453.
- Bowmaker JK, Hunt DM (2006) Evolution of vertebrate visual pigments. *Curr Biol* 16(13):R484–R489.
- Seehausen O, et al. (2008) Speciation through sensory drive in cichlid fish. *Nature* 455(7213):620–626.
- Yokoyama S (2008) Evolution of dim-light and color vision pigments. *Annu Rev Genomics Hum Genet* 9:259–282.
- Rennison DJ, Owens GL, Taylor JS (2012) Opsin gene duplication and divergence in ray-finned fish. *Mol Phylogenet Evol* 62(3):986–1008.
- Near TJ, et al. (2013) Phylogeny and tempo of diversification in the superradiation of spiny-rayed fishes. *Proc Natl Acad Sci USA* 110(31):12738–12743.
- Spady TC, et al. (2006) Evolution of the cichlid visual palette through ontogenetic subfunctionalization of the opsin gene arrays. *Mol Biol Evol* 23(8):1538–1547.
- Nakamura Y, et al. (2013) Evolutionary changes of multiple visual pigment genes in the complete genome of Pacific bluefin tuna. *Proc Natl Acad Sci USA* 110(27):11061–11066.
- Minamoto T, Shimizu I (2005) Molecular cloning of cone opsin genes and their expression in the retina of a smelt, Ayu (*Plecoglossus altivelis*, Teleostei). *Comp Biochem Physiol B Biochem Mol Biol* 140(2):197–205.
- Katju V, Bergthorsson U (2010) Genomic and population-level effects of gene conversion in *caenorhabditis* paralogs. *Genes (Basel)* 1(3):452–468.
- Mighell AJ, Smith NR, Robinson PA, Markham AF (2000) Vertebrate pseudogenes. *FEBS Lett* 468(2–3):109–114.
- Lynch M, Conery JS (2000) The evolutionary fate and consequences of duplicate genes. *Science* 290(5494):1151–1155.
- Near TJ, et al. (2012) Resolution of ray-finned fish phylogeny and timing of diversification. *Proc Natl Acad Sci USA* 109(34):13698–13703.
- Betancur-R R, et al. (2013) The tree of life and a new classification of bony fishes. *PLoS Curr* 5:5.
- Gojobori J, Innan H (2009) Potential of fish opsin gene duplications to evolve new adaptive functions. *Trends Genet* 25(5):198–202.
- Hofmann CM, et al. (2009) The eyes have it: Regulatory and structural changes both underlie cichlid visual pigment diversity. *PLoS Biol* 7(12):e1000266.
- Cheng CL, Flammarique IN (2007) Chromatic organization of cone photoreceptors in the retina of rainbow trout: Single cones irreversibly switch from UV (SWS1) to blue (SWS2) light sensitive opsin during natural development. *J Exp Biol* 210(Pt 23):4123–4135.
- Siebeck UE, Marshall NJ (2001) Ocular media transmission of coral reef fish—can coral reef fish see ultraviolet light? *Vision Res* 41(2):133–149.
- Jokela M, Vartio A, Paulin L, Fyhrquist-Vanni N, Donner K (2003) Polymorphism of the rod visual pigment between allopatric populations of the sand goby (*Pomatoschistus minutus*): A microspectrophotometric study. *J Exp Biol* 206(Pt 15):2611–2617.
- Carleton KL, Parry JW, Bowmaker JK, Hunt DM, Seehausen O (2005) Colour vision and speciation in Lake Victoria cichlids of the genus *Pundamilia*. *Mol Ecol* 14(14):4341–4353.
- Carleton KL, Spady TC, Cote RH (2005) Rod and cone opsin families differ in spectral tuning domains but not signal transducing domains as judged by saturated evolutionary trace analysis. *J Mol Evol* 61(1):75–89.
- Maddison WP, Maddison DR (2014) *Mesquite: A Modular System for Evolutionary Analysis, Version 3.0*. Available at [mesquiteproject.org](http://mesquiteproject.org). Accessed September 7, 2014.
- Hart NS, Theiss SM, Harahush BK, Collin SP (2011) Microspectrophotometric evidence for cone monochromacy in sharks. *Naturwissenschaften* 98(3):193–201.

# Supporting Information

Cortesi et al. 10.1073/pnas.1417803112

## SI Materials and Methods

**Study Species.** This study included 97 fish species, of which molecular data for 44 species were available from public databases (Table S1), and 53 species were sequenced specifically for this study; 38 species were part of the teleost/Acanthomorpha whole-genome sequencing project at the Centre for Ecological and Evolutionary Synthesis, and 12 samples were obtained from the aquarium trade to be newly sequenced. Fin clips of seven species from the aquarium trade were preserved in 95% ethanol (95:5, ethanol:ddH<sub>2</sub>O) until total DNA was extracted using a QiaGen DNeasy Tissue commercial kit ([www.qiagen.com](http://www.qiagen.com)), and of the remaining five species, retinas were preserved in RNAlater ([www.lifetechnologies.com](http://www.lifetechnologies.com)) for subsequent transcriptome sequencing (Table S1). Three dottyback species (Pseudochromidae) were caught at Lizard Island (14°40' S, 145°27' E), Great Barrier Reef, Australia between 2007 and 2013 (Table S1). Dottybacks were collected on snorkel from shallow reefs (depth of 2–5 m) surrounding the island using an anesthetic clove oil solution (10% clove oil, 40% ethanol, and 50% seawater) and hand nets. A fin clip was preserved in 95% ethanol (95:5, ethanol:ddH<sub>2</sub>O) until total DNA was extracted using a standard salt precipitation protocol (1). In addition, several dusky dottyback (*Pseudochromis fuscus*) tissues were preserved on RNAlater for subsequent transcriptome sequencing and gene expression analysis. Larval dusky dottybacks were caught overnight using light traps during the summer recruitment pulses in November of 2007 and October and November of 2013 and either directly used for MSP measurements or kept on RNAlater for subsequent gene expression analysis.

## SWS2 Gene Synteny.

**Transcriptome sequencing and SWS2 reference mapping.** Total RNA from various dusky dottyback tissues was extracted using a QiaGen RNeasy Plus Universal Kit (QiaGen): skin, liver, eyes, and gonads from a brown male individual [total length (TL) = 69 mm]; skin, brain, anal fin, caudal fin, and gonads from a yellow female individual (TL = 71 mm); and one entire small immature individual (TL = 22 mm). BioAnalyzer ([www.genomics.agilent.com](http://www.genomics.agilent.com)) was used to measure the initial concentration of the different extracts, after which they were diluted to the same concentration and pooled. The pool was then used to prepare a library for high-throughput sequencing using the Dynabeads mRNA Purification Kit (LifeTechnologies) for mRNA selection and the Ion Total RNA-Seq Kit (LifeTechnologies) for standard steps, such as RNA-to-cDNA transcription and size selection. Transcriptome sequencing was performed on an Ion-Torrent PGM platform (LifeTechnologies) using a 316 chip, standard run conditions, and a 120-bp length restriction. The run produced >3.4 million unique reads (70% efficiency) with a mean length of 113 bp, equaling a total number of 389.06 Mbp, of which 330.67 Mbp had a Phred quality score of Q20 or higher (i.e., >99% base call accuracy). Subsequent quality filtering of reads was performed on the Galaxy online web server ([usegalaxy.org](http://usegalaxy.org)). Data were initially trimmed using a sliding window approach with a window size of 20 and step size of 1, and reads were trimmed from both sides until reaching a base pair with a score of ≥Q20. Reads with a read length of zero were discarded, and the trimmed reads were filtered for quality so that 95% of a single read had an overall score of Q20 or higher (Q20/95). After quality filtering and removal of sequencing artifacts, the library contained >2.5 million reads with a mean length of 80 bp. Filtered reads were mapped against publicly avail-

able SWS2A and SWS2B coding sequences of the Nile tilapia (*Oreochromis niloticus*; Cichlidae) in Geneious v.6.0.2 ([www.geneious.com](http://www.geneious.com)) using customized sensitivity settings (index word length = 11; maximal gap size = 2,000 bp). Assembled reads with an average depth of 16× per gene were manually assigned to the different copies before generating their consensus. The resulting sequences were scored for similarity to publicly available genes using BLASTN ([www.ncbi.nlm.nih.gov/BLAST](http://www.ncbi.nlm.nih.gov/BLAST)). This approach produced three distinct gene products, which were thereafter used as references for mapping of orthologous genes (see below). To verify the synteny of the dusky dottyback SWS2 copies, we furthermore sequenced the genomic region containing the three genes using a combination of long-amplicon sequencing on Ion-Torrent and Sanger sequencing (see below). The dusky dottyback transcriptome is made available on the short-read archive database in GenBank ([www.ncbi.nlm.nih.gov/genbank](http://www.ncbi.nlm.nih.gov/genbank)) (Table S1).

Additionally, we used a HiSeq 2000 DNA sequencer from Illumina ([www.illumina.com](http://www.illumina.com)) to generate retina-specific transcriptomes for five species of labrids (Labridae) and cardinalfishes (Apogonidae) (Table S1). Raw reads from these approaches were then mapped against the dusky dottyback SWS2 genes in Geneious v.6.0.2 (average depth of 250–2,500× per SWS2 gene), and genes were extracted as previously described for the dusky dottyback.

**Public data mining.** Whole-genome sequences of 24 species and the transcriptome sequences of 1 species (*Tripterygion delaisi*; average depth of 360–620× per SWS2 gene) were accessed from the Ensembl Genome browser ([www.ensembl.org](http://www.ensembl.org)) or the Assembly (assembled contigs or scaffolds) and the short-read archive databases in GenBank (Table S1). Initially, the raw reads from unassembled datasets were mapped against SWS2 exons from the three dusky dottyback SWS2 genes in Geneious v.6.0.2 using medium-sensitivity settings (70% identity threshold for mapping) to efficiently recover all SWS2 copies. Matching reads were then manually split by copies (if more than one gene copy was present in the species) and de novo assembled, and their consensus was used as a species-specific reference for subsequent low-sensitivity mapping (only reads over 90% sequence identity map) in Geneious v.6.0.2. During this cyclic mapping, unassembled reads were mapped repeatedly against the prolonging reference (originally single exons) until the mapped regions would overlap and could be connected into an entire gene. The cyclic mapping continued the same way until the genes could not be prolonged anymore or could be connected into a genomic region (~30 kbp) that contained the highly conserved up- and downstream neighboring genes HCFC1 and LWS or GNL3L (in case of LWS loss), respectively. Alignments were continuously inspected visually to exclude ambiguous mapping of genes. In species that retained all three SWS2 paralogs, genes were interspaced by around 1,500 bp with an upstream SWS2Aβ, middle SWS2Aα, and downstream SWS2B copy (Fig. 1).

**Sequencing of the SWS2 target region.** The synteny of SWS2 genes in nine species was investigated by sequencing the SWS2 target region between HCFC1 and LWS. The region was initially separated into three overlapping stretches, and universal primers were designed to amplify each stretch separately (Table S2). Long PCR was used to amplify the 5- to 13-kbp-long products using the TaKaRa LA polymerase (TaKaRa Bio Inc.; program: 35× 98 °C for 10 s, 60–68 °C for 1 min, and 68 °C for 20 min), and the QIAquick PCR Purification Kit (QiaGen) was used to purify the products cut from the electrophoresis gel. After purified, products were used to prepare a long-amplicon library following the

genomic DNA library preparation protocol (Ion Xpress Plus gDNA and Amplicon Library Preparation; LifeTechnologies) and sequenced on IonTorrent PGM using a 316 v2 ChIP combined with the Ion PGM Sequencing 400 Kit (LifeTechnologies). Reads were quality filtered (same as for the dusky dotyback transcriptome; see above) and de novo assembled in Geneious v.6.0.2. In several species, the consensus sequences would not cover the entire genomic region, and we, therefore, designed specific primers to sequence the missing parts by Sanger on an Applied Biosystems 3130xl Genetic Analyzer ([www.appliedbiosystems.com](http://www.appliedbiosystems.com)) (Table S2). Additionally, the genomic raw reads and scaffolds of 38 species that were part of the whole-genome sequencing project at the Centre for Ecological and Evolutionary Synthesis were used to BLAST search and assemble the target SWS2 genomic region (HCFC1 upstream and LWS or GNL3L downstream) (Table S1).

SWS2 presence and synteny were assessed by mapping single exons from the dusky dotyback against the target region in Geneious v.6.0.2 using high-sensitivity settings (see above). Coding regions of SWS2 copies were subsequently extracted from the region and used for phylogenetic analyses.

**Phylogenetic analyses.** SWS2 coding sequences from 67 species were cut from genomic regions and combined with the transcriptome sequences from 7 species and publicly available single-gene coding sequences of 23 species (Table S1). Sequences were aligned using MAFFT v.6.8 (2), and the most appropriate model of sequence evolution was estimated in jModeltest v.2 (3) using the Akaike information criterion as the criterion for model selection. Subsequent Bayesian inference was conducted on the CIPRES platform (4) using the GTR+I+ $\Gamma$  model in MrBayes v.3.2.1 (5) and a Markov chain Monte Carlo search with two independent runs and four chains each. Each run was set to 10 million generations, with trees sampled every 1,000 generations (i.e., 10,000 trees per run) with 25% of burn in after the sampling. SWS2 sequences from eel (*Anguilla anguilla*), zebrafish (*Danio rerio*), carp (*Cyprinus carpio*), and salmon (*Salmo salar* and *Oncorhynchus keta*) were used as outgroups to reconstruct phylogenetic relationships between SWS2 copies. This approach produced a partly unresolved gene tree with low phylogenetic support for SWS2A $\alpha$  genes in particular (Fig. S5). Consequently, to increase the phylogenetic signal, we repeated the analysis after removing the genetic regions that were affected by gene conversion (see below for gene conversion approaches) (Fig. S1).

#### Gene Conversion.

**Single-exon phylogenies.** To investigate which SWS2 copies and what genetic regions would be affected by gene conversion, we ran additional MrBayes analyses under the same conditions as mentioned above but for each exon separately (five in total) (Fig. S2).

**Sliding window analysis of gene conversion.** To measure the divergence between SWS2 genes, we calculated the dS (neutral process) along the coding sequences of gene copies using a sliding window strategy with a step size of 1 and a window of 30 in DNAsp v.5.10.1 (6). To avoid a bias toward clades with more representatives, we calculated the rates for one fish species per family that possesses more than one SWS2 copy. Converted regions were identified based on a sharp drop in dS between genes, which is equivalent to high sequence similarities (Fig. S3). These regions were subsequently removed from the coding sequence alignment to generate the final SWS2 gene tree (see above) (Fig. S1).

**Gene resurrection: gene conversion from pseudogenes.** Pseudogenes with the potential to be resurrected by converting with functional paralogs were identified in five species/lineages (Fig. 1 and Fig. S3). To test for potential gene resurrection, we ran phylogenetic analyses with the aforementioned dataset (i.e., genes without converted regions) and additionally included the converted region of the pseudogene and its functional paralog of the species

of interest (Fig. S4). Analyses were run for each species separately (i.e., a total of five analyses) in MrBayes under the same conditions as described above. Two out of five analyses were found to support the proposed gene resurrection scenario (Fig. S4).

#### Functional Analysis.

**Neofunctionalization of SWS2 genes.** Putative amino acid substitutions of importance for spectral tuning were searched for by comparing amino acid alignments of known (7) and potential key tuning sites (i.e., retinal binding pocket sites) of SWS2 genes from one fish species per family (based on alignments in ref. 8). Initially, sites were extracted based on differences in clade consensus (majority rule applied after removal of converted regions of sequences) between paralogs (Fig. S5). To identify those sites with clade specificity, we reconstructed their ancestral state (under maximal parsimony) in Mesquite v.3.0 (9). Additionally, all species were screened for the specific substitution of A269T, which is known to cause a positive shift in spectral sensitivity of 6 nm (7).

**Function of the percomorph-specific SWS2A paralogs.** A functional analysis of the percomorph-specific SWS2A duplication was conducted in the dusky dotyback using a combination of MSP and quantitative real-time RT-PCR (qRT-PCR) approaches.

For MSP, adult ( $n = 3$ ) and larval ( $n = 1$ ) dusky dotybacks were dark-adapted overnight and euthanized with an overdose of MS222 (1:2,000). Eyes were removed and dissected under IR illumination with the aid of an IR-sensitive image converter. Small pieces ( $\sim 1\text{--}3\text{ mm}^2$ ) of retinal tissue were mounted on a no. 1 glass coverslip in a drop of PBS (410 mOsm  $\text{kg}^{-1}$ , pH 7.2) containing 4% dextran (molecular weight of 282,000; D-7265; Sigma). This preparation was covered with a smaller no. 0 coverslip, and the edges of the top coverslip were sealed with nail varnish to prevent dehydration. Absorbance spectra of individual photoreceptor outer segments were measured using a single-beam wavelength-scanning microspectrophotometer and analyzed as described in detail elsewhere (10, 11).

For qRT-PCR, RNA was extracted from retina tissues (adults) or the whole head (larvae) using TriZol following the protocol of the manufacturer (LifeTechnologies). To remove possible genomic contamination, we treated the RNA extract with DNase according to the DNA Free protocol from the manufacturer (LifeTechnologies). RNA was subsequently reverse-transcribed to cDNA using the High-Capacity RNA-to-cDNA Kit (Applied Biosystems), and the resulting concentration was measured on a NanoDrop1000 Spectrophotometer (ThermoScientific).

The relative expression of the SWS opsin genes (SWS1 and SWS2s) was quantified by qRT-PCR on a StepOnePlus Real-Time PCR System (LifeTechnologies). A 20- $\mu\text{L}$  reaction volume was prepared using SYBR Green Master (Rox) dye ([www.lifescience.roche.com](http://www.lifescience.roche.com)) with a final cDNA concentration of 10 ng/ $\mu\text{L}$  and a final primer concentration of 200 nM. The qRT-PCR was then performed under the following cycling conditions: 95  $^{\circ}\text{C}$  for 10 min, 40 cycles at 95  $^{\circ}\text{C}$  for 15 s, and 61  $^{\circ}\text{C}$  for 60 s. All qRT-PCR amplifications included a melt curve step after cycling. Unique primers for each opsin gene were designed with a primer specificity of  $\geq 90\%$  and either the forward or the reverse primer spanning an exon-exon boundary to ensure cDNA-specific amplification of the product (60–100 bp) (Table S2). Products were furthermore sequenced by Sanger to assure accuracy of the reaction.

All primers were initially validated on a dilution series of factor 5 of a species-specific pool containing equal ratios of fragments (molarity measured on BioAnalyzer) of each of the gene copies with a starting concentration of 0.1–0.5 nM/ $\mu\text{L}$ . qRT-PCR efficiencies ( $E_s$ ) were calculated for each reaction from the slope of the standard curve using the equation  $E = 10^{(-1/\text{slope})}$  as implemented in the StepOnePlus software (LifeTechnologies), with an efficiency of 2 being equal to 100% ( $E\% = [10^{(-1/\text{slope})} - 1] \times 100$ ) and an indicator of a robust assay. All experiments were



carried out with three technical replicates, and the opsin pool was added to each plate as an internal reference. The relative expression of each gene was then calculated as described in detail elsewhere (12).

We used *t* and Wilcoxon rank sum tests to examine whether the expression of SWS2 genes between larval and adult fish differed (SWS1 was found not to be expressed). Expression data were ini-

tially ln-transformed and assessed for normality and homogeneity of variance using histograms, residuals plots, and quantile–quantile plots. Because SWS2A copies did not conform to normality, we used Wilcoxon tests to compare their expression between larval and adult dotybacks. To account for multiple comparisons of tests, we used Bonferroni corrections (13) to adjust *P* values. All statistical analyses were performed in SPSS v.15.0 (SPSS).

1. Miller SA, Dykes DD, Polesky HF (1988) A simple salting out procedure for extracting DNA from human nucleated cells. *Nucleic Acids Res* 16(3):1215.
2. Katoh K, Toh H (2008) Recent developments in the MAFFT multiple sequence alignment program. *Brief Bioinform* 9(4):286–298.
3. Darriba D, Taboada GL, Doallo R, Posada D (2012) jModelTest 2: More models, new heuristics and parallel computing. *Nat Methods* 9(8):772–772.
4. Miller MA, Pfeiffer W, Schwartz T (2010) Creating the CIPRES Science Gateway for inference of large phylogenetic trees. *Proceedings of the Gateway Computing Environments Workshop (GCE)* (IEEE, New Orleans), pp 1–8.
5. Ronquist F, et al. (2012) MrBayes 3.2: Efficient Bayesian phylogenetic inference and model choice across a large model space. *Syst Biol* 61(3):539–542.
6. Librado P, Rozas J (2009) DnaSP v5: A software for comprehensive analysis of DNA polymorphism data. *Bioinformatics* 25(11):1451–1452.
7. Yokoyama S (2008) Evolution of dim-light and color vision pigments. *Annu Rev Genomics Hum Genet* 9:259–282.
8. Carleton KL, Spady TC, Cote RH (2005) Rod and cone opsin families differ in spectral tuning domains but not signal transducing domains as judged by saturated evolutionary trace analysis. *J Mol Evol* 61(1):75–89.
9. Maddison WP, Maddison DR (2014) *Mesquite: A Modular System for Evolutionary Analysis, Version 3.0*. Available at [mesquiteproject.org](http://mesquiteproject.org). Accessed September 7, 2014.
10. Hart NS, Theiss SM, Harahush BK, Collin SP (2011) Microspectrophotometric evidence for cone monochromacy in sharks. *Naturwissenschaften* 98(3):193–201.
11. Hart NS, Coimbra JP, Collin SP, Westhoff G (2012) Photoreceptor types, visual pigments, and topographic specializations in the retinas of hydrophiid sea snakes. *J Comp Neurol* 520(6):1246–1261.
12. Carleton KL, Kocher TD (2001) Cone opsin genes of african cichlid fishes: Tuning spectral sensitivity by differential gene expression. *Mol Biol Evol* 18(8):1540–1550.
13. Rice WR (1989) Analyzing tables of statistical tests. *Evolution* 43(1):223–225.

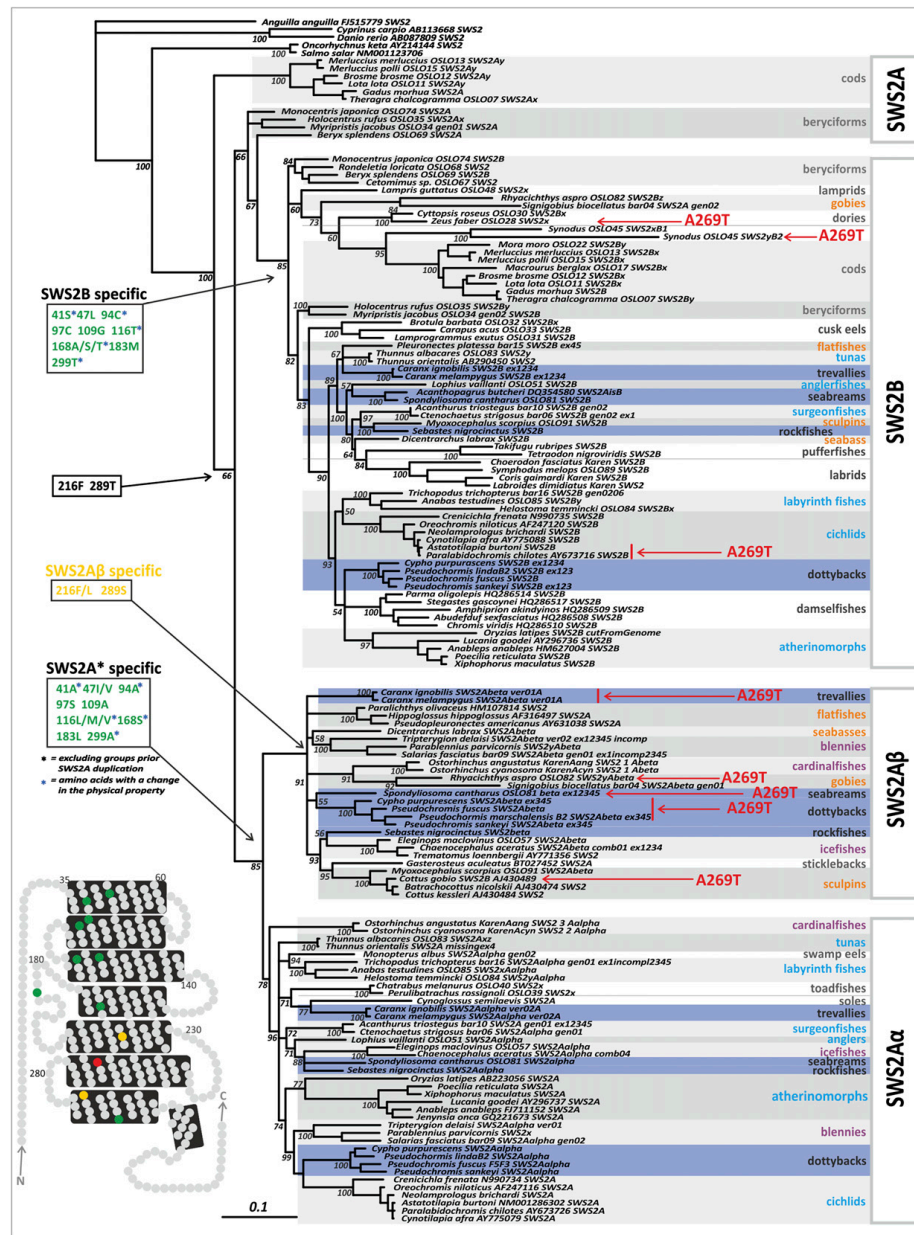
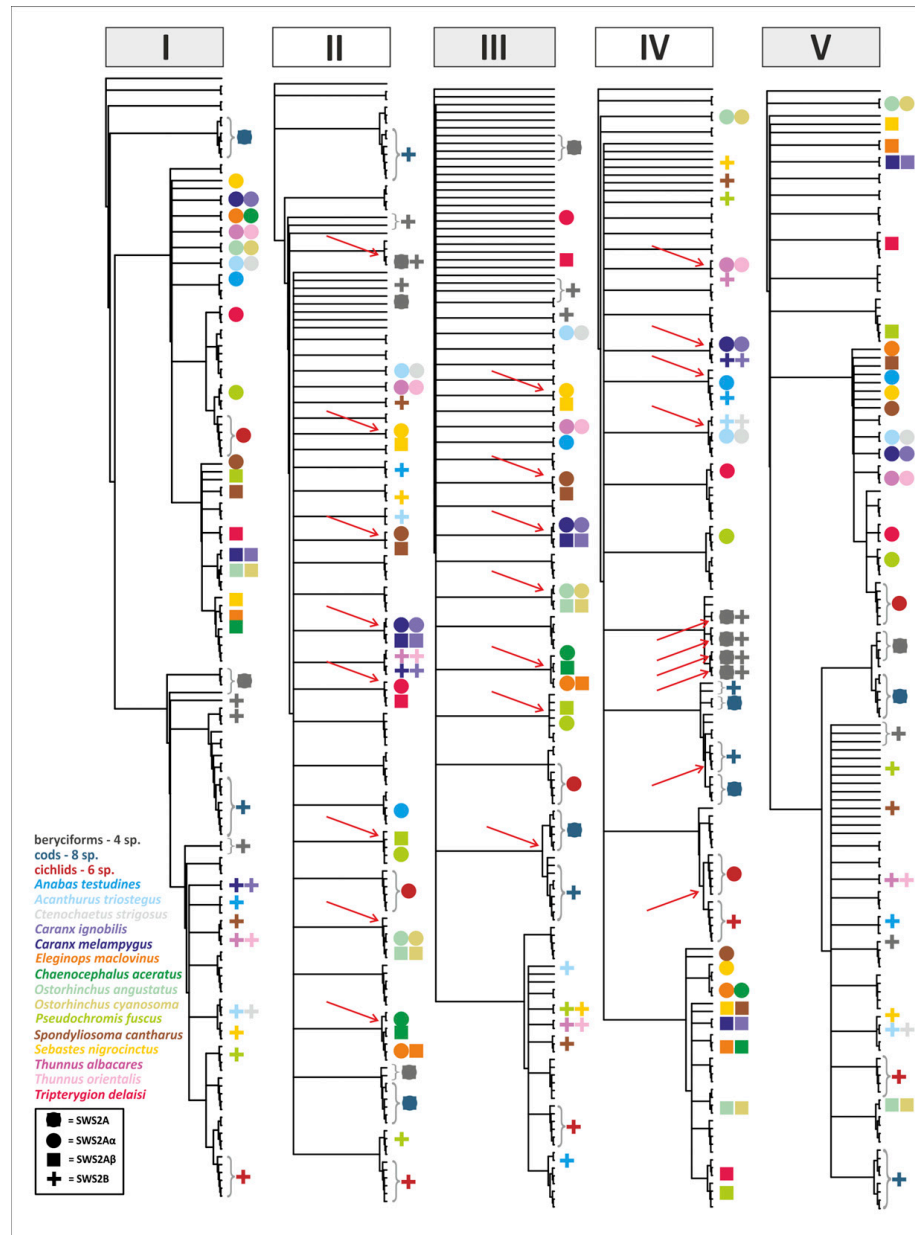


Fig. S1. SWS2 gene phylogeny and potential key amino acid substitutions. Consensus phylogeny based on the coding region of SWS2 genes without converted parts. Bayesian posterior probabilities are shown for deeper nodes (i.e., maximum one value per lineage). Lineages that retained all three SWS2 copies are shaded in blue; those with two copies are highlighted by two shades of gray. No shading means one copy retained. Common names are color-coded according to the identity of retained genes based on currently available data: blue, SWS2A $\alpha$  + SWS2B; orange, SWS2A $\beta$  + SWS2B; violet, SWS2A $\alpha$  + SWS2A $\beta$ . The boxes show clade-specific amino acid substitutions (as per ancestral state reconstruction; standardized to bovine rhodopsin) between SWS2A and SWS2B (green) and for SWS2A $\beta$  (yellow). Amino acid substitutions that vary in physical properties are marked with blue asterisks. Species with a substitution of A269T,

Legend continued on following page

which is likely to cause a positive shift in spectral sensitivity of 6 nm, are indicated with red arrows (1). *Lower Left* shows a schematic drawing of the bovine rhodopsin (based on ref. 2), with potentially important amino acid substitutions marked accordingly.

1. Yokoyama S (2008) Evolution of dim-light and color vision pigments. *Annu Rev Genomics Hum Genet* 9:259–282.
2. Palczewski K, et al. (2000) Crystal structure of rhodopsin: A G protein-coupled receptor. *Science* 289(5480):739–745.



**Fig. S2.** Single-exon phylogenies used to identify regions under gene conversion. SWS2 copies are clustered as sisters if exons were affected by gene conversion (red arrows). Most of the conversions in exons 2 and 3 happened between SWS2A $\alpha$  and SWS2A $\beta$ , whereas the conversions of exon 4 happened mostly between SWS2B and one of the SWS2A copies. Gene conversions of different phylogenetic age can be detected based on the tree [e.g., family-specific gene conversion in cichlids (Cichlidae; exon 4) and cods (Gadiformes; exon 3), genus-specific conversion in *Caranx* (Carangiformes; exons 2–4) and *Ostorhinchus* (Apogonidae; exons 2 and 3), or species-specific conversion in icefishes (Notothenioidei; *E. maclovinus* and *C. aceratus*; exons 2 and 3) and beryciforms (Beryciformes; exon 4)]. Note that, for beryciforms, the exon 4 of SWS2A and SWS2B always cluster as sisters within species, indicating that conversion occurred independently multiple times over in this lineage.

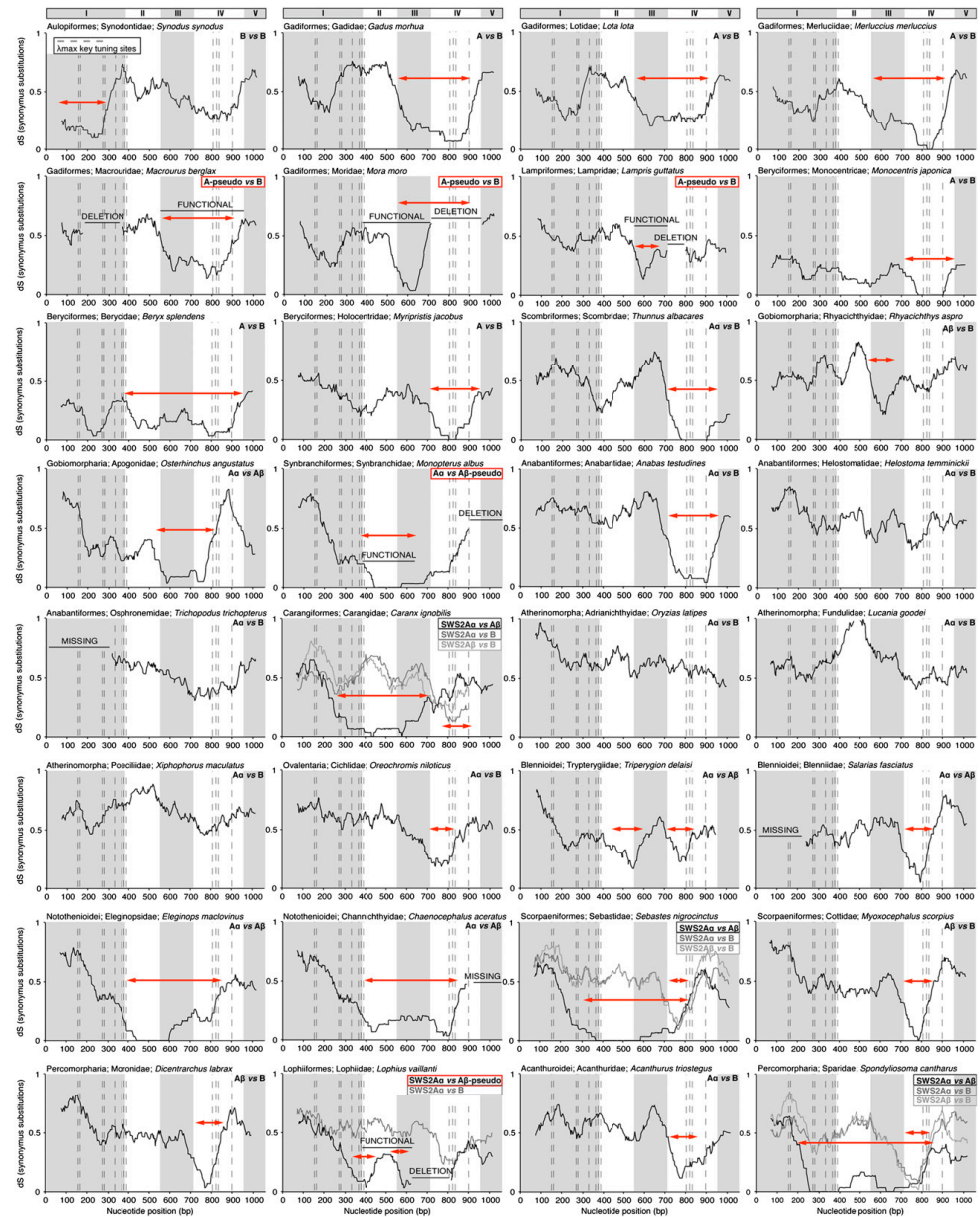
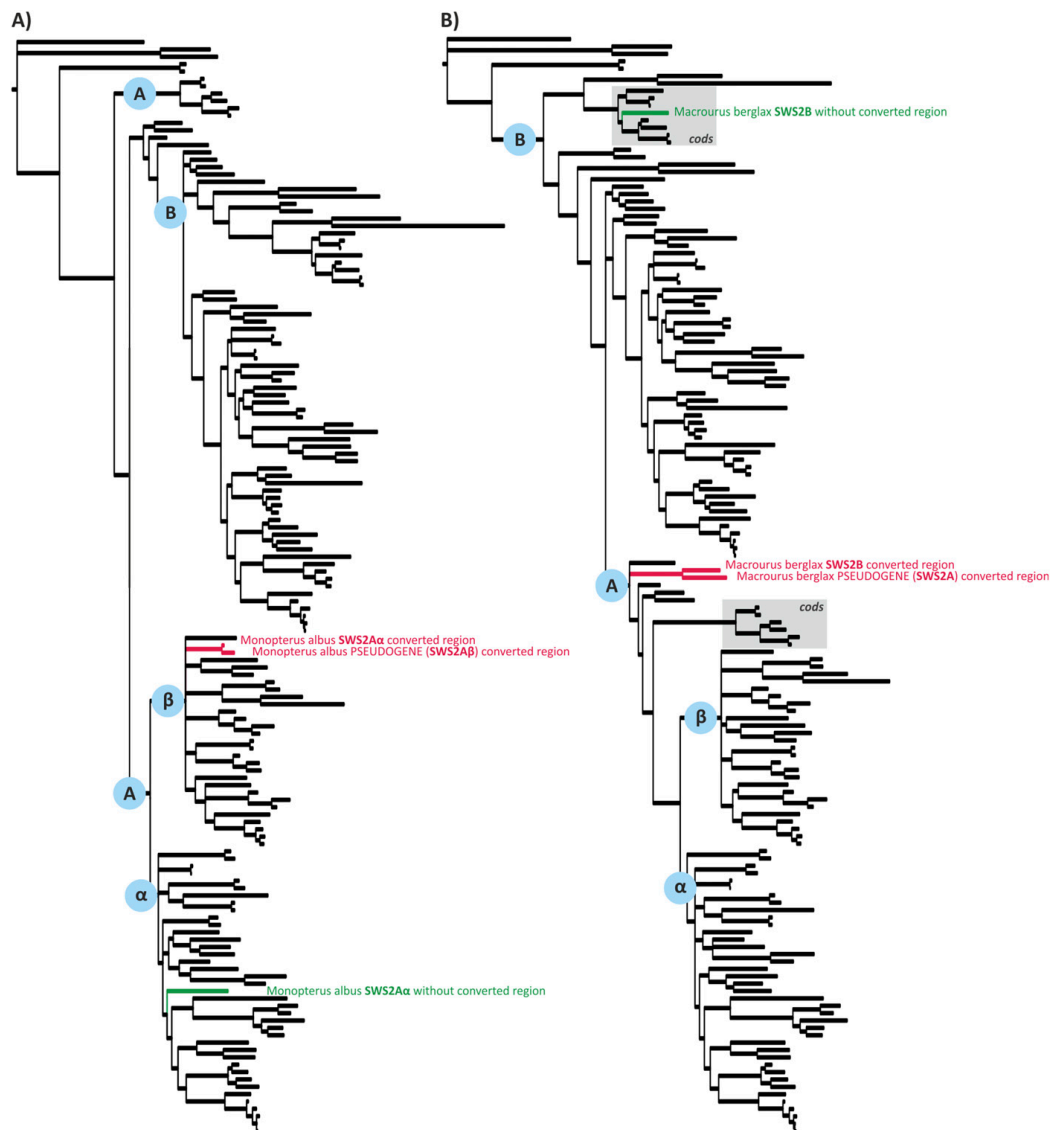


Fig. S3. Sequence comparison of SW52 genes from one representative fish species per family. Synonymous substitution rates (dS) along gene sequences were assessed by sliding windows (size of 30 bp; step size = 1). Probable regions under gene conversion, which were removed to generate the final gene phylogeny (Fig. S1), are identified by a drop in dS and marked by red arrows. Note that, in several families, pseudogenized genes are likely to have contributed to gene conversion (framed in red) (also see Fig. S4).



**Fig. S4.** Conversion from pseudogene to functional paralog potentially leading to gene resurrection. Phylogenies based on the coding genes without converted regions (all species) (similar to Fig. S1) and the converted region of the pseudogene and the target paralog (of a tested species) identified potential gene resurrection in two cases. (A) Asian swamp eel (*Monopterus albus*; Synbranchiformes). Red shows the converted regions of SWS2A $\alpha$  and the SWS2A $\beta$  pseudogene; green shows SWS2A $\alpha$  without the converted region. The phylogenetic position of SWS2A $\alpha$  converted region in the SWS2A $\beta$  clade clearly suggests the origin of the converted region in the SWS2A $\beta$  pseudogene. (B) Roughhead grenadier (*Macrourus berglax*; Gadiformes). Red shows the converted regions of SWS2B and the SWSA pseudogene; green shows SWS2B without the converted region. Shaded in gray is the position of other cod species (Gadiformes).





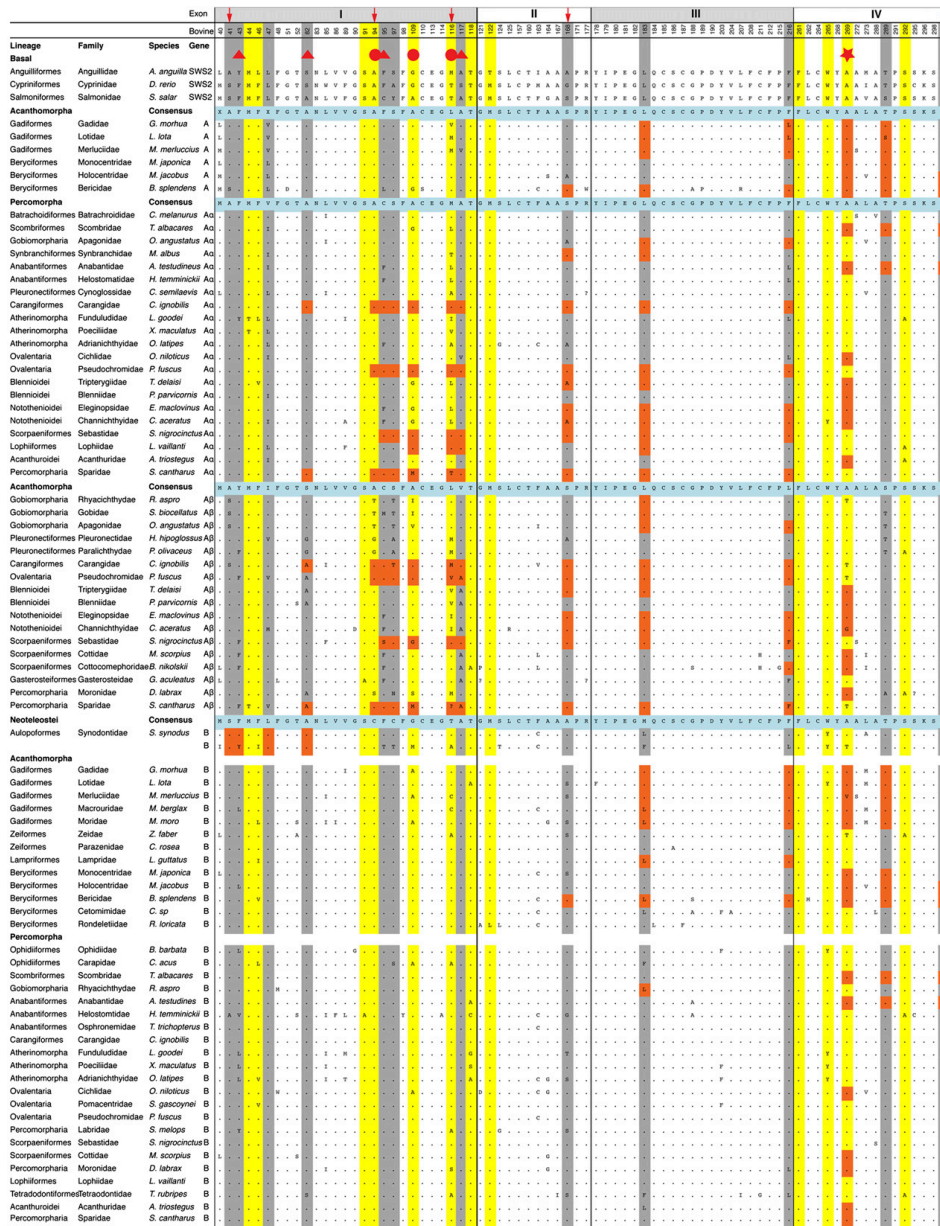


**Fig. S6.** SWS2 amino acid alignments (standardized to bovine rhodopsin) of known key tuning (yellow) (1) and retinal binding pocket sites. Pictured is one representative fish species per family. Highlighted in gray or marked by a red sphere are potentially functional amino acid substitutions that were identified based on clade consensus (after removing amino acids affected by conversion; orange). The red asterisk marks site 269, at which a substitution of A269T is known to cause a positive shift of 6 nm. Red triangles mark sites that did not confer to clade specificity based on an ancestral state reconstruction (after maximum parsimony). Arrows indicate those potential key substitutions that also vary in physical properties between SWS2 genes. Additional information is in Fig. S1.

1. Yokoyama S (2008) Evolution of dim-light and color vision pigments. *Annu Rev Genomics Hum Genet* 9:259–282.

Cortesi et al. [www.pnas.org/cgi/content/short/1417803112](http://www.pnas.org/cgi/content/short/1417803112)

10 of 16



Cortesi et al. [www.pnas.org/cgi/content/short/1417803112](http://www.pnas.org/cgi/content/short/1417803112)Percomorpha—basal

Cortesi et al. [www.pnas.org/cgi/content/short/1417803112](http://www.pnas.org/cgi/content/short/1417803112)

Order	Family	Species	Source/locality	Type of data	Database	Accession no.	Blue opsins	
Batrachoidiformes	Batrachoididae	<i>Chatrabius melanurus</i>	Teleost Genome Project	Genomic region	GenBank*	KP004287, KP004296, KP004265, KP004267	SW52Aα + pseudogene	
	Batrachoididae	<i>Perulibatrachus rossignoli</i>	Teleost Genome Project	Genomic region	GenBank*	KP004254, KP004308, KP004263	SW52Aα	
Scomberiformes	Scombridae	<i>Thunnus albacares</i>	Teleost Genome Project	Genomic region	GenBank*	KP004306, KP004291	SW52Aα + SW52B	
	Scombridae	<i>Thunnus orientalis</i>	Public database	Single-gene sequence(s); genome assembly	GenBank	AB290450, BADN01000000	SW52Aα + SW52B	
Gobiomorphia	Gobiidae	<i>Signigobius biocellatus</i>	Aquarium trade	Long PCR genomic region	GenBank*	KP004338, KP004332	SW52Aα + SW52B	
		<i>Rhyacichthys aspro</i>	Teleost Genome Project	Genomic region	GenBank*	KP004301	SW52Aα + SW52B	
		<i>Ostrochinchus cyanosoma</i>	Aquarium trade	Transcriptome	GenBank*	KP004342, KP004343	SW52Aα + SW52Aβ	
		<i>Ostrochinchus angustatus</i>	Aquarium trade	Transcriptome	GenBank*	KP004345, KP004341	SW52Aα + SW52Aβ	
	Carangomorphariae and anabantomorphariae							
		Anabantidae	<i>Anabas testudineus</i>	Teleost Genome Project	Genomic region	GenBank*	KP004316, KP004284	SW52Aα + SW52B + pseudogene
	Anabantiformes	Osphronemidae	<i>Trichopodus trichopterus</i>	Aquarium trade	Long PCR genomic region	GenBank*	KP004337	SW52Aα, SW52B
		Helostomatidae	<i>Helostoma temminckii</i>	Teleost Genome Project	Genomic region	GenBank*	KP004249	SW52Aα + SW52B + pseudogene
	Carangiformes	Carangidae	<i>Caranx melampygus</i>	Public database	Genomic raw reads	SRA GenBank	SRX360285	SW52Aα + SW52Aβ + SW52B
	Carangiformes	Carangidae	<i>Caranx ignobilis</i>	Public database	Genomic raw reads	SRA GenBank	SRX360276	SW52Aα + SW52Aβ + SW52B
Pleuronectiformes	Cynoglossidae	<i>Cynoglossus semilaevis</i>	Public database	Genome assembly; raw reads	GenBank	AGRG000000000.1, SRX100168	SW52Aα	
Pleuronectiformes	Pleuronectidae	<i>Hippoglossus hippoglossus</i>	Public database	Single-gene sequence(s)	GenBank	AF316497	SW52Aβ	
Pleuronectiformes	Pleuronectidae	<i>Pseudopleuronectes americanus</i>	Public database	Single-gene sequence(s)	GenBank	AY631038	SW52Aβ	
Pleuronectiformes	Paralichthyidae	<i>Paralichthys olivaceus</i>	Public database	Single-gene sequence(s)	GenBank	HM107814	SW52Aβ	
Pleuronectiformes	Pleuronectidae	<i>Pleuronectes platessa</i>	Trade	Long PCR genomic region	GenBank*	KP004328	SW52B (partial)	
Synbranchiformes	Synbranchidae	<i>Monopterus albus</i>	Public database	Genomic raw reads	SRA GenBank	SRX218061	SW52Aα + pseudogene	
Ovalentaria								
Former Perciformes	Cichlidae	<i>Oreochromis niloticus</i>	Public database	Genome assembly	Ensembl	Oreni11.0.76	SW52Aα + SW52B + pseudogene	
Former Perciformes	Cichlidae	<i>Astatotilapia burtoni</i>	Public database	Genome assembly	GenBank	AFNZ000000000.1	SW52Aα + SW52B + pseudogene	
Former Perciformes	Cichlidae	<i>Neolamprologus brichardi</i>	Public database	Genome assembly	GenBank	AFNY000000000.1	SW52Aα + SW52B + pseudogene	
Former Perciformes	Cichlidae	<i>Cynotilapia afra</i>	Public database	Single-gene sequence(s)	GenBank	AY775088, AY775079	SW52Aα + SW52B	
Former Perciformes	Cichlidae	<i>Paralabidochromis chilotes</i>	Public database	Single-gene sequence(s)	GenBank	AY673716, AY673726	SW52Aα + SW52B	
Former Perciformes	Cichlidae	<i>Crenicichla frenata</i>	Public database	Single-gene sequence(s)	GenBank	JN90735, JN990734	SW52Aα + SW52B	
Cyprinodontiformes	Poeciliidae	<i>Poecilia reticulata</i>	Public database	Single-gene sequence(s)	GenBank	AZHG000000000.1	SW52Aα + SW52B	
Cyprinodontiformes	Poeciliidae	<i>Xiphophorus maculatus</i>	Public database	Genome assembly	GenBank	AGA000000000.1	SW52Aα + SW52B	
Cyprinodontiformes	Fundulidae	<i>Lucania goodei</i>	Public database	Single-gene sequence(s)	GenBank	AY296736, AY296737	SW52Aα + SW52B	
Cyprinodontiformes	Anablepidae	<i>Anableps anableps</i>	Public database	Single-gene sequence(s)	GenBank	HM627004, FJ711152	SW52Aα + SW52B	
Belontiiformes	Adrianichthyidae	<i>Oryzias latipes</i>	Public database	Genome assembly	Ensembl	MEDAKA1.76	SW52Aα + SW52B	

Table S1. Cont.

Order	Family	Species	Source/locality	Type of data	Database	Accession no.	Blue opsins
Former Perciformes	Pomacentridae	<i>Stegastes partitus</i>	Public database	Genome assembly; raw reads	GenBank	JMKM000000000.1, SRX526491	SW52B
Former Perciformes	Pomacentridae	<i>Stegastes gascognei</i>	Public database	Single-gene sequence(s)	GenBank	HQ286517	SW52B
Former Perciformes	Pomacentridae	<i>Parma oligolepis</i>	Public database	Single-gene sequence(s)	GenBank	HQ286514	SW52B
Former Perciformes	Pomacentridae	<i>Amphiprion akindynos</i>	Public database	Single-gene sequence(s)	GenBank	HQ286509	SW52B
Former Perciformes	Pomacentridae	<i>Abudefduf sexfasciatus</i>	Public database	Single-gene sequence(s)	GenBank	HQ286508	SW52B
Former Perciformes	Pomacentridae	<i>Chromis viridis</i>	Public database	Single-gene sequence(s)	GenBank	HQ286510	SW52B
Blennioidei (former Perciformes)	Tripterygiidae	<i>Tripterygion delaisi</i>	Public database	Transcriptomic raw reads	SRA GenBank	SRX237746	SW52Aα + SW52Aβ
Blennioidei (former Perciformes)	Blenniidae	<i>Salarias fasciatus</i>	Aquarium trade	Long PCR genomic region	GenBank*	KP004330	SW52Aα + SW52Aβ
Blennioidei (former Perciformes)	Blenniidae	<i>Parablennius parvicornis</i>	Teleost Genome Project	Genomic region	GenBank*	KP004303, KP004304, KP004315	SW52Aα + SW52Aβ
Former Perciformes	Pseudochromidae	<i>Pseudochromis fuscus</i>	Lizard Island, Australia	Long PCR genomic region; transcriptome	GenBank*, SRA GenBank	KP004335, SRX736911, KP017246, KP017247	SW52Aα + SW52Aβ + SW52B
Former Perciformes	Pseudochromidae	<i>Pseudochromis sankaei</i>	Aquarium trade	Long PCR genomic region	GenBank*	KP004334	SW52Aα + SW52Aβ + SW52B
Former Perciformes	Pseudochromidae	<i>Pseudochromis marshallensis</i>	Lizard Island, Australia	Long PCR genomic region	GenBank*	KP004331	SW52Aα + SW52Aβ + SW52B
Former Perciformes	Pseudochromidae	<i>Cypho purpurascens</i>	Lizard Island, Australia	Long PCR genomic region	GenBank*	KP004327	SW52Aα + SW52Aβ + SW52B
Percomorphia							
Former Perciformes	Acanthuridae	<i>Acanthurus triostegus</i>	Aquarium trade	Long PCR genomic region	GenBank*	KP004336	SW52Aα + SW52B
Former Perciformes	Acanthuridae	<i>Ctenochaetus strigosus</i>	Aquarium trade	Long PCR genomic region	GenBank*	KP004329, KP004333	SW52Aα + SW52B
Former Perciformes	Labridae	<i>Symphodus melops</i>	Teleost Genome Project	Genomic region	GenBank*	KP004320, KP004281, KP004250	SW52B
Former Perciformes	Labridae	<i>Choerodon fasciatus</i>	Aquarium trade	Transcriptome	GenBank*	KP004344	SW52B
Former Perciformes	Labridae	<i>Coris gaimardi</i>	Aquarium trade	Transcriptome	GenBank*	KP004340	SW52B
Former Perciformes	Labridae	<i>Labroides dimidiatus</i>	Aquarium trade	Transcriptome	GenBank*	KP004339	SW52B
Lophiiformes	Lophiidae	<i>Lophius vaillanti</i>	Teleost Genome Project	Genomic region	GenBank*	KM978047	SW52Aα + SW52B + pseudogene
Gasterosteiformes	Gasterosteidae	<i>Gasterosteus aculeatus</i>	Public database	Genome assembly	Ensembl	BROADS1.76	Pseudogene + SW52Aβ + SW52B
Former Perciformes	Moronidae	<i>Dicentrarchus labrax</i>	Public database	Genome assembly	GenBank	FQ310506.3	SW52Aβ + SW52B
Tetraodontiformes	Tetraodontidae	<i>Tetraodon nigriviridis</i>	Public database	Genome assembly	Ensembl	TETRAODON8.75	SW52B
Tetraodontiformes	Tetraodontidae	<i>Takifugu rubripes</i>	Public database	Genome assembly	Ensembl	FUGU4.76	SW52B
Notothenioidae	Eleginopsidae	<i>Eleginops macdonovi</i>	Public database	Genomic region	GenBank*	KP004292, KP004268	SW52Aα + SW52Aβ
Notothenioidae	Channichthyidae	<i>Channichthys aceratus</i>	Public database	Genomic raw reads	SRA GenBank	SRX272123	SW52Aα + SW52Aβ
Notothenioidae	Nototheniidae	<i>Trematomus loennbergii</i>	Public database	Single-gene sequence(s)	GenBank	AY771356	SW52Aβ
Scorpaeniformes	Sebastidae	<i>Sebastes nigrocinctus</i>	Public database	Genome assembly	GenBank	AUPR000000000.1	SW52Aα + SW52Aβ + SW52B
Scorpaeniformes	Cottidae	<i>Myoxocephalus scorpius</i>	Teleost Genome Project	Genomic region	GenBank*	KM978045, KM978046	Pseudogene + SW52Aβ + SW52B
Scorpaeniformes	Cottidae	<i>Cottus gobio</i>	Public database	Single-gene sequence(s)	GenBank	AJ430489	SW52Aβ
Scorpaeniformes	Cottocomphoridae	<i>Batrachocottus nikolskii</i>	Public database	Single-gene sequence(s)	GenBank	AJ430474	SW52Aβ
Scorpaeniformes	Cottocomphoridae	<i>Cottus kessleri</i>	Public database	Single-gene sequence(s)	GenBank	AJ430484	SW52Aβ

Cortesi et al. [www.pnas.org/cgi/content/short/1417803112](http://www.pnas.org/cgi/content/short/1417803112)

13 of 16

Cortesi et al. [www.pnas.org/cgi/content/short/1417803112](http://www.pnas.org/cgi/content/short/1417803112)

\*Data obtained within this study.

**Table S2. Primer list for this study**

Method and targeted region: gene/exon or intron	Primer name	Orientation	Primer sequence	Species
Long PCR				
HCFC1/ex1	<i>D1_DUP_HCFC1_F1</i>	Forward	CTCCTTTATAGCCACAGCTCTGTGTCC	<i>P. fuscus</i>
SWS2A $\beta$ /intron1	<i>D10_fus_SWS2Abet_exintr1_R1</i>	Reverse	GTACCAAACTCATCTTACCTCCAAGTGTG	
Long PCR				
SWS2B/ex4	<i>D6_DUP_SWS2Abet_F1</i>	Forward	GAGCGGGAGGTGACCAGGATGGTGG	<i>P. fuscus,</i> <i>T. trichopterus</i> <i>C. strigosus</i>
LWS/ex2	<i>D9_DUP_LWS_ex2_R2</i>	Reverse	CCAGTTTAGAGGRTGACGGAGTTTCTTG	
Long PCR				
SWS2A $\beta$ /ex3	<i>ENDF1</i>	Forward	CCTATGTGATRTTCTCTCTGCTTCTGCTTCG	<i>P. fuscus, P. sankeyi,</i> <i>P. marshallensis</i> <i>Cypho purpurescens</i>
SWS2B/ex3	<i>BEGR1</i>	Reverse	GCAGTGCTCCTGTGGACCAGACTGGTACACCAC	
Long PCR				
HCFC1/ex1	<i>D1_DUP_HCFC1_F1</i>	Forward	Sequence above	<i>A. triostegus</i>
SWS2B/ex3	<i>D16_DUP_SWS2B_ex3_R1</i>	Reverse	GTTTCATTGTTAAACTTGTTCCTGTTG	
Long PCR				
HCFC1/ex1	<i>D1_DUP_HCFC1_F1</i>	Forward	Sequence above	<i>C. strigosus</i>
SWS2B/ex3	<i>D18_DUP_SWS2B_ex1_R3</i>	Reverse	TGTATCTGAAGGCAAAGCAGTAGAAGCAG	
Long PCR				
SWS2A $\alpha$ /ex2	<i>D6_DUP_SWS2Abet_F1</i>	Forward	Sequence above	<i>S. biocellatus</i>
SWS2B/ex5	<i>D5_DUP_SWS2B_R2</i>	Reverse	GCAAGATTGAAGGATTACAGCAAC	
Long PCR				
SWS2A $\alpha$ /ex3	<i>ENDF1</i>	Forward	Sequence above	<i>T. trichopterus</i>
SWS2B/ex3	<i>BEGR1</i>	Reverse	Sequence above	
Long PCR				
SWS2B/ex4	<i>D6_DUP_SWS2Abet_F1</i>	Forward	Sequence above	<i>S. biocellatus,</i> <i>P. platessa</i> <i>A. triostegus</i>
LWS/ex2	<i>D8_DUP_LWS_ex2_R1</i>	Reverse	CTGGTTGCAYACACTGATGGTCTGGC	
Long PCR				
SWS2A $\beta$ /ex2	<i>D6_DUP_SWS2Abet_F1</i>	Forward	Sequence above	<i>S. fasciatus</i>
SWS2A $\alpha$ /ex5	<i>D5_DUP_SWS2B_R2</i>	Reverse	Sequence above	
Long PCR				
SWS2A $\beta$ /SWS2A $\alpha$ /ex1	<i>D22_DUP_beta_ex1_F1</i>	Forward	ATGAAGCACGGCCGTGTCACRGAGC	<i>S. fasciatus</i>
LWS/ex2	<i>D8_DUP_LWS_ex2_R1</i>	Reverse	Sequence above	
Long PCR				
SWS2A $\alpha$ /ex3	<i>D17_DUP_SWS2A_ex3_F1</i>	Forward	GACTGGTACACCACAACAAACAATAC	<i>S. fasciatus</i>
LWS/ex2	<i>D9_DUP_LWS_ex2_R2</i>	Reverse	Sequence above	
Sanger sequencing				
SWS2A $\beta$ /ex1	<i>SWS2A_betF6</i>	Forward	CATCAATGCGCTTACCG	<i>P. fuscus</i>
SWS2A $\beta$ /ex4	<i>SWS2A_betR1</i>	Reverse	GAAGGAGGTGTAGGGGG	
Sanger sequencing				
SWS2B/intron3	<i>BF5_intron34</i>	Forward	CACATCTAAACTTCACCAGG	<i>P. fuscus</i>
SWS2B/ex5	<i>ABbetR6</i>	Reverse	CCCACTTTGGAGACTTC	
Sanger sequencing				
SWS2B/ex1	<i>D27_Ctenoch_SWS2ex1_F</i>	Forward	GCGCTCTTTTATTCAATGTCAGC	<i>A. triostegus</i>
SWS2B/ex4	<i>D26_Acanth_ex4_R2</i>	Reverse	GTAGATAACAGGGTTGTAGAC	
Sanger sequencing				
SWS2B/ex1	<i>D27_Ctenoch_SWS2ex1_F</i>	Forward	Sequence above	<i>C. strigosus</i>
SWS2B/ex4	<i>D28_Ctenoch_SWS2ex4_R</i>	Reverse	GATAACAGGGTTATAGACGGTG	
Sanger sequencing				
SWS2B/ex2	<i>D29_Tricho_ex2_F</i>	Forward	TACAGCGTAATCATCGTCAGTC	<i>T. trichopterus</i>
SWS2B/ex4	<i>D30_Tricho_ex4_R</i>	Reverse	CCACCTGTTTATTGAGGAGTATG	
Sanger sequencing				
SWS1	<i>POOL_Pfus_SWS1_F</i>	Forward	CTGTGTGCCATGGAGTCTGCC	<i>P. fuscus</i>
Pool for quantitative PCR reference	<i>SWS1_R2d_dam</i>	Reverse	TCGTTGTGGGTGTACCAGTC	
Sanger sequencing				
SWS2B	<i>POOL_Pfus_SWS2B_F</i>	Forward	GTGACTGGTACTGCCATCAATATC	<i>P. fuscus</i>
Pool for quantitative PCR reference	<i>POOL_Pfus_SWS2B_R</i>	Reverse	AACGATGGTGAAGAAGGGGATGGAA	
Sanger sequencing				
SWS2A $\alpha$	<i>POOL_Pfus_SWS2Aalfa_F</i>	Forward	CTCACTATTGCATGCACCGCC	<i>P. fuscus</i>
Pool for quantitative PCR reference	<i>POOL_Pfus_SWS2Aalfa_R</i>	Reverse	GCCCATGCCAGCATCGCT	

Method and targeted region:  
gene/exon or intron

Method and targeted region: gene/exon or intron	Primer name	Orientation	Primer sequence	Species
Sanger sequencing				
SWS2α	<i>POOL_Pfus_SWS2Abeta_F</i>	Forward	CTTACCGTTGCATGACCCGTG	<i>P. fuscus</i>
Pool for quantitative PCR reference	<i>POOL_Pfus_SWS2Abeta_R</i>	Reverse	TCCACTCATCCCCAGCATCTTC	
qRT-PCR				
SWS1 (efficiency: 90%)	<i>Pfus_SWS1_2F</i>	Forward	TTTGGAGCCTTCAAGTTACCAG	<i>P. fuscus</i>
SWS1 (efficiency: 90%)	<i>Pfus_SWS1_23R</i>	Reverse	GATGTACCTGCTCCAGCCAAAG	
qRT-PCR				
SWS2B (efficiency: 94%)	<i>Pfus_SWS2B_1F1</i>	Forward	CCGTGGGCTCCTTACCTG	<i>P. fuscus</i>
SWS2B (efficiency: 94%)	<i>Pfus_SWS2B_12R1</i>	Reverse	GGCTCACCATGCCTCCAATC	
qRT-PCR				
SWS2α (efficiency: 96%)	<i>Pfus_SWS2Aalfa_12F1</i>	Forward	CATGGCAACACTCGGGGGTATG	<i>P. fuscus</i>
SWS2α (efficiency: 96%)	<i>Pfus_SWS2Aalfa_2R1</i>	Reverse	CGCAACACCCAGGTGAACC	
qRT-PCR				
SWS2α (efficiency: 96%)	<i>Pfus_SWS2Abeta_1F2</i>	Forward	GGTGAACTTGGCTGCCGCG	<i>P. fuscus</i>
SWS2α (efficiency: 96%)	<i>Pfus_SWS2Abeta_12R1</i>	Reverse	CCATACCTCCAAGTGTGCTAC	

# Seeing is believing: Dynamic evolution of gene families

Rayna M. Harris and Hans A. Hofmann<sup>1</sup>

Department of Integrative Biology, Center for Computational Biology, Institute for Cellular and Molecular Biology, The University of Texas at Austin, Austin, TX 78712

Educated by his deep appreciation of nature, Darwin observed that “from so simple a beginning endless forms most beautiful” have arisen throughout the evolutionary history of life on earth (1). The spectacular diversity of orchids (2) and beetles (3) has long fascinated naturalists and casual observers alike. More recently, the adaptive radiations of Hawaiian drosophilids (4), Caribbean *Anolis* lizards (5), and African cichlid fishes (6) have become prime examples for understanding the mechanisms that give rise to phenotypic diversity (7). Following gene duplication and loss, adaptation and speciation appear to proceed through a combination of both structural and *cis*-regulatory changes in one or more paralogous genes (8). Recent advances in sequencing technology have enabled researchers to make significant progress in understanding the molecular evolution that has facilitated diversification. In PNAS, Cortesi et al. (9) examine the evolution of vertebrate opsin genes as a spectacular example of how gene duplication and deletion events that affect spectral sensitivity have driven adaptation to diverse light environments and visual displays.

Gene families comprise several to many genes of similar nucleotide or amino acid sequences; they share similar cellular functions and commonly arise as a result of gene or genome duplication events. The expansion or contraction of gene families over evolutionary time in different lineages can be random or the result of natural selection, although demonstrating the latter can be difficult (10). Several mechanisms, such as tandem duplications, segmental duplications, or even whole-genome duplications can lead to the expansion of gene families. Importantly, during the evolution of chordates, the ancestral deuterostome genome (likely in a cephalochordate ancestor) experienced two rounds of whole-genome duplication followed by a genome

duplication in actinopterygian (ray-finned) fishes, but not in the sarcopterygian (lobe-finned) fishes, the lineage that includes land vertebrates (11). Even though most duplicated genes were secondarily lost, many evolved new functions, in support of the notion that gene and genome duplications might provide a major mechanism for generating phenotypic diversity in evolution (7).

## Opsin Gene Family Expansion and Light Sensitivity

Opsin genes expressed in photoreceptor cells are fundamental to animal vision and are a major force underlying the evolutionary adaptation to variable photic environments (12). The diversity of these genes is achieved by gene duplication followed by changes in amino acid sequence at key tuning sites. Opsins have been crucial to the successful colonization of diverse habitats, especially in teleost fishes, the most species-rich lineage of vertebrates. In a tour de force comparative genomics analysis, Cortesi et al. (9) describe a newly discovered violet/blue short wavelength-sensitive 2 (SWS2) opsin, which arose alongside the radiation of the highly diverse percomorph fishes (which include cichlid fishes, wrasses, and other diverse and colorful families). Specifically, the authors compared almost 100 fish genomes to examine the complex evolutionary history of SWS2, including numerous duplication, deletion, and pseudogenization events, and possibly even the “resurrection” of functional genes from pseudogenes (Fig. 1). Several amino acid substitutions are described that likely facilitated the adaptive differentiation between SWS2 gene copies, probably by conferring sensitivities to different wavelengths of light or by being differentially expressed as organisms move through their ontogenetic and life history stages. The study by Cortesi et al. (9) illustrates the complexity that results from gene duplication and loss, and which in turn enables the evolution of animal diversity.

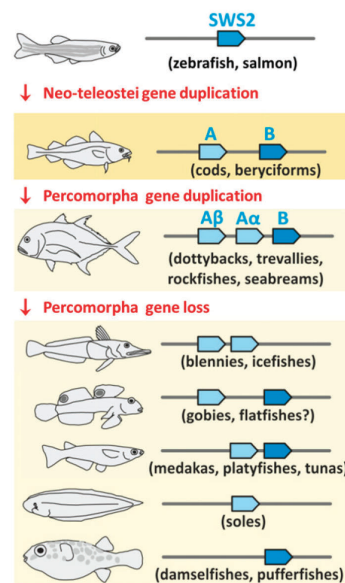


**Fig. 1.** Abbreviated history of violet-blue-sensitive (SWS2) genes in teleost fishes. The SWS2 gene was present in a single copy before the neo-teleostei gene duplication, which gave rise to SWS2A (light blue) and SWS2B paralogs (dark blue). In the percomorpha lineage, a subsequent duplication event gave rise to SWS2A $\alpha$  and SWS2 $\beta$  paralogs. Although these three paralogs have been retained in many species, one or more paralogs have been lost in percomorph fishes. The syntenic relationship is shown to illustrate that these were tandem duplications occurring on the same chromosome, with example species listed below in parentheses. Modified from ref. 9.

## Gene Family Evolution and Phenotypic Diversification

The evolution of opsin genes has received ample scrutiny, yet several other gene families deserve mention because of their likely role in phenotypic diversification. One of the most spectacular examples comprises the large and diverse family of olfactory receptor

Author contributions: R.M.H. and H.A.H. wrote the paper.

The authors declare no conflict of interest.

See companion article on page 1493.

<sup>1</sup>To whom correspondence should be addressed. Email: hans@utexas.edu.



genes, which vary widely in number across vertebrate genomes (13). For example, although rodents have approximately 1,000 olfactory receptor genes, humans have only around 400 (a reduction likely caused by massive loss and pseudogenization of olfactory receptor genes in the human lineage). Compared with mammals, the olfactory receptor gene family is considerably more diverse in fishes (eight subfamilies are present), yet the total number of olfactory receptor genes is much smaller, suggesting that the mammalian olfactory receptor gene family is much less complex compared with that in the ancestor of vertebrates. Even though it is often assumed that gene families evolve adaptively, signatures of selection are often difficult to demonstrate. In this regard olfactory receptor genes also serve as a warning against adaptive scenarios because the number and types of olfactory receptor genes apparently have evolved only in part in response to environmental needs (13).

Voltage-gated sodium channels provide another compelling example, as they form the basis for electrical excitability in animals (14). These sodium channels evolved from calcium channels and were present in the last common ancestor of choanoflagellates and metazoa (animals), thus they already existed when neurons first evolved. A motif that evolved early in chordate evolution allows voltage-gated sodium channels to cluster where action potentials are generated to greatly enhance conduction velocity. After the late Devonian extinction, when teleosts and tetrapods each diversified in their respective habitats and the complexity of their brains increased concomitantly, the voltage-gated sodium channel gene family expanded in parallel in tetrapods and teleosts, possibly allowing more complex neural computations along with energy savings. In addition, these channels have been selected to encode diverse communication signals in weakly electric fish (15) and to protect against lethal sodium channel toxins (e.g., in snakes, newts, pufferfish, insects), providing unprecedented opportunities for drug design and therapeutic applications (16).

Gene families involved in cell-to-cell signaling appear to expand less in the course of evolution, possibly because the genes that encode the receptors and ligands need to evolve in a coordinated manner. Examples include steroid hormones, which classically

bind to receptors that belong to the nuclear receptor family of transcription factors. These genes have coevolved with those that encode the enzymes that synthesize steroids at key transitions in the evolution of vertebrates and during gene family expansion (17), likely contributing to the diversification of vertebrates through their fundamental roles in reproduction, development, homeostasis, and stress response.

#### Integration of Functional and Evolutionary Genomics

The study by Cortesi et al. (9) does not describe any analyses of regulatory sequence evolution, nor do the authors investigate tissue- or temporally specific gene-expression patterns that may have arisen following regulatory changes. Coyne and Hoekstra (8) argue that adaptation and speciation proceed through a combination of both structural and *cis*-regulatory changes in one or more paralogous genes. Regrettably, much of our knowledge regarding the influence of structural and regulatory contribution to phenotypic diversity comes from studies examining these two mechanisms in isolation rather than through concurrent examination in the same system. However, a recent study by Harris et al. (18) combined structural, functional, and regulatory analyses to examine the evolution of the pro-opiomelanocortin gene family. By integrating temporal and spatial expression measurements with sequence variation and regulatory interactions, these authors were able to shed new light on the mechanisms of phenotypic diversification.

It would be interesting to see future studies on the opsin gene family that incorporate both an analysis of gene expression across time or cell type with a bioinformatic analysis of regulatory sequence evolution.

#### The Power of the Comparative Approach

All these studies underscore the power of the comparative approach for understanding gene family evolution and, ultimately, the origins of animal diversity. Aristotle (in his book *Peri Zoon Morion*) already championed the promise of comparing different species for achieving a deep understanding about nature. If conducted within a phylogenetic framework, comparative analyses can provide inference similar to that obtainable with experimental approaches (19). Furthermore, a deeper understanding of the detailed relationship between orthologous and paralogous genes is crucial if we want to fully capitalize on the wealth of data generated with comparative omics approaches. In an era where biologists use fewer and fewer model systems, to the detriment of the entire biomedical research enterprise (20), the Cortesi et al. (9) paper provides a timely reminder for this notion, as it convincingly demonstrates a likely role for opsin gene evolution in the ability of animals to conquer new niches and acquire new modes of communication.

**ACKNOWLEDGMENTS.** Research in our laboratory is supported by National Science Foundation Grants IOS-0843712 and IOS-1354942 (to H.A.H.) and DBI-0939454 for the BEACON Center for the Study of Evolution in Action.

- 1 Darwin C (1859) *On the Origin of Species by Means of Natural Selection*. (J Murray, London).
- 2 Dressler RL (1993) *Phylogeny and Classification of the Orchid Family* (Timber Press, Portland, OR).
- 3 Farrell BD (1998) "Inordinate Fondness" explained: Why are there so many beetles? *Science* 281(5376):555–559.
- 4 Kambyseis MP, Craddock EM (1997) Ecological and reproductive shifts in the diversification of the endemic Hawaiian *Drosophila*. *Molecular Evolution and Adaptive Radiation*, eds Givnish TJ, Sytsma KJ (Cambridge Univ Press, Cambridge, UK), pp 475–509.
- 5 Losos JB (2001) Evolution: A lizard's tale. *Sci Am* 284(3):64–69.
- 6 Bravard D, et al. (2014) The genomic substrate for adaptive radiation in African cichlid fish. *Nature* 513(7518):375–381.
- 7 Ohno S (1970) *Evolution by Gene Duplication* (Springer, New York).
- 8 Coyne JA, Hoekstra HE (2007) Evolution of protein expression: New genes for a new diet. *Curr Biol* 17(23):R1014–R1016.
- 9 Cortesi F, et al. (2015) Ancestral duplications and highly dynamic opsin gene evolution in percomorph fishes. *Proc Natl Acad Sci USA* 112:1493–1498.
- 10 Hartl DL, Clark AG (2007) *Principles of Population Genetics* (Sinauer Associates, Sunderland, MA), 4th Ed.
- 11 Meyer A, Van de Peer Y (2005) From 2R to 3R: Evidence for a fish-specific genome duplication (FSGD). *BioEssays* 27(9): 937–945.

- 12 Carleton K (2009) Cichlid fish visual systems: Mechanisms of spectral tuning. *Integr Zool* 4(1):75–86.
- 13 Nimura Y, Nei M (2006) Evolutionary dynamics of olfactory and other chemosensory receptor genes in vertebrates. *J Hum Genet* 51(6):505–517.
- 14 Zakon HH (2012) Adaptive evolution of voltage-gated sodium channels: The first 800 million years. *Proc Natl Acad Sci USA* 109(Suppl 1):10619–10625.
- 15 Zakon HH, Lu Y, Zwickl DJ, Hillis DM (2006) Sodium channel genes and the evolution of diversity in communication signals of electric fishes: Convergent molecular evolution. *Proc Natl Acad Sci USA* 103(10):3675–3680.
- 16 Billen B, Bosmans F, Tytgat J (2008) Animal peptides targeting voltage-activated sodium channels. *Curr Pharm Des* 14(24):2492–2502.
- 17 Baker ME, Nelson DR, Studer RA (2014) Origin of the response to adrenal and sex steroids: Roles of promiscuity and co-evolution of enzymes and steroid receptors. *J Steroid Biochem Mol Biol*, 10.1016/j.jsmb.2014.10.020.
- 18 Harris RM, Dijkstra PD, Hofmann HA (2014) Complex structural and regulatory evolution of the pro-opiomelanocortin gene family. *Gen Comp Endocrinol* 195:107–115.
- 19 Maynard-Smith J, Holliday R, eds (1979) *Preface to Evolution of Adaptation by Natural Selection. Evolution of Adaptation by Natural Selection* (The Royal Society, London).
- 20 Bolker J (2012) Model organisms: There's more to life than rats and flies. *Nature* 491(7422):31–33.



## Side Projects

Evolution of colourful signals in marine sea slugs, and the use of facial colour patterns in the Princess of Burundi cichlid *Neolamprologus Brichardi*



## Chapter 4

# Conspicuousness is correlated with toxicity in marine opisthobranchs

F. Cortesi, K. L. Cheney,

Journal of Evolutionary Biology (2010)

4.1. Manuscript p. 95 – 104

4.2. Supporting Information p. 105

This paper emerged early on during my PhD and the work presented in it was performed as part of my honours thesis (equivalent to a Swiss Masters), which was conducted under the supervision of Dr. Cheney in Australia.



## Conspicuousness is correlated with toxicity in marine opisthobranchs

F. CORTESI & K. L. CHENEY

School of Biological Sciences, The University of Queensland, QLD, Australia

### Keywords:

aposematic colouration;  
marine invertebrates;  
nudibranchs;  
secondary defences;  
visual signalling.

### Abstract

Aposematism is defined as the use of conspicuous colouration to warn predators that an individual is chemically or otherwise defended. Mechanisms that drive the evolution of aposematism are complex. Theoretical and empirical studies show that conspicuousness can be either positively or negatively correlated with toxicity as once aposematism is established, species can allocate resources into becoming more conspicuous and/or increase secondary defences. Here, we investigated the evolution of conspicuousness and toxicity in marine opisthobranchs. Conspicuousness of colour signals was assessed using spectral reflectance measurements and theoretical vision models from the perspective of two reef fish signal receivers. The relative toxicity of chemicals extracted from each opisthobranch species was then determined using toxicity assays. Using a phylogenetic comparative analysis, we found a significant correlation between conspicuousness and toxicity, indicating that conspicuousness acts as an honest signal when signifying level of defence and provides evidence for aposematism in opisthobranchs.

### Introduction

Aposematism is defined as the use of conspicuous colouration to warn predators that a species is chemically or otherwise defended (Poulton, 1890; Cott, 1940). The mechanisms that drive the evolution of aposematic signals are complex and have received much attention in recent literature (Speed & Ruxton, 2005a, 2007; Darst *et al.*, 2006; Blount *et al.*, 2009). Aposematic species are thought to initially evolve from defended, inconspicuous (cryptic) species (e.g. Sillén-Tullberg & Bryant, 1983; Guilford, 1988). Once aposematism is established, resource allocation by a species becomes an important evolutionary factor: should a species invest in becoming more conspicuous, more defended or both? A positive correlation between signal strength and level of toxicity has been shown in the conspicuous and highly toxic Dendrobatid frog family and in the Asian lady bird beetle *Harmonia axyridis* (Summers & Clough, 2001; Bezzerides *et al.*, 2007). However, theory also predicts that highly defended prey should evolve less conspicuous colour-

ation because their chances of surviving attacks are enhanced, and therefore, costs involved with conspicuous signalling can be reduced (Leimar *et al.*, 1986; Speed, 2001; Speed & Ruxton, 2005b). Support for this contradictory theory has been shown in three closely related Dendrobatid frog species: *Epipedobates parvulus*, *E. bilineatus* and *E. hahneli*. The most toxic species was only moderately conspicuous (*E. parvulus*), and the most conspicuous species was only moderately toxic (*E. bilineatus*) (Darst *et al.*, 2006).

Empirical evidence to corroborate these two hypotheses is limited, and studies have generally failed to consider the phylogenetic relatedness between large numbers of species (Darst *et al.*, 2006) or conspicuousness from a signal receiver's perspective (e.g. Summers & Clough, 2001; Bezzerides *et al.*, 2007; but see Darst *et al.*, 2006). Indeed, when investigating the function or evolution of coloured signals, it is important to consider the spectral sensitivity and visual abilities of the signal receiver, the light environment and the background against which the signal is viewed (Endler, 1990).

On coral reefs, marine opisthobranchs (which include Nudibranchia) provide an ideal model system to investigate the co-evolution of conspicuousness and toxicity. They display some of the most diverse and spectacular

Correspondence: Karen L. Cheney, School of Biological Sciences, The University of Queensland, St Lucia, QLD 4072, Australia.  
Tel.: +61 7 3365 2855; fax: +61 7 3365 1655; e-mail: k.cheney@uq.edu.au

colours and patterns found in nature, which function as advertisement signals (aposematism and deimatism) and provide concealment (crypsis) to protect themselves from predation (Edmunds, 1987). Indeed, Gosliner & Behrens, (1990) estimated that 50% of opisthobranch species are aposematic. As a secondary defence, opisthobranchs contain chemicals that are produced *de novo* or deposited as secondary metabolites from their diet (Cimino & Ghiselin, 1998, 1999; Cimino *et al.*, 1999; Marin *et al.*, 1999). Defensive chemicals found within opisthobranchs are mainly alkaloids, many of which are terpenes and their derivatives, and are typically stored in the outer body parts of the opisthobranch, either in the epidermal layer or in mantle glands (Carte & Faulkner, 1983; Cimino *et al.*, 1999; Fontana *et al.*, 1999, 2000; Ungur *et al.*, 1999).

To examine whether a positive correlation between conspicuousness and toxicity exists in marine opisthobranchs, we first measured the spectral reflectance of opisthobranch colour signals and their background habitat. Second, a colour opponent discrimination theoretical vision model was used (Vorobyev & Osorio, 1998) to quantify the conspicuousness of opisthobranch colour patches in terms of spectral contrast, both against their background and between colours within an opisthobranch pattern. This was carried out from the perspective of two distinct reef fish visual systems, with and without ultraviolet (UV) sensitivity. Third, toxicity assays were conducted on extracted opisthobranch chemicals using a brine shrimp assay following the protocol of Meyer *et al.* (1982). Finally, a phylogenetic comparative analysis was used to test for a correlation between conspicuousness and toxicity.

## Materials and methods

### Study site and species

Twenty opisthobranch species ( $n = 3\text{--}10$  per species), comprising of members from the suborders Nudibranchia ( $n = 14$  species), Cephalaspidea ( $n = 3$ ) and Sacoglossa ( $n = 3$ ), were located using SCUBA on coral reefs around Lizard Island (14°40'S; 145°28'E), Great Barrier Reef, Australia; North Stradbroke Island (27°35'S; 153°27'E), and Mooloolaba (26°40'S; 153°07'E), Southeast Queensland, Australia, at depths between 3 and 7 m. Opisthobranchs were placed in plastic vials, transported back to shore and then held in tanks with running sea water or air pumps for no longer than 48 h until their spectral reflectance could be measured. After measurements were taken, opisthobranchs were frozen and stored at  $-18^\circ\text{C}$ .

### Spectral reflectance measurements of opisthobranchs and background habitat

Spectral reflectance measurements of opisthobranch colours were obtained using an Ocean Optics (Dunedin,

FL, USA) USB2000 spectrometer and a laptop computer running Ocean Optics OOIBASE32 software. Opisthobranchs were measured in the laboratory in a tray containing enough sea water to cover each individual completely. The spectral reflectance of each distinct colour patch  $> 4\text{ mm}^2$  ( $n = 1\text{--}6$  depending on species) was measured through a 200- $\mu\text{m}$  bifurcated optic UV/visible fibre connected to a PX-2 pulse xenon light (Ocean Optics). A Spectralon 99% white reflectance standard (LabSphere, NH, USA) was used to calibrate the percentage of light reflected at each wavelength from 300–800 nm. The bare end of the fibre was held at a 45° angle to prevent specular reflectance. At least ten measurements per colour patch were taken and then averaged. Colour measurements were taken from at least three individuals per species, with the exception of *Chelidonura inornata* and *Chelidonura varians*, of which we only acquired two individuals. Spectra were categorized by the wavelength at which light was reflected and the shape of reflectance curves, as per a previous categorization of reef fish colours (Marshall, 2000).

We also measured the spectral reflectance of background habitats that each individual was found upon using an underwater spectrometer. At the location where each opisthobranch was collected, measurements of the respective background habitat within a 5 cm radius of the opisthobranch were taken using the USB2000 spectrometer enclosed in an underwater housing (Wills Camera Housings, Vic., Australia). Data were stored using a Palm-Spec computer running PALM-SPEC software (Ocean Optics). Measurements were taken with a modified (shortened, 60 cm) 1000- $\mu\text{m}$  UV/visible fibre using underwater video lights (Sunray 200; Light and Motion, USA) that emit light in the 350–800 nm range. At least ten measurements were taken of the substrate and then averaged. A Spectralon 99% white reflectance standard was again used to calibrate the percentage of light reflected. For heterogeneous backgrounds, equally coloured areas were judged by eye, and then each substrate type was measured.

### Visual modelling of colour signals

We used the Vorobyev–Osorio colour opponent discrimination model (Vorobyev & Osorio, 1998; Vorobyev *et al.*, 2001) to assess the conspicuousness of different opisthobranch species in terms of spectral contrast from the perspective of two potential trichromatic fish species: the UV-sensitive damselfish, *Stegastes fasciatus* ( $\lambda_{\text{max}} = 363\text{ nm}$ , 470 and 528 nm) (Losey *et al.*, 2003), and the blue/green-sensitive triggerfish, *Rhinecanthus aculeatus* ( $\lambda_{\text{max}} = 420, 480$  and 530 nm) (NJ Marshall, unpublished data). These fish were chosen because they have markedly different visual sensitivities, and both fish are likely to encounter opisthobranchs. Although they themselves may not be potential predators of opisthobranchs, they are used in this study to represent the visual systems of a

range of reef fish species (Losey *et al.*, 2003). Many opisthobranch species reflect colours in the ultraviolet (UV, < 400 nm) (Fig. 1, unpublished data); therefore, sensitivity in the UV may affect the way in which opisthobranch colours are perceived. These species will subsequently be referred to by their genus name only.

The model calculates the 'distance' ( $\Delta S$ ) between the colours in a dichromatic, trichromatic or tetrachromatic visual space, depending on the number of receptor types of the signal receiver. Colours that appear similar within each visual system result in low  $\Delta S$  values, whereas those that are chromatically contrasting are high in value. This model assumes that the luminosity signal is disregarded, that colours are encoded by an opponent mechanism judged using the known cone sensitivity of the signal receiver and that colour discrimination in the perceptual space is limited by noise originating in the receptors and determined by the relative proportion of each photoreceptor (Vorobyev & Osorio, 1998; Vorobyev *et al.*, 2001). The receptor quantum catch,  $q_i$ , in photoreceptor of type  $i$  (i.e. cone cell) is calculated as (modified from eqn 1 of Vorobyev & Osorio, 1998):

$$q_i = \int_{\lambda} R_i(\lambda) S(\lambda) I(\lambda) d\lambda \quad (1)$$

where  $\lambda$  denotes wavelength,  $R_i(\lambda)$  denotes the spectral sensitivity of a receptor  $i$ ,  $S(\lambda)$  is the reflectance spectrum

of the colour patch,  $I(\lambda)$  is the irradiance spectrum entering the eye and integration is over the range 300–700 nm. Colour distances were calculated with an illumination measured at 5 m depth.

Colour distances were calculated between each opisthobranch colour patch and the corresponding background habitat (colour/background) for each individual and then averaged for each species. Colour distances were also calculated between each adjacent colour patch on the opisthobranch (colour/colour). The maximum colour distance ( $\Delta S$ ) for each species was used as our measure of conspicuousness and varied considerably between opisthobranch species for both signal receivers (Table S1).

The Weber fraction ( $\omega$ ) was based on the relative proportion of receptor types, and here, we assumed a 1 : 2 : 2 ratio [short-wavelength-sensitive (SWS) cones to medium-wavelength-sensitive cones (MWS) to long-wavelength-sensitive cones (LWS); S : M : L] for our signal receivers, which was set according to morphological studies of fish retina (NJ Marshall, unpublished data). Because of the lack of behavioural data, the LWS noise threshold was set at 0.05, which represents a conservative visual performance, being half the sensitivity of the human LWS system (Wyszecki & Styles, 1982).

To compare the spectral contrast of colours while considering a coral reef environment, colour distances were calculated using illumination measurements at a

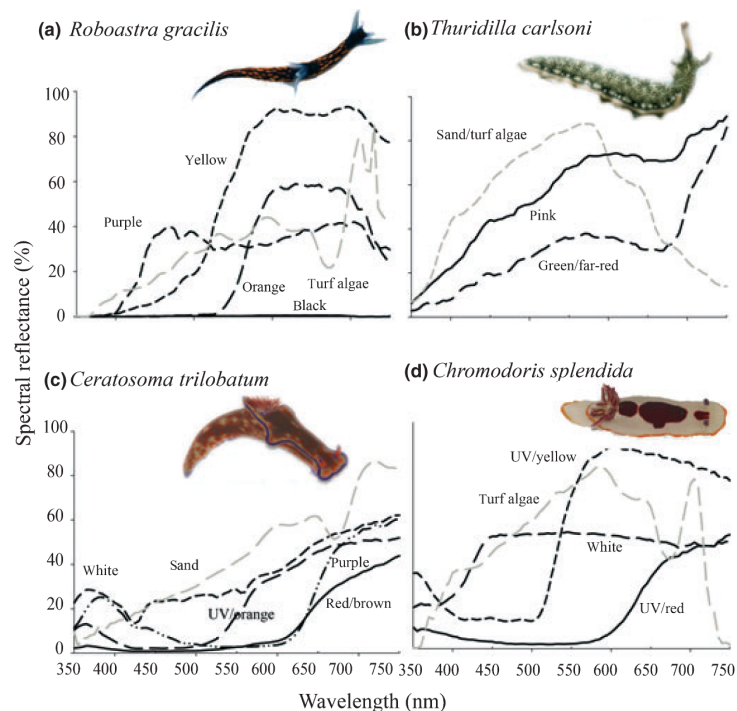


**Fig. 1** Spectral reflectance (%) of four representative opisthobranch species. Grey lines indicate background colours.

water depth of 5 m. Illumination measurements were taken using the underwater spectrometer on reefs at each study site with a cosine corrector providing an 180° hemisphere. We measured both down-welling light (by holding the fibre 1 m away from the reef and pointing upwards) and side-welling light (holding the fibre at a distance of 1–2 m from and pointing horizontally at the reef); however, we found no significant differences in our overall conclusions, regardless of which measure we used.

### Toxicity bioassay

We tested the relative toxic properties of extracted chemicals from each species of opisthobranch with a brine shrimp lethality assay, which is considered a useful tool for preliminary assessment of toxicity in marine organisms (Carballo *et al.*, 2002), and has been used previously when assessing opisthobranch toxicity (Gunthorpe & Cameron, 1987). Chemical extractions were conducted as per a previous study investigating the toxicity of opisthobranchs (Gunthorpe & Cameron, 1987). Briefly, frozen opisthobranchs were thawed at room temperature and homogenized using a mortar and pestle. The resulting mass was soaked for 72 h in 200 mL methanol at 4 °C. The methanol was decanted and evaporated using a rotary evaporator under reduced pressure in a water bath at 40 °C. The resulting aqueous–organic solution was then partitioned in a separating funnel in a 1 : 1 dichloromethane : distilled water mixture. The dichloromethane was evaporated using a rotary evaporator under reduced pressure in a water bath at 35 °C, and crude chemicals were transferred into 10-mL glass vials. Remaining chemical extracts that could not be transferred easily were diluted in 100% ethanol, transferred into 10-mL glass vials and left under a fume hood to ensure ethanol evaporation. All chemicals were then frozen at –4 °C until further use.

Brine shrimp bioassays were then conducted as per Meyer *et al.*, 1982. Frozen chemicals were thawed, and the weight of the compound was recorded. A solution of 10 mg compound per mL methanol was prepared. We then transferred 5, 50 and 500 µL of the solution to 1.5-cm discs of filter paper. The discs were placed in 5-mL plastic vials and left to dry for 24 h. Final concentrations of 10, 100 and 1000 µg mL<sup>–1</sup> were obtained by adding 5 mL seawater to each vial during the process (see below). Control discs were prepared using methanol alone. Three replicates per dose level and control, per species of opisthobranch were prepared. Brine shrimp eggs (San Francisco Bay Brand, NY, USA) were hatched in a 1-litre glass bottle filled with double-distilled water. The hatch mix was suspended in the water and kept under aeration for 48 h, before the phototropic nauplii could be collected by pipette. Ten of the nauplii were counted against a lighted background and transferred into the test vials, which were then filled with artificial

sea water to make 5 mL. A drop of dry yeast suspension was added for food supply. The vials were kept under constant illumination over a 24-h time period before survivors from each dose and control were counted out under a 4.5× dissecting microscope. The percentage of death per treatment was calculated as: % deaths = (1 – test population after treatment/control population after treatment) \* 100 (Abbott, 1987) (Table 1; Fig. 3).

### Phylogenetic comparative analysis

#### Sequence acquisition and alignment

Partial 16S rDNA gene sequences of fourteen species were taken directly from GenBank (<http://www.ncbi.nlm.nih.gov/>). However, sequence data were not available for six species. In these cases, we used species from the same genus: *Phyllidia elegans* for *Phyllidia picta*, *Glossodoris pallida* for *Glossodoris atromarginata*, *Flabellina verrucosa* for *Flabellina rubrolineata*, *Hypselodoris bennetti* for *Hypselodoris whitei*, *Aegires punctilucens* for *Notodoris citrina* and *Notodoris gardineri* (also known as *Aegires citrina* and *Aegires gardineri*; Fahey & Gosliner, 2004) to generate branch structure, and then species used in this study were added as polytomies. *Onchidella floridana* (Pulmonata) was included as an out-group species for rooting (Vonnemann *et al.*, 2005). Sequences were initially aligned using CLUSTALW (Thompson *et al.*, 1994) in BioEdit (Hall, 1999), and manual adjustments were made afterwards by eye. Alignment gaps, representing putative insertion–deletion (indel) sites, were coded as character

**Table 1** Mortality (%) of brine shrimp (*n* = 30) after 24 h of exposure to opisthobranch chemical extracts.

Opisthobranch species	Lethality (%)		
	10 µg mL <sup>–1</sup>	100 µg mL <sup>–1</sup>	1000 µg mL <sup>–1</sup>
<i>Chelidonura inornata</i>	25	100	100
<i>Roboastra gracilis</i>	0	45	100
<i>Sagaminopteron ornatum</i>	50	89	100
<i>Phyllidiella pustulosa</i>	0	10	97
<i>Phyllidia varicosa</i>	0	17	67
<i>Phyllidia picta</i>	0	0	60
<i>Glossodoris atromarginata</i>	3	12	47
<i>Ceratosoma trilobatum</i>	0	14	35
<i>Chromodoris splendida</i>	0	21	32
<i>Flabellina rubrolineata</i>	0	11	30
<i>Elysia ornata</i>	0	0	27
<i>Chelidonura varians</i>	0	0	24
<i>Phyllidia ocellata</i>	3	11	24
<i>Notodoris gardineri</i>	0	0	17
<i>Thuridilla gracilis</i>	0	0	11
<i>Hypselodoris whitei</i>	0	10	10
<i>Notodoris citrina</i>	0	0	10
<i>Risbecia tryoni</i>	0	0	8
<i>Hypselodoris obscura</i>	0	0	7
<i>Thuridilla carlsoni</i>	0	0	0



states (1 = character present, 0 = character absent). The total analysed alignment length of 16S comprised 463 base pairs. The alignment and resulting trees are deposited in TREEBASE (<http://www.treebase.org>).

#### Phylogenetic reconstruction

We assessed the phylogenetic relationship using Maximum likelihood (ML) and Bayesian inference approaches. RAXML version 7.0.4 (Stamatakis *et al.*, 2005) was used for ML reconstruction with default settings (GTRGAMMA model) on the web-interface (<http://www.phylo.org/>) using rapid bootstrap analysis (1000 replicates) and the search option for best scoring ML tree (Stamatakis *et al.*, 2008). Bayesian inference was conducted using MRBAYES v3.1.2 (Huelsenbeck & Ronquist, 2001), using a Metropolis Chain Monte Carlo search. Each set produced five million generations by sampling every 1000 generations. The first 1000 trees (=1 000 000 generations) were removed as burn-in. Only clades with significant support values (> 70% bootstrap; > 0.80 posterior probabilities) were used for subsequent analysis; others were collapsed and treated as polytomies for the comparative analysis (Fig. 2).

#### Statistical analysis

Colour distances ( $\Delta S$ ) were first log-transformed to meet the assumptions of parametric testing. To assess whether colour distances were significantly different between signal receivers, we used a General Linear Mixed Model (GLMM) with log colour distance as the response variable, signal receiver and colour category as fixed factors and opisthobranch species as a random factor. Highly nonsignificant interactions ( $P > 0.25$ ) were omitted from the model. There was a significant difference in colour distances between signal receivers for opisthobranch colours against their background ( $F_{1,19.5} = 125.3$ ,  $P < 0.001$ ) and between colours within an opisthobranch pattern ( $F_{1,115} = 14.3$ ,  $P = 0.001$ ); therefore, analyses for each signal receiver were conducted separately.

A linear regression model was first used to test for a relationship between conspicuousness and toxicity without considering the relatedness of species. Relative toxicity was defined as the percentage of dead brine shrimps at a concentration of 1000  $\mu\text{g/mL}$ . To consider whether a correlation existed between conspicuousness and toxicity while considering phylogenetic relatedness between species, we used a Generalized Least Squares (GLS) regression model. To select the most parsimonious model, we ran the analysis using the Grafen (1989), Martins & Hansen (1997), Brownian (Felsenstein, 1985) models using corGrafen, corMartins, corBrownian packages in the ape package (<http://ape.mpl.ird.fr>) and selected the model with the lowest AIC value (corGrafen). To resolve polytomies, we used the multi2di function in the ape package for R and introduced zero-length branch lengths for the branch within the polytomy. We adjusted the degrees of freedom to account for soft polytomies in

our phylogenetic tree (Garland & Diaz-Uriarte, 1999). All phylogenetic regression analysis was conducted in R v. 2.4.1. (<http://www.r-project.org/>).

## Results

### Conspicuousness of opisthobranchs

The most common colour categories found on opisthobranch molluscs were white ( $n = 9$  species), black ( $n = 8$ ), brown ( $n = 8$ ) and purple ( $n = 8$ ). Opisthobranchs were found on turf algae, sand, live coral, sponge and tunicates (Fig. 1, Table S1). Overall, colour distances were significantly higher for the UV-sensitive fish *Stegastes* compared to *Rhinecanthus* (mean  $\pm$  SE: colour/background *Rhinecanthus*  $8.8 \pm 7.4$ , *Stegastes*  $20.7 \pm 1.6$ , paired  $t$ -test  $t_{55} = 9.6$ ,  $P < 0.001$ ; colour/colour: *Rhinecanthus*  $13.5 \pm 1.8$ , *Stegastes*  $20.1 \pm 2.3$ , paired  $t$ -test  $t_{57} = 4.80$ ,  $P < 0.001$ ). The highest colour distances were found on *Roboastra gracilis* between colour (orange) and background and between colours within the pattern (black and orange) (Fig. 1; Table S1). The lowest colour distances were found on *Thuridilla carlsoni* between colours and background (*Rhinecanthus*: green/far-red; *Stegastes*: pink) and between colours within the pattern (green/far-red and pink, for both signal receivers) (Fig. 1; Table S1).

### Toxicity of opisthobranchs

Toxic extractions from each opisthobranch species showed partial or total lethality to brine shrimps at a concentration of 1000  $\mu\text{g/mL}$ , with the exception of *Thuridilla carlsoni*. *Roboastra gracilis*, *Chelidonura inornata* and *Sagaminopteron ornatum* were found to cause 100% lethality at this concentration (Table 1).

### Phylogenetic analysis

The results of the phylogenetic analysis were in general agreement with previously published trees on opisthobranch phylogenies (Wollscheid-Lengeling *et al.*, 2001; Vonnemann *et al.*, 2005) (Fig. 2). There was a significant association between conspicuousness and toxicity from the perspective of both signal receivers for colour/background measurements (*Rhinecanthus*:  $r^2 = 0.27$ ,  $n = 20$ ,  $P = 0.02$ ; *Stegastes*:  $r^2 = 0.35$ ,  $n = 20$ ,  $P = 0.01$ ; Fig. 3) and for colour/colour measurements (*Rhinecanthus*:  $r^2 = 0.25$ ,  $n = 19$ ,  $P = 0.03$ ; *Stegastes*:  $r^2 = 0.27$ ,  $n = 19$ ,  $P = 0.03$ ; Fig. 3).

Using the phylogenetic generalized least squares (GLS) regression model, there was also a significant association between conspicuousness and toxicity for colour/background measurements (*Rhinecanthus*:  $t_{17} = 2.62$ ,  $P = 0.019$ ; *Stegastes*:  $t_{17} = 3.11$ ,  $P = 0.007$ ) and colour/colour measurements (*Rhinecanthus*:  $t_{17} = 2.37$ ,  $P = 0.03$ ; *Stegastes*:  $t_{17} = 2.40$ ,  $P = 0.03$ ). However, we

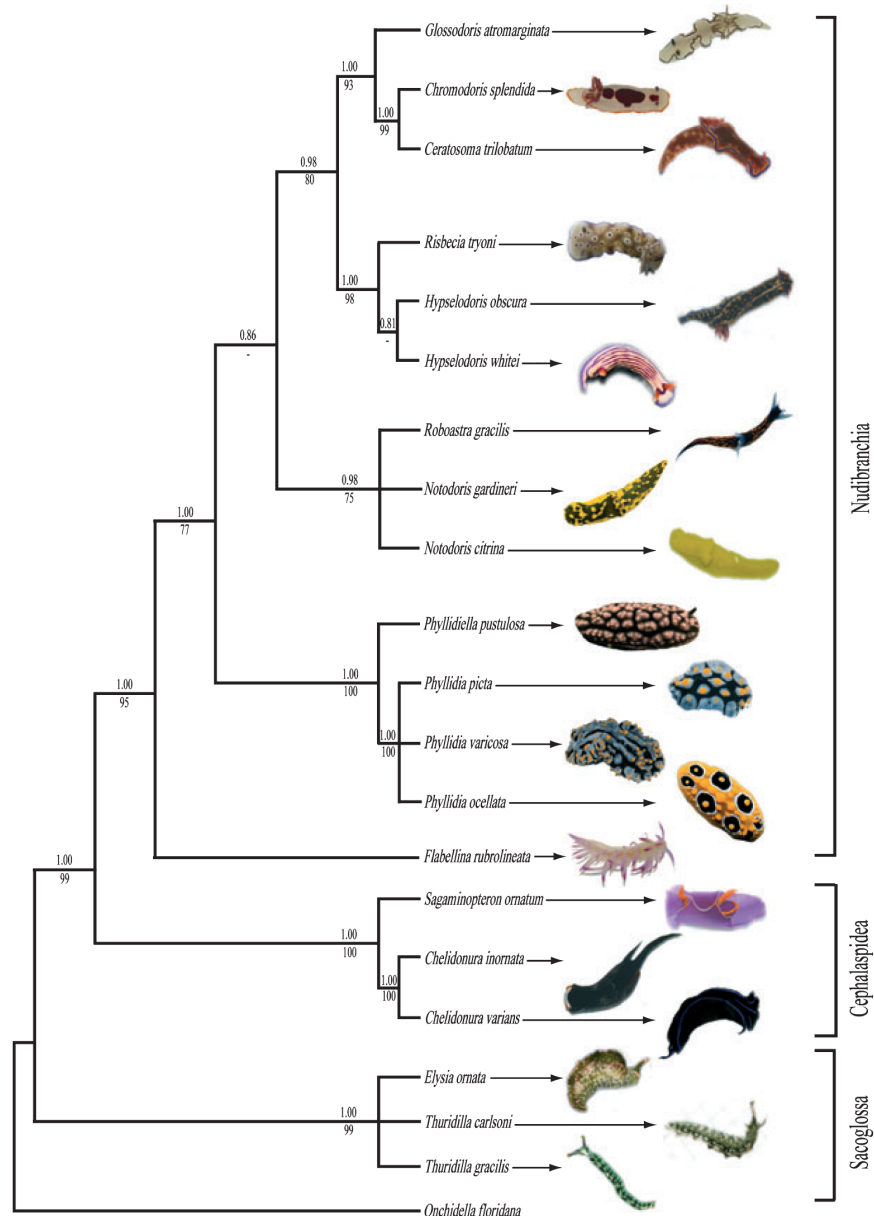


**Fig. 2** Bayesian majority rule consensus phylogram of the 16S rDNA gene. Numbers above branches represent posterior probabilities from Bayesian analysis, and numbers below branches represent bootstrap values for nodes obtained by RAxML. Only values greater or equal to 0.8 and 70 are shown.

found little phylogenetic signal in our data (Grafen's  $\rho < 0.26$ ), and there was little difference between the GLS regression model and ordinary linear model for each signal receiver (ANOVA, d.f. = 3,  $P > 0.93$ ).

## Discussion

Our study reveals that the conspicuousness of marine opisthobranchs, measured in terms of maximum spectral

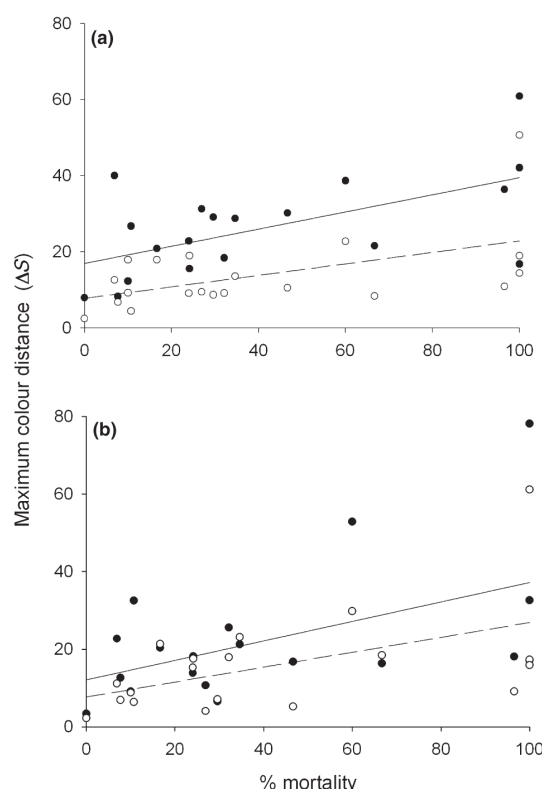


**Fig. 3** Mortality of brine shrimp (%) in relation to maximum colour distance for (a) colour/background contrast and (b) colour/colour contrast. Dark circles and solid lines represent *Stegastes*, open circles and dashed lines *Rhinecanthus*.

contrast of an opisthobranch colour patch against its background, and between two colours within a pattern, was correlated with toxicity. This was found to be the case when we considered colour signals from the perspective of two reef fish visual systems, with and without UV sensitivity. Therefore, conspicuousness appears to be an honest signal of the strength of secondary defences within opisthobranchs and provides evidence that aposematism has evolved as a defensive strategy in this family (Yachi & Higashi, 1998; Servedio, 2000; Summers & Clough, 2001).

Contrasting theories predict that conspicuousness should either evolve with increased toxicity (Summers & Clough, 2001) or the evolution of aposematic displays favours conspicuousness or toxicity, but not both (Darst *et al.*, 2006). Speed & Ruxton (2007) developed an optimization model to account for differences between these two scenarios. The model predicts that when the costs (in terms of fecundity) involved in producing a warning display vary, but the costs of producing secondary

defences are fixed, then a negative correlation will exist between conspicuousness and toxicity. In this scenario, prey species benefit from diminishing resource allocation into a warning display and increasing investment into secondary defences. However, if the costs of producing a warning display and secondary defence increase in relation to each other, then a positive correlation between warning display and toxicity can exist. In support of this, it has been suggested that antioxidant molecules may be used for both pigmentation and protection against accumulated toxins; therefore, their presence may explain a positive correlation between conspicuousness and toxicity (Blount *et al.*, 2009).

Other factors may also influence the coevolution of conspicuousness and toxicity within a species (Guilford, 1988). Sexual selection may favour brightly coloured males or females (Andersson & Iwasa, 1996), which may increase detection rates by predators and thus increase rates of mortality. An increase in secondary defence mechanisms may then evolve in response to this. However, opisthobranchs have very primitive eyes; therefore, colouration is very unlikely to be used in intraspecific communication (Edmunds, 1987).

We found little phylogenetic signal in our data, indicating that the correlation between conspicuousness and toxicity was independent of the relationship between organisms. If colour signals of a particular species are a function of diet and chemicals sequestered, then an apparent multiple evolution of conspicuousness may be caused by the diet specialization of individual species independent of their phylogenetic relationship. For example, *Phyllidia ocellata*, which was found to be mildly toxic and relatively inconspicuous, is known to sequester the toxins 10 $\alpha$ -Isocyano-4-amorphene and Cavernothiocyanate from the sponge *Acanthella cf. Cavernosa*. *Phyllidia varicosa* on the other hand, a sister species of *P. ocellata* (Fig. 2), sequesters 2-Isocyanopupukeanane and 9-Isocyanopupukeanane from the sponge *Hymeniacidon* sp. and was found to be more toxic and more conspicuous than *P. ocellata* (Garson & Simpson, 2004). The ancestral Sacoglossans appeared more cryptic than the more recently derived Nudibranchia; therefore, conspicuousness may have evolved from cryptic ancestral states. However, this needs to be investigated further using more comprehensive analyses. Colour variation may also exist within an opisthobranch species. Juveniles are sometimes more lightly pigmented than adults, and pigments from food are often used to create colouration; therefore, individuals within the same species can differ in colour depending on the availability of particular foods (e.g. *Pteraeolidia ianthina*). However, for this study, we used species that showed little intraspecific variability in colour patterns.

Phylogenetic signals may also be clouded by the accuracy of trait data. We measured the maximum spectral contrast between two colours as our measure of conspicuousness. However, aposematic signals are

generally multimodal (Ruxton *et al.*, 2004); therefore, other visual components of colour patterns may be important in effective signalling to predators, such as luminance contrast and spatial distribution of colours within a pattern. For example, *Phyllidia ocellata* appeared to be relatively inconspicuousness in our measure of spectral contrast, but its distinct bold patterning (Fig. 2) suggests that luminance contrast may be important in interspecific signalling. However, colour contrast is considered more critical to the effectiveness of aposematic signalling than luminance contrast when predators have colour vision (Osorio *et al.*, 1999; Gamberale-Stille & Guilford, 2003). We also only investigated how potential reef fish predators with trichromatic visual systems viewed opisthobranch colour signals. Unfortunately, little is known about the identity of opisthobranch predators, so this was our best estimate of the selective pressures that could drive the evolution of colour signals in marine opisthobranchs derived from predation attempts observed in the field. However, other predators may include dichromatic reef fish, sea spiders and crabs, whose visual systems may also influence the evolution of warning signals in opisthobranchs.

Our measures of toxicity were somewhat crude; however, brine shrimp assays have been shown to provide a suitable initial screening for marine natural chemicals (Carballo *et al.*, 2002) and gave us a suitable relative measure of toxicity between species. Furthermore, brine shrimp assays have shown similar results to ichthyologic assays on *Cyprinodon variegatus* when assaying toxins from a marine dinoflagellate (Moeller *et al.*, 2001). When consumed, terpenes and their derivatives affect the central nervous system; therefore, terpenes would likely affect vertebrates in a similar manner to invertebrates. Defensive chemicals may also be nontoxic but unpalatable, and responses may vary between taxa. Although many opisthobranchs contain chemicals that are unpalatable to a variety of species (e.g. Long & Hay, 2006), the link between toxicity and unpalatability has yet to be determined.

Why the appearance of prey varies from the highly cryptic to the very bright and conspicuous remains an intriguing phenomenon. Conspicuousness is costly in terms of attracting the attention of predators, and only well-protected species can generally afford this type of advertisement (Speed, 2000). Indeed, our results suggest that the most conspicuous marine opisthobranchs are the most toxic. However, further information is needed on the costs involved in producing warning displays and storing defence chemicals to fully understand the evolution of such signals.

## Acknowledgments

We thank Justin Marshall for discussions on visual ecology and modelling; Cynthia Riginos, Lyn Cook and Simon Blomberg for discussion on phylogenetic analysis

and Tane Sinclair-Taylor, Peter Waldie, Eva McClure, Cait Newport, Anna Mirams, Libby Liggins, Dave Aguirre, Emma Lewis and Eric Trembl for help in the field. This work was supported by an Australian Research Council grant to K. L. C.

## References

- Abbott, W.S. 1987. Abbott's formula – A method of computing the effectiveness of an insecticide. *J. Am. Mosq. Control Assoc.* **3**: 302–303.
- Andersson, M. & Iwasa, Y. 1996. Sexual selection. *TREE* **11**: 53–58.
- Bezzarides, A.L., McGraw, K.J., Parker, R.S. & Hussein, J. 2007. Elytra color as a signal of chemical defense in the Asian ladybird beetle *Harmonia axyridis*. *Behav. Ecol. Sociobiol.* **61**: 1401–1408.
- Blount, J.D., Speed, M.P., Ruxton, G.D. & Stephens, P.A. 2009. Warning displays may function as honest signals of toxicity. *Proc. Roy. Soc. Lond. B* **276**: 871–877.
- Carballo, J.L., Hernandez-Inda, Z.L., Perez, P. & Garcia-Gravalos, M.D. 2002. A comparison between two brine shrimp assays to detect in vitro cytotoxicity in marine natural products. *BMC Biotechnol.* **2**: 17–22.
- Carte, B. & Faulkner, D.J. 1983. Defensive metabolites from 3 nembrothid nudibranchs. *J. Org. Chem.* **48**: 2314–2318.
- Cimino, G. & Ghiselin, M.T. 1998. Chemical defense and evolution in the Sacoglossa (Mollusca: Gastropoda: Opisthobranchia). *Chemoecology* **8**: 51–60.
- Cimino, G. & Ghiselin, M.T. 1999. Chemical defense and evolutionary trends in biosynthetic capacity among dorid nudibranchs (Mollusca: Gastropoda: Opisthobranchia). *Chemoecology* **9**: 187–207.
- Cimino, G., Fontana, A. & Gavagnin, M. 1999. Marine opisthobranch molluscs: chemistry and ecology in sacoglossans and dorids. *Curr. Org. Chem.* **3**: 327–372.
- Cott, H.B. 1940. *Adaptive Coloration in Animals*. Methuen, London.
- Darst, C.R., Cummings, M.E. & Cannatella, D.C. 2006. A mechanism for diversity in warning signals: conspicuousness versus toxicity in poison frogs. *Proc. Nat. Acad. Sci. USA* **103**: 5852–5857.
- Edmunds, M. 1987. Color in opisthobranchs. *Amer. Malacol. Bull.* **5**: 185–196.
- Endler, J.A. 1990. On the measurement and classification of color in studies of animal color patterns. *Biol. J. Linn. Soc.* **41**: 315–352.
- Fahey, J.S. & Gosliner, T.M. 2004. A phylogenetic analysis of the Aegiridae Fischer, 1883 (Mollusca, Nudibranchia, Phanerobranchia) with descriptions of eight new species and a reassessment of phanerobranch relationships. *Proc. Calif. Acad. Sci.* **55**: 613–689.
- Felsenstein, J. 1985. Phylogenies and the comparative method. *Amer. Nat.* **125**: 1–15.
- Fontana, A., Ciavatta, M.L., Miyamoto, T., Spinella, A. & Cimino, G. 1999. Biosynthesis of drimane terpenoids in dorid molluscs: pivotal role of 7-deacetoxyolepupane in two species of *Dendrodoris* nudibranchs. *Tetrahedron* **55**: 5937–5946.
- Fontana, A., Cavaliere, P., Wahidulla, S., Naik, C.G. & Cimino, G. 2000. A new antitumor isoquinoline alkaloid from the



- marine nudibranch *Jorunna funebris*. *Tetrahedron* **56**: 7305–7308.
- Gamberale-Stille, G. & Guilford, T. 2003. Contrast versus colour in aposematic signals. *Anim. Behav.* **65**: 1021–1026.
- Garland, T. Jr & Diaz-Uriarte, R. 1999. Polytomies and phylogenetically independent contrasts: examination of the bounded degrees of freedom approach. *System. Biol.* **48**: 547–558.
- Garson, M.J. & Simpson, J.S. 2004. Marine isocyanides and related natural products - structure, biosynthesis and ecology. *Nat. Prod. Rep.* **21**: 164–179.
- Gosliner, T.M. & Behrens, D.W. 1990. Special resemblance, aposematic coloration, and mimicry in opisthobranch gastropods. In: *Adaptive Coloration in Invertebrates* (M. Wicksten, ed), pp. 127–138. University Press, Texas A&M.
- Grafen, A. 1989. The phylogenetic regression. *Phil. Trans. Roy. Soc. Lond. B* **326**: 119–157.
- Guilford, T. 1988. The evolution of conspicuous coloration. *Am. Nat.* **131**: S7–S21.
- Gunthorpe, L. & Cameron, A.M. 1987. Bioactive properties of extracts from Australian dorid nudibranchs. *Mar. Biol.* **94**: 39–43.
- Hall, T.A. 1999. BioEdit: a user-friendly biological sequence alignment editor and analysis program for Windows 95/98/NT. *Nucleic Acids Symp. Ser.* **41**: 95–98.
- Huelsenbeck, J.P. & Ronquist, F. 2001. MRBAYES: Bayesian inference of phylogenetic trees. *Bioinformatics* **17**: 754–755.
- Leimar, O., Enquist, M. & Sillén-tullberg, B. 1986. Evolutionary stability of aposematic coloration and prey unprofitability – A theoretical analysis. *Am. Nat.* **128**: 469–490.
- Long, J.D. & Hay, M.E. 2006. Fishes learn aversions to a nudibranch's chemical defense. *Mar. Ecol. Prog. Ser.* **307**: 199–208.
- Losey, G.S., McFarland, W.N., Loew, E.R., Zamzow, J.P., Nelson, P.A. & Marshall, N.J. 2003. Visual biology of Hawaiian coral reef fishes. I. Ocular transmission and visual pigments. *Copeia* **2003**: 433–454.
- Marin, A., Alvarez, L.A., Cimino, G. & Spinella, A. 1999. Chemical defence in cephalaspidean gastropods: origin, anatomical location and ecological roles. *J. Moll. Stud.* **65**: 121–131.
- Marshall, N.J. 2000. The visual ecology of reef fish colours. In: *Animal Signals: Signalling and Signal Design in Animal Communication* (Y. Espmark, T. Amundsen & G. Rosenqvist, eds), pp. 83–120. Tapir Academic Press, Trondheim.
- Martins, E.P. & Hansen, T.F. 1997. Phylogenies and the comparative method: a general approach to incorporating phylogenetic information into the analysis of interspecific data. *Am. Nat.* **149**: 646–667.
- Meyer, B.N., Ferrigni, N.R., Putnam, J.E., Jacobsen, L.B., Nichols, D.E. & McLaughlin, J.L. 1982. Brine shrimp – A convenient general bioassay for active plant constituents. *Planta Med.* **45**: 31–34.
- Moeller, P.D.R., Morton, S.L., Mitchell, B.A., Sivertsen, S.K., Fairey, E.R., Mikulski, T.M., Glasgow, H., Deamer-Melia, N.J., Burkholder, J.M. & Ramsdell, J.S. 2001. Current progress in isolation and characterization of toxins isolated from *Pfiesteria piscicida*. *Environ. Health Persp.* **109**: 739–743.
- Osorio, D., Jones, C.D. & Vorobyev, M. 1999. Accurate memory for colour but not pattern contrast in chicks. *Curr. Biol.* **9**: 199–202.
- Poulton, E.B. 1890. *The Colours of Animals*. Trübner, London.
- Ruxton, G.D., Sherratt, T.N. & Speed, M.P. 2004. *Avoiding Attack: The Evolutionary Ecology of Crypsis, Warning Signals and Mimicry*. Oxford University Press, Oxford, UK.
- Servedio, M.R. 2000. The effects of predator learning, forgetting, and recognition errors on the evolution of warning coloration. *Evolution* **54**: 751–763.
- Sillén-Tullberg, B. & Bryant, E.H. 1983. The evolution of aposematic coloration in distasteful prey – an individual selection model. *Evolution* **37**: 993–1000.
- Speed, M.P. 2000. Warning signals, receiver psychology and predator memory. *Anim. Behav.* **60**: 269–278.
- Speed, M.P. 2001. Can receiver psychology explain the evolution of aposematism? *Anim. Behav.* **61**: 205–216.
- Speed, M.P. & Ruxton, G.D. 2005a. Aposematism: what should our starting point be? *Proc. Roy. Soc. B Biol. Sci.* **272**: 431–438.
- Speed, M.P. & Ruxton, G.D. 2005b. Warning displays in spiny animals: one (more) evolutionary route to aposematism. *Evolution* **59**: 2499–2508.
- Speed, M.P. & Ruxton, G.D. 2007. How bright and how nasty: explaining diversity in warning signal strength. *Evolution* **61**: 623–635.
- Stamatakis, A., Ott, M. & Ludwig, T. 2005. RAXML-OMP: an efficient program for phylogenetic inference on SMPs. In: *Parallel Computing Technologies* (V. Malyskin, ed), pp. 288–302. Springer-Verlag, Berlin.
- Stamatakis, A., Hoover, P. & Rougemont, J. 2008. A rapid bootstrap algorithm for the RAXML web servers. *Syst. Biol.* **57**: 758–771.
- Summers, K. & Clough, M.E. 2001. The evolution of coloration and toxicity in the poison frog family (Dendrobatidae). *Proc. Nat. Acad. Sci. USA* **98**: 6227–6232.
- Thompson, J.D., Higgins, D.G. & Gibson, T.J. 1994. CLUSTAL W: improving the sensitivity of progressive multiple sequence alignment through sequence weighting, position-specific gap penalties and weight matrix choice. *Nucl. Acids Res.* **22**: 4673–4680.
- Ungur, N., Gavagnin, M., Fontana, A. & Cimino, G. 1999. Absolute stereochemistry of natural sesquiterpenoid diacylglycerols. *Tetrahedron: Asymmetry* **10**: 1263–1273.
- Vonnemann, V., Schrod, M., Klussmann-Kolb, A. & Wagele, H. 2005. Reconstruction of the phylogeny of the Opisthobranchia (Mollusca: Gastropoda) by means of 18s and 28s rRNA gene sequences. *J. Mollus. Stud.* **71**: 113–125.
- Vorobyev, M. & Osorio, D. 1998. Receptor noise as a determinant of colour thresholds. *Proc. Roy. Soc. B Biol. Sci.* **265**: 351–358.
- Vorobyev, M., Brandt, R., Peitsch, D., Laughlin, S.B. & Menzel, R. 2001. Colour thresholds and receptor noise: behaviour and physiology compared. *Vis. Res.* **41**: 639–653.
- Wollscheid-Lengeling, E., Boore, J., Brown, W. & Wagele, H. 2001. The phylogeny of Nudibranchia (Opisthobranchia, Gastropoda, Mollusca) reconstructed by three molecular markers. *Org. Divers. Evol.* **1**: 241–256.
- Wyszecki, G. & Styles, W. 1982. *Color Science: Concepts and Methods, Quantitative Data and Formulae*. John Wiley and Sons, New York.
- Yachi, S. & Higashi, M. 1998. The evolution of warning signals. *Nature* **394**: 882–884.

### Supporting information

Additional Supporting Information may be found in the online version of this article:

**Table S1** Maximum colour distances ( $\Delta S$ ) found between colour patch on a species and its background.

As a service to our authors and readers, this journal provides supporting information supplied by the authors.

Such materials are peer-reviewed and may be reorganized for online delivery, but are not copyedited or typeset. Technical support issues arising from supporting information (other than missing files) should be addressed to the authors.

*Received 4 January 2010; revised 8 April 2010; accepted 12 April 2010*

## 4.2. Supporting Information

**Table S1** Maximum colour distance ( $\Delta S$ ) found between any colour patch on a species and its background (colour/background) and between adjacent colour patches within species (colour/colour) for: a) *Rhinecanthus aculeatus* and b) *Stegastes fasciatus* (1 = turf algae; 2 = sand; 3 = coral; 4 = sponge; 5 = tunicates. na = only one colour category is found on this species).

### a) *Rhinecanthus aculeatus*

Opisthobranch species	Against background colour measurements (colour/background)			Within opisthobranch colour measurements (colour/colour)		
	Colour	Background	Colour distance ( $\Delta S$ )	Colour 1	Colour 2	Colour distance ( $\Delta S$ )
<i>Ceratosoma trilobatum</i>	purple	1,2	13.59	purple	brown	23.07
<i>Chelidonura inornata</i>	UV/orange	1,3	14.41	white	UV/orange	17.28
<i>Chelidonura varians</i>	UV/blue	2	18.95	black	UV/blue	17.59
<i>Chromodoris splendida</i>	UV/yellow	1	9.14	UV/yellow	UV/red	17.87
<i>Elysia ornata</i>	orange	1	9.46	green/far red	orange	4.04
<i>Flabellina rubrolineata</i>	purple	1	8.68	pink	purple	7.08
<i>Glossodoris atromarginata</i>	white	1,5	10.55	brown	white	5.21
<i>Hypselodoris obscura</i>	UV/blue	1,5	12.58	UV/yellow	black	11.12
<i>Hypselodoris whitei</i>	purple	1,2	9.21	purple	white	8.78
<i>Notodoris citrina</i>	yellow	1,4	17.88	n/a	n/a	n/a
<i>Notodoris gardineri</i>	yellow	1,4	17.9	yellow	brown	21.36
<i>Phyllidia ocellata</i>	UV/yellow	1	9.11	UV/yellow	white	15.26
<i>Phyllidia picta</i>	yellow	1	22.78	yellow	black	29.78
<i>Phyllidia varicosa</i>	UV/blue	1,2	8.35	UV/yellow	black	18.42
<i>Phyllidiella pustulosa</i>	black	1	10.9	pink	black	9.07
<i>Risbecia tryoni</i>	purple	1	6.78	white	purple	6.88
<i>Roboastra gracilis</i>	orange	1	50.68	black	orange	61.12
<i>Sagaminopteron ornatum</i>	purple	1	19	UV/orange	purple	15.87
<i>Thuridilla carlsoni</i>	green/far red	1,2	2.43	green/far red	pink	2.2
<i>Thuridilla gracilis</i>	brown	1,2	4.42	brown	white	6.36

### b) *Stegastes fasciatus*

Opisthobranch species	Against background colour measurements (colour/background)			Within opisthobranch colour measurements (colour/colour)		
	Colour	Background	Colour distance ( $\Delta S$ )	Colour 1	Colour 2	Colour distance ( $\Delta S$ )
<i>Ceratosoma trilobatum</i>	purple	1,2	28.78	purple	brown	21.26
<i>Chelidonura inornata</i>	black	1,3	16.75	black	UV/orange	32.61
<i>Chelidonura varians</i>	UV/blue	2	15.57	black	UV/blue	18.2
<i>Chromodoris splendida</i>	UV/yellow	1	18.38	white	UV/red	25.56
<i>Elysia ornata</i>	brown	1	31.24	green/far red	brown	10.69
<i>Flabellina rubrolineata</i>	purple	1	29.1	white	magenta	6.53
<i>Glossodoris atromarginata</i>	white	1,5	30.16	white	orange	16.75
<i>Hypselodoris obscura</i>	UV/blue	1,5	40.03	UV/blue	black	22.7
<i>Hypselodoris whitei</i>	purple	1,2	12.28	purple	white	9.08
<i>Notodoris citrina</i>	yellow	1,4	12.35	n/a	n/a	n/a
<i>Notodoris gardineri</i>	yellow	1,4	20.89	yellow	brown	20.39
<i>Phyllidia ocellata</i>	white	1	22.86	UV/yellow	white	13.87
<i>Phyllidia picta</i>	black	1	38.69	yellow	black	52.85
<i>Phyllidia varicosa</i>	black	1,2	21.56	UV/yellow	black	16.3
<i>Phyllidiella pustulosa</i>	black	1	36.39	pink	black	18.12
<i>Risbecia tryoni</i>	white	1	8.26	white	brown	12.64
<i>Roboastra gracilis</i>	orange	1	60.86	black	orange	78.20
<i>Sagaminopteron ornatum</i>	purple	1	42.09	UV/orange	purple	17.12
<i>Thuridilla carlsoni</i>	pink	1,2	7.89	pink	green/far red	3.39
<i>Thuridilla gracilis</i>	brown	1,2	26.75	brown	white	32.53





## Chapter 5

# Conspicuous visual signals do not coevolve with increased body size in marine sea slugs

K. L. Cheney, F. Cortesi, M. J. How, N. G. Wilson,  
S. P. Blomberg, A. E. Winters, S. Umzör, N. J. Marshall

Journal of Evolutionary Biology (2014)

5.1. Cover work p. 109

5.2. Manuscript p. 110 – 121

5.3. Supporting Information p. 122 – 126

I contributed to this work by reconstructing phylogenies, taking spectral measurements of sea slugs and handling sea slug images for subsequent image statistical analysis.



ISSN 1010-061X

JOURNAL OF  
**Evolutionary  
Biology**

VOLUME 27 ISSUE 4 APRIL 2014



**WILEY** Blackwell

 **eseb**  
European Society for Evolutionary Biology

## Conspicuous visual signals do not coevolve with increased body size in marine sea slugs

K. L. CHENEY\*, F. CORTESI\*†, M. J. HOW‡, N. G. WILSON§, S. P. BLOMBERG\*,  
A. E. WINTERS\*, S. UMANZÖR¶ & N. J. MARSHALL‡

\*School of Biological Sciences, The University of Queensland, St Lucia, Qld, Australia

†Zoological Institute, The University of Basel, Basel, Switzerland

‡Queensland Brain Institute, The University of Queensland, St Lucia, Qld, Australia

§The Australian Museum, Sydney, NSW, Australia

¶Department of Biology, New Mexico State University, Las Cruces, NM, USA

### Keywords:

animal patterns;  
aposematism;  
image statistics;  
nudibranchs;  
spectral contrast;  
visual signalling.

### Abstract

Many taxa use conspicuous colouration to attract mates, signal chemical defences (aposematism) or for thermoregulation. Conspicuousness is a key feature of aposematic signals, and experimental evidence suggests that predators avoid conspicuous prey more readily when they exhibit larger body size and/or pattern elements. Aposematic prey species may therefore evolve a larger body size due to predatory selection pressures, or alternatively, larger prey species may be more likely to evolve aposematic colouration. Therefore, a positive correlation between conspicuousness and body size should exist. Here, we investigated whether there was a phylogenetic correlation between the conspicuousness of animal patterns and body size using an intriguing, understudied model system to examine questions on the evolution of animal signals, namely nudibranchs (opisthobranch molluscs). We also used new ways to compare animal patterns quantitatively with their background habitat in terms of intensity variance and spatial frequency power spectra. In studies of aposematism, conspicuousness is usually quantified using the spectral contrast of animal colour patches against its background; however, other components of visual signals, such as pattern, luminance and spectral sensitivities of potential observers, are largely ignored. Contrary to our prediction, we found that the conspicuousness of body patterns in over 70 nudibranch species decreased as body size increased, indicating that crypsis was not limited to a smaller body size. Therefore, alternative selective pressures on body size and development of colour patterns, other than those inflicted by visual hunting predators, may act more strongly on the evolution of aposematism in nudibranch molluscs.

### Introduction

Animals that contain toxic or unpalatable chemicals often use conspicuous colouration and distinct body patterning to communicate unprofitability to visual hunting predators. Such warning colouration, or

aposematism, is found in a wide range of organisms including insects, snakes, molluscs, fish and amphibians (Poulton, 1890; Cott, 1940; Ruxton *et al.*, 2004). How such warning or aposematic colouration evolves has puzzled scientists for decades and has been limited by a lack of comparative studies investigating real prey species. Conspicuousness is a key feature of warning signals, as conspicuous signals are more likely to be detected and learned by predators, and memorized for longer (Rothschild, 1984; Roper, 1994; Lindstrom *et al.*, 2001; Aronsson & Gamberale-Stille, 2008). A conspicuous

Correspondence: Karen L. Cheney, School of Biological Sciences, The University of Queensland, St Lucia, Qld 4072, Australia  
Tel.: +61 7 3365 7386; fax: +61 7 3365 1655;  
e-mail: k.cheney@uq.edu.au

signal must differ from its background in colour, pattern and/or luminance from the perspective of the intended receiver (Endler, 1978, 1991). High contrast against the background increases signal efficiency and initial wariness by predators (Roper & Cook, 1989; Lindstrom *et al.*, 2001; Ruxton *et al.*, 2004), and the speed and strength of avoidance learning (Gittleman & Harvey, 1980). However, no simple method exists for quantifying the conspicuousness of an object against its background (but see Endler, 2012). Furthermore, the relative importance of each component and how they interact is often unclear (but see Osorio *et al.*, 1999; Aronsson & Gamberale-Stille, 2008).

Experimental evidence suggests that an increase in body size and/or in pattern element size within the visual display strengthens the avoidance response of warning colouration by predators (Gamberale & Tullberg, 1996b, 1998; Lindstrom *et al.*, 1999; Nilsson & Forsman, 2003). Domestic chicks have been shown to have an unlearned aversion to larger-sized insect prey (Gamberale & Tullberg, 1996a, 1998), and larger pattern elements in artificial prey caused blue tits to learn signals more rapidly and provided enhanced avoidance of unpalatable prey (Lindstrom *et al.*, 1999). Predator selective pressures may therefore cause species that have acquired aposematic colouration to increase overall body size and/or increase body pattern elements relative to body size (e.g. widening of stripes or size of dots). Alternatively, species with larger body size may be more likely to evolve conspicuous colouration. If predator selective pressures influence the evolution of aposematic displays, we would expect to find an evolutionary correlation between conspicuousness and body size of aposematic species. Indeed, a comparative analysis of poison frogs (Dendrobatidae) (Hagman & Forsman, 2003) indicated that body size was correlated with an increase in conspicuous colouration, in terms of brightness quantified by human assessment and computer analysis of digital colour photographs. However, Nilsson & Forsman (2003) failed to find such a correlation in moths, but lifestyle was thought to confound the results as a shift from lone behaviour to gregariousness was also partnered with a decrease in body size.

In this study, we examined this hypothesis using an intriguing, understudied model system, namely nudibranchs (opisthobranch molluscs, commonly known as sea slugs). To do this, we quantified the conspicuousness of animal body colouration using new ways of quantifying the spatial frequency of body patterns (intensity variance and power spectrum analysis) and compared this to spectral contrast measurements, which is frequently the sole measure of conspicuousness in studies of animal colour patterns. We then used Bayesian phylogenetic regression analysis to assess how these measures of conspicuousness related to animal body size.

## Materials and methods

### Study species

Nudibranchs exhibit tremendous species-level diversity with over 3000 species worldwide. Our sampling covered representative species from infraorder Doridacea (families: Aegiridae, Chromodoridae, Dendrodorididae, Discodoridae, Dorididae, Phyllidiidae and Polyceridae) and infraorder Aeolidida (families: Glaucidae, Facelinidae and Flabellinidae) (Table S1). Most nudibranchs contain secondary metabolites, including isocyanides, diterpenes and sesquiterpenes (Faulkner & Ghiselin, 1983; Cimino *et al.*, 1985; Avila, 1995), which protect the animals from predatory attacks (Avila, 1995; Mollo *et al.*, 2005). These chemicals are often localized in selected parts of the body (Avila & Paul, 1997; Somerville *et al.*, 2006; Wagele *et al.*, 2006) and can be diet-derived or produced *de novo* (Cimino *et al.*, 1983; Cimino & Sodano, 1993; Fontana *et al.*, 1994). Nudibranchs also range in their visual displays and include those that are highly cryptic against their background habitat to those that exhibit bold and distinct body colouration, which are used as aposematic signals. Although information on the identity of potential nudibranch predators is limited, predators are thought to include fish (e.g. pufferfish, triggerfish and wrasse) and other invertebrates such as crabs, sea spiders and other opisthobranchs. However, fish predators are considered to be the main selective pressure that drives the evolution of conspicuous colours and patterns due to their ability to detect colour (Siebeck *et al.*, 2008) and their di- or trichromatic visual system (Marshall *et al.*, 2006). We measured nudibranch body lengths from live individuals that were collected for spectral reflectance measurements and used nudibranch identification books with detailed body length information (Cobb & Willian, 2006; Debelius & Kuitert, 2007; Coleman, 2008). We used mean body length from a minimum of eight individual measurements for each species; measurements for juveniles were omitted. In this study, average body size ranged from 1.0 to 10.0 cm (Table S1).

### Phylogenetic reconstruction

We used a Bayesian inference approach to estimate the phylogenetic relationships between 76 nudibranch species for which we were able to collect pattern and/or colour data. Phylogenetic relationships were reconstructed using published COI and 16S gene sequences from GenBank (<http://www.ncbi.nlm.nih.gov/genbank/>) for 49 species. We also sequenced both genes for an additional 16 species, COI for an additional eight species and 16S for an additional three species (Accession Numbers listed in Table S1). Three pleurobranch species: *Pleurobrancha meckeli*, *Bathyerthella antarctica* and *Thompsonia antarctica* were used as outgroups to root the trees.

DNA was extracted using a Qiagen DNAeasy blood and tissue kit, and sequences were amplified using primers and protocols as in Wilson *et al.*, (2009). PCRs were carried out using illustra PuRe taq Ready-to-go beads (GE Healthcare, Piscataway, NJ, USA), and amplicons were directly purified using ExoSAP-IT (USB, Cleveland, OH, USA) prior to sequencing. Sequences were edited and reconciled in Sequencher (Genecodes, Ann Arbor, MI, USA). Sequences were aligned using the Q-INS-i strategy in Multiple Alignment using Fast Fourier Transform (MAFFT) (Katoh & Toh, 2008), which takes into account secondary structure. The resulting alignment length of COI data comprised 658 bp and 16S data comprised 527 bp. We then used Gblock (Castresana, 2000) for the 16S alignment, implementing the least stringent options to remove areas of ambiguous alignment in an explicit, repeatable manner. This resulted in a 391 bp alignment, comprising 74% of the original 527 positions. Geneious v6.0.5 (Cimino & Sodano, 1993) was used to concatenate COI and 16S alignments, which resulted in a final dataset of 1049 bp.

We used PartitionFinder v1.1.0 (Lanfear *et al.*, 2012) to search for the best partitioning scheme and model of sequence evolution for our dataset. Evolutionary models were chosen from the ones available in MrBayes, with linked branch lengths, a search for all possible schemes, and the Bayesian information criterion (BIC) as criterion for model selection. The resulting partitioning scheme comprised four subsets: 16S, first, second and third COI codon positions. GTR + G was chosen to be the best model of evolution for the second codon position of COI, and GTR + G + I was chosen to be the best model for 16S, the first and third codon position of COI. Subsequent Bayesian inference was conducted using MrBayes, v.3.2.1 (Ronquist *et al.*, 2012), using a MCMC search with two independent runs and four chains each. All partitions were set to be variable, and parameters (shape, pinvar, statefreq and revmat) were unlinked to allow each partition to evolve independently. Each run produced ten million generations, with trees sampled every 1000 generations (10 000 trees per run). A majority-rule consensus tree (Fig. 1) was constructed to illustrate the phylogenetic relationship between nudibranch species. We also show density plots of 1000 trees created in DensiTree v2.0.1 (Bouckaert, 2010) (Fig. S2).

### Quantification of conspicuousness

We focused on quantifying two main aspects of conspicuousness: (i) analysis of first- and second-order image statistics to determine the brightness contrast and spatial frequency of the nudibranchs' pattern and how closely the pattern matches the background (as per Zylinski *et al.*, 2011); and (ii) spectral contrast both within the nudibranch body pattern and against background (as per Dalton *et al.*, 2010; Wang, 2011).

#### (i) First- and second-order image statistics

We obtained digital images of nudibranch species taken in the Indo-Pacific region by ourselves, a variety of other scientific researchers and recreational divers. Any photographs that were under or over exposed (i.e. containing large areas of white or black), or not focused, were excluded and only photographs that had >85% background habitat in the images were included. We ensured that we had a minimum of eight independent (e.g. different individuals and locations) images for each species (range 8–48 per species; Table S1). For this analysis, we had a total of 61 species.

The average length of each nudibranch species was used to calibrate image scale relative to known average body lengths (Table S1). Each photograph was scaled to approximate a scene viewed by a fish observer with an optical resolution of 10 cycles per degree (Collin & Pettigrew, 1989) and a viewing distance of 10 cm. This scaling method provided an estimate of the visual information available to a hypothetical fish predator, which is the most relevant perspective for an analysis of nudibranch conspicuousness.

The position of each nudibranch was manually identified by tracing the animal's outline with a computer mouse. Six background samples were then identified by shifting the nudibranch outline to random positions within the background area of the image. Each of these seven image samples (one nudibranch and six background samples) was split into its three RGB colour channels. Fish are thought to use their double cones for luminance vision (Kelber *et al.*, 2003), which generally lie in the green part of the visual spectrum at around 500 nm (Lythgoe, 1979; Marshall *et al.*, 2006); therefore, we used only the green channel for our analysis to approximate likely photon catch and therefore intensity viewed by such fish predators (for full discussion of this see Vorobyev *et al.*, 2001; Stevens *et al.*, 2007).

First- and second-order image statistics were then calculated for each nudibranch and background sample. The first-order statistic used was intensity variance, a measure of the distribution of brightness contrast within the sample. This was calculated as the standard deviation of pixel intensity values. Samples containing a range of intensity values, for example a pattern with mixture of light and dark patches, generate a high intensity variance value, whereas plain patterns produce a low value. The second-order statistic used was the two-dimensional power spectrum, an estimate of the spatial frequency of patterns within the sample area. This is calculated in a similar way to one-dimensional frequency analysis, in which a sequence of values (e.g. a line of pixel values extracted from an image transect; Fig. 2a,b) is converted into a measure of its frequency components using a Fourier transform (Fig. 2c; Fig. S1 for more examples). Each image



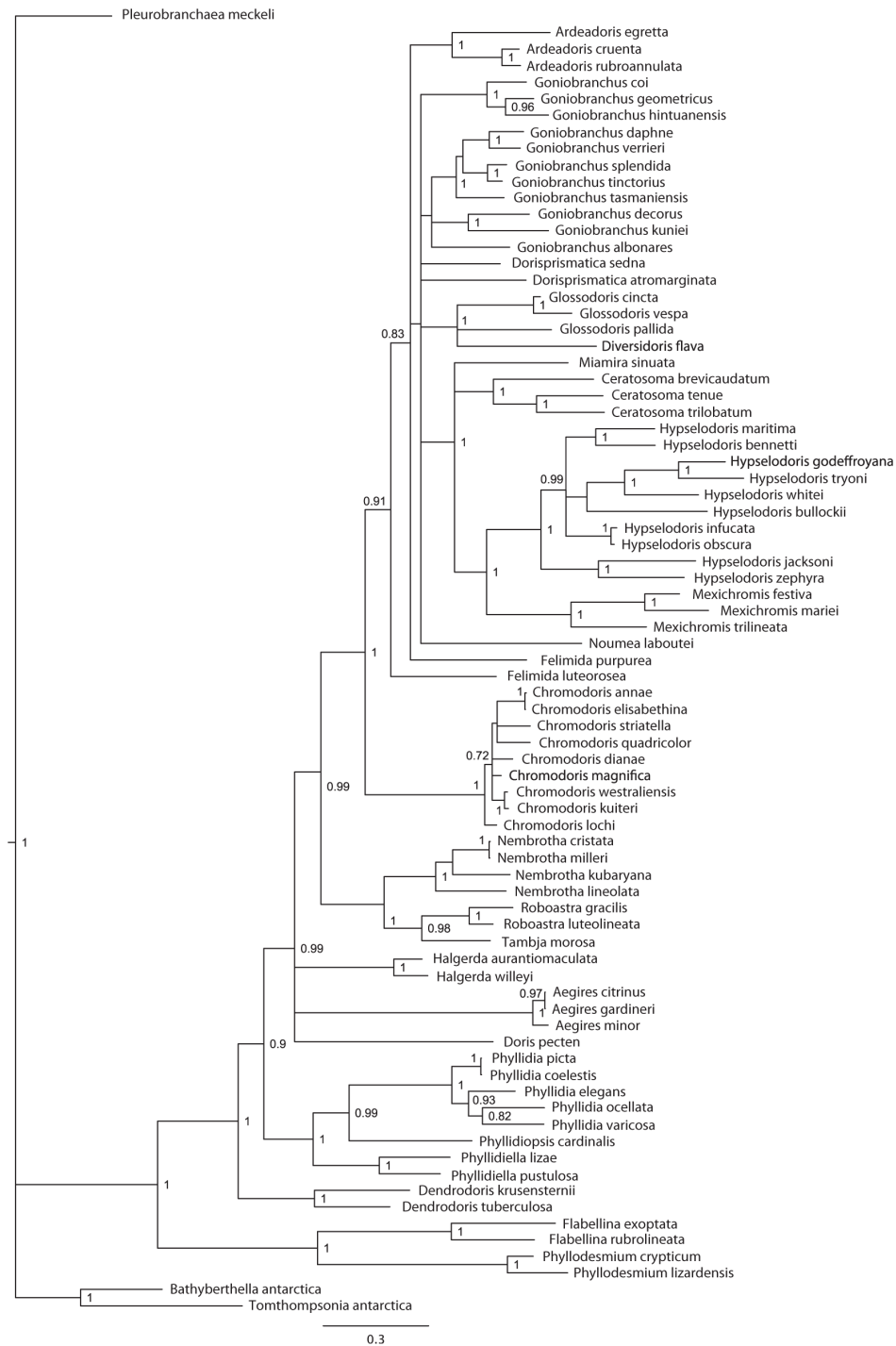


**Fig. 1** Bayesian 50% majority rule consensus phylogram based on CO1 and 16S rDNA sequence data. Only support values for Bayesian posterior probabilities ( $\geq 0.7$ ) are shown.

sample was extracted from the image and padded with black pixels to make a rectangular shape. A two-dimensional discrete Fourier transform (Matlab function *fft2*) was performed on the sample (Fig. 2d), and the resulting amplitudes were rotationally averaged to produce a log-scaled power spectrum curve (Fig. 2e; see Field, 1987 for details). These image statistics were then used to quantify the conspicuousness of each nudibranch against their background by calculating the difference in area beneath power spectrum curves (nudibranch – background curve) and absolute difference between power spectrum curves. Both of these measurements gave similar results, so we present the former. This method could not be used to compare patterns between images (within pattern analysis) due to edge effects from the border between the sample and the padded area. Image intensity variance and power spectrum are potentially vulnerable to changes in camera exposure settings; however, performing within-image comparisons of sample and background measures largely controls for such effects.

#### (ii) Spectral contrast

To assess conspicuousness in terms of spectral contrast, spectral reflectance measurements were collected for 61 nudibranch species ( $n = 1\text{--}6$  individuals per species). Nudibranchs were located using SCUBA on coral reefs at depths from 1 to 15 m in Australia: Lizard Island (14°40'S; 145°28'E) and Heron Island (23°29'S; 151°11'E), Great Barrier Reef; North Stradbroke Island (27°35'S; 153°27'E), Mooloolaba (26°40'S; 153°07'E) and Gold Coast (27°25'S; 153°25'E), Southeast Queensland; and in Indonesia: Palau Hoga, (05°28'S; 123°45'E). Nudibranchs were placed in plastic vials or bags and held in containers with air pumps for no longer than 48 h. Spectral reflectance measurements of nudibranch colours were measured using an Ocean Optics (Dunedin, FL, USA) USB2000 spectrometer and a laptop computer running Ocean Optics OOIBASE32 software. Nudibranchs were placed in a tray containing enough seawater to cover each individual completely, and the spectral reflectance of each distinct colour patch  $> 4\text{ mm}^2$  was measured through a 200- $\mu\text{m}$  bifurcated optic UV/visible fibre connected to a PX-2 pulse xenon light (Ocean Optics). A Spectralon 99% white reflectance standard (LabSphere, North Sutton, NH, USA) was used to calibrate the percentage of light reflected at each wavelength from 300 to 800 nm. The bare end of the fibre was held at a 45° angle to prevent specular reflectance. At least ten measurements per colour patch per individual were taken and then averaged.

To estimate the conspicuousness of nudibranch colour pattern based on spectral contrast from the perspective of a potential trichromatic reef fish predator, we used the Vorobyev–Osorio theoretical vision model (Vorobyev & Osorio, 1998). As per previous studies (Cheney & Marshall, 2009; Cortesi & Cheney,

2010), we assumed a 1 : 2 : 2 ratio for the weber fraction ( $\omega$ ), LWS noise threshold was set at 0.05. To account for the light environment in which the colours would be viewed, colours were modelled using illumination measurements at a water depth of 5 m (as per Cheney & Marshall, 2009). We considered the effects of signal transmission through water to be negligible, as most coral reef fish would view nudibranchs from a relatively close distance (approximately 1–2 m).

The model calculates the 'colour distance' ( $\Delta S$ ) between colours in a trichromatic visual space. Colours that appear similar within each visual system result in low  $\Delta S$  values, whereas those that are chromatically contrasting are high in value. We modelled colours from the perspective of a trichromatic, benthic feeding fish species: the Picasso triggerfish, *Rhinecanthus aculeatus* ( $\lambda_{\text{max}} = 413, 480, 530\text{ nm}$ ; Cheney *et al.*, 2013). This fish was chosen because they are likely to encounter nudibranchs and are representative of a common visual system found in a range of reef fish species (Losey *et al.*, 2003; Marshall *et al.*, 2006). We also show results from a potential dichromatic fish predator in the supplementary information (Fig. S4).

To measure **against background spectral contrast**, we measured the spectral reflectance of coral reef background habitats (coral, turf algae, sponge, sand and specific habitats such as xeniid soft corals, which are used by the cryptic nudibranch *Phyllodesmium lizardensis*) using an underwater spectrophotometer (as per Cortesi & Cheney, 2010). Colour distances were calculated between each nudibranch colour patch and the background habitat on which it was found most frequently. To estimate **within pattern spectral contrast**, colour distances were calculated between each nudibranch colour patch with a diameter (circular) or width (stripe)  $> 3\text{ mm}$  for each individual and then averaged for each species. Species that only had one colour patch ( $n = 4$ ) were removed from this analysis ( $n = 59$  species).

#### Comparative analysis of traits

We used a Bayesian approach, employing the methods outlined in de Villemereuil *et al.* (2012). We took the first 10 000 trees (with branch lengths) from the output of two MrBayes chains. We discarded the first 2500 of each as burn-in, and combined the two resulting sets of trees (15 000 trees). Species that did not have trait data (pattern data or spectral contrast) for a particular analysis were pruned from trees. The trees were then converted to correlation matrices using the function *vcv.phylo* in package *ape* version 3.0-8 for R version 3.0.1 (Paradis *et al.*, 2004; R Core Team, 2013). The trait data and the correlation matrices were used as input to a Markov Chain Monte Carlo analysis using program JAGS (Plummer, 2012). We ran three separate chains for each analysis, with different starting values. We fitted simple linear regression models, regressing each col-



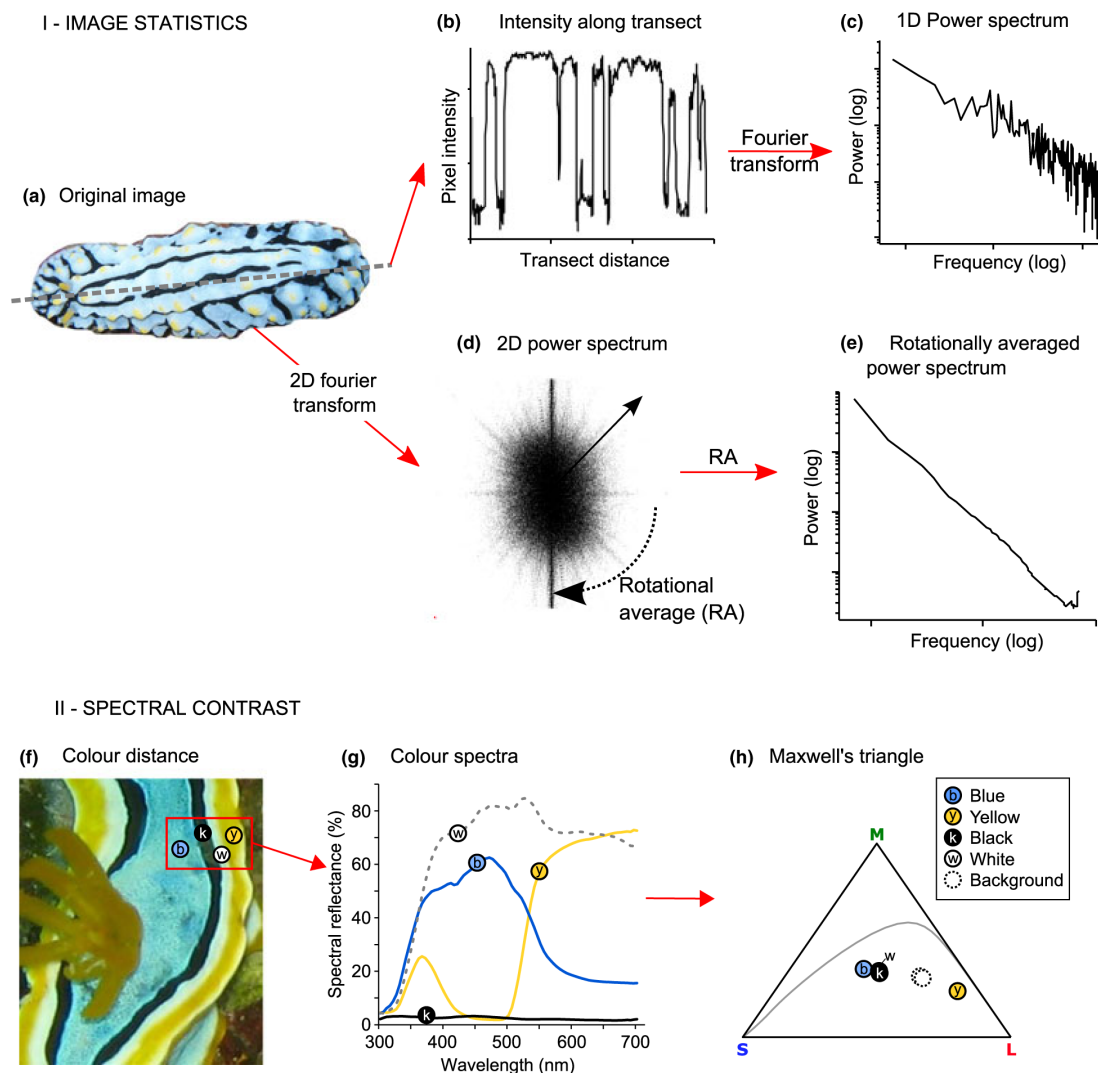


**Fig. 2** Methods used for quantifying conspicuousness. (I) Spatial frequency was calculated using the two-dimensional Fourier transform. The principle is first illustrated in one dimension. A transect through an image (a – grey dashed line) is used to extract a slice of pixel intensity values (b), and the frequencies contained within are characterized with a Fourier transform (c). The slope of the frequency–power relationship is a rough measure of the distribution of frequencies within the image. Two-dimensional Fourier transforms have a similar approach, but transects are sampled through the image in all orientations, producing a two-dimensional map of frequency distributions (d) which is then rotationally averaged into a one-dimensional power spectrum (e). (II) Distance in visual space between different nudibranch colours: blue [b], black [k], white [w] and yellow [y] patches on a nudibranch (f). First the reflectance spectral frequency is measured for each colour (g). This is then modelled from the perspective of the colour vision system of a potential fish predator (e.g. *R. aculeatus*, this study) (h) and colour distances between spectra calculated using the Vorobyev–Osorio model (Vorobyev & Osorio, 1998).

our or pattern variable on body size (cm), accounting for phylogenetic uncertainty by randomly sampling from the set of phylogenetic correlation matrices. In addition, we estimated Pagel's  $\lambda$  for each regression,

which is a measure of phylogenetic signal in the data and flexibly accommodates some branch-length uncertainty (Pagel, 1999). We computed the posterior distributions (conditional on the observed data) for the slope

and intercept of the regression, the residual standard deviation ( $\sigma$ ), and  $\lambda$ . We used Normal priors for the intercept and slope, both with zero mean and precision  $10^{-6}$ . For  $\sigma$ , we used a Uniform prior on [0, 100] (Gelman, 2006). For  $\lambda$ , we used a Uniform prior on [0, 1]. Post-processing and convergence diagnostics were performed in R using the coda package (Plummer *et al.*, 2006). In addition, we performed checks of the models by comparing the discrepancy (we used square-root mean squared error) for the real data and simulated data from the models, and calculated posterior predictive  $P$ -values (Gelman *et al.*, 2004).

## Results

Bayesian searches produced a tree similar to recently published work on nudibranchs (Johnson & Gosliner, 2012), with high support for many nodes (Fig. 1).

For all of our measures of conspicuousness, values close to 0 represent nudibranchs that closely match their substrate [e.g. *Phyllodesmium lizardensis*: intensity variance (against background) = 1.61; power spectra = 0.01; spectral contrast (against background) = 0.26; Fig. 3], whereas values further away from 0 indicate an increase in conspicuousness (e.g. *Chromodoris magnifica*: intensity variance (against background) = 28.7; power spectra = 0.07; spectral contrast (against background) = 31.2; Fig. 3).

There was a significant positive relationship between first-order (intensity variance against background) and second-order (power spectra) image statistics ( $r^2_{59} = 0.06$ ,  $P = 0.04$ ). However, we did not find a significant relationship between intensity variance (against background) or power spectra and spectral contrast (against background) (intensity variance:  $r^2_{45} = -0.015$ ,  $P = 0.57$ ; power spectra:  $r^2_{45} = -0.02$ ,  $P = 0.93$ ). There was also no relationship between intensity variance (within pattern) and spectral contrast (within pattern) ( $r^2_{45} = 0.003$ ,  $P = 0.30$ ).

Using phylogenetic regression models, there was a negative relationship between intensity variance (against background) and power spectra against body size, with the highest-density predicted interval (HDPI) not exceeding 0 for both variables (intensity variance: HDPI  $-2.72$  to  $-0.18$ ; power spectra: HDPI  $-0.007$  to  $-0.003$ ; Fig. 3i, ii). However, there was no relationship between intensity variance (within pattern) and body size (HDPI  $-1.78$  to  $1.10$ ; Fig. 3iv).

There was also no relationship between spectral contrast (against background) and body size (HDPI  $-0.57$  to  $1.18$ ; Fig. 3iii), or spectral contrast (within pattern) and body size (HDPI  $-0.07$  to  $2.30$ ; Fig. 3v).

## Discussion

Here, we have used an understudied model system to investigate the hypothesis that the conspicuousness of

aposematic signals coevolves with an increase in body size, using a new way of assessing the conspicuousness of animal signals by considering both pattern analysis and spectral contrast measurements. We did not find any evidence to support this hypothesis in our subsample of nudibranch species, on the contrary, we found that as body size increased, patterns in nudibranchs became less conspicuous, indicating that relatively large nudibranchs are capable of being cryptic. We found no relationship between spectral contrast and body size; nudibranchs that displayed the highest spectral contrast against the background habitat were only moderately sized, such as *Chromodoris elisabethina* (average 41 mm) and *Chromodoris magnifica* (45 mm).

Animals with large body size are predicted to evolve conspicuous colouration as cryptic colouration is often difficult to achieve in larger individuals (Cott, 1940). Indeed, cryptic colouration functions to decrease prey detection risk but may be costly in heterogeneous habitats, as it is difficult to match more than one visual background (Merilaita *et al.*, 2001). Many cryptic nudibranch species are indeed reliant on one habitat type, such as in this study, *Phyllodesmium lizardensis*, which closely resembles the xeniid soft corals it is found upon. This highly cryptic but moderately sized species (average 36 mm) is able to remain stationary as they house zooxanthellae in their digestive gland branches enabling individuals to meet their energy requirements through photosynthesis (Burghardt *et al.*, 2008). However, other large nonphotosynthetic cryptic nudibranchs including *Dendrodoris krusensternii* and *D. tuberculosa* were also located and included in our study. These species have an outer surface covered in tubercules, which helps skin texture to match their habitat. Other species such as octopi commonly use changes in skin texture to camouflage themselves against their background (Hanlon *et al.*, 2011). Conspicuous species should be easier to detect on coral reefs; therefore, our sampling may have been biased towards species with highly contrasting patterns. However, we also specifically targeted cryptic species using knowledge of their ecology to locate individuals.

Our prediction that an increase in body size and/or in pattern element size within the visual display strengthens the avoidance response of warning colouration by predators was based on behaviour responses of avian predators, but to our knowledge, this prediction has not been explicitly tested in fish. The light environment of marine habitats and differences in the visual systems of fish (Marshall *et al.*, 2006) may impact the way in which fish predators respond to visual stimuli and may explain why we did not find any evidence to support our prediction. Marine fish have been shown to avoid unpalatable prey based on visual cues (colour and pattern) alone (Miller & Pawlik, 2013), and fish exhibit response bias towards particular colours (Cheney *et al.*, 2013); however, more behavioural experiments are needed with marine predators.

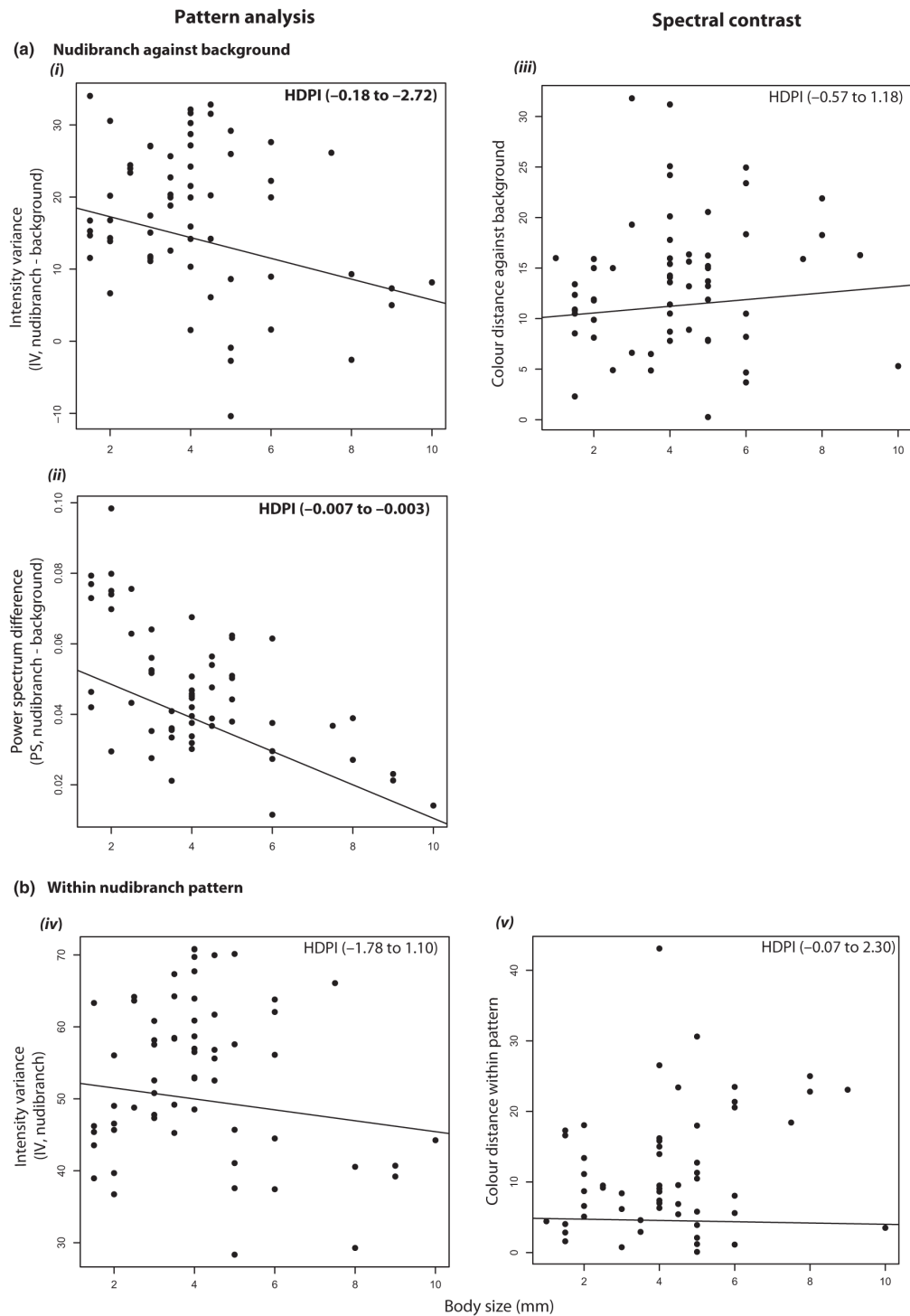


**Fig. 3** Scatterplot of image statistics (intensity variance, difference in power spectrum slope) and spectral contrast (colour distance) against average body size of each nudibranch species, (a) against the background habitat and (b) within animal colour pattern. Highest-density predicted interval (HDPI) and regression lines show results of phylogenetic regression analysis. Bold HDPI values indicate those that did not exceed 0.

Factors other than an increase in body size and/or in pattern element size within the visual display may impact the avoidance response of warning colouration by predators. Although most nudibranchs are thought to contain some level of chemical defence, little is known about the abundance, relative strength and chemical profiles of these toxins and how they influence warning signal form and function (but see Cortesi & Cheney, 2010). However, highly conspicuous nudibranchs, which may have the strongest chemical defences (Cortesi & Cheney, 2010), should maximize the deviation of their visual signals from the natural spatial frequency of the surrounding visual environment to elicit a strong avoidance response by predators (Zylinski *et al.*, 2011; Stevens & Ruxton, 2012). Olfactory cues may also increase avoidance response by predators (Ritson-Williams & Paul, 2007). This may be enhanced by the secretion of pungent substances (Behrens, 2005; personal observations) in some species, for example *Phyllidiella pustulosa*, that may be detected before an attack.

The ability of nudibranchs to produce certain colours and patterns may also be restricted by diet, habitat and physiological mechanisms, as found in many colourful animals (Fox & Vevers, 1960). However, the variety of colours produced by the relatively closely related bivalve marine molluscs, such as the giant clam family (Tridacnidae), suggests that the palette available to this phylum, using both pigmentary and structural mechanisms, is large. Additional selective pressures that have confounded results from terrestrial model systems (e.g. insects, frogs) such as thermoregulation and intra-specific signalling (e.g. individual recognition and sexual signalling) are not applicable to our system. Nudibranch eyes are simple structures; their visual abilities are limited and only used for simple behaviours such as phototaxis (Barth, 1964).

As expected, both measures of pattern (intensity variance and spatial frequency power spectra) were highly correlated; however, we found no relationship between pattern statistics and spectral contrast, a measurement that is frequently used in studies investigating the function and evolution of animal visual signals. Therefore, nudibranchs that exhibited the most highly contrasting patterns compared with their background, did not necessarily exhibit the most contrasting colours. The relative importance of each signal component (e.g. colour, pattern, luminance) and how they interact is often unclear. In terrestrial systems, chicks appear to use colours, rather than pattern, when learning and memorizing a signal (Osorio *et al.*, 1999; Aronsson & Gamble-Stille, 2008), indicating that specific colours may

transmit information, but pattern may attract attention to the signal and increase learning of a specific signal (Osorio *et al.*, 1999). Pigeons appear to use only one visual cue (shape or colour) when discriminating between visual stimuli (Reynolds, 1961; Johnson & Cumming, 1968). However, Spottiswoode & Stevens (2010) found that host birds use both colour and pattern to discriminate and reject parasitic eggs from nests. Furthermore, honeybees use more than one cue when processing information about signals (shape, colour and scent), and are able to store information about each one (Gould, 1984). To our knowledge, there has been little work done on the importance of colour and pattern in aquatic signalling systems.

Often studies use spectral contrast as a sole measure of conspicuousness, which may be misleading as colour distance may not be a linear measure of conspicuousness: once colour distance goes beyond the threshold of just noticeable differences, we do not know how spectral information is processed. Also, two spectra that are separated by equal distances in different directions in the colour space may not be equally distinguishable. Whether an increase in colour distance is directly related to an increase in conspicuousness or detectability of a colour signal should be tested empirically with behavioural experiments. Measures of conspicuousness are largely based on estimates of retinal input but do not consider neural processing of visual information. Until more is known on the relative roles and perception of visual cues component, multiple measures of conspicuousness should be used when addressing the function and evolution of visual signals.

In conclusion, we show that in nudibranch molluscs crypsis is not limited to small individuals, and we highlight the need to consider pattern in addition to spectral contrast when investigating the function and evolution of animal visual signals. We would also encourage more studies into the relative importance of colour, pattern and luminance in visual cues. We believe that that nudibranchs will be a fruitful model system in which to test a number of evolutionary hypotheses regarding the evolution of visual signals, but further information is needed on the relative strength of their chemical defences.

## Acknowledgments

We thank Eva McClure, Marie Mauffrey, Deb Aston and Derek Sun for help in the field and with spectral reflectance measurements. The following people provided photographs for the pattern analysis: Steve Clay,



Deb Aston, Astrid Lefringhausen, Chris Holman, Cory Pittman, Doug Perrine, Eric Mills, Gary Cobb, Ian Robertson, Jenny Ough, Julia DeMartini, Leanne Thompson, LeRoy Deters, Maxi Eckes, Michael Sawyer, Patti Jones, Scott Johnson, Jeanette Johnson, Stephen Grail, Terry Gosliner, Tom Davis, Johanna Werminghausen; and finally, to Britta Meyer and Michael Matschner for help with the phylogeny. This work was supported by the Australian Research Council and The University of Queensland.

## References

- Aronsson, M. & Gamberale-Stille, G. 2008. Domestic chicks primarily attend to colour, not pattern, when learning an aposematic coloration. *Anim. Behav.* **75**: 417–423.
- Avila, C. 1995. Natural products of opisthobranch molluscs: a biological review. *Oceanogr. Mar. Biol.* **33**: 487–559.
- Avila, C. & Paul, V.J. 1997. Chemical ecology of the nudibranch *Glossodoris pallida*: is the location of diet-derived metabolites important for defense? *Mar. Ecol. Prog. Ser.* **150**: 171–180.
- Barth, J. 1964. Intracellular recording from photoreceptor neurons in the eyes of a nudibranch mollusc (*Hermisenda crassicornis*). *Comp. Biochem. Physiol.* **11**: 311–315.
- Behrens, D.W. 2005. *Nudibranch Behaviour*. New World Publications Inc, Jacksonville, FL.
- Bouckaert, R.R. 2010. DensiTree: making sense of sets of phylogenetic trees. *Bioinformatics* **26**: 1372–1373.
- Burghardt, I., Schroedl, M. & Wagele, H. 2008. Three new solar-powered species of the genus *Phyllodesmium* Ehrenberg, 1831 (Mollusca: Nudibranchia: Aeolidioidea) from the tropical Indo-Pacific, with analysis of their photosynthetic activity and notes on biology. *J. Molluscan Stud.* **74**: 277–292.
- Castresana, J. 2000. Selection of conserved blocks from multiple alignments for their use in phylogenetic analysis. *Mol. Biol. Evol.* **17**: 540–552.
- Cheney, K.L. & Marshall, N.J. 2009. Mimicry in coral reef fish: how accurate is this deception in terms of color and luminance? *Behav. Ecol.* **20**: 459–468.
- Cheney, K.L., Newport, C., McClure, E.C. & Marshall, N.J. 2013. Colour vision and response bias in a coral reef fish. *J. Exp. Biol.* **216**: 2967–2973.
- Cimino, G. & Sodano, G. 1993. Biosynthesis of secondary metabolites in marine mollusks. *Top. Curr. Chem.* **167**: 77–115.
- Cimino, G., Derosa, S., Destefano, S., Sodano, G. & Villani, G. 1983. Dorid nudibranch elaborates its own chemical defense. *Science* **219**: 1237–1238.
- Cimino, G., Derosa, S., Destefano, S., Morrone, R. & Sodano, G. 1985. The chemical defense of nudibranch mollusks – structure, biosynthetic origin and defensive properties of terpenoids from the dorid nudibranch *Dendrodoris grandiflora*. *Tetrahedron* **41**: 1093–1100.
- Cobb, G. & Willian, R.C. 2006. *Undersea Jewels: A Colour Guide to Nudibranchs*. ABRs, Canberra.
- Coleman, N. 2008. *Nudibranchs Encyclopedia – Catalogue of Asia and Indo-Pacific Sea Slugs*. Neville Coleman's Underwater Geographic Pty Ltd., Springwood, Qld, Australia.
- Collin, S.P. & Pettigrew, J.D. 1989. Quantitative comparison of the limits on visual spatial resolution set by the ganglion cell layer in twelve species of reef teleosts. *Brain Behav. Evol.* **34**: 184–192.
- Cortesi, F. & Cheney, K.L. 2010. Conspicuousness is correlated with toxicity in marine opisthobranchs. *J. Evol. Biol.* **23**: 1509–1518.
- Cott, H.B. 1940. *Adaptive Coloration in Animals*. Methuen, London.
- Dalton, B.E., Cronin, T.W., Marshall, N.J. & Carleton, K.L. 2010. The fish eye view: are cichlids conspicuous? *J. Exp. Biol.* **213**: 2243–2255.
- Debelius, H. & Kuitert, R.H. 2007. *Nudibranchs of the World*. IKAN-Unterwasserarchiv, Frankfurt, Germany.
- Endler, J.A. 1978. A predator's view of animal colour patterns. In: *Evolutionary Biology*, Vol. **11** (M.K. Hecht, W.C. Steere & B. Wallace, eds), pp. 319–364. Plenum Press, New York.
- Endler, J.A. 1991. Variation in the appearance of guppy color patterns to guppies and their predators under different visual conditions. *Vision. Res.* **31**: 587–608.
- Endler, J.A. 2012. A framework for analysing colour pattern geometry: adjacent colours. *Biol. J. Linn. Soc.* **107**: 233–253.
- Faulkner, D.J. & Ghiselin, M.T. 1983. Chemical defense and evolutionary ecology of dorid nudibranchs and some other opisthobranch gastropods. *Mar. Ecol. Prog. Ser.* **13**: 295–301.
- Field, D.J. 1987. Relations between the statistics of natural images and then response properties of cortical cells. *J. Opt. Soc. Am. A* **4**: 2379–2394.
- Fontana, A., Gimenez, F., Marin, A., Mollo, E. & Cimino, G. 1994. Transfer of secondary metabolites from the sponges *Dysidea fragilis* and *Pleraplysilla spinifera* to the mantle dermal formations (MdFs) of the nudibranch *Hypselodoris webbi*. *Experientia* **50**: 510–516.
- Fox, H.M. & Vevers, G. 1960. *The Nature of Animal Colours*. Macmillan, New York.
- Gamberale, G. & Tullberg, B.S. 1996a. Evidence for a more effective signal in aggregated aposematic prey. *Anim. Behav.* **52**: 597–601.
- Gamberale, G. & Tullberg, B.S. 1996b. Evidence for a peak-shift in predator generalization among aposematic prey. *Proc. R. Soc. Lond. B Biol. Sci.* **263**: 1329–1334.
- Gamberale, G. & Tullberg, B.S. 1998. Aposematism and gregariousness: the combined effect of group size and coloration on signal repellence. *Proc. R. Soc. Lond. B Biol. Sci.* **265**: 889–894.
- Gelman, A. 2006. Prior distributions for variance parameters in hierarchical models (Comment on an Article by Browne and Draper). *Bayesian Analysis* **1**: 515–533.
- Gelman, A., Carlin, J.B., Stern, H.S. & Rubin, D.B. 2004. *Bayesian Data Analysis*, 2nd edn. Chapman & Hall/CRC, Boca Raton, FL.
- Gittleman, J.L. & Harvey, P.H. 1980. Why are distasteful prey not cryptic? *Nature* **286**: 149–150.
- Gould, J.L. 1984. The natural history of honey bee learning. In: *The Biology of Learning* (P. Marler & H. Terrace, eds), pp. 149–180. Springer-Verlag, Berlin.
- Hagman, M. & Forsman, A. 2003. Correlated evolution of conspicuous coloration and body size in poison frogs (Dendrobatidae). *Evolution* **57**: 2904–2910.
- Hanlon, R.T., Chiao, C.C., Mäthger, L.M., Buresch, K.C., Barbosa, A., Allen, J.J. et al. 2011. Rapid adaptive camouflage in cephalopods. In: *Animal Camouflage: Mechanisms and Function*

- (M. Stevens & S. Merilaita, eds), pp. 145–163. University Press, Cambridge.
- Johnson, D.F. & Cumming, W.W. 1968. Some determiners of attention. *J. Exp. Anal. Behav.* **11**: 157–166.
- Johnson, R.F. & Gosliner, T.M. 2012. Traditional taxonomic groupings mask evolutionary history: a molecular phylogeny and new classification of the chromodorid nudibranchs. *PLoS One* **7**: e33479.
- Katoh, K. & Toh, H. 2008. Improved accuracy of multiple ncRNA alignment by incorporating structural information into a MAFFT-based framework. *BMC Bioinformatics* **9**: 212.
- Kelber, A., Vorobyev, M. & Osorio, D. 2003. Animal colour vision – behavioural tests and physiological concepts. *Biol. Rev. (Camb.)* **78**: 81–118.
- Lanfear, R., Calcott, B., Ho, S.Y.W. & Guindon, S. 2012. PartitionFinder: combined selection of partitioning schemes and substitution models for phylogenetic analyses. *Mol. Biol. Evol.* **29**: 1695–1701.
- Lindstrom, L., Alatalo, R.V., Mappes, J., Riipi, M. & Vertainen, L. 1999. Can aposematic signals evolve by gradual change? *Nature* **397**: 249–251.
- Lindstrom, L., Alatalo, R.V., Lyytinen, A. & Mappes, J. 2001. Predator experience on cryptic prey affects the survival of conspicuous aposematic prey. *Proc. R. Soc. Lond. B Biol. Sci.* **268**: 357–361.
- Loosey, G.S., McFarland, W.N., Loew, E.R., Zamzow, J.P., Nelson, P.A. & Marshall, N.J. 2003. Visual biology of Hawaiian coral reef fishes. I. Ocular transmission and visual pigments. *Copeia* **2003**: 433–454.
- Lythgoe, J.N. 1979. *The Ecology of Vision*. Clarendon Press, Oxford.
- Marshall, N.J., Vorobyev, M. & Siebeck, U.E. 2006. What does a reef fish see when it sees a reef fish? Eating ‘Nemo’. In: *Communication in Fishes*, Vol. 2 (F. Ladich, S.P. Collin, P. Møller & B.G. Kapoor, eds), pp. 393–422. Science Publishers, Enfield, NH.
- Merilaita, S., Lyytinen, A. & Mappes, J. 2001. Selection for cryptic coloration in a visually heterogeneous habitat. *Proc. R. Soc. Lond. B Biol. Sci.* **268**: 1925–1929.
- Miller, A.M. & Pawlik, J.R. 2013. Do coral reef fish learn to avoid unpalatable prey using visual cues? *Anim. Behav.* **85**: 339–347.
- Mollo, E., Gavagnin, M., Carbone, M., Guo, Y.W. & Cimino, G. 2005. Chemical studies on Indopacific *Ceratosoma nudibranchs* illuminate the protective role of their dorsal horn. *Chemoecology* **15**: 31–36.
- Nilsson, M. & Forsman, A. 2003. Evolution of conspicuous colouration, body size and gregariousness: a comparative analysis of lepidopteran larvae. *Evol. Ecol.* **17**: 51–66.
- Osorio, D., Jones, C.D. & Vorobyev, M. 1999. Accurate memory for colour but not pattern contrast in chicks. *Curr. Biol.* **9**: 199–202.
- Pagel, M. 1999. Inferring the historical patterns of biological evolution. *Nature* **401**: 877–884.
- Paradis, E., Claude, J. & Strimmer, K. 2004. APE: analyses of phylogenetics and evolution in R language. *Bioinformatics* **20**: 289–290.
- Plummer, M. 2012. *JAGS Version 3.3.0 User Manual*, Lyon, France. [Computer software manual]. <http://mcmc-jags.sourceforge.net/>.
- Plummer, M., Best, N., Cowles, K. & Vines, K. 2006. CODA: convergence diagnosis and output analysis for MCMC. *R News* **6**: 7–11.
- Poulton, E.B. 1890. *The Colours of Animals*. Kegan Paul, London.
- R Core Team 2013. *R: A Language and Environment for Statistical Computing*. R Foundation for Statistical Computing, Vienna, Austria. ISBN 3-900051-07-0. <http://www.R-project.org/>.
- Reynolds, G.S. 1961. Attention in the pigeon. *J. Exp. Anal. Behav.* **4**: 203–208.
- Ritson-Williams, R. & Paul, V.J. 2007. Marine benthic invertebrates use multimodal cues for defense against reef fish. *Mar. Ecol. Prog. Ser.* **340**: 29–39.
- Ronquist, F., Teslenko, M., van der Mark, P., Ayres, D.L., Darling, A., Höhna, S. et al. 2012. MrBayes 3.2: efficient Bayesian phylogenetic inference and model choice across a large model space. *Syst. Biol.* **61**: 539–542.
- Roper, T.J. 1994. Conspicuousness of prey retards reversal of learned avoidance. *Oikos* **69**: 115–118.
- Roper, T.J. & Cook, S.E. 1989. Responses of chicks to brightly colored insect prey. *Behaviour* **110**: 276–293.
- Rothschild, M. 1984. Aide-memoire mimicry. *Ecol. Entomol.* **9**: 311–319.
- Ruxton, G.D., Sherratt, T.N. & Speed, M.P. 2004. *Avoiding Attack: The Evolutionary Ecology of Crypsis, Warning Signals, and Mimicry*. Oxford University Press, Oxford.
- Siebeck, U.E., Wallis, G.M. & Litherland, L. 2008. Colour vision in coral reef fish. *J. Exp. Biol.* **211**: 354–360.
- Somerville, M.J., Mollo, E., Cimino, G., Rungprom, W. & Garson, M.J. 2006. Spongian diterpenes from Australian nudibranchs: an anatomically guided chemical study of *Glossodoris atomarginata*. *J. Nat. Prod.* **69**: 1086–1088.
- Spottiswoode, C.N. & Stevens, M. 2010. Visual modeling shows that avian host parents use multiple visual cues in rejecting parasitic eggs. *Proc. Natl. Acad. Sci. USA* **107**: 8672–8676.
- Stevens, M. & Ruxton, G.D. 2012. Linking the evolution and form of warning coloration in nature. *Proc. R. Soc. Lond. B Biol. Sci.* **279**: 417–426.
- Stevens, M., Parraga, C.A., Cuthill, I.C., Partridge, J.C. & Troscianko, T.S. 2007. Using digital photography to study animal coloration. *Biol. J. Linn. Soc.* **90**: 211–237.
- de Villemereuil, P., Wells, J.A., Edwards, R.D. & Blomberg, S.P. 2012. Bayesian models for comparative analysis integrating phylogenetic uncertainty. *BMC Evol. Biol.* **12**: 102.
- Vorobyev, M. & Osorio, D. 1998. Receptor noise as a determinant of colour thresholds. *Proc. R. Soc. Lond. B Biol. Sci.* **265**: 351–358.
- Vorobyev, M., Marshall, J., Osorio, D., de Ibarra, N.H. & Menzel, R. 2001. Colourful objects through animal eyes. *Color Res. Appl.* **26**: S214–S217.
- Wagele, H., Ballesteros, M. & Avila, C. 2006. Defensive glandular structures in opisthobranch molluscs – from histology to ecology. *Ocean. Mar. Biol.* **44**: 197–276.
- Wang, I.J. 2011. Inversely related aposematic traits: reduced conspicuousness evolves with increased toxicity in a polymorphic poison-dart frog. *Evolution* **65**: 1637–1649.
- Wilson, N.G., Schrödl, M. & Halaných, K.M. 2009. Ocean barriers and glaciation: evidence for explosive radiation of mitochondrial lineages in the Antarctic sea slug *Doris kerguelensis* (Mollusca, Nudibranchia). *Mol. Ecol.* **18**: 965–984.
- Zylinski, S., How, M.J., Osorio, D., Hanlon, R.T. & Marshall, N.J. 2011. To be seen or to hide: visual characteristics of body patterns for camouflage and communication in the Australian Giant Cuttlefish *Sepia apama*. *Am. Nat.* **177**: 681–690.

### Supporting information

Additional Supporting Information may be found in the online version of this article:

**Figure S1** Spatial frequency analysis of six simulated and real example images.

**Figure S2** Density plots of 1000 trees obtained from MrBayes analysis to highlight phylogenetic uncertainty.

**Figure S3** Relative measurements of traits plotted on phylogenetic tree.

**Figure S4** Scatterplot of spectral contrast (colour distance) as perceived by a dichromatic reef fish (*Chaetodon kleinii*;  $\lambda$  max = 496, 530) against average body size of each nudibranch species, (a) against the background habitat and (b) within animal colour pattern.

**Table S1** Species and data used in each analysis and GenBank Accession Numbers.

Received 25 September 2013; revised 13 January 2014; accepted 23 January 2014

### 5.3. Supporting Information

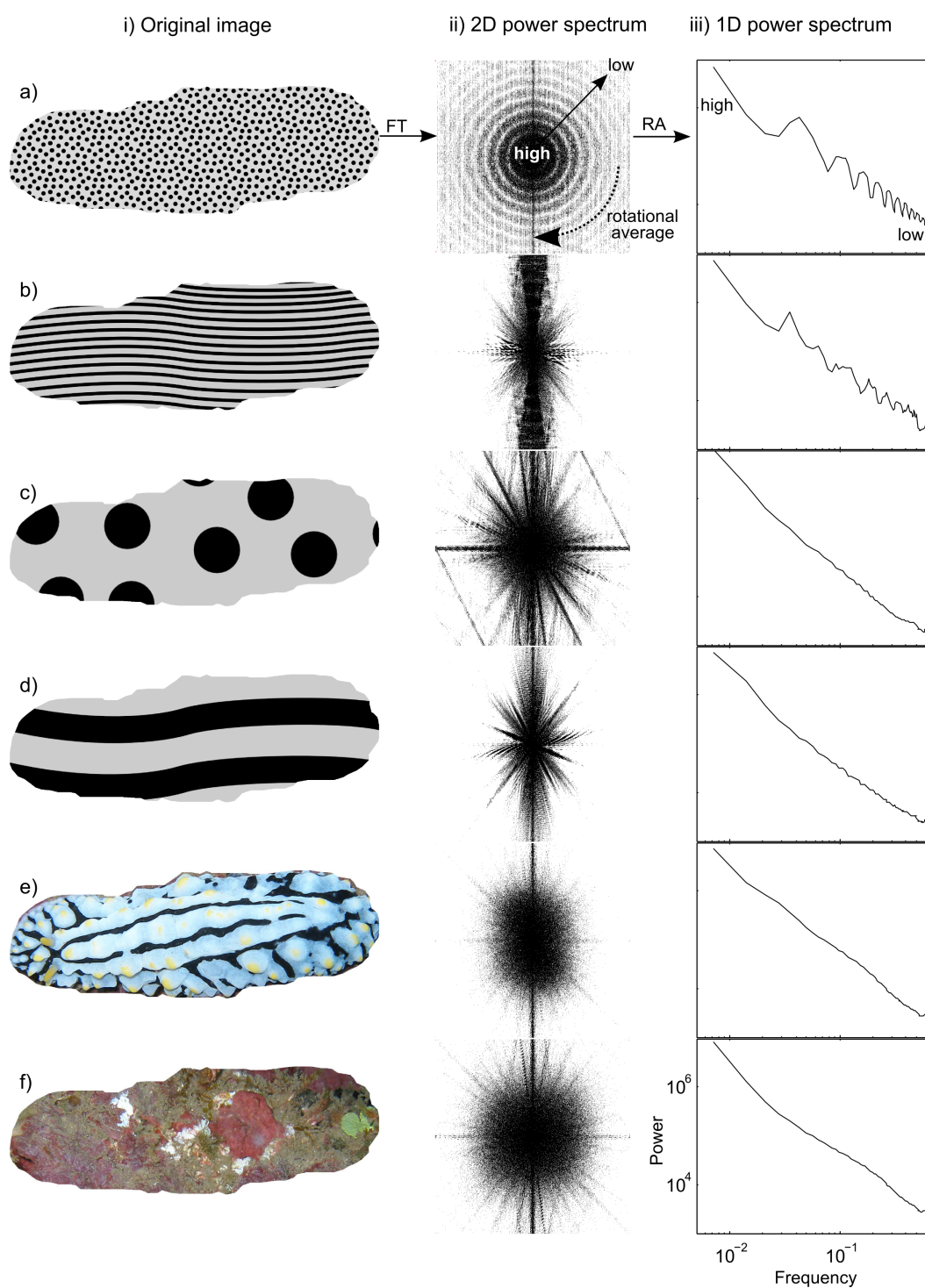
Supplementary Table Sg1: Species and data used in each analysis, and Genbank accession numbers

Family	Species Name (as per WoRMS: <a href="http://www.marinespecies.org">www.marinespecies.org</a> )	Recent synonyms	COI	16S	Mean body size (cm)	Spectral data	Number of image (for pattern analysis)
Aegiridae	<i>Aegires citrinus</i> (Bergh, 1875)	<i>Notadoris citrina</i>	KJ001313	KJ018905	4	YES	-
Aegiridae	<i>Aegires gardineri</i> (Eliot, 1906)	<i>Notadoris gardineri</i>	DQ991934	DQ991934	6	YES	14
Aegiridae	<i>Aegires minor</i> (Eliot, 1904)	<i>Notadoris minor</i>	KJ001314	KJ018906	6	YES	-
Chromodorididae	<i>Ardeadoris cruenta</i> (Rudman, 1986)	<i>Glossodoris cruenta</i>	KJ001298	KJ018907	4	YES	-
Chromodorididae	<i>Ardeadoris egretta</i> (Rudman, 1984)		EU982713	EU982762	5	YES	14
Chromodorididae	<i>Ardeadoris rubroannulata</i> (Rudman, 1986)	<i>Glossodoris rubroannulata</i>	JQ727873	JQ727755	5	YES	-
Chromodorididae	<i>Ceratosoma brevicaudatum</i> (Abraham, 1876)		EU512141	EU512052	9	-	11
Chromodorididae	<i>Ceratosoma tenue</i> (Abraham, 1876)		KJ001300	JQ727696	8	YES	9
Chromodorididae	<i>Ceratosoma trilobatum</i> (Gray, 1827)		EU982730	EU982784	9	YES	8
Chromodorididae	<i>Chromadoris annae</i> (Bergh, 1877)		JQ727829	JQ727704	5	YES	20
Chromodorididae	<i>Chromadoris striatella</i> (Bergh, 1876)		KJ001302	KJ018908	4	-	8
Chromodorididae	<i>Chromadoris diana</i> (Gosliner & Behrens, 1998)		JQ727836	JQ727712	3	YES	22
Chromodorididae	<i>Chromadoris elisabethina</i> (Bergh, 1877)		JQ727837	JQ727713	4.5	YES	27
Chromodorididae	<i>Chromadoris kuiteri</i> (Rudman, 1982)		AF249804	AF249240	6	YES	20
Chromodorididae	<i>Chromadoris lachi</i> (Rudman, 1982)		JQ727850	JQ727728	4	YES	32
Chromodorididae	<i>Chromadoris magnifica</i> (Quoy & Gaimard, 1832)		EU982736	EU982787	4	YES	24
Chromodorididae	<i>Chromadoris quadricolor</i> (Ruppell & Leuckhart, 1828)		AF249802	AF249241	4	-	25
Chromodorididae	<i>Chromadoris westraliensis</i> (O'Donoghue, 1924)		JQ727860	JQ727742	3.5	-	10
Chromodorididae	<i>Diversidoris flava</i> (Eliot, 1904)	<i>Noumea flava</i>	EU512164	JQ727805	1.5	YES	12
Chromodorididae	<i>Dorisprismatica atromarginata</i> (Cuvier, 1804)	<i>Glossodoris atromarginata</i>	JQ727864	JQ727746	5	YES	51
Chromodorididae	<i>Dorisprismatica sedna</i> (Marcus & Marcus, 1967)	<i>Glossodoris sedna</i>	JQ727878	JQ727760	3	-	16
Chromodorididae	<i>Felimida luteoasea</i> (von Rapp, 1827)	<i>Chromodoris luteoasea</i>	AJ223259	AJ225183	2.5	-	11
Chromodorididae	<i>Felimida purpurea</i> (Risso in Guérin, 1831)	<i>Chromodoris purpurea</i>	AJ223260	AJ225184	2	-	16
Chromodorididae	<i>Glossodoris cincta</i> (Bergh, 1888)		EU982740	EU982792	6	YES	8
Chromodorididae	<i>Glossodoris pallida</i> (Ruppell & Leuckhart, 1828)		EU982742	EU982794	2	YES	14
Chromodorididae	<i>Glossodoris vespa</i> (Rudman, 1990)		EU512160	EU925586	8	YES	9
Chromodorididae	<i>Goniobranchus albonares</i> (Rudman, 1990)	<i>Chromadoris albonares</i>	KJ001299	KJ018909	2	YES	10

Family	Species	Recent synonyms	COI	16S	Mean body size (cm)	Spectral data	Number of image (for pattern analysis)
Chromodorididae	<i>Goniobranchus coi</i> (Risbec, 1956)	<i>Chromadoris coi</i>	EU982734	EU982785	4	YES	17
Chromodorididae	<i>Goniobranchus daphne</i> (Angus, 1864)	<i>Chromadoris daphne</i>	KJ001297	KJ018921	2.5	YES	12
Chromodorididae	<i>Goniobranchus decorus</i> (Pease, 1860)	<i>Chromodoris decora</i>	EU982735	EU982786	1.5	YES	18
Chromodorididae	<i>Goniobranchus geometricus</i> (Risbec, 1928)	<i>Chromadoris geometrica</i>	JQ727841	JQ727718	1.5	YES	20
Chromodorididae	<i>Goniobranchus hintuanensis</i> (Gosliner & Behrens, 1998)	<i>Chromadoris hintuanensis</i>	JQ727845	JQ727721	2	YES	11
Chromodorididae	<i>Goniobranchus kuniei</i> (Pruvot-Fol, 1930)	<i>Chromadoris kuniei</i>	EF535112	JQ727724	4.5	-	9
Chromodorididae	<i>Goniobranchus splendida</i> (Angus, 1864)	<i>Chromadoris splendida</i>	EU982738	EU982789	4	YES	32
Chromodorididae	<i>Goniobranchus tasmaniensis</i> (Bergh, 1905)	<i>Chromadoris tasmaniensis</i>	EF535113	AY458817	3	-	14
Chromodorididae	<i>Goniobranchus tinctorius</i> (Ruppell & Leuckart, 1828)	<i>Chromadoris tinctoria</i>	KJ001315	KJ018910	3.5	-	15
Chromodorididae	<i>Goniobranchus verrieri</i> (Crosse, 1875)	<i>Chromadoris verrieri</i>	JQ727858	JQ727740	2	YES	13
Chromodorididae	<i>Hypselodoris bennetti</i> (Angas, 1864)		EF535131	EF534059	3	-	50
Chromodorididae	<i>Hypselodoris bullockii</i> (Collingwood, 1881)		JQ727888	JQ727772	3.5	-	11
Chromodorididae	<i>Hypselodoris godeffroyana</i> (Bergh, 1977)	<i>Risbecia godeffroyana</i>	EU512124	EU512097	4.5	YES	20
Chromodorididae	<i>Hypselodoris infucata</i> (Ruppell & Leuckhart, 1828)		JQ727891	JQ727776	3.5	-	12
Chromodorididae	<i>Hypselodoris jacksoni</i> (Wilson & Willan, 2007)		JQ727892	JQ727778	4	YES	13
Chromodorididae	<i>Hypselodoris maritima</i> (Baba, 1949)		JQ727897	JQ727788	2.5	YES	-
Chromodorididae	<i>Hypselodoris obscura</i> (Stimpson, 1855)		EU982745	EU982797	3.5	YES	25
Chromodorididae	<i>Hypselodoris tryoni</i> (Garrett, 1873)	<i>Risbecia tryoni</i>	EU982755	EU982808	4.5	YES	32
Chromodorididae	<i>Hypselodoris whitei</i> (Adams & Reeve, 1850)		JQ727903	JQ727794	3.5	YES	11
Chromodorididae	<i>Hypselodoris zephyra</i> (Gosliner & Johnson, 1999)		JQ727904	JQ727796	3	YES	14
Chromodorididae	<i>Mexichromis festiva</i> (Angas, 1864)		EF535124	EF534051	1.5	YES	14
Chromodorididae	<i>Mexichromis mariei</i> (Crosse, 1872)		EU982749	EU982801	1.5	YES	10
Chromodorididae	<i>Mexichromis trilineata</i> (Adams & Reeve, 1850)	<i>Pectenodoris trilineata</i>	EU982753	EU982806	1	YES	-
Chromodorididae	<i>Miamira sinuata</i> (van Hasselt, 1824)	<i>Ceratosoma sinuata</i>	EU982733	EU982783	5	YES	-
Chromodorididae	<i>Noumea laboutei</i> (Rudman, 1986)		KJ001301	KJ018911	1.5	YES	-
Dendrodorididae	<i>Dendrodoris krusensternii</i> (Gray, 1850)	<i>Dendrodoris denisoni</i>	GQ292047	AF430350	6	YES	10
Dendrodorididae	<i>Dendrodoris tuberculosa</i> (Quoy & Gaimard, 1832)		KJ001303	AF430352	10	YES	8
Discodorididae	<i>Halgerda aurantiomaculata</i> (Allan, 1932)		KJ001312	KJ018912	6	YES	-
Discodorididae	<i>Halgerda willeyi</i> (Eliot, 1904)		AY128129.1	KJ018913	5	YES	-
Dorididae	<i>Doris pecten</i> (Collingwood 1881)	<i>Doriopsis pecten</i>	KJ001311	KJ018914	1.5	YES	8
Facelinidae	<i>Phyllodesmium crypticum</i> (Rudman, 1981)		HQ010507	HQ010543	5	YES	8

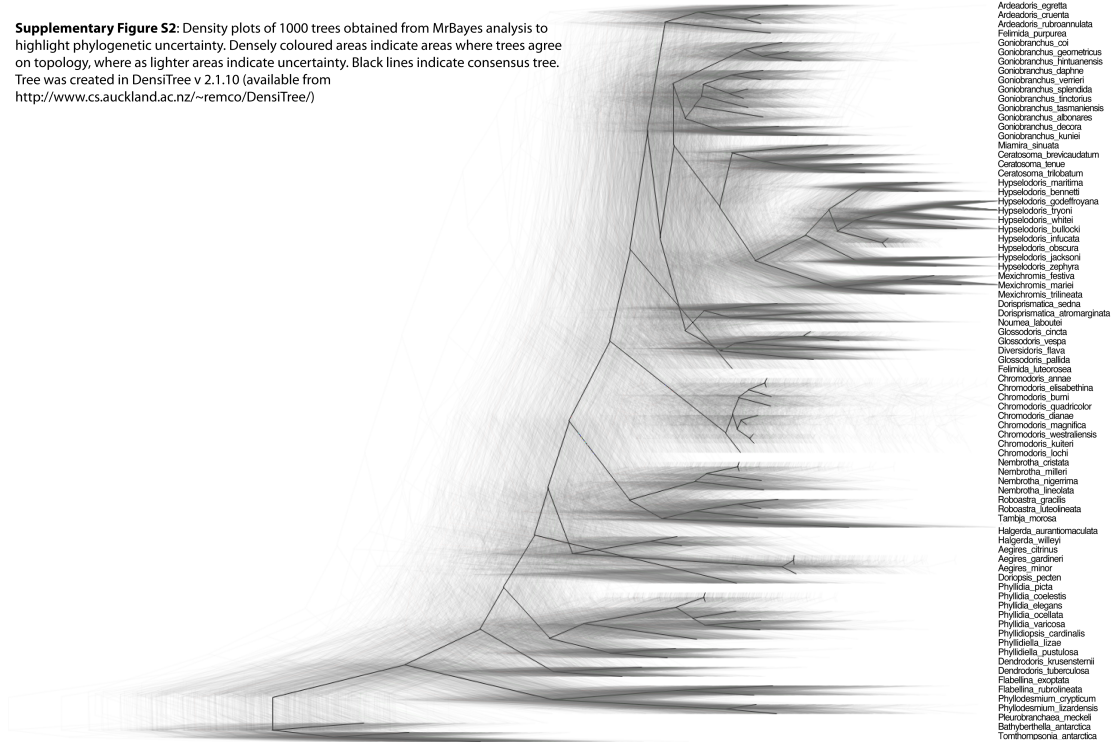
Family	Species	Recent synonyms	COI	16S	Mean body size (cm)	Spectral data	Number of image (for pattern analysis)
Facelinidae	<i>Phyllodesmium lizardensis</i> (Burghardt, Schrödl & Wägele, 2008)		HQ010505	HQ010540	6	YES	8
Flabellinidae	<i>Flabellina exoptata</i> (Gosliner & Willan, 1991)		JQ699572	JQ699485	2	YES	11
Flabellinidae	<i>Flabellina rubrolineata</i> (O'Donoghue, 1929)		KJ001316	KJ018915	2	YES	-
Phyllidiidae	<i>Phyllidia picta</i> (Pruvot-Fol, 1957)	<i>Fryeria picta</i>	KJ001304	KJ018916	4	YES	-
Phyllidiidae	<i>Phyllidia coelestis</i> (Bergh, 1905)		KJ001305	KJ018917	4	YES	18
Phyllidiidae	<i>Phyllidia elegans</i> (Bergh, 1869)		AJ223276	AJ225201	4	YES	22
Phyllidiidae	<i>Phyllidia ocellata</i> (Cuvier, 1804)		KJ001307	AF430363	4	YES	22
Phyllidiidae	<i>Phyllidia varicosa</i> (Lamarck, 1801)		KJ001306	AF430364	7.5	YES	26
Phyllidiidae	<i>Phyllidiella lizae</i> (Brunckhorst, 1993)		KJ001309	KJ018918	2.5	-	9
Phyllidiidae	<i>Phyllidiella pustulosa</i> (Cuvier, 1804)		KJ001310	AF249232	4	YES	48
Phyllidiidae	<i>Phyllidiopsis cardinalis</i> (Bergh, 1876)		KJ001308	AF430367	4	YES	-
Polyceridae	<i>Nembrotha cristata</i> (Bergh, 1877)		EF142893	EF142942	4.5	YES	17
Polyceridae	<i>Nembrotha kubaryana</i> (Bergh, 1877)	<i>Nembrotha nigerrima</i>	DQ231007	KJ018919	5	YES	20
Polyceridae	<i>Nembrotha lineolata</i> (Bergh, 1905)		EF142885	EF142937	3	YES	8
Polyceridae	<i>Nembrotha milleri</i> (Gosliner & Behrens, 1997)		EF142896	KJ018920	6	YES	-
Polyceridae	<i>Tambja morosa</i> (Bergh, 1877)		EF142867	EF142917	5	YES	8
Polyceridae	<i>Roboastra gracilis</i> (Bergh, 1877)		EF142863	EF142912	3	YES	14
Polyceridae	<i>Roboastra luteolineata</i> (Baba, 1936)		EF142861	EF142911	4	YES	8
Pleurobranchaeidae	<i>Pleurobranchaea meckeli</i> (Blainville, 1825)		FJ917499	FJ917439			
Pleurobranchaeidae	<i>Bathyberthella antarctica</i> (Willan & Bertsch, 1987)		FJ917487	FJ917429			
Pleurobranchaeidae	<i>Tomthompsonia antarctica</i> (Thiele, 1912)		DQ237992	EF489330			

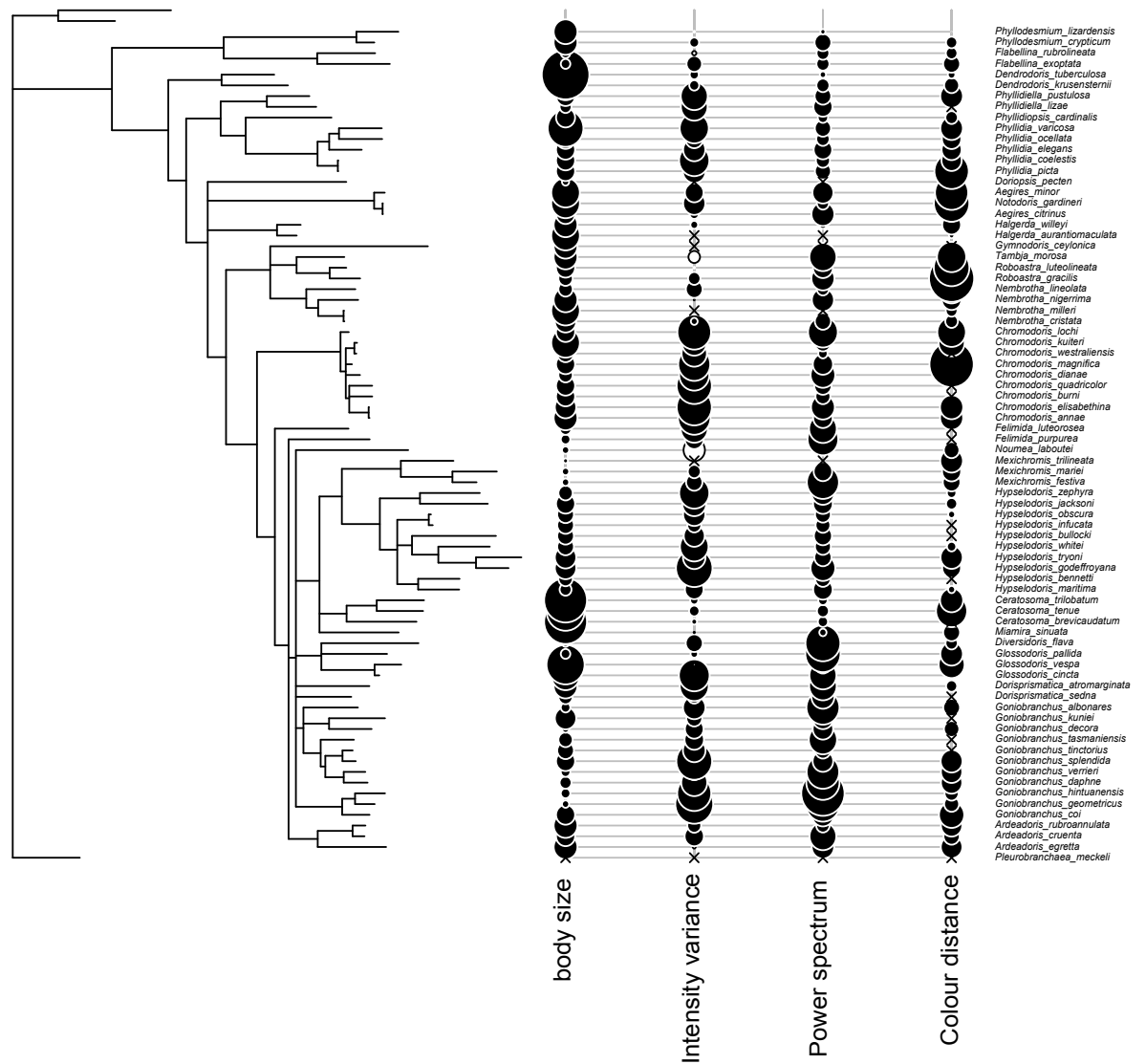




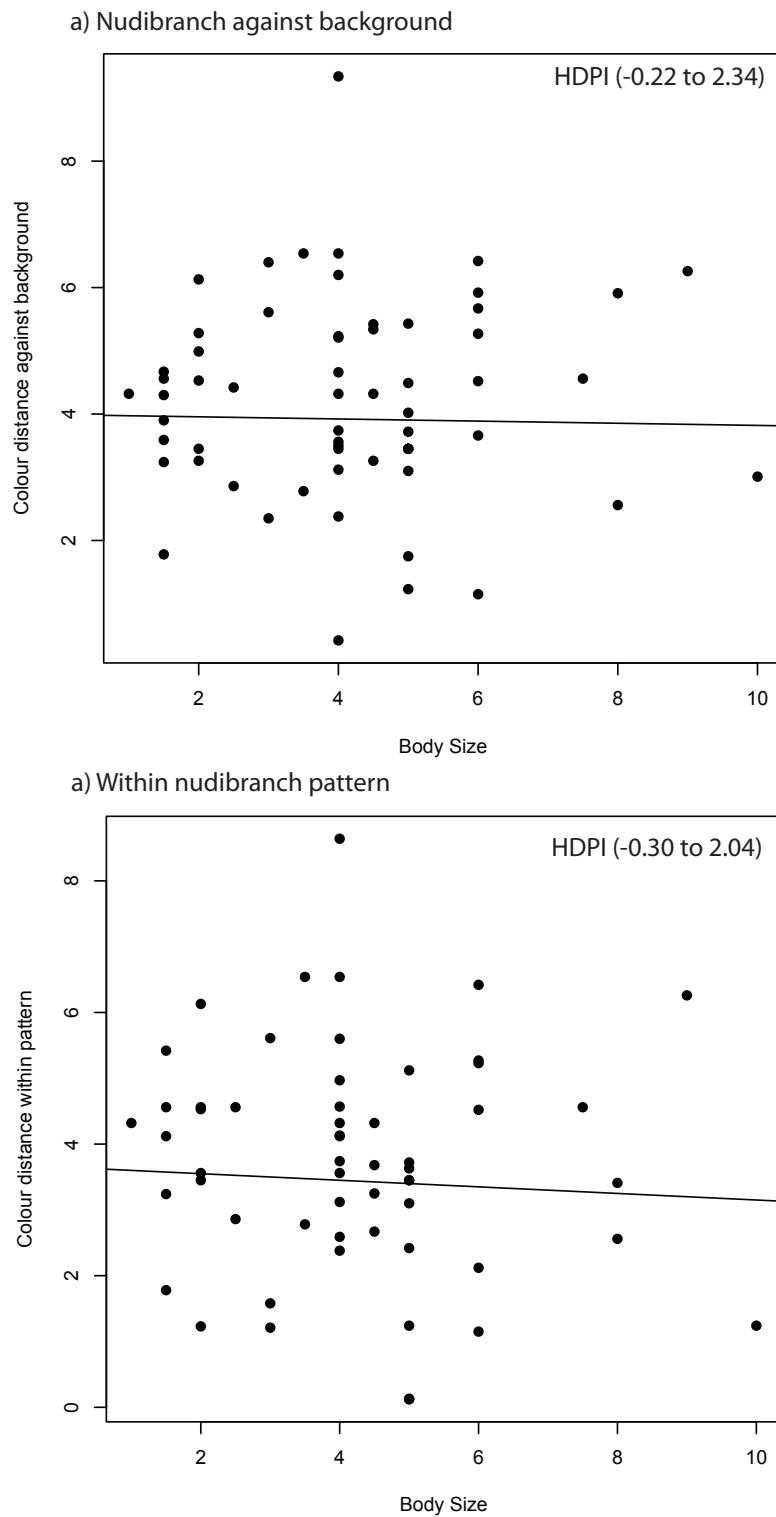
**Supplementary Figure S1:** Spatial frequency analysis of 6 simulated and real example images. Each image (i) is analyzed using a two-dimensional Fourier transform (ii), which is then rotationally averaged to produce a one dimensional power spectrum. The simulated images (a-d) contain strict periodic patterns, which produce clear peaks and troughs in the frequency analysis. In contrast, more natural scenes (e-f) contain a wider distribution of frequencies, and therefore exhibit smoother power spectrum relationships.

**Supplementary Figure S2:** Density plots of 1000 trees obtained from MrBayes analysis to highlight phylogenetic uncertainty. Densely coloured areas indicate areas where trees agree on topology, where as lighter areas indicate uncertainty. Black lines indicate consensus tree. Tree was created in DensiTree v 2.1.10 (available from <http://www.cs.auckland.ac.nz/~remco/DensiTree/>)





**Supplementary Figure S3:** Relative measurements of traits plotted on phylogenetic tree. As the diameter of circle increase, the respective trait value increases (body size, pattern measurements, colour distance measurement). X indicates value not available for the trait, white circles indicate a negative value (in the case of intensity variance, nudibranch has a solid coloration compared to their background).



**Supplementary Figure S4:** Scatterplot of spectral contrast (colour distance) as perceived by a dichromatic reef fish (*Chaetodon kleinii*;  $\lambda$  max = 496, 530) against average body size of each nudibranch species, a) against the background habitat and b) within animal colour pattern. Highest-density predicted interval (HDPI) and regression lines show results of phylogenetic regression analysis.

## Chapter 6

# Honesty of a plastic visual signal is maintained by receiver retaliation

J. C. Bachmann, F. Cortesi, M. D. Hall,  
N. J. Marshall, W. Salzburger, H. F. Gante

Current Biology (In review)

6.1. Manuscript p. 129 – 138

6.2. Supporting Information p. 139 – 160

This work was part of J. C. B. master thesis at the Universit of Basel. I contributed to her work by taking spectral reflectance measurements of fish, performed the theoretical fish visual models and participated in the writing of the manuscript.



# Honesty of a plastic visual signal is maintained by receiver retaliation

Judith C. Bachmann,<sup>1</sup> Fabio Cortesi,<sup>1,2</sup> Matthew D. Hall<sup>1,3</sup>, N. Justin Marshall<sup>2</sup>, Walter Salzburger<sup>1</sup>, Hugo F. Gante<sup>1\*</sup>

## Affiliations:

<sup>1</sup>Zoological Institute, Vesalgasse 1, University of Basel, 4051 Basel, Switzerland

<sup>2</sup>Queensland Brain Institute, University of Queensland, Brisbane Queensland 4072, Australia

<sup>3</sup>School of Biological Sciences, Monash University, Melbourne 3800, Australia

\*To whom correspondence should be addressed. E-mail: hugo.gante@unibas.ch

## Abstract

How reliable signals evolve is a question that has been hotly debated by theoreticians and for which empirical evidence has been difficult to obtain. Due to strong conflicts of interest, theory predicts that communication in territorial species should be under strong selection for clear, reliable, signaling. On the other hand, context-dependent signaling increases cheating opportunities, depending on how different receivers – mates, competitors or potential predators – acquire and process information. Using signaling theory, visual models and behavioral experimentation, we characterize reliability sources of the facial pattern as a visual signal in the territorial cichlid *Neolamprologus brichardi*. This signal evolved constant conspicuous chromatic properties for efficient detection in the aquatic medium, while allowing for context-dependent achromatic plasticity to communicate aggressive intent during territorial bouts. Importantly, we provide behavioral evidence that signal honesty is maintained by receiver retaliation costs, keeping the chances for cheating at a low.

**One Sentence Summary:** Receiver retaliation maintains honesty of a plastic visual signal in cichlid fish.

## Main Text

Animals use a variety of strategies to signal threat, attract mates and advertise territory ownership (1, 2). However, because signaling systems are open to exploitation from individuals who would rather provide unreliable information (i.e. cheaters), the interests of senders and receivers rarely coincide (1, 2). Then what prevents animals from cheating and getting fitness benefits at the expense of direct competitors? Due to advances in game-theoretical modeling over the past three decades, costly signaling theory has emerged as the ultimate adaptive explanation for the evolution of reliable communication and hinges on differential production costs of signals (1–5). Yet identifying the proximate mechanisms that generate reliable signals in the face of conflicts of interest has proven difficult, and empirical evidence for production costs in support of theoretical models remains scarce and mixed. In fact, signals thought to be reliable often have low production costs (6). Recognition that the potential costs of cheating, rather than their realized costs, can maintain signal reliability (7–9), offers a solution to the issue of reliable communication when strategic production costs are not evident (10). Here a third type of cost – receiver retaliation – is context-dependent and entirely conditional on receiver responses to the signal displayed by the sender. In this case, a signal needs only to incur efficacy production costs to guarantee unambiguous communication while honesty is socially mediated.

The evolution of reliable signals further depends on the spatial and temporal features of communication, yet this aspect is rarely considered. Dominant territorial males of sexually dichromatic birds (11), lizards (12) and fish (13), for example, display vibrant costly colors and contrasting color patches that are used in male-male competition and to attract choosy females (Fig. 1A). Expression of these signals, however, needs to be status-dependent, such that non-territorial individuals and territorial neighbors do not elicit unnecessary aggression from territory owners. But how can year-round territorial species reliably signal ownership while dominant, and not incur in physical injury while subordinate? These changes in conspicuousness require specific behavioral or morphological adaptations, such that signals are conveniently hidden or absent when not in use but still maximize signal reception when needed (14, 15). In the present study we characterize a plastic visual signal that is used to communicate aggressive intent, and identify mechanisms guaranteeing honest communication by simulating a cheater invasion (Fig. 1B). Moreover, we provide a general framework to characterize visual signals and offer empirical evidence that selection for signal conspicuousness, rapid physiological color changes and receiver retaliation costs can act as the proximate mechanisms that guarantee the efficacy and reliability of such signals.

We chose to examine the design and conspicuousness of a facial coloration pattern in the cichlid fish *Neolamprologus brichardi*, a lifelong territorial species that shows elaborate social habits (Fig. 1A). Our model system is a sexually monochromatic substrate spawner of the species-rich tribe Lamprologini (16) and has emerged as a model in cooperative breeding studies (17). Like other members of this tribe, individuals of both sexes look alike and share



similar tasks such as territory maintenance, defense and brood care. The reproductive couple has the peculiarity of being aided by up to 25 helpers in these tasks, organized in a strict linear hierarchy (18, 19). As a consequence of cooperative breeding and colony life, individuals repeatedly and regularly interact (20), using visual signals to recognize mates, kin and neighbors (21–23). Importantly, the rocky territories they inhabit are a valuable resource that provides substrate for reproduction and shelter against predation (3–50 m depth; (24, 25). Against this background, we characterized the conspicuousness of the *N. brichardi* facial pattern, the information it transmits to conspecifics (territoriality), and determined whether and how honesty of the signal is maintained.

**Conspicuousness of the *N. brichardi* facial pattern (Fig. 2A, B).** Selection for honest communication favors signaling systems that maximize signal reception relative to environmental noise and signal degradation. A visual signal in a particular light environment is most conspicuous when adjacent color elements have greater contrasts than non-adjacent elements (26–29). High conspicuousness is achieved by stimulation of adjacent photoreceptors in opposite ways by complementary radiance spectra (30, 31). Design strategies for signal conspicuousness and efficacy therefore include; (i) use of white or highly reflective colors adjacent to dark patches; (ii) use of patches that reflect high-intensity ambient wavelengths adjacent to patches that reflect low-intensity wavelengths; (iii) use of adjacent patches with complementary colors; and, (iv) the latter being centered in the greatest light intensity of the transmission medium (27).

Using spectral reflectance and theoretical fish visual models ((32, 33); Fig. S1 – 4 and Table S1 – 3) we show that the conspicuousness of the facial pattern is achieved by highly contrasting adjacent colors, ensuring detection efficacy in the aquatic medium (linear mixed-effects model (LMM):  $F_{1,9} = 207.31$ ,  $P < 0.001$ ; Fig. 2C). In support of signal theory (27), we show that conspicuousness is accomplished by the use of highly reflective elements, such as structural blue coloration and white adjacent to dark elements, in particular both black horizontal and vertical stripes composed of melanophores (black pigment cells). This combination is exceptionally effective since white reflects everywhere in the available light spectrum and the blue element reflects the high-intensity wavelengths of the aquatic medium, while the black stripes absorb most incident light (Fig. S *tba*). Chromatic contrast is further achieved by use of complementary colors, blue and yellow, centered in the highest light intensity of water transmission (Fig. S *tba*). By contrast, the achromatic signals do not seem to contribute much to conspicuousness, as brightness contrasts between adjacent and non-adjacent elements do not significantly differ from one another (LMM:  $F_{1,9} = 4.61$ ,  $P = 0.06$ ; Fig. 2D).

**Context-dependent use of facial color pattern.** Highly contrasting facial patterns implicate selection for the honest exchange of information. To test this, we investigated the function of the facial pattern in a territorial context by staging combat situations (fight for a ‘flower pot’ territory)

in laboratory aquaria between pairs of fish ( $n = 20$  pairs, 20 females and males each; Fig. S5 and Table S4). We found that irrespective of sex (outcome  $\times$  females LMM:  $F_{1,18} = 0.44$ ,  $P = 0.52$ ; outcome  $\times$  males LMM:  $F_{1,18} = 0.58$ ,  $P = 0.46$ ), body size (LMM:  $F_{1,18} = 8.02$ ,  $P = 0.01$ ) and fighting ability (LMM:  $F_{1,18} = 67.31$ ,  $P < 0.001$ ) determined the outcome of staged dyadic combats. Most importantly, we uncovered that losers of the combat rapidly paled their horizontal facial stripe (generalized linear mixed-effects model (GLMM) with binomial error distribution:  $X^2_1 = 14.97$ ,  $P < 0.001$ ; Figs. 2B, 3A) and that the initial brightness of the stripe does not influence contest outcome (GLMM, binomial:  $X^2_1 = 0.01$ ,  $P = 0.93$ ). Rapid physiological color changes are response available to all lower vertebrates and many invertebrates, can occur as fast as in a few seconds (34), and have previously been found to be used to alter signals during social interactions in other cichlid species (35).

Next, we used the theoretical vision models ([32, 33]; see above) to test if the changes in brightness of the horizontal facial stripe would also implicate an alteration in conspicuousness of the facial pattern in general. We found that even after paling, chromatic contrasts of adjacent colors stayed higher than that of non-adjacent colors and all pairwise comparisons remained well above the threshold of one for just noticeable differences (JND) of the signal receiver ([28]; Fig. 2C]. Whereby, adjacency of the color elements accounted for 96.5% of the variance of chromatic contrasts, while changes in the brightness of horizontal stripes explained less than 3% (Table S *tba*). Therefore, conspicuousness of the facial pattern in terms of chromatic contrast seems unaffected by the paling of the horizontal facial stripe. On the other hand, we observed a significant decrease of brightness contrasts when comparing facial pattern elements to the pale horizontal stripe, except for the contrast involving the vertical stripe, since the latter remains black (Fig. 2D). Hence, changes in brightness of the horizontal stripe explain most of the variance in achromatic contrasts (68.5%; Table S *tba*). From this it follows that information about aggressiveness is solely encoded by changes in brightness of the horizontal facial stripe while white, yellow and blue elements of the facial pattern act as amplifiers to enhance the chromatic contrast of the signal.

Behavioral in combination with fish visual modeling results suggest that individuals use the achromatic channel to communicate aggressive intent and territory ownership, while signal conspicuousness is kept intact by use of the chromatic channel. Using this dual mechanism is an elegant way to ensure that communication efficacy does not decrease due to context-dependent signaling. This always 'on' strategy to communicate territorial ownership and aggressive intent is somewhat surprising as it is temporally opposite to common intraspecific signaling systems used by e.g. anoles lizards or chameleons (12, 36, 37). Our findings could possibly be explained by lifelong territoriality and different predation escape strategies. While stenotopic cichlids rely on their rocky territories for shelter (and breeding) and conspicuously signal their ownership at all times, chameleons and anoles lizards have to rely on immobility and camouflage to escape avian predation and become only momentarily conspicuous while

displaying to conspecifics (37). Instead, a continuously conspicuous signaling strategy is more similar to that of aposematic species, which rely on high conspicuousness to signal their distastefulness (38, 39).

**Proximate mechanisms producing an evolutionary stable signaling strategy.** Theoretically, plastic changes in brightness of the horizontal facial stripe, because they are relatively cheap and quick to achieve, would be a prime candidate for cheating behavior to evolve. However, no such behavior was observed from the experiments above. Therefore, to test why plastic signals remain honest in *N. brichardi*, we simulated a cheater invasion of the signaling system by manipulating the brightness of the horizontal facial stripe (darkening or paling) and presenting fish to their mirror images. Our setup was opposite to the commonly used approach of displaying manipulated individuals to territory owners (2), but had the advantage of testing behavior of non-territorials (i.e. the receivers of the mirror image), which are the ones most interested in detecting unreliable signals if used by 'fake' territorial, dominant individuals. Manipulation of the horizontal stripe had a significant effect on the number of aggressive bouts received (LMM:  $F_{2,45} = 13.73$ ,  $P < 0.001$ ; Fig. 3B) irrespective of sex (LMM:  $F_{1,47} = 0.04$ ,  $P = 0.85$ ). Individuals with darkened stripes received significantly more aggression compared to individuals with pale stripes (TukeyHSD:  $z = -3.89$ ,  $P < 0.001$ ) and controls (TukeyHSD:  $z = -6.59$ ,  $P < 0.001$ ). Importantly, individuals with pale stripes also received more aggression than controls (TukeyHSD:  $z = -2.97$ ,  $P = 0.008$ ). Since aggressive intent is not a quality that can be easily handicapped (2), receivers can assess the reliability of signals of aggressive intent with relative ease (8) and impose social costs on cheaters.

Reliable communication is expected in aggressive contexts, such as territorial defense, since fighting is costly to all individuals (1, 2, 4). As predicted by theoretical models (7–9), we show that honest communication can be guaranteed by punishing cheaters. We thereby provide some rare empirical evidence that, like in wasps (6, 40), fish are able to detect and punish individuals who signal unreliably, be they cheaters signaling strength (bluffers) or modest liars (Trojans) (41). Our study furthermore supports the theory that commitment to a resource can generate broad conditions of reliability even if the resource is of high value (41). The territory is a non-divisible resource, essential for survival and reproduction in *N. brichardi*, and losing it has potential lifetime fitness consequences. Furthermore, the fact that these fish live in close proximity to conspecifics creates conditions for repeated interactions among individuals, which favors identification and punishment of cheaters. Here, we show that receiver retaliation is a powerful mechanism maintaining the honesty and stability of visual signals in territorial cichlid fishes. The physiological changes of the facial stripe rival the morphological and behavioral strategies presented by other territorial species (14, 15) and allow fish to communicate their intention to retreat from a combat to avoid escalation and associated costs which are typically imposed on species that use more static visual signals.

## References and Notes

1. W. A. Searcy, S. Nowicki, *The evolution of animal communication: reliability and deception in signaling systems* (Princeton University Press, Princeton, 2005).
2. J. W. Bradbury, S. L. Vehrencamp, *Principles of Animal Communication, Second Edition* (Sinauer Associates, Inc.; 2 edition, 2011).
3. A. Zahavi, *J. Theor. Biol.* **53**, 205–214 (1975).
4. John Maynard-Smith, D. Harper, *Animal Signals* (Oxford University Press, Oxford, First edit., 2003).
5. P. L. Hurd, M. Enquist, *Anim. Behav.* **70**, 1155–1170 (2005).
6. E. A. Tibbetts, J. Dale, *Nature*. **432**, 218–22 (2004).
7. P. L. Hurd, *J. Theor. Biol.* **174**, 217–222 (1995).
8. M. Lachmann, S. Számadó, C. T. Bergstrom, *Proc. Natl. Acad. Sci. U. S. A.* **98**, 13189–94 (2001).
9. S. Számadó, *Anim. Behav.* **81**, 3–10 (2011).
10. Production costs can be split into efficacy and strategic costs – the former are paid to transmit information unambiguously, while the latter are those that maintain signal reliability by making cheating unaffordable to low-quality individuals (3, 4).
11. S. R. Pryke, S. Andersson, *Behav. Ecol. Sociobiol.* **53**, 393–401 (2003).
12. J. B. Losos, *Lizards in an evolutionary tree: ecology and adaptive radiation of anoles* (University of California Press, Berkeley, 2009).
13. A. Kodric-Brown, *Integr. Comp. Biol.* **38**, 70–81 (1998).
14. A. J. Hansen, S. Rohwer, *Anim. Behav.* **34**, 69–76 (1986).
15. K. J. Metz, P. J. Weatherhead, *Anim. Behav.* **43**, 223–229 (1992).
16. H. F. Gante, W. Salzburger, *Curr. Biol.* **22**, R956–8 (2012).
17. M. Wong, S. Balshine, *Biol. Rev. Camb. Philos. Soc.* **86**, 511–30 (2011).
18. M. Taborsky, D. Limberger, *Behav. Ecol. Sociobiol.* **8**, 143–145 (1981).
19. S. Balshine et al., *Behav. Ecol. Sociobiol.* **50**, 134–140 (2001).
20. A. R. Reddon et al., *Anim. Behav.* **82**, 93–99 (2011).
21. S. Balshine-Earn, A. Lotem, *Behaviour*. **135**, 369–386 (1998).
22. P. Frostman, P. T. Sherman, *Ichthyol. Res.* **51**, 8–10 (2004).
23. A. L. Le Vin, B. K. Mable, K. E. Arnold, *Anim. Behav.* **79**, 1109–1114 (2010).
24. M. Taborsky, *Anim. Behav.* **32**, 1236–1252 (1984).
25. D. Heg, Z. Bachar, L. Brouwer, M. Taborsky, *Proc. Biol. Sci.* **271**, 2367–74 (2004).
26. J. A. Endler, *Biol. J. Linn. Soc.* **41**, 315–352 (1990).
27. J. A. Endler, *Am. Nat.* **139**, S125–S153 (1992).
28. J. A. Endler, *Biol. J. Linn. Soc.* **107**, 233–253 (2012).
29. T. Guilford, M. S. Dawkins, *Trends Neurosci.* **16**, 430–436 (1993).
30. J. N. Lythgoe, *The ecology of vision* (Clarendon Press, Oxford, 1979).

31. L. M. Hurvich, *Colour vision* (Sinauer Associates Inc., U.S., 1981).
32. M. Vorobyev, D. Osorio, *Proc. Biol. Sci.* **265**, 351–8 (1998).
33. M. Vorobyev, R. Brandt, D. Peitsch, S. B. Laughlin, R. Menzel, *Vision Res.* **41**, 639–53 (2001).
34. R. Fujii, *Pigment Cell Res.* **13**, 300–319 (2000).
35. L. E. Muske, R. D. Fernald, *J. Comp. Physiol. A.* **160**, 89–97 (1987).
36. M. Leal, L. J. Fleishman, *Am. Nat.* **163**, 26–39 (2004).
37. D. Stuart-Fox, A. Moussalli, *PLoS Biol.* **6**, e25 (2008).
38. C. R. Darst, M. E. Cummings, D. C. Cannatella, *Proc. Natl. Acad. Sci. U. S. A.* **103**, 5852–7 (2006).
39. K. L. Cheney et al., *J. Evol. Biol.* **27**, 676–87 (2014).
40. E. A. Tibbetts, A. Izzo, *Curr. Biol.* **20**, 1637–1640 (2010).
41. S. Számadó, *Anim. Behav.* **82**, 295–302 (2011).
42. S. Rohwer, *Evolution (N. Y.)* **29**, 593–610 (1975).
43. J. C. Senar, in *Proceedings of the International Ornithological Congress*, N. J. Adams, R. H. Slotow, Eds. (BirdLife South Africa, Johannesburg, 1999), pp. 1669–1686.

### Acknowledgments

Photographs of the anole and widowbird are courtesy of Melisa Losos and Jan Willem Steffelaar. We thank designers Inês Santiago and Marco Silva.

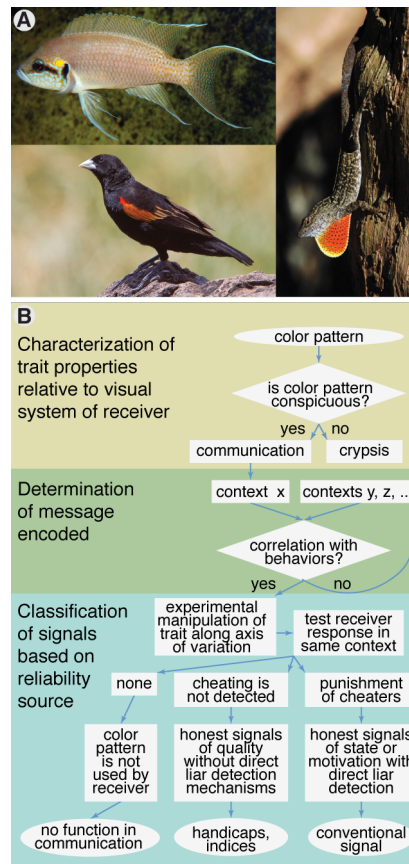


**Figure 1.** (A) Territorial species display a variety of conspicuous visual signals to communicate aggressive intent. To decrease predation pressure, during non-breeding season and other non-aggressive contexts several species use morphological or behavioral adaptations to conceal signals. We propose that rapid physiological color change is the proximate mechanism responsible for turning ‘off’ a visual signal of aggressive intent in lifelong territorial fish. Clockwise from top left: facial color pattern in Princess of Burundi cichlid (*Neolamprologus brichardi*); extended dewlap in trunk-ground Brown Anole (*Anolis sagrei*); partially covered epaulette in Fan-tailed Widowbird (*Euplectes axillaris*). (B) Flowchart to illustrate the general approach proposed for studying visual signals by determining signal efficacy, function and proximate reliability mechanisms.

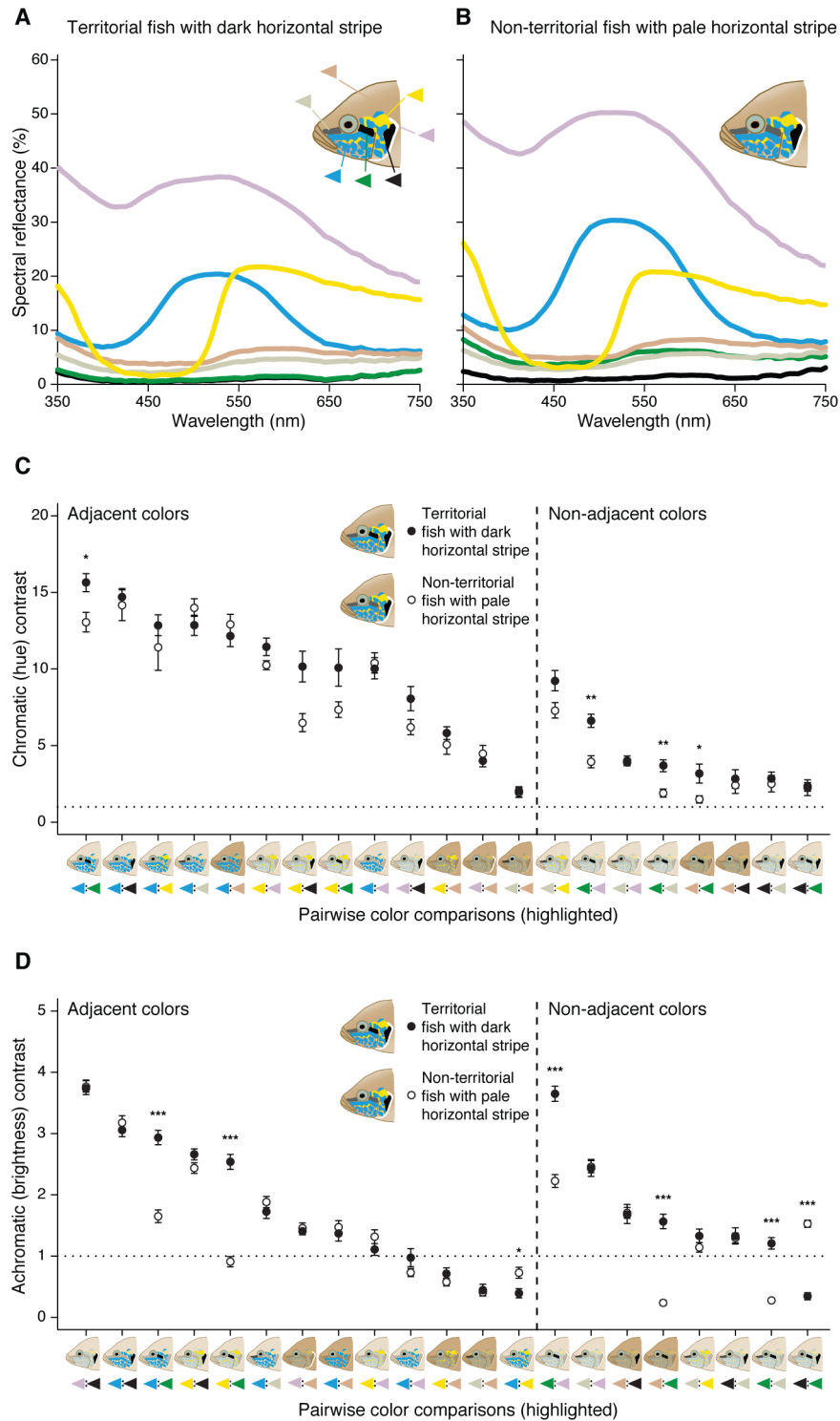


**Figure 2.** Color properties of facial elements in dominant and non-dominant *Neolamprologus brichardi*. (**A and B**) Average spectral reflectance of facial color pattern elements. Horizontal (green triangle) and vertical (black triangle) facial stripes have the same reflectance in territorial fish (**A**). Losing a combat (and territory) significantly increases reflectance of horizontal facial stripe in non-territorial fish, i.e. paling occurs (**B**). (**C and D**) Chromatic and achromatic contrasts between pairs of adjacent and non-adjacent color elements as perceived by *N. brichardi*, ordered from highest to lowest in territorial fish. High chromatic contrast is achieved by color combinations involving blue and yellow (**C**), while high brightness contrast is achieved by color combinations involving dark stripes (**D**). Stippled line marks the 1 JND, threshold after which two patches are thought to be perceived as different (28). Asterisks illustrate significant differences in contrast between territorial and non-territorial fish (\*\* $P < 0.001$ , \*\*  $P < 0.01$ , \*  $P < 0.05$ ).



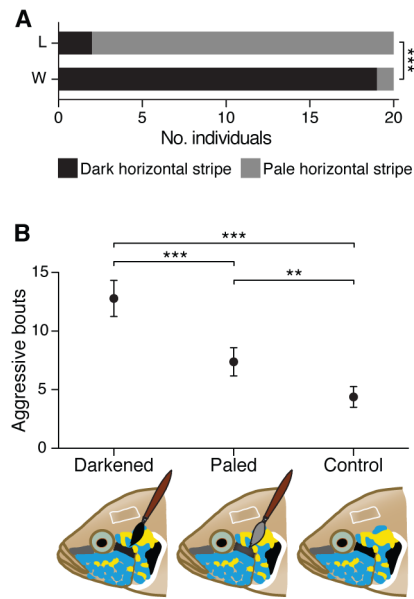


**Figure 3.** Horizontal facial stripe provides reliable information on aggressive intent. **(A)** Brightness of the facial stripe is associated with fighting ability (winning or losing) at end of combat. L: losers; W: winners. **(B)** Unreliable signaling of strength (darkened stripe) or weakness (paled stripe) is punished by increased receiver retaliation costs relative to reliable signaling. Asterisks illustrate significant differences in facial stripe luminance at end of combat and of Tukey-Kramer *post-hoc* tests between treatments (\*\*\*  $P < 0.001$ , \*\*  $P < 0.01$ ).

## 6.2. Supporting Information

### Materials and Methods

#### *Choice of species*

The Princess of Burundi, *Neolamprologus brichardi* (Teleostei: Cichlidae), is a small (up to 8 cm in standard length) fish native to Lake Tanganyika, eastern Africa. Together with *N. pulcher*, it has emerged as a model system in studies on the evolution of cooperative breeding behavior (1). Recently, substantial genomic and transcriptomic resources have become available for *N. brichardi* (2). These resources make this species an excellent system for the study of speciation, evolution of cooperative behavior and communication from a genetic perspective. Moreover, *N. brichardi* performs the complete range of behaviors observed in the wild under laboratory conditions, which also makes it an optimal species for behavioral studies (3). Phylogenetic relationships have been recently studied (4), which led some authors to synonymize it with *N. pulcher*. The two species differ in their facial pigmentation patterns, but are thought to behave similarly. We adopt the pre-synonymy taxonomy because it highlights the differences in facial pigmentation pattern, which are the focus of our study. This should not create taxonomic confusion and favors the accumulation of clear information for each of the pigmentation phenotypes. Like most other species of the tribe Lamprologini, *N. brichardi* is sexually monochromatic, i.e. the color of fish does not differ between males and females. The facial pigmentation of *N. brichardi* consists of two black stripes, arranged in a horizontal T-shape, surrounded by structural blue coloration, yellow pigmentation elements and a white branchiostegal membrane. Another less conspicuous stripe is present in the pre-orbital (lacrimal) area. From a human perspective, the species has a beige body with fine orange elements in the posterior half and white-fringed fins (see Fig. 1 in main text).

Substantial data on life history and behavioral traits have been documented for these species. Social groups of *N. brichardi* can be found on coastal rocky substrates of Lake Tanganyika between 3 – 50 m deep. The rocky substrate provides a territory with shelters and breeding grounds where adhesive eggs are spawned. The breeding male is always the largest individual of the group, usually followed by the breeding female and subordinate helpers (which can number up to 25) are the smallest (1). Groups aggressively defend their territory and dominant females and males behave similarly, and both show high testosterone levels and brain arginine vasotocin expression [a neuropeptide involved in vertebrate territorial, reproductive and social behaviors; (5)]. Group hierarchy is based on size, is relatively stable over time and, subordinate fish either stay in their natal group or they disperse to a new group to queue and breed (1). Territories are clustered into colonies, separated by a mean distance adjacent of 1.6 m (6). These life history and behavioral traits create conditions for repeated interactions among individuals. Most of which involve submissive behaviors, followed by aggressive behaviors and only then territory maintenance (such as digging) and broodcare (7).

### *Husbandry of study animals*

*N. brichardi* were raised and kept under controlled captive conditions at the Zoological Institute, University of Basel, Switzerland. Tanks had a constant water temperature of  $27 \pm 1$  °C, a 12:12 h light:dark regime and contained ~ 1.5 cm of sand on the bottom, a foam filter, a heater and terracotta flowerpots that are readily accepted as shelters. Fish were fed commercial flakes or frozen cichlid food twice daily. All experiments were authorized by the Cantonal Veterinary Office, Basel, Switzerland (permit numbers 2317 & 2356) and performed at the Zoological Institute, University of Basel.

### *Color spectra and theoretical visual modeling experiment*

Spectral reflectance measurements of *N. brichardi* facial patterns were taken using a USB4000 spectrophotometer (Ocean Optics Inc.) and DH-2000-DUV Mikropack deuterium-halogen light source, connected to a laptop computer running Ocean Optics SpectraSuite software. Twenty individuals were tranquilized using a solution of KOIMED Sleep (KOI&BONSAI, 0.5% v/v 2-Phenoxyethanol) before being transferred to a shallow tray filled with sufficient water to fully cover the fish. Because tranquilizing the fish before measuring their spectral reflectance may induce a short term darkening of their skin pigmentation we took care to measure reflectance after original conditions were re-established (~15 seconds). Spectral reflectance of various facial color patches (Fig. 2A-B in main text) was measured with a 200µm bifurcated optic UV/visible fiber. The bare end of the fiber was held at a 45° angle to prevent specular reflectance. A Spectralon 99% white reflectance standard was used to calibrate the percentage of light reflected at each wavelength from 350 – 750 nm. At least ten measurements per facial pattern per individual were taken and subsequently averaged. Spectra were assessed based on the wavelength at which light was reflected and the shape of the reflectance curves, and classified into previously established categories of reef fish colors (8).

To characterize the visual system of *N. brichardi*, we used published quantitative opsin data (2, 9) and amino acid sequences from eye RNAseq data (2) done on our stock of *N. brichardi*, and collected new transmission measurements of the crystalline lens from wild specimens. Laboratory reared *N. brichardi* expressed the UV-sensitive SWS1, and the two green-sensitive RH2A and RH2B opsin genes, which is a common opsin expression palette in cichlid species, including the ones from lake Malawi [(Figure S1; (10)]. On comparisons of amino acid sequences of these three genes to the sequences of their lake Malawi relatives we found that there are only minor differences between species (Tables S1 – S3). In particular, *N. brichardi* and *Metriaclima (Maylandia) zebra* show amino acid similarity of 95.4% ( $\pm 1.1\%$ , s.e.) at SWS1, 98% ( $\pm 0.7\%$ , s.e.) at RH2A $\alpha$  and 97.7% ( $\pm 0.8\%$ , s.e.) at RH2B [calculated in MEGA6; (11)].

Finally, we measured ocular media transmission of the whole eye, cornea, and the lens from wild caught *N. brichardi* (Cape Kachese, Zambia; n = 3) to gain an understanding of the physical light filtering properties of the eye. Briefly, we followed previously established protocols

(10, 13) and measured transmission by cutting a window into the back of the respective ocular media before mounting it above a pinhole. Light from a pulsed xenon light source (Jaz-PX, Ocean Optics Inc.) was directed through the pinhole and the ocular media and collected by a 100  $\mu\text{m}$  optical fiber attached to a Jaz spectrometer (Ocean Optics Inc.). A Spectralon 99% white standard was used as a reflection standard. At least three measurements per media were taken and subsequently averaged. Spectra were thereafter normalized using their maximum transmission and the wavelength at which 50% transmission (T50) was reached was determined within the 300 – 750 nm interval (10, 13). We found the lens to be the limiting light transmission media of the *N. brichardi* eye with a T50 cut-off value of 359 nm (Figure S2).

In the absence of physiological measurements for *N. brichardi* and based on our molecular assessment, we followed (14) and used opsin absorbance spectra [ $\lambda_{\text{max}} = 368$  nm for short wavelength (SWS),  $\lambda_{\text{max}} = 488$  nm for mid wavelength (MWS),  $\lambda_{\text{max}} = 533$  nm for long wavelength (LWS); (15, 16)] from *Metriacalma* (*Maylandia*) *zebra*, a rock-dwelling cichlid species from lake Malawi, to reconstruct the visual sensitivities of *N. brichardi* (Figure S3A). We then incorporated our lens transmission measurements to create a template of the visual system of *N. brichardi* (Figure S3B), which was later on used to model how *N. brichardi* perceives color differences between facial patterns of individuals with dark and pale horizontal stripes.

We took measurements of the natural ambient light under which the fish color patterns have evolved. Measurements were taken at Isanga Bay, Zambia (Lake Tanganyika, Africa) in September 2011 at depths of 3 m and 7 m (Figure S4). Illumination was measured using a USB2000 spectrometer attached to a PALM-SPEC computer running native software (Ocean Optics), enclosed in an underwater housing (Wills Camera Housings, Victoria, Australia). We used a shortened (60cm) 1000  $\mu\text{m}$  UV/visible optical-fiber with a cosine corrector to provide an 180° hemisphere to measure both, down-welling (by pointing the fiber upwards) and side-welling light (pointing the fiber horizontally into the middle or towards the shore of the lake). However, there was no substantial difference in our overall conclusion when using either of the measurements.

We used theoretical fish vision models (17, 18) to quantify the chromatic (hue) and achromatic (luminance or brightness) color contrasts between the facial patterns of *N. brichardi* with dark and pale horizontal stripes. The difference between adjacent and non-adjacent color patches was calculated using the *N. brichardi* visual system and assuming ambient light conditions as measured from their natural habitat (see above).

The chromatic model calculates the color distance ( $\Delta S$ ) within the visual ‘space’ of the fish, where low values of  $\Delta S$  denote similar colors and high values of  $\Delta S$  indicate chromatically different colors. When calculating chromatic distances between color patches luminosity is disregarded within the model, the colors are assumed to be encoded by an opponency mechanism based on the sensitivities of the fish visual system, and color discrimination is thought to be limited by photoreceptor noise determined by the relative proportion of each

photoreceptor type (17, 18). The receptor quantum catch ( $q_i$ ) in the photoreceptor cell of type  $i$  is calculated as:

$$q_i = \int R_i(\lambda)S(\lambda)I(\lambda)d\lambda$$

where  $\lambda$  denotes the wavelength,  $R_i(\lambda)$  the spectral sensitivity of the photoreceptor cell,  $S(\lambda)$  the spectral reflectance of the color patch,  $I(\lambda)$  the illumination spectrum entering the eye and integration is over the range of 350 – 750 nm [equation 1 of (17)]. Illumination was set as measured at a depth of 7 m and coming from above (no difference was found when using spot tests and illumination at 3 m). In the absence of physiological data for our study species we based the relative proportion of cone receptors on morphological studies from other cichlid fishes (Marshall N.J. personal communication) to assume a ratio of 1:2:2 (SWS:MWS:LWS). The weber fraction ( $\omega$ ) was set to assume a 0.05 LWS noise threshold, which is a conservative approach representing approximately half the sensitivity of the human LWS cone system (19).

In addition to the chromatic contrast we also calculated achromatic, brightness contrast as a second property of the visual signal. Long wavelength receptors are thought to be responsible when perceiving differences in brightness [for discussion see (20)] and we therefore, used the differences in the natural logarithm quantum catch ( $Q$ ) of the long wavelength receptor ( $L$ ) to calculate achromatic differences between color patches:

$$\Delta L = \ln(Q_{LpatchX}) - \ln(Q_{LpatchY})$$

We predict that the more  $\Delta S$  and  $\Delta L$  increase above the threshold of 1 JND (just noticeable difference) the more distinguishable colors become from one another, which might be especially important for long-range signals where intervening water and particles start to blur colors (20).

To determine which color elements changed in achromatic or chromatic contrast between territorial and non-territorial fish, pairwise Mann-Whitney U tests were calculated for each comparison. False discovery rate (FDR) was applied to correct for multiple testing. To detect overall differences between adjacent and non-adjacent color patches in achromatic and chromatic contrasts in territorial and non-territorial fish, we ran linear mixed-effects models (LMM) using the R package nlme (21). As we measured several color patches per fish and then used them in different comparisons, all adjacent and all non-adjacent color or brightness contrasts were averaged per individual. ‘Individual’ was then used as random effect. Shapiro tests confirmed normality of the residuals. As achromatic contrast deviated from normality, it was square-root transformed. First, to test whether the facial color pattern is conspicuous to the fish eye, we compared hue and achromatic contrasts between adjacent and non-adjacent color patches of territorial fish (i.e. fish with dark horizontal stripes, which is the state in which the phenotype is normally expressed). In a second step we further analyzed non-territorial fish (i.e. fish with pale horizontal stripes) to investigate how changes in facial stripe intensity affected the phenotype. We ran mixed models with ‘adjacency’, ‘stripe intensity’ and their interaction as fixed effects and ‘individual’ as random effect.

### **Resource contest experiment**

A total of 40 *N. brichardi* (20 males and 20 females) originating from several stock tanks were sexed (by examination of the genital papilla), measured (standard length (SL), taken as the distance between the tip of the snout and the insertion of caudal fin rays) and weighed (body mass (BM), taken after one day fasting). Female SL was  $5.41 \pm 0.55$  cm (mean  $\pm$  standard deviation) and BM was  $4.30 \pm 1.34$  g. Male SL was  $5.62 \pm 0.56$  cm and BM  $4.67 \pm 1.48$  g. To control for daily variation in behaviors, all territorial dyadic combats were conducted between 11AM and 1PM (22). Combats were performed in an aquarium (60  $\times$  30  $\times$  30 cm) divided at the middle of the long side into two equal compartments by a removable opaque plastic barrier. The conditions in both compartments were the same: each had a filter, a heater, ca. 2 cm of sand on the bottom, and a quarter of a terracotta flowerpot (12 cm in diameter, 10 cm long) adjacent to the barrier (Figure S5). Due to the social nature of these fish, small opposite-sexed conspecifics (one per compartment) were introduced in transparent plastic bottles to encourage territory establishment of the focal fish. Dyads of fish were matched by sex, SL (Wilcoxon signed-rank test,  $2V = 233$ ,  $P = 0.27$ ) and BM ( $V = 316$ ,  $P = 0.21$ ). Test fish were caught from their tanks of origin and released into one of the two randomly chosen compartments to establish a territory for three days. Fish were fed commercial flakes or frozen cichlid food twice a day and one hour before starting the trial to control for effects of feeding regime (23). Following this acclimation period the visual barrier was removed, thereby merging the territories of the two fish and the flowerpot shelter into one. This procedure guaranteed that both fish had simultaneous ownership over a territory and that they could not divide the resource after the barrier was removed. Because *N. brichardi* is highly territorial (24, 25), fish started immediately to combat for ownership of the shelter. To avoid disturbances from a possible human observer, the interactions of the fish were videotaped with a Sony HDR XR 550VE camcorder. After each trial ended, fish were moved to separate holding nets in their original tanks.

Intensity of the horizontal facial stripe (pale or dark) was recorded at the beginning and end of experiments. Outcome and behaviors of the 20 min combats were recorded via video analysis (see Table S2 for a detailed ethogram of the species). The winner was that fish from which the loser fled three times without counterstrike or constantly held a submissive posture (25, 26). Alternatively, a fish was declared winner if it owned the flowerpot at the end of the combat (i.e. the most valuable resource of the territory). Behaviors of both fish were recorded and separated into four different categories (Table S2). Diving observations into categories has previously been used when studying *Neolamprologus spp.* behavior (24, 27, 28). A fighting ability index for each fish was calculated by subtracting the total of submissive behaviors from the sum of territorial, display and contact aggressive behaviors [a.k.a. dominance index (5)].

Factors determinant for the outcome of resource contests were identified with linear mixed models with 'body mass' and 'fighting ability' (or dominance index, the difference between aggressive and submissive behaviors) as response and 'outcome', 'sex' and their

interaction as explanatory variables. We fit a generalized linear mixed model (GLMM) with binomial error distribution, logit link function and 'pair' as random effect, to test whether outcome is significantly associated to the intensity of the facial stripe at the beginning or at the end of the contest. For this analysis we used the R package lme4 (29).

#### ***Facial stripe manipulation and standard mirror image stimulation experiment***

Standard mirror image stimulation (MIS) experiments were used to determine if *N. brichardi* are able to recognize and punish unreliable signaling by measuring the response of each individual to its image. MIS is a very powerful method as it provides instantaneous feedback without the confounding factors that might result from using live fish as stimuli (30). Cichlids, including *Neolamprologus spp.*, are known to react aggressively towards their mirror images (3, 26, 31). Additionally, *N. pulcher* has been found to show similar behaviors towards mirror images and actual live conspecifics (Taborsky, unpublished).

The test setup consisted of an aquarium (40 × 25 × 25 cm) with a 2.84 mm-thick glass mirror (25 × 25 cm) placed inside the tank, behind a terracotta flowerpot arch (10 cm in diameter; 3 cm wide) on one of the sidewalls (Figure S6). Using a flowerpot arch instead of a closed flowerpot guaranteed that the fish could see their reflection at all times including inside the shelter, avoiding the generation of impossible reflection angles that could confuse the test fish. At the beginning the arch and the mirror were hidden behind an opaque plastic barrier. After removal of the opaque barrier, the mirror image usually reflects a conspecific territory owner to the test fish (control fish). This setup further addresses the limitations faced when presenting manipulated individuals to dominant, territorial individuals (32). In our setup, the focal fish act as intruders and test the repellent effect of the manipulated signals in individuals of the same size they perceive as territory owners.

A total of 49 *N. brichardi* (25 males and 24 females) originating from several stock tanks were sexed, measured (SL), and weighed (BM) as in resource contest experiment (above). Female SL was  $5.90 \pm 0.74$  cm (mean  $\pm$  standard deviation) and BM was  $5.19 \pm 2.21$  g. Male SL was  $5.92 \pm 0.84$  cm and BM  $5.20 \pm 2.62$  g. Before fish were tested, they were separated from their social group for two days and kept in a pre-test tank (40 × 25 × 25 cm), covered on all four sides to minimize disturbance. This tank contained a flowerpot arch placed adjacent to one wall so fish learned to use this as a shelter and territory instead of a closed flowerpot.

After two days, fish were gently netted out of the pre-test tank, partially anesthetized with of KOI MED Sleep (KOI&BONSAI, 0.5% v/v 2-Phenoxyethanol) and the horizontal facial stripe was randomly manipulated in one of three different ways:

1. *Darkened facial stripe:* The facial stripe was brushed with black waterproof eyeliner (Collection 2000, USA). To control for the covering treatment (below), wound snow and wound spray (KOI MED®) were applied on the head above the facial stripes.

2. *Paled facial stripe*: To control for the darkening treatment, the facial stripe was first painted with the black waterproof eyeliner (Collection 2000, USA) and then covered up with Wound Snow and Wound Spray (KOI MED).

3. *Control sham-manipulation*: Same treatment as 2, applied on the head above the facial stripe as in 1, so the facial stripe was left un-manipulated.

Spectral reflectance measurements show that treatments result in the desired effect of darkening and paling, similar to non-manipulated horizontal stripes. A principal components analysis of spectral reflectance data clearly groups black 'eyeliner' with dark melanistic stripes and groups 'Wound Snow' with pale horizontal stripe, lachrymal stripe and head (Figure S7). A cluster analysis conducted with R package mclust (33) was subsequently used to confirm our visual assessments (Table S5).

After facial stripe manipulation, fish were released into the test tank compartment without the flowerpot arch and mirror, and allowed to recover for 5 min from anesthesia and treatment. To ease acclimation to new surroundings fish were fed a little amount of newly hatched *Artemia nauplii*. After the recovery period, the opaque barrier was removed and the fish could interact with its mirror image. To control for diurnal variation in behavior, all experiments were conducted between 9 AM and 11:30 AM (22). To control for individual effects of aggression (34), fish were tested twice with two different treatments. Order of treatment was randomized. All aggressive (display and contact) and submissive behaviors (Table S4) towards the mirror image were counted during a period of 2.5 min from a video recording (Sony camcorder, see above), starting after the removal of the opaque barrier.

We fit a linear mixed model with 'aggressive bouts' as response and 'treatment', 'sex' and their interaction as explanatory variables. To normalize the residuals, 'aggressive bouts' was square-root transformed. As fish were tested twice, 'individual' was added as a random effect. TukeyHSD post-hoc analysis was performed to test for differences among treatment levels.

## Results

### *Color spectra and theoretical visual modeling experiment*

The paling of the horizontal facial stripe did not result in significant changes to the reflectance of other facial color elements (see Fig. 2 in main text, Figures S7 and S8). These results support our observations that aggressive behavior is signaled only by changes in brightness of the horizontal facial stripe. The changes do not affect the chromatic difference between adjacent and non-adjacent patterns but they do change achromatic contrasts (Figure S9). In particular, we found that high chromatic contrast is achieved by adjacency of color patterns (LMM:  $F_{1,18} = 208.21$ ,  $P < 0.001$ ) and not by the brightness of the horizontal stripe (LMM:  $F_{1,18} = 3.48$ ,  $P = 0.08$ ) or interaction between the two fixed effects (LMM:  $F_{1,18} = 0.05$ ,  $P = 0.82$ ). The model explains 99.31% of the variance in chromacy, 96.5% of which comes from adjacency of the color patterns, while changes in the brightness of the horizontal stripe explain the remaining ~ 3%. On



the other hand, we found that achromatic contrasts are strongly influenced by changes in the brightness of the horizontal stripe (LMM:  $F_{1,18} = 9.11$ ,  $P = 0.007$ ). Consequently, the relationship between adjacent and non-adjacent contrasts (LMM:  $F_{1,18} = 5.07$ ,  $P = 0.037$ ) as well as the interaction between the two (LMM:  $F_{1,18} = 6.78$ ,  $P = 0.018$ ) becomes significant. This model explains 95.9% of the achromatic contrast variance, 68.53% of which is explained by changes in brightness of the horizontal stripe, 22.34% by signal design and the remainder 5.02% by their interaction.

### ***Resource contest experiment***

*N. brichardi* is highly territorial and engaged immediately in ownership combat for the flower pot shelter after the opaque divider was removed. Fish performed a variety of behaviors, showing clear differences between winners and losers of the territorial bouts (Figure S10). The differences between winners and losers can be best seen when analyzing fish in dyads. Previously we have shown that combat winners display dark, conspicuous horizontal facial stripes, whereas losers signal their inferior fighting ability by paling their stripe (Figs. 2 and 3 in the main text). Here we show that winning is associated with higher fighting abilities, while the effect of body size for contest outcome is less pronounced (Figure S11; see main text for statistics). Different amounts of aggressive and submissive behaviors are performed by individuals of different rank and size even in social groups with stable hierarchies (5).

### ***Facial stripe manipulation and standard mirror image stimulation experiment***

We tested for contest-dependent costs of signaling by simulating an invasion by cheaters. We found that cheaters, falsely signaling strength (bluffers) or weakness (Trojans) incur an increased cost relative to honest signalers (controls). This is an important aspect of signal reliability because it is the marginal costs of cheating that should make signaling prohibitive for cheaters (35). Physiological color changes have previously been implicated in signaling aggressive intent in a number of taxa, in particular fish (36–39). Increased levels of aggression toward the signal were reported in some of these studies, suggesting that reliability of these signals could also be maintained by receiver retaliation costs. We show that individuals consistently direct more aggression toward unreliable than reliable signalers, and more to bluffers than to Trojans (Figure S12). Therefore, consistent with our dyadic combat results that showed stripe intensity at the beginning of a combat does not determine outcome (GLMM with binomial error distribution:  $\chi^2_1 = 0.01$ ,  $P = 0.93$ ), brightness of the stripe alone does not have an effect if its not backed-up by the appropriate postural and aggressive behaviors of individuals.

### ***Aggressive territorial display of *N. brichardi* and signal classification based on honesty***

The complex facial color pattern of *N. brichardi* is an important component of its overall aggressive behavior. The facial color pattern can be thought of as the fish's equivalent of the colorful masks used by human wrestlers in Mexican free wrestling, Lucha Libre. *N. brichardi*'s mask is located prominently in the head region, where it can best be seen by an opponent during agonistic interactions (Figure S10). We found that information about aggressiveness is encoded by changes in brightness of the horizontal stripe, while the vertical stripe, white, yellow and blue elements of the facial color pattern change little during aggressive displays (Fig. 3A, Figure S8). Rather, these bright color elements act as amplifiers to enhance conspicuousness in the aquatic ambient light in which the signal has evolved (Fig. 2, Figure S9). This guarantees signal efficacy, but what guarantees signal honesty? Aggressive intention is not a quality that can be easily handicapped, so quality handicaps do not likely serve as mechanisms guaranteeing reliability of such signals about the sender (32). By contrast, receivers can directly assess reliability of signals of aggressive intent with relative ease and in real time. Accordingly, we found strong receiver retaliation costs associated with unreliable signaling (Fig. 3B), which indicates the color pattern can be classified as a conflict conventional signal of fighting ability with socially imposed costs.

This visual color signal is used in conjunction with non-contact aggressive behaviors, such as puffed throat and aggressive posture, which are pre-injury inflicting behaviors. These are likely perceived as intention movements, used as cues to enforce information content of the signal and favor efficient communication. At the same time subordinate animals behave with opposite, antithetical, signals such as submissive posture. These behavioral and postural aggressive signals are likely to be reliable due to differential costs of production or bearing. In the case of puffed throat, only fish in good condition can maintain the opercular display for longer periods, making it a quality handicap signal with a cost directly associated to the key quality feature. Such behavior interferes with respiration and restricts oxygen uptake by the gills, which limits energy available to fight and cannot be faked. Reliability of the opercular display is likely also maintained by other mechanisms. Similar to the lateral display with extended fins during aggressive display, puffed throat is probably a body size indicator. Body size is important for winning a contest (Figure S11). Extended fins and gill covers are apparent-size enhancing structures that amplify signals encoding body size information, and convert body size cues into physically constrained index signals. Both fins and gill covers have contrasting outlining pigmentation, so that signals are easier to detect by receivers. Overall, data suggest that aggressive territorial displays in cichlids are kept reliable by several mechanisms.

## References and Notes

1. M. Wong, S. Balshine, *Biol. Rev. Camb. Philos. Soc.* **86**, 511–530 (2011).
2. D. Brawand et al., *Nature*. **513**, 375–381 (2014).
3. S. Balshine-Earn, A. Lotem, *Behaviour*. **135**, 369–386 (1998).
4. N. Duftner et al., *Mol. Phylogenet. Evol.* **45**, 706–715 (2007).
5. N. Aubin-Horth, J. K. Desjardins, Y. M. Martei, S. Balshine, H. A. Hofmann, *Mol. Ecol.* **16**, 1349–1358 (2007).
6. K. A. Stiver et al., *Mol. Ecol.* **16**, 2974–2984 (2007).
7. M. Taborsky, A. Grantner, *Anim. Behav.* **56**, 1375–1382 (1998).
8. N. J. Marshall, in *Animal signals: signalling and signal design in animal communication*, Y. Espmark, T. Amundsen, G. Rosenqvist, Eds. (Tapir Academic Press, Trondheim, Norway, 2000), pp. 83–120.
9. J. E. Schulte, C. S. O'Brien, M. A. Conte, K. E. O'Quin, K. L. Carleton, *Mol. Biol. Evol.* **31**, 2297–308 (2014).
10. C. M. Hofmann, K. E. O'Quin, N. Justin Marshall, K. L. Carleton, *Vision Res.* **50**, 357–63 (2010).
11. K. Tamura, G. Stecher, D. Peterson, A. Filipowski, S. Kumar, *Mol. Biol. Evol.* **30**, 2725–2729 (2013).
12. C. M. Hofmann et al., *J. Mol. Evol.* **75**, 79–91 (2012).
13. U. E. Siebeck, N. J. Marshall, *Vision Res.* **41**, 133–149 (2001).
14. B. E. Dalton, T. W. Cronin, N. J. Marshall, K. L. Carleton, *J. Exp. Biol.* **213**, 2243–2255 (2010).
15. J. S. Levine, E. F. MacNichol, *Sens. Processes*. **3**, 95–131 (1979).
16. K. L. Carleton, F. I. Ha, T. D. Kocher, *Vision Res.* **40**, 879–890 (2000).
17. M. Vorobyev, D. Osorio, *Proc. Biol. Sci.* **265**, 351–8 (1998).
18. M. Vorobyev, R. Brandt, D. Peitsch, S. B. Laughlin, R. Menzel, *Vision Res.* **41**, 639–53 (2001).
19. G. Wyszecki, Stiles. W. S., *Color science — concepts and methods, quantitative data and formulae* (Wiley, New York, ed. 2nd, 2000).
20. N. J. Marshall, K. Jennings, W. N. McFarland, E. R. Loew, G. S. Losey, *Copeia*. **2003**, 467–480 (2003).
21. P. J, B. D, D. S, S. D, *nlme: Linear and Nonlinear Mixed Effects Models* (2012).
22. R. F. Oliveira, M. Lopes, L. A. Carneiro, A. V. M. Canário, *Nature*. **409**, 2001 (2001).
23. H. S. Fisher, G. G. Rosenthal, *Behav. Ecol.* **17**, 979–981 (2006).
24. M. D. Taves, J. K. Desjardins, S. Mishra, S. Balshine, *Gen. Comp. Endocrinol.* **161**, 202–207 (2009).

25. A. R. Reddon et al., *Anim. Behav.* **82**, 93–99 (2011).
26. P. D. Dijkstra, S. M. Schaafsma, H. A. Hofmann, T. G. G. Groothuis, *Physiol. Behav.* **105**, 489–92 (2012).
27. S. Balshine et al., *Behav. Ecol. Sociobiol.* **50**, 134–140 (2001).
28. N. M. Sopinka et al., *J. Fish Biol.* **75**, 1–16 (2009).
29. D. Bates, M. Maechler, B. Bolker, S. Walker, lme4: Linear mixed-effects models using Eigen and S4 (2014), (available at <http://cran.r-project.org/package=lme4>).
30. W. J. Rowland, *Environ. Biol. Fishes.* **56**, 285–305 (1999).
31. A. R. Reddon, S. Balshine, *Behav. Processes.* **85**, 68–71 (2010).
32. J. W. Bradbury, S. L. Vehrencamp, *Principles of Animal Communication*, Second Edition (Sinauer Associates, Inc.; 2 edition, 2011).
33. C. Fraley, A. Raftery, L. Scrucca, mclust: Normal Mixture Modeling for Model-Based Clustering, Classification, and Density Estimation (2014).
34. A. M. Bell, *Proc. R. Soc. B Biol. Sci.* **274**, 755–761 (2007).
35. W. A. Searcy, S. Nowicki, *The evolution of animal communication: reliability and deception in signaling systems* (Princeton University Press, Princeton, 2005).
36. L. E. Muske, R. D. Fernald, *J. Comp. Physiol. A.* **160**, 89–97 (1987).
37. W. Korzan, T. Summers, C. Summers, *Gen. Comp. Endocrinol.* **128**, 153–161 (2002).
38. J. A. Moretz, M. R. Morris, *Proc. R. Soc. B Biol. Sci.* **270**, 2271–7 (2003).
39. R. R. Rodrigues, L. N. Carvalho, J. Zuanon, K. Del-claro, *Neotrop. Ichthyol.* **7**, 641–646 (2009).

**Table S1.** Alignment of short wavelength UV-sensitive opsin SWS1 [(modified after (12)).

Figure 1 displays a multiple sequence alignment of the SWS1 protein across various species, including *Maylandia zebra*, *Neolamprologus brichardi*, and *Rhamphocharax* (RH1, RH2, SW52, SW51 or LWS). The alignment highlights conserved regions and key sites (1-5) that are critical for retinal binding and tuning. The sequences are shown in a color-coded format, with key sites marked by colored boxes: green for known tuning site RH1, blue for known tuning site RH2, red for known tuning site SW52, pink for known tuning site SW51 or LWS, and yellow for known tuning site SW51 or LWS. A legend at the bottom defines the colors and the key sites. The alignment also includes a retinal binding pocket site in bovine rhodopsin (grey box) and a transmembrane region (white box).

Figure 1 displays the sequence alignment and conservation of bovine rhodopsin (RH1) and cone opsins (RH2, SWS2, SWS1 or LWS) across different species. The figure is organized into several rows, each representing a different species and its corresponding opsin type. The sequences are aligned, and key sites are highlighted with colored boxes (green, blue, pink, red) and numbered (1-5). A legend at the bottom explains the color coding and site numbers.

**Species and Opsin Types:**

- Maylandia zebra JF262089.1 RH2B** (RH1, RH2, SWS2, SWS1 or LWS)
- Neolamprologus brichardi FR4 eye RH2B comp45\_c0\_seq1** (RH1, RH2, SWS2, SWS1 or LWS)
- Maylandia zebra JF262089.1 RH2B** (RH1, RH2, SWS2, SWS1 or LWS)
- Neolamprologus brichardi FR4 eye RH2B comp45\_c0\_seq1** (RH1, RH2, SWS2, SWS1 or LWS)
- Maylandia zebra JF262089.1 RH2B** (RH1, RH2, SWS2, SWS1 or LWS)
- Neolamprologus brichardi FR4 eye RH2B comp45\_c0\_seq1** (RH1, RH2, SWS2, SWS1 or LWS)
- Maylandia zebra JF262089.1 RH2B** (RH1, RH2, SWS2, SWS1 or LWS)
- Neolamprologus brichardi FR4 eye RH2B comp45\_c0\_seq1** (RH1, RH2, SWS2, SWS1 or LWS)
- Maylandia zebra JF262089.1 RH2B** (RH1, RH2, SWS2, SWS1 or LWS)
- Neolamprologus brichardi FR4 eye RH2B comp45\_c0\_seq1** (RH1, RH2, SWS2, SWS1 or LWS)
- Maylandia zebra JF262089.1 RH2B** (RH1, RH2, SWS2, SWS1 or LWS)
- Neolamprologus brichardi FR4 eye RH2B comp45\_c0\_seq1** (RH1, RH2, SWS2, SWS1 or LWS)
- Maylandia zebra JF262089.1 RH2B** (RH1, RH2, SWS2, SWS1 or LWS)
- Neolamprologus brichardi FR4 eye RH2B comp45\_c0\_seq1** (RH1, RH2, SWS2, SWS1 or LWS)
- Maylandia zebra JF262089.1 RH2B** (RH1, RH2, SWS2, SWS1 or LWS)
- Neolamprologus brichardi FR4 eye RH2B comp45\_c0\_seq1** (RH1, RH2, SWS2, SWS1 or LWS)
- Maylandia zebra JF262089.1 RH2B** (RH1, RH2, SWS2, SWS1 or LWS)
- Neolamprologus brichardi FR4 eye RH2B comp45\_c0\_seq1** (RH1, RH2, SWS2, SWS1 or LWS)
- Maylandia zebra JF262089.1 RH2B** (RH1, RH2, SWS2, SWS1 or LWS)
- Neolamprologus brichardi FR4 eye RH2B comp45\_c0\_seq1** (RH1, RH2, SWS2, SWS1 or LWS)

**Key Sites:**

- Site 1:** Known tuning site, RH1
- Site 2:** Known tuning site, RH2
- Site 3:** Known tuning site, SWS2
- Site 4:** Known tuning site, SWS1 or LWS
- Site 5:** Known tuning site, SWS1 or LWS

**Legend:**

- Green box:** Known tuning site, RH1
- Blue box:** Known tuning site, RH2
- Pink box:** Known tuning site, SWS2
- Red box:** Known tuning site, SWS1 or LWS
- Numbered box (1-5):** Variable AA properties in site known to tune some other opsin
- Grey box:** Retinal binding pocket site in bovine rhodopsin
- White box:** Transmembrane region

**Table S3.** Alignment of long wavelength green-sensitive opsin RH2A [modified after (12)].

**RH2A**

RH1  
RH2  
SWS2  
SWS1 or LWS  
Key sites

Maylandia zebra JF262089.1 RH2Aalpha  
Neolamprologus brichardi fR4 eye RH2Aalpha comp39\_c0\_seq1

MAWDGGIEPNGTGEKKNFYIPMSNRTGIVRSPPFEYTYQYYMVDPIIYKVLAFAFMFFLICTGT  
MAWDGGIEPNGTGEKKNFYIPMSNRTGIVRSPPYEYNQYYMVDPIIYKVLAFAFMFFLICTGT

**RH1**  
**RH2**  
**SWS2**  
**SWS1 or LWS**  
**Key sites**

Maylandia zebra JF262089.1 RH2Aalpha  
Neolamprologus brichardi fR4 eye RH2Aalpha comp39\_c0\_seq1

PINGLTLFTVAQNKKLRQLPNLYILVNLAVAGLMCCFCGFTITITSALNNGYFILGPTTFCAI  
PINGLTLFTVAQNKKLRQLPNLYILVNLAVAGLMCCFCGFTITITSALNNGYFILGPTTFCAI

**RH1**  
**RH2**  
**SWS2**  
**SWS1 or LWS**  
**Key sites**

Maylandia zebra JF262089.1 RH2Aalpha  
Neolamprologus brichardi fR4 eye RH2Aalpha comp39\_c0\_seq1

EFGFMATLGGEVALWSLVVLAVERYIVVCCKPMGSFKFSGAHAGAGVFFTWVMAMACAAPPL  
EFGFMATLGGEVALWSLVVLAVERYIVVCCKPMGSFKFSGAHAGAGVFFTWVMAMACAAPPL

**RH1**  
**RH2**  
**SWS2**  
**SWS1 or LWS**  
**Key sites**

Maylandia zebra JF262089.1 RH2Aalpha  
Neolamprologus brichardi fR4 eye RH2Aalpha comp39\_c0\_seq1

F G W S R Y I P E G M Q C S C G P D Y Y T L A P G F N N E S Y V I I M F V V H F F V P V F V I F F T Y G S L V M T V K A  
F G W S R Y I P E G M Q C S C G P D Y Y T L A P G F N N E S Y V I I M F I V H F I P V F V I F F T Y G S L V L T V K A

**RH1**  
**RH2**  
**SWS2**  
**SWS1 or LWS**  
**Key sites**

Maylandia zebra JF262089.1 RH2Aalpha  
Neolamprologus brichardi fR4 eye RH2Aalpha comp39\_c0\_seq1

A A A Q Q Q D S A S T Q K A E K E V T R M C V L M V M G F L V A W T P Y A S F A G W I F M N K G A S F T A L T A A L P A  
A A A Q Q Q D S A S T Q K A E K E V T R M C V L M V L G F L V A W T P Y A S F A G W I F M N K G A S F T A L T A A L P A

**RH1**  
**RH2**  
**SWS2**  
**SWS1 or LWS**  
**Key sites**

Maylandia zebra JF262089.1 RH2Aalpha  
Neolamprologus brichardi fR4 eye RH2Aalpha comp39\_c0\_seq1

F F A K S S A L Y N P V I Y V L M N N K Q F R N C M L S T I G M G G M V E D E T S V S T S K T E V S S V S  
F F A K S S A L Y N P V I Y V L M N N K Q F R N C M L T T I G M G G M V E D E T S V S T S K T E V S S V S

**RH1**  
**RH2**  
**SWS2**  
**SWS1 or LWS**  
**Key sites**

Maylandia zebra JF262089.1 RH2Aalpha  
Neolamprologus brichardi fR4 eye RH2Aalpha comp39\_c0\_seq1

F F A K S S A L Y N P V I Y V L M N N K Q F R N C M L S T I G M G G M V E D E T S V S T S K T E V S S V S  
F F A K S S A L Y N P V I Y V L M N N K Q F R N C M L T T I G M G G M V E D E T S V S T S K T E V S S V S

known tuning site, RH1  
known tuning site, RH2  
known tuning site, SWS2  
known tuning site, LWS  
known tuning site, SWS1

variable AA properties in transmembrane region  
variable AA properties in retinal binding pocket as defined by bovine RH  
variable AA properties in site known to tune some other opsin  
variable AA properties in site known to tune this opsin

retinal binding pocket site in bovine rhodopsin  
transmembrane region

Table S4. Ethogram of behavioral repertoire of *N. brichardi* [modified after (24, 28)]

Category	Behavior	Description
Contact aggression	Bite	Focal fish bites another fish
	Chase	Focal fish follows another fish
	Displace	Focal fish swim towards another fish, forcing it to move
	Mouth-lock*	Two fish lock jaws and push against each other
	Ram	Focal fish hits another fish with its head, but jaws remain closed
Display aggression	Aggressive posture	Focal fish lowers its head towards another fish and shows the side of its body with spread fins
	Head shake	Fish tosses its head from left to right
	Puffed throat	Fish opens operculum and lower jaw cavity
Submission	Bitten	Focal fish gets bitten by another fish
	Flee	Focal fish swim away from another fish
	Submissive posture	The focal fish has a (nearly) vertical position, with the head directing upwards
	Submissive display	The fish is positioned with a submissive posture accompanied by a quivering caudal fin
Territoriality	Body digging	Focal fish quivers its body on the substrate and moves sand
	Digging	Focal fish takes sand in its mouth, sometimes swims to a different area and spits it out
	Lookout	Focal fish observes another fish from its shelter
	Hover	Focal fish defends brood chamber, inhibit other fish from entering
	Cleaning	Focal fish removes algae from shelter by nibbling on them

\* both fish get the score



**Table S5.** Cluster analysis of principal components of spectral data. Five clusters were identified. ‘Eyeliner’ clusters together with black stripes (cluster 2), while ‘Wound Snow’ clusters with pale horizontal stripe, lachrymal stripe and head (cluster 1). D: dark. P: pale.

Color patch	Clusters				
	1	2	3	4	5
Eyeliner	0	1	0	0	0
Wound Snow	1	0	0	0	0
Vertical facial stripe (D)	0	10	0	0	0
Vertical facial stripe (P)	0	10	0	0	0
Horizontal facial stripe (D)	1	9	0	0	0
Horizontal facial stripe (P)	10	0	0	0	0
Lachrymal stripe (D)	8	2	0	0	0
Lachrymal stripe (P)	10	0	0	0	0
Head (D)	9	1	0	0	0
Head (P)	10	0	0	0	0
Blue (D)	0	0	10	0	0
Blue (P)	0	0	10	0	0
Branchiostegal (D)	0	0	0	0	10
Branchiostegal (P)	0	0	1	0	9
Yellow (D)	0	0	0	9	1
Yellow (P)	0	0	0	9	1

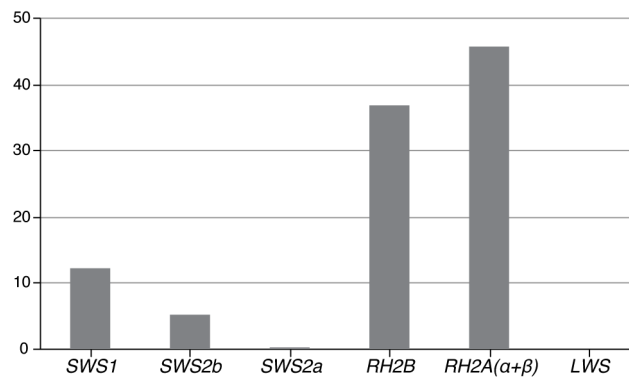


Figure S1. Relative opsin expression of *N. brichardi* determined by RNAseq. Modified from (9).

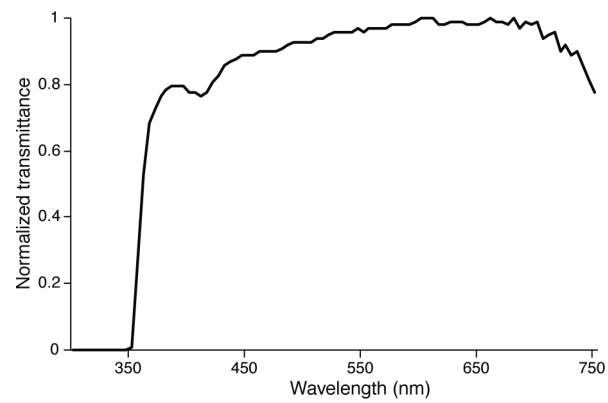


Figure S2. Normalized transmittance of *N. brichardi* crystalline lens.

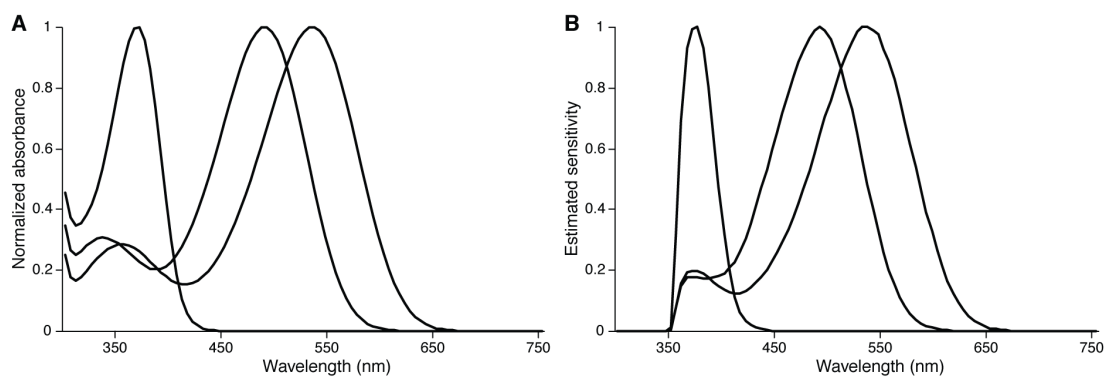
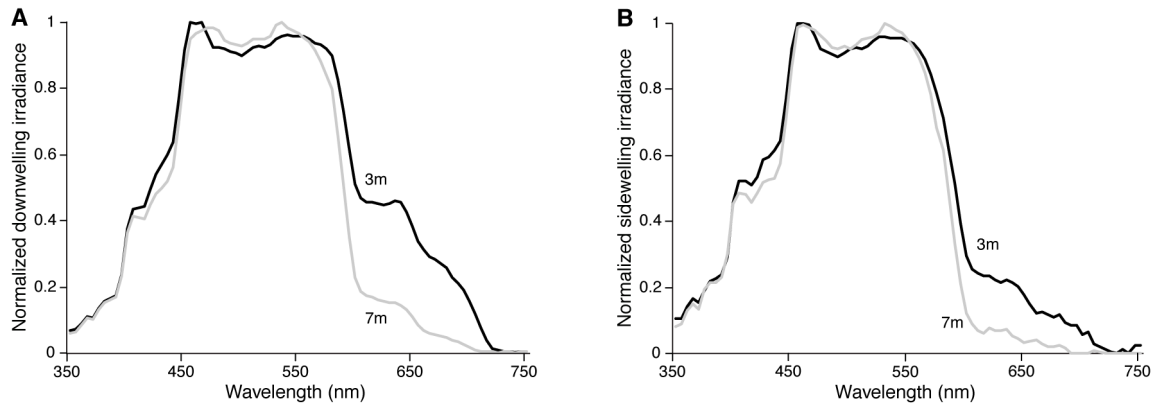
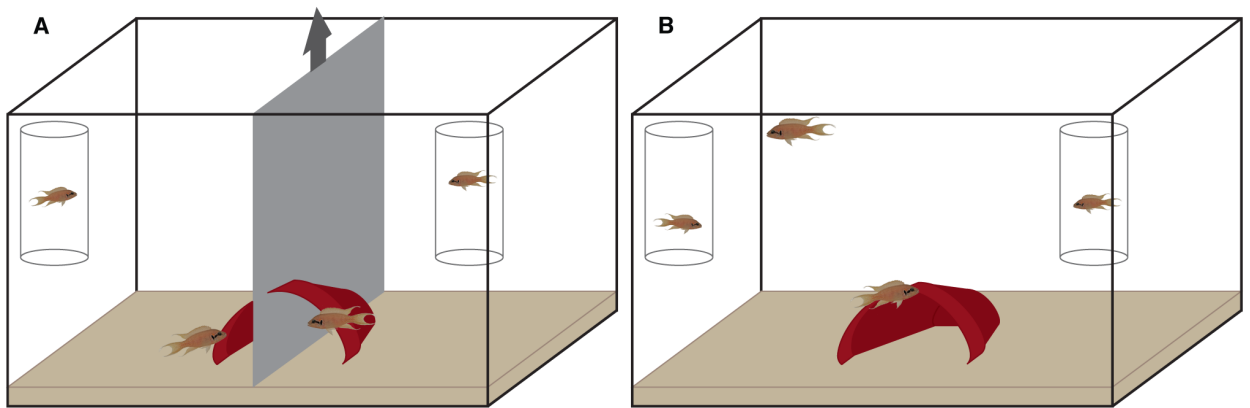


Figure S3. Visual system of *N. brichardi*. **(A)** Normalized absorbance of SWS1, RH2B and RH2A. **(B)** Estimated visual sensitivities incorporating crystalline filtering media.



**Figure S4.** Light environment of *N. brichardi* habitat. **(A)** Normalized down-welling and **(B)** side-welling irradiance at two depths. Increasing water depth reduces available longer light wavelengths.



**Figure S5.** Schematic representation of territory contest experimental setup. **(A)** Fish are visually separated and allowed to establish their territory in the terracotta flowerpot for three days until divider is removed and territories/shelters were merged. **(B)** Individuals are allowed to fight over the non-divisible territorial resource for 20 minutes.

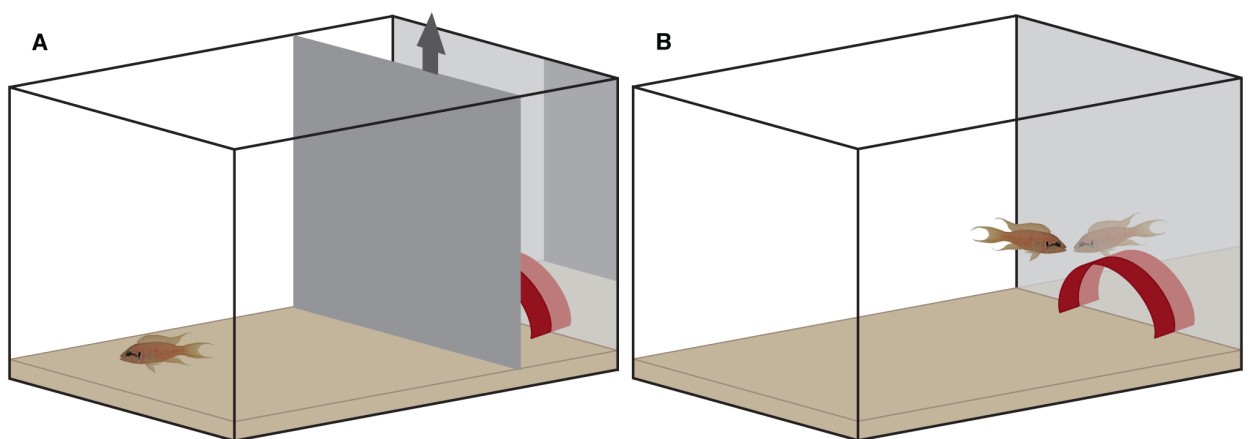


**Figure S6.** Schematic representation of standard mirror image stimulation setup. **(A)** Fish with manipulated signals are introduced to a bare side of the tank with no shelters. **(B)** After opaque divider is removed, individuals can see a shelter and a territorial fish next to it (i.e. their mirror image) and are allowed to interact with it.

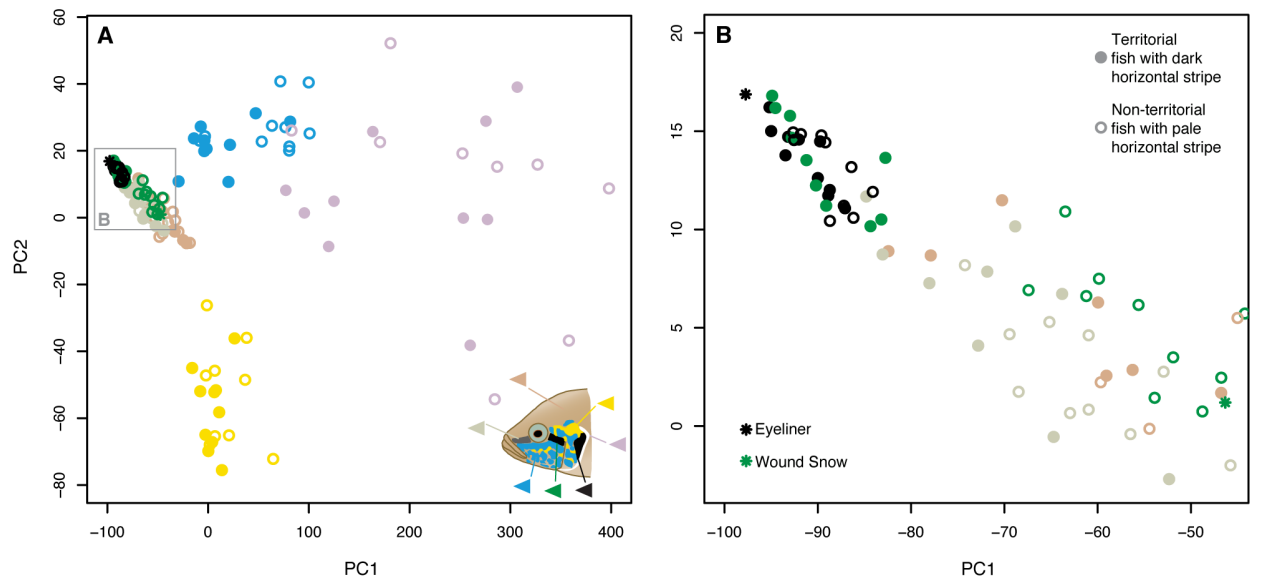


**Figure S7.** Principal components analysis of spectral data. **(A)** PC1 and PC2 explain 96.5% of the variance (90.8% and 5.7%, respectively) and clearly separates different colors. **(B)** Zoom in at the dark/black area of the plot shows that 'Eyeliner' is similar to dark stripes, while 'Wound Snow' is similar to pale stripes and head.

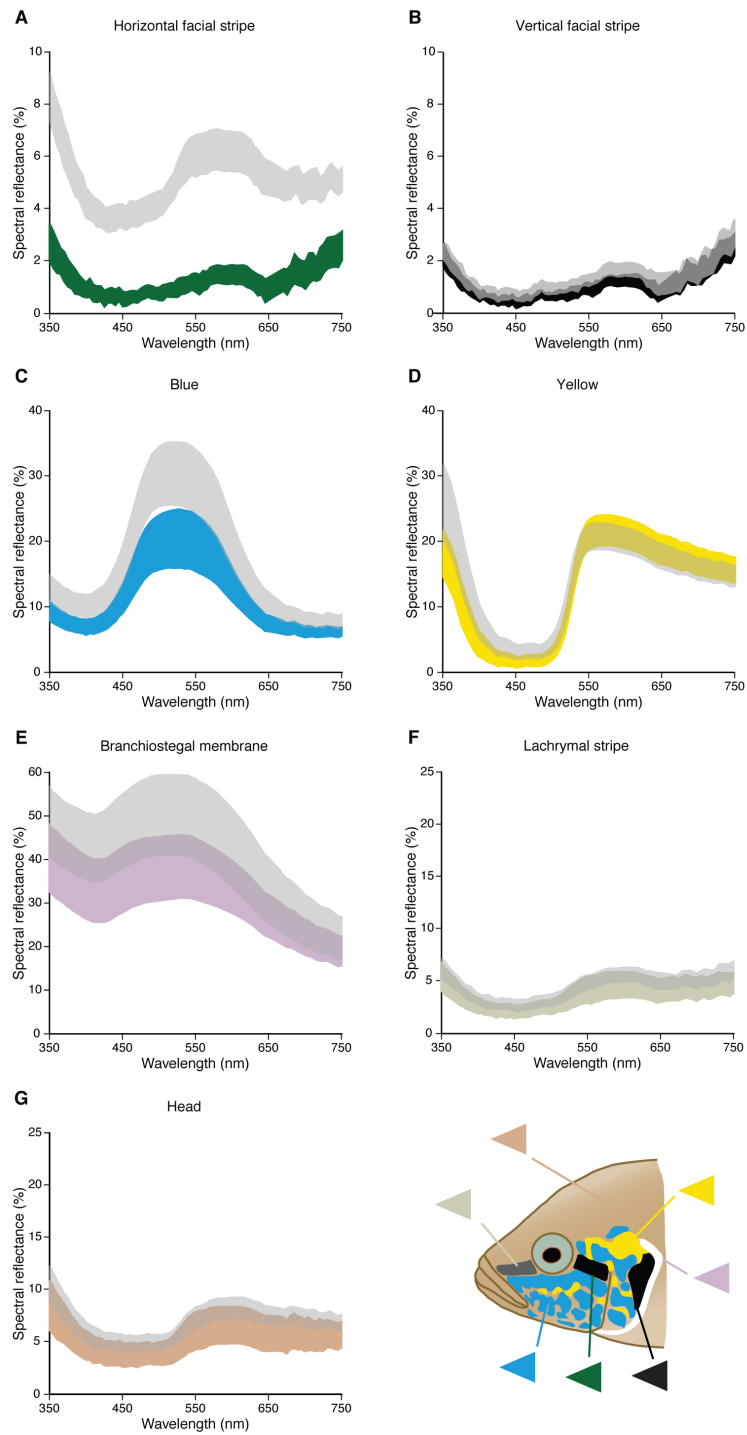


**Figure S8.** 95% confidence intervals of spectral data. Only horizontal facial stripe spectra significantly differ between dark and pale fish (**A**), while spectral curves of other colors overlap to various degrees (**B – G**). Colored curves refer to color pattern elements in individuals with dark horizontal stripe, while light grey curves refer to equivalent elements in individuals with pale horizontal stripe.

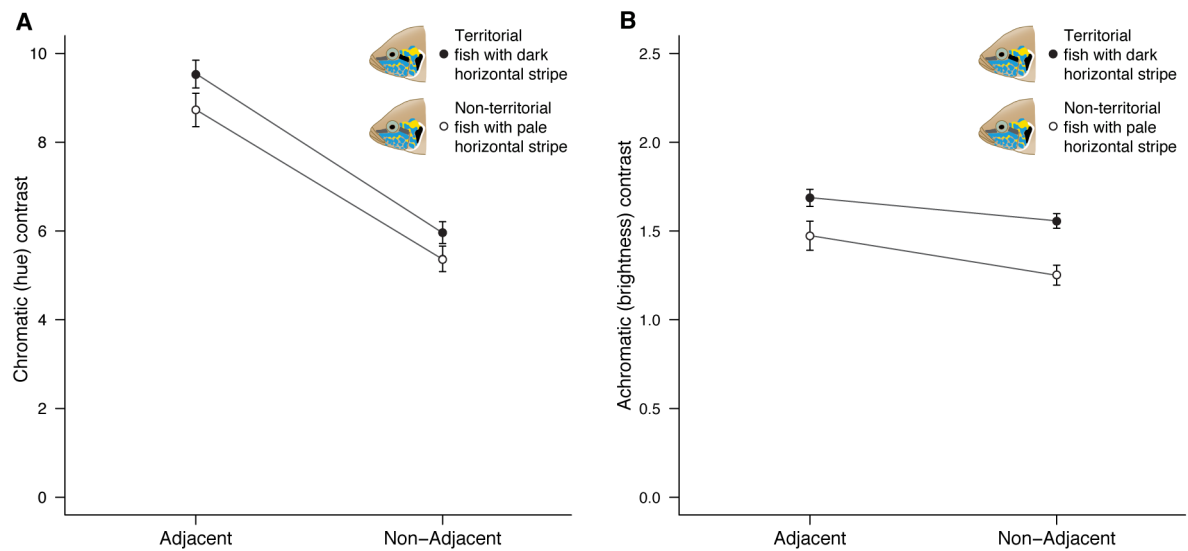


**Figure S9.** Color contrasts of adjacent and non-adjacent elements in fish with dark or pale horizontal facial stripes. **(A)** Chromatic contrast is achieved by adjacency of color elements and not influenced by brightness of horizontal stripe. **(B)** Achromatic contrast is achieved by paling of the horizontal stripe and its differential influence on adjacent and non-adjacent color elements.

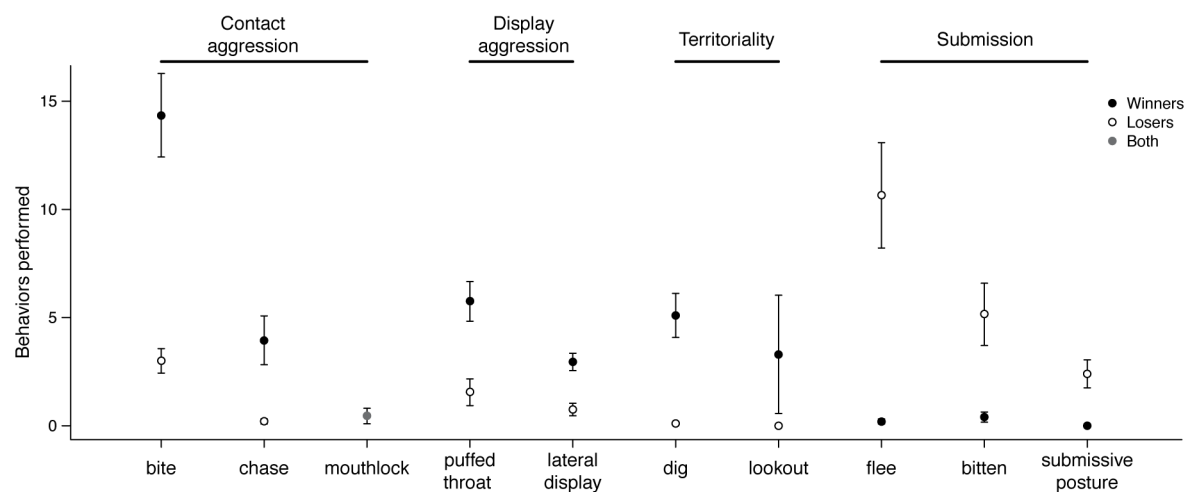


**Figure S10.** Behaviors performed by winners and losers during territory combat. Winners did most of the aggressive behaviors, while losers did most of the submissive behaviors.

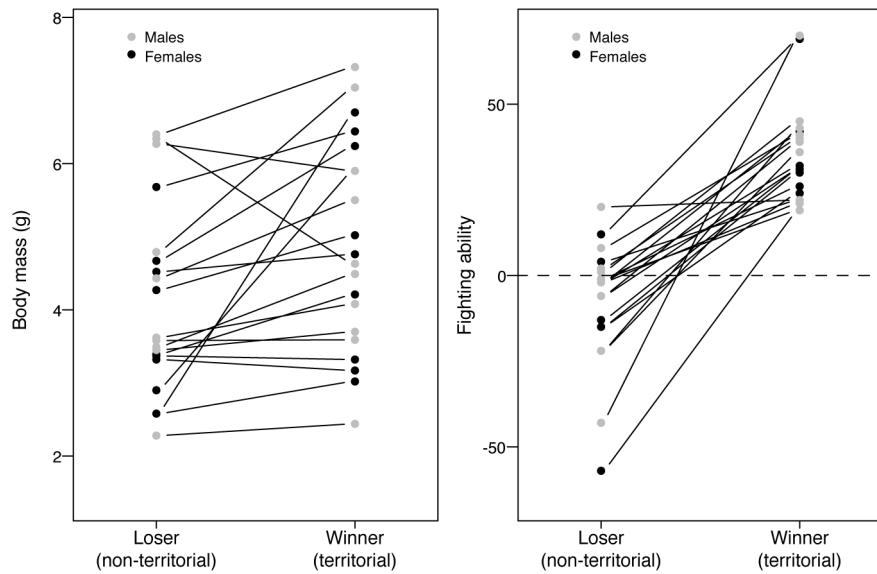


Figure S11. Reaction norms of winner-loser body mass and fighting ability during territorial combat. Winners are larger and fight more aggressively compared to losers.

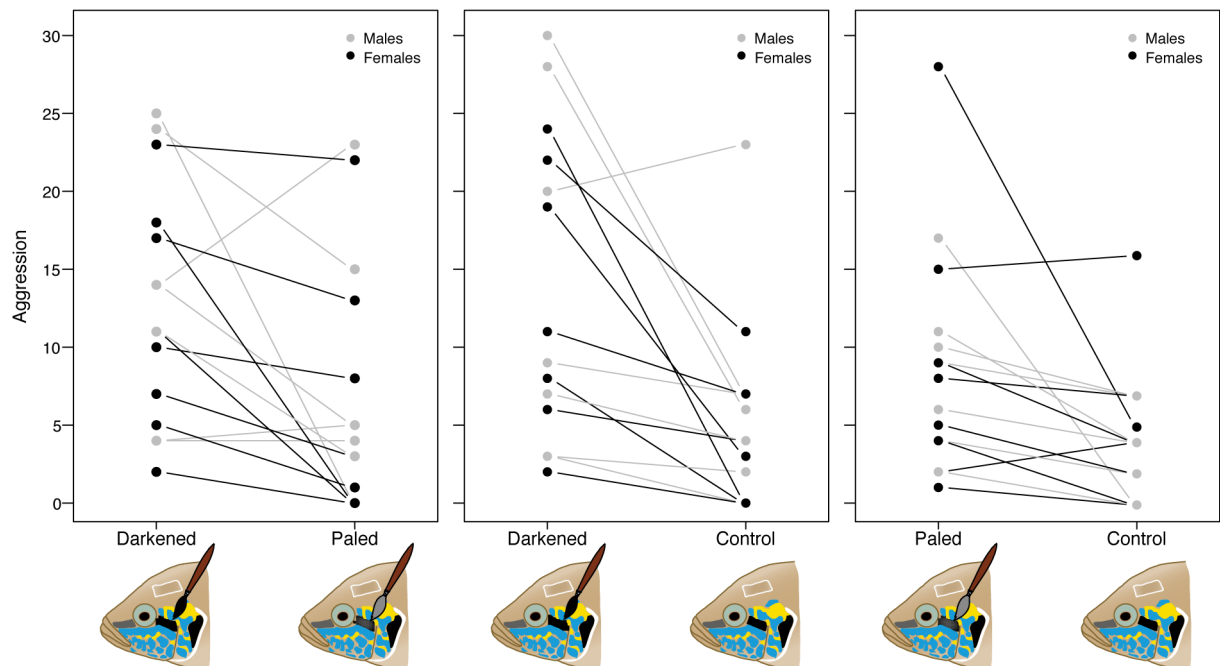


Figure S12. Reaction norms of amount of aggression incurred during reliable and unreliable signaling. Retaliation costs are highest for bluffers, followed by Trojans, and then controls (i.e. reliable signalers), which were the ones that received the lowest amount of aggression.

# Discussion and Future Perspectives

Aquatic animals are among the most colourful and beautifully patterned organisms on the planet; however, understanding the function and evolution of such coloured visual signals is unclear. My dissertation has furthered our knowledge on the selective pressures shaping colourful signals in aquatic media by providing a number of important insights into signal design and function in mimic (Chapters 1 – 3), aposematic (Chapters 4 & 5), and territorial species (Chapter 6).

In Chapter 1, I report a novel way to mediate frequency-dependent constraints of deceptive signals in animals. That is to say, mimics can avoid being found out by plastically changing their phenotypes to impersonate various models and thus deceive perceivers with multiple guises ([1]; Thesis Chapter 1). I then show that the function of colourful signals can change with ontogeny, and that these changes may interrelate with other morphological and/or physiological adaptations through development such as that of the visual system ([2]; Thesis Chapter 2). Indeed, although animal colouration may also function for thermoregulation [3], when used to transfer information, the evolution of animal signals will necessarily depend on the way the intended receiver perceives them [4, 5]. Hence, an in-depth knowledge of the visual system of potential receivers (mates, competitors or predators) is needed when studying the design and evolution of visual signals [4, 6]. In Chapter 3, I report the findings from what is to date the most thorough investigation of the evolutionary history of the SWS2 opsin gene family, responsible for violet-blue vision in fishes ([7]; Thesis Chapter 3). Despite the fact that opsin genes are amongst the best-studied and functionally best-characterised vertebrate gene families [8, 9], this study shows that when explored over a broad phylogenetic framework, the evolutionary history of opsins may be more complex than previously assumed, ultimately calling for a re-evaluation of previous work ([7]; Thesis Chapter 3).

Although the importance of integrative approaches to study evolutionary questions is consistently being emphasized, this has not truly been feasible until very recently, when advances in sequencing, functional genetic essays and microscopy techniques have reached a level where researchers could expand to non-model systems to study the processes that shape organismal diversity from ecology to development to evolution (*eco-evo-devo*) *in-situ*. The investigation of the dottyback mimicry system represents an attempt at this, and by combining behavioural, molecular, histological, and neurophysiological approaches I was able to elucidate the triggers for, and consequences of colour changes and polymorphism in this species. However, old and new questions provide the substrate for future studies.

For example, the molecular base for colour changes and mimicry in dottybacks and for that matter, vertebrates in general remains to be investigated. By generating a reference transcriptome and sequencing of the dottyback genome, the foundations to study the molecular characteristics of colourful traits and plastic changes thereof in the dottyback have been laid. In



a further step, comparative transcriptomics throughout dottyback development (from larval to yellow and brown stages as adults) should be used to generate a list of candidate genes for colour change. Since colour changes in adult dottybacks occur as a relative change in the proportion of chromatophore types within the skin of fish ([1]; Thesis Chapter 1), the molecular bases for colour changes in this instance are likely to be of gene regulatory origin. Therefore, transcriptomic approaches should be combined with quantitative genetic approaches to affirm the appropriateness of candidate genes when being mapped to genomic regions of interest. This could be done using different approaches. For example, advantage could be taken of an orange dottyback morph that reportedly is restricted to Papua New Guinean populations [10]. First, the ecology of colour changes in orange morphs should be investigated ([1]; Thesis Chapter 1). If it would turn out that they are unable to change colour, then genome wide association mappings (see e.g. [11]) and the mapping of quantitative trait loci (QTL's) from F2 crosses between yellow/brown and orange morphs in combination with genome wide single nucleotide polymorphism (SNPs) screens (see e.g. [12]), could be used to narrow down the genomic region of interest. Laboratory based trans-genesis essays and knock-in, knock-out experiments could then serve to test the functionality of identified genes, promoters etc. [13]. Finally, the origin and novelty of a 'colour change' trait could be investigated by mapping the trait onto a detailed phylogeny of the Pseudochromidae complex (~ 150 species in 24 genera; <http://fishbase.org>). Similar approaches could also be used to investigate the molecular origin of the 'hybrid' chromatophore cells in dottybacks (see [2]; Thesis Chapter 2), and functional approaches especially, would be useful to test the significance of the newly described opsin genes in fishes (see [2, 7]; Thesis Chapters 2 & 3).

Chapters four and five focus on the evolution of aposematic signals in nudibranchs. Called the 'butterflies' of the ocean, nudibranchs have lost their protective shell and instead evolved a variety of signalling strategies ranging from being almost indistinguishable from their food source (crypsis) to being brightly coloured to advertise unpalatability (aposematism) and avoid potential predators ([14, 15]; Thesis chapters 4 & 5). Nudibranchs are ideal to study the evolution of colourful signals, because as a consequence of having bad eyesight, colourful displays serve purely to communicate to visually hunting predators. During my dissertation I was involved in a number of projects investigating the correlation between toxic properties and conspicuous signals in this group. First results from the work show that in nudibranchs levels of toxicity and conspicuousness co-evolve ([15]; Thesis Chapter 4), but that this co-evolution does not correlate with the body size of animals ([14] Thesis Chapter 5). These two studies now serve as a springboard to investigate further questions within the system as well as aposematic theory in general. For example, it is still unclear how aposematic colours evolve in the first place: are animals to begin with conspicuous and/or unpalatable or do these two traits (co-) evolve from an initially cryptic undefended stage? Furthermore, nudibranchs show a tremendous variability in colouration between, but also within species, which is ideal to test long-standing theories of

signalling such as the assumption that signals need to be consistent in order to be learned by receivers.

Finally, in Chapter 6, I report how plastic visual signals may be used by territorial species to avoid costly combat situations, whereby receiver retaliation was found responsible to maintain signal honesty of such cheap and easily to achieve modifications ([16]; Thesis Chapter 6). Future work in this system should focus on closely related species to see if the mechanisms we uncovered are generally applicable and if they are, if they share a common evolutionary origin.

## References

1. Cortesi F., Feeney W.E., Ferrari M.C.O., Waldie P.A., Phillips G.A.C., McClure E.C., Sköld H.N., Salzburger W., Marshall J., Cheney K.L. 2015 Phenotypic plasticity confers multiple fitness benefits to a mimic. *Current Biology* **25**, 949-954.
2. Cortesi F., Musilová Z., Stieb S.M., Hart N.S., Siebeck U.E., Cheney K.L., Salzburger W., Marshall N.J. 2016 From crypsis to mimicry: changes in colour and the configuration of the visual system during ontogenetic habitat transitions in a coral reef fish. *Journal of Experimental Biology*, **219**, 2545-2558.
3. Stuart-Fox D., Moussalli A. 2009 Camouflage, communication and thermoregulation: lessons from colour changing organisms. *Philosophical Transactions of the Royal Society of London B Biological Sciences* **364**, 463-470.
4. Endler J.A. 1992 Signals, signal conditions, and the direction of evolution. *The American Naturalist* **139**, 125-153.
5. Marshall N.J., Cheney K.L. 2011 Color vision and color communication in reef fish. In *Encyclopedia of fish physiology: from genome to environment* (ed. Farrell A.P.), pp. 150-158. San Diego, Academic Press.
6. Espmark Y., Amundsen T., Rosenqvist G. 2000 *Animal signals: signalling and signal design in animal communication*. Tapir Academic Press.
7. Cortesi F., Musilová Z., Stieb S.M., Hart N.S., Siebeck U.E., Malmstrøm M., Tørresen O.K., Jentoft S., Cheney K.L., Marshall N.J., et al. 2015 Ancestral duplications and highly dynamic opsin gene evolution in percomorph fishes. *Proceedings of the National Academy of Sciences of the United States of America (USA)*, **112**, 1493-1498.
8. Bowmaker J.K., Hunt D.M. 2006 Evolution of vertebrate visual pigments. *Current Biology* **16**, R484-R489.
9. Yokoyama S. 2008 Evolution of dim-light and color vision pigments. *Annual Review Genomics and Human Genetics* **9**, 259-282.
10. Messmer V., van Herwerden L., Munday P.L., Jones G.P. 2005 Phylogeography of colour polymorphism in the coral reef fish *Pseudochromis fuscus*, from Papua New Guinea and the Great Barrier Reef. *Coral Reefs* **24**, 392-402.
11. Comeault A.A., Soria-Carrasco V., Gompert Z., Farkas T.E., Buerkle C.A., Parchman T.L., Nosil P. 2014 Genome-wide association mapping of phenotypic traits subject to a range of intensities of natural selection in *Timema cristinae*. *The American Naturalist* **183**, 711-727.
12. Berner D., Moser D., Roesti M., Buescher H., Salzburger W. 2014 Genetic architecture of skeletal evolution in European lake and stream stickleback. *Evolution* **68**, 1792-1805.

13. Santos M.E., Braasch I., Boileau N., Meyer B.S., Sauteur L., Böhne A., Belting H.-G., Affolter M., Salzburger W. 2014 The evolution of cichlid fish egg-spots is linked with a cis-regulatory change. *Nature communications* **5**.
14. Cheney K.L., Cortesi F., How M.J., Wilson N.G., Blomberg S.P., Winters A.E., Umanzör S., Marshall N.J. 2014 Conspicuous visual signals do not coevolve with increased body size in marine sea slugs. *Journal of Evolutionary Biology* **27**, 676-687.
15. Cortesi F., Cheney K.L. 2010 Conspicuousness is correlated with toxicity in marine opisthobranchs. *Journal of Evolutionary Biology* **23**, 1509-1518.
16. Bachmann J.C., Cortesi F., Hall M.D., Marshall N.J., Salzburger W., Gante H.F. (in review) Honesty of a plastic visual signal is maintained by receiver retaliation.



# Acknowledgement

First and foremost I'm grateful to **Prof. Dr. Walter Salzburger**, **Dr. Karen Cheney** and **Prof. Dr. Justin Marshall** for giving me the opportunity to conduct my dissertation in their groups, for the guidance and support over the years, and for keeping me grounded when my ideas went a bit too far off the charts.

A big thank you goes to **Prof. Redouan Bshary** who agreed to be the external examiner for my thesis.

I would like to acknowledge the **Basler Stiftung fuer Biologische Forschung**, the **Janggen Poehn Stiftung**, the **Fondazione Felix Leemann**, the **Australian Government for an Endeavour Fellowship**, the **Swiss National Science Foundation**, the **Swiss Zoological Society**, and the **Australian Museum for a Lizard Island Doctorol Fellowship**. Without the funding support from these agenices my work would not have been possible.

I'm grateful to **Associate Prof. Karen Carleton**, never has there been a PI answering quicker and more throroughly to emails.

A big enormous thank you goes to all the members of the **Salzburger**, the **Cheney** and the **Marshall lab**, both past and present. For being great colleagues and friends, for having time to listen to me whenever needed, and especially for the times spent sitting on the bank of the Rhein or on the beach at Lizard and philosophing over a beer or two about the true meaning of life.

In particular I would like to thank **Zuzana Musilová**, **Sara Stieb** and **Hugo Gante** for countless hours spent talking about opsin genes, and **Zuza** especially for the never-ending brain storming on how double stranded DNA really works - How did it go again? I would also like to thank **Yuri Klaefiger**, **Wen-sung Chung** and **Hanne Thoen** for their company and patience throughout. Merci vilmol to **Brigitte Aeschbach**, **Nicolas Boileau**, **Alan Goldizen** and **Kyra Hay**, they are the wizards that keep the boat afloat. **Anya Theis**, **Florian Meury** and **Adrian Indermaur** were my lifeline during the writing up phase of the dissertation, and amongst many other things made sure that I would not only live of sugary food and coffee alone, but instead would also consume my daily portions of fruit and vegs. Grazcha fich also to **Fabrizia Ronco**, without you my thesis document would have had more formatting styles to it than pages.

A special thanks goes to all my co-authors. Without you many things would not have been possible! I would like to especially mention the people that have helped me times over in the

field, Eva – Ewa – McClure, Peter – the Caveman – Waldie, Derek Sun, Genevieve Phillips, and William Feeney.

The staff at the Lizard Island Research Station, especially **Anne Hogget and Lyle Vail**, deserve a special mentioning. Thank you for putting up with me and my sometimes unbelievable clumsiness over the years.

**Eric, Lena Kathrin** and the lil baba **Elin Fischer** (who to this day still insists on calling me opa), you guys are an amazing family and very close friends to me. No doubt that without your constant support, input and shelter it would have been very tedious to accomplish this work.

For activities, both in and outside the lab I'm very grateful to, **Pete, Zuza, Andy (Mather), Emi (Santos), Nico, Hugo, Will, Derek, Sasha (alias Alex Barras), and Mike (Wagner)**.

Over the years I have parasitized quite a few different flats and I would like to thank all the people giving me a roof over the head at times, including **the Ryffstrasse mob, Muespi Wg vegetarians, and the Wettsteinplatz house of music**.

It goes without saying that the biggest gratitude goes to my families, both in Switzerland and in Australia. I would like to thank you for giving me love, courage, and the perspective on what is truly important in life. Grazcha fich, mum **Rita Cortesi**, dad **Sergio Cortesi**, sis **Sara Cortesi**, dog **Rocky** and the cats **Ela, Tizza and Nicki**. **Daphnie Leo** and especially **Lawrie Fabian** and dog **Mollymoo**, without you Australia would only be half a home to call.

Last but not least, to all the people I may have forgotten. **Thank you all, Grazcha fich, Merci eu allne, Danke vielmals, Grazie mille, Terima kasih, Děkuji!**

# Curriculum Vitae

## Fabio Cortesi

### PRESENT ADDRESS:

Zoological Institute

University of Basel

Vesalgasse 1, CH-4051 Basel, Switzerland

eMail: [Fabio.cortesi@uqconnect.edu.au](mailto:Fabio.cortesi@uqconnect.edu.au)

home: [http://www.salzbungerlab.org/team/fabio\\_cortesi/](http://www.salzbungerlab.org/team/fabio_cortesi/)

<http://web.qbi.uq.edu.au/ecovis/fabio.htm>

tel.: +41 61 267 0303; fax.: +41 61 267 0301



**PRIVATE ADDRESS:** Strada principale 19B, CH-7516 Maloja, Switzerland,  
tel.: + 41 78 761 24 41 (mobile)

**DATE OF BIRTH:** June 4<sup>th</sup> 1985 (in Samedan, Switzerland)

**NATIONALITY:** Swiss

**LANGUAGES:** Swiss German: mother tongue  
German: first spoken language  
English: spoken and written fluently  
Italian: spoken and written fluently  
Rhaeto-Romanic: spoken and written fluently  
French: spoken and written fluently

### Higher Education

<b>2010 – 2014</b>	<b>PhD in Zoology</b> Zoological Institute, University of Basel, Switzerland
<b>2009</b>	<b>Honours degree</b> School of Biological Sciences, University of Queensland, Australia
<b>2008</b>	<b>Bachelor degree</b> Biozentrum, University of Basel, Switzerland
<b>2005 – 2008</b>	<b>Study of Plant and Animal Biology</b> University of Basel, Switzerland

### Research Experience

<b>2010 – 2014</b>	<b>Dissertation on colour change and mimicry in <i>Pseudochromis fuscus</i></b>  Under supervision of Prof. Walter Salzburger, Zoological Institute, University of Basel, Switzerland, and Dr. Karen
--------------------	--



- Cheney and Prof. Justin Marshall, School of Biological Sciences & QBI, University of Queensland, Australia
- 2012 – present**      **Research project: Testing the functionality of facial stripes in the cichlid fish *Neolamprologus brichardi***
- Ongoing collaboration with Judith Bachman, Dr. Matthew Hall, Dr. Hugo Gante and Prof. Walter Salzburger, Zoological Institute, University of Basel, Switzerland
- 2009 – present**      **Research project: The evolution of aposematism in marine opisthobranchs (sea slugs)**
- Ongoing collaboration with Dr. Karen Cheney, School of Biological Sciences, University of Queensland, Australia
- April 2012**          **Research project: The role of cleaning behaviour in juvenile reef fish**
- Field assistant for Derek Sun, School of Biological Sciences, The University of Queensland, Australia
- September 2011**      **Research project: Quantifying the light environment of Lake Tanganyika**
- Collaboration with Prof. Walter Salzburger and Dr. Hugo Gante, Zoological Institute, University of Basel, Switzerland
- 2010**                **Research project: Unveiling the ecology of the Mary river turtle**
- Field assistant for Dr. Marianna Campbell and Dr. Hamish Campbell, School of Biological Sciences, The University of Queensland
- December 2009**      **Research project: The relative importance of pattern and colour contrast in the evolution of aposematic colouration in marine opisthobranchs**
- One month part-time work for Prof. Justin Marshall and Dr. Karen Cheney, QBI & School of Biological Sciences, The University of Queensland
- 2009**                **Honours thesis on the relationship between conspicuousness and toxicity in marine opisthobranchs**
- Under supervision of Dr. Karen Cheney, Dr. Alexandra Grutter, and Prof. Justin Marshall, School of Biological Sciences & QBI, The University of Queensland, Australia

**Sep – Dec 2008      Research project: The genetics of adaptive radiation in ice fishes (Nothothenioidae)**

Four months internship at the Zoological Institute, University of Basel, group of Prof. Walter Salzburger in collaboration with Dr. Michael Matschner

**2007/2008      Bachelor year at the University of Basel**

Block-courses in: Plant biology, Parasitism and Infection Biology, Ecology, Evolution and Zoology

### **Academic Certificates**

**2014      PhD in Science in the field of Zoology; grade ‘Summa cum laude’**

Zoological Institute, University of Basel, Switzerland

**2009      Bachelor in Science with Honours Class I (85% score) in the field of Marine Biology**

School of Biological Sciences, University of Queensland, Australia

**2008      Bachelor in Science with Major in Plant and Animal Biology; total grade of 5.31<sup>1</sup>**

Biozentrum, University of Basel, Switzerland

<sup>1</sup>(6 = excellent, 5 = good, 4 = pass, 3 = fail, 2 = poor, 1 = very poor)

### **Further Certificates**

**2010      ADAS Scientific diver certificate**

**2010      Marine RMDL licence**

**2008      TOEFL English certificate,**

Computer-based test, score; 110/120

**2005      English Advanced certificate**

Byron Bay English Language School, Australia

**2004      Matura Diploma**

Academia Engiadina, Samedan, Switzerland

### **Grants, Fellowships & Awards**

**2013/14      Swiss National Science Foundation (SNSF) Doc.Mobility Fellowships (N° 148460 & 155248)**

9 & 3 months research abroad towards PhD in home country, (51'400 CHF)

- 2013**                      **Swiss Zoological Society Travel award**  
(1'500 CHF)
- 2013**                      **Lizard Island Doctoral Fellowship (2013); an Institution of the Australian Museum**  
(8'000 AUD)
- 2012**                      **Australian Endeavour Research Fellowship**  
From the Australian Government, 6 months research abroad towards PhD in home country, (23'500 AUD)
- 2011**                      **Janggen-Pöhn Stiftung – One year PhD Fellowship –**  
(38'000 CHF)
- 2011**                      **Fondazione Felix Leemann study Award**  
(2'000 CHF)
- 2010**                      **Basler Stiftung für Biologische Forschung**  
**– PhD Start up grant –**  
(10'000 CHF)
- 2009**                      **Study Abroad Award – Honours Thesis –**  
From the Kanton Graubünden, Switzerland, (11'000 CHF)

#### **Conference Presentations and Workshops**

- 2013 August**              Poster at the European Society of Evolutionary Biology (ESEB) meeting, Lisbon, Portugal. "Ecological and Molecular cues for colour change in a marine fish"
- 2013 February**          Poster at the Swiss Biological Science meeting (Biology13), Basel, Switzerland. "Ecological and Molecular Cues for Colour Polyphenism in a Putative Coral Reef Fish Mimic"
- 2013 January**          Workshop NCBI/LUMC/WUR advanced NGS course "*de novo* Assembly of NGS data"
- 2012 July**                Talk at the 12th International Coral Reef Symposium (ICRS2012), Cairns, Australia. "Being yellow or brown: ecological and molecular base for colour adaptation in a marine fish"
- 2011 August**            Poster at the European Society of Evolutionary Biology (ESEB) meeting, Tuebingen, Germany. "A novel System for the Study of Aposematism: Conspicuousness and Toxicity in Marine Opisthobranchs"

**2011 July**                      Talk at the European Meeting for PhD Students in Evolutionary Biology (EMPSEB17), Seia, Portugal. "Being yellow or brown: Ecological base for colour adaptation in a marine fish"

#### **Affiliations & Societies**

Swiss Zoological Society (SZS)  
European Society of Evolutionary Biology (ESEB)  
Australian Coral Reef Society (ACRS)

#### **National Collaborations**

Prof. Walter Salzburger, University of Basel, Switzerland  
Dr Hugo Gante, University of Basel, Switzerland  
Dr Zuzana Musilová, University of Basel, Switzerland  
Dr Sara Mae Stieb, University of Basel, Switzerland

#### **International Collaborations**

Prof. Justin Marshall, University of Queensland, Australia  
Dr Karen Cheney, University of Queensland, Australia  
Prof. Karen Carleton, University of Maryland, USA  
Prof. Terry Ord, University of New South Wales, Australia  
Dr Sara Mae Stieb, University of Queensland, Switzerland  
Dr William Feeney, University of Queensland, Australia  
Dr Fanny De Busserolles, University of Queensland, Australia

#### **Teaching experience**

**2011**                      **School for International training (SIT), USA**  
Supervision of Ms Megan Sherman (4 weeks) at LIRS

#### **Media Coverage Selected:**

**2015**                      **Spiegel Online**  
Fische am Great Barrier Reef: Doppelte Täuschung hält besser

**2015**                      **BBC Earth**  
Dottyback's deadly colour trick revealed

**2015**                      **The Washington Post**  
This innocuous-looking reef fish is actually a vicious killer

- 2015                      The Conversation**  
The dusky dottyback, a master of disguise in the animal world
- 2015                      Blick Am Abend**  
Kleiner Fisch mit grossem Trick
- 2015                      Canadian National Broadcasting Radio, CBC**  
Interview on dottyback colour change and deception
- 2015                      The Conversation**  
Strange tale of fish eye evolution shows how new species could be born
- 2015                      Laborpraxis Deutschland**  
Farbwahrnehmungsgen zeigt seltene Wege der Evolution
- 2013                      <http://www.qbi.uq.edu.au/events-winter-2013>**
- 2010                      ‘Unsere Abhängigkeit vom Meer’ (Juli 2010)**  
Engadiner Wochenzeitung (Switzerland), by Barbara Schellenberg

#### **Publications Peer-Reviewed Articles**

- 2015                      Cortesi, F., et al. (2015)** Phenotypic plasticity confers multiple fitness benefits to a mimic. *Current Biology* 25 (7), 949-954.
- 2015                      Cortesi, F., Musilová, Z., et al. (2015)** Ancestral duplications and highly dynamic opsin gene evolution in percomorph fishes. *PNAS*, 112(5), 1493-1498.
- 2014                      Cheney, K. L., Cortesi, F., et al. (2014)** Conspicuous visual signals do not coevolve with increased body size in marine sea slugs. *Journal of Evolutionary Biology* 27 (4), 676 -687.
- 2010                      Cortesi, F., and Cheney, K.L. (2010)** Conspicuousness is correlated with toxicity in marine opisthobranchs. *Journal of Evolutionary Biology* 23, 1509-1518.
- Submitted**
- 2015                      Bachmann J.C., Cortesi F., et al. (In review)** Social selection maintains honesty of a plastic visual signal in fish.

## **Popular Press**

**2015**

### **The Conversation**

The dusky dottyback, a master of disguise in the animal world by William E. Feeny & Fabio Cortesi

## **Referees**

### **Professor Walter Salzburger**

Zoologisches Institut, Evolutionsbiologie,  
Vesalgasse 1, Universität Basel,  
4051 Basel, Switzerland,  
Phone: +41 61267 0303  
Email: [Walter.salzburger@unibas.ch](mailto:Walter.salzburger@unibas.ch)

### **Dr Karen Cheney**

School of Biological Sciences,  
The University of Queensland,  
St. Lucia, QLD 4072, Australia,  
Phone: +61 73365 5582  
Email: [k.cheney@uq.edu.au](mailto:k.cheney@uq.edu.au)

### **Professor Justin Marshall**

Queensland Brain Institute,  
The University of Queensland,  
St. Lucia, QLD 4072, Australia,  
Phone: +61 7334 51397  
Email: [Justin.marshall@uq.edu.au](mailto:Justin.marshall@uq.edu.au)